Ion beam patterning and directed self-assembly) Class 2

MICRO-724 (2022)

Advanced topics in micro- and nanomanufacturing: top-down meets bottom-up

Francesc Pérez-Murano
IMB-CNM, CSIC
Francesc.Perez@csic.es

Centro Nacional de Microelectrónica IMB

CSIC Consejo Superior de Investigaciones Científicas

www.imb-cnm.csic.es

STRUCTURE

Introductory lectures

A. Electron and ion beam lithography

- Recap on principles and limitations
- Relevant examples of ion-beam patterning

B. Directed self-assembly (DSA)

- Bottom-up vs top down fabrication
- DSA for high volume manufacturing
- Principles of DSA of block co-polymers

Advanced lessons

- Ion beam patterning for the fabrication of Nanoelectronic and nanomechanical devices

Advanced DSA aspects: Creation of guiding paterns and applications

Lithographies

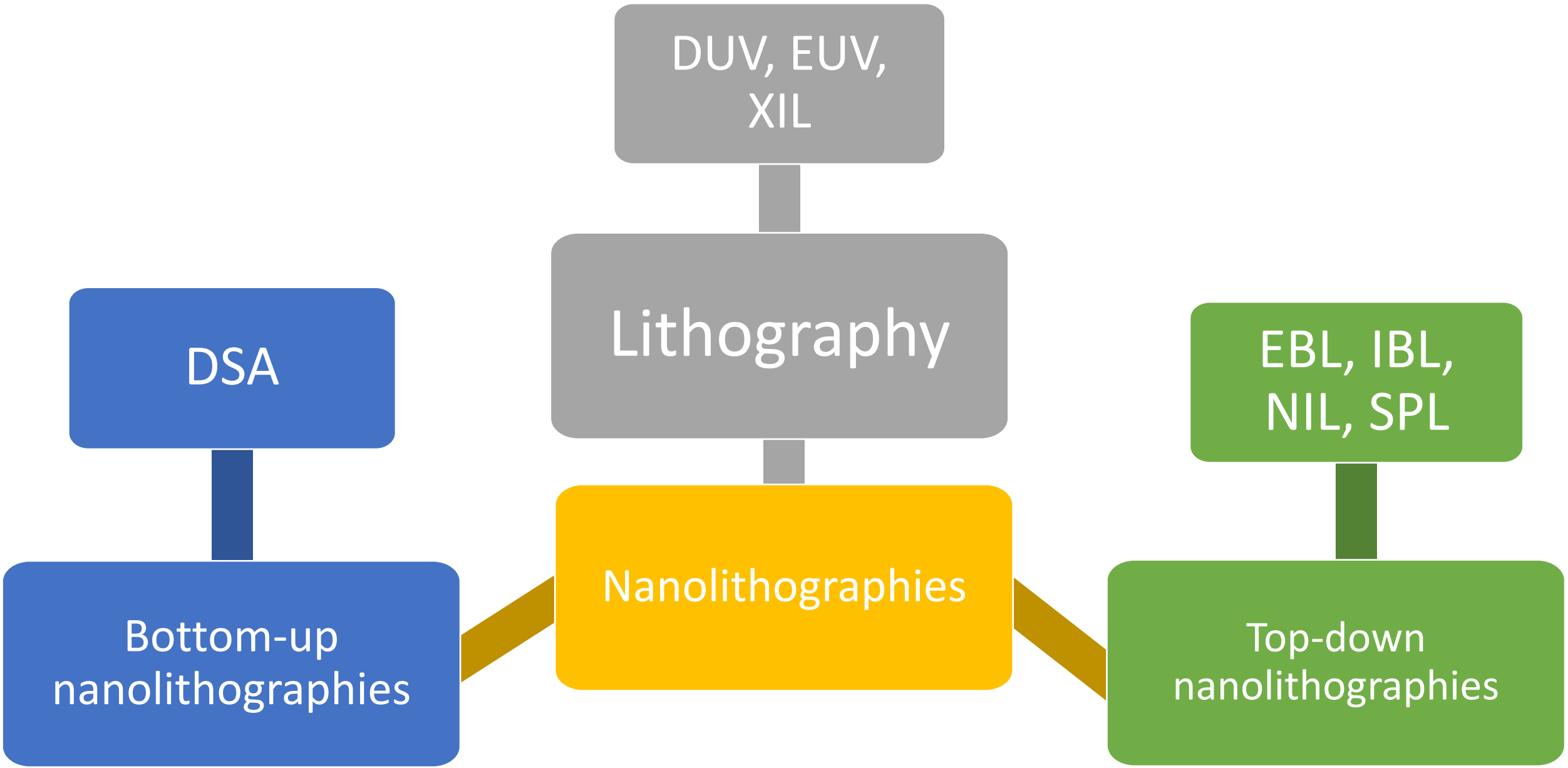

Recommended bibliography

Nanofabrication

Nanolithography techniques and their applications

Edited by JoséMaría De Teresa

ISBN 978-0-7503-2608-7 (ebook)

ISBN 978-0-7503-2606-3 (print)

ISBN 978-0-7503-2609-4 (myPrint)

ISBN 978-0-7503-2607-0 (mobi)

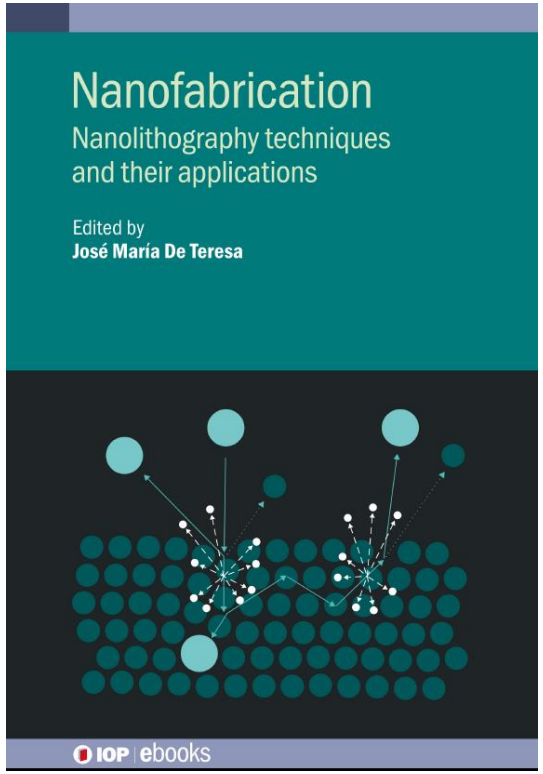

- J. E. E. Baglin, “Ion beam enabled nanoscale fabrication, surface patterning, and self-assembly” Applied Physics Reviews 7, 011601 (2020). https://doi.org/10.1063/1.5143650
- P. Li, et al. “Recent advances in focused ion beam nanofabrication for nanostructures and devices: fundamentals and applications,” Nanoscale 13, 1529–1565 (2021), http://dx.doi.org/10.1039/D0NR07539F
- Ji S, Wan et al. Directed self-assembly of block copolymers on chemical patterns: A platform for nanofabrication Prog. Polym. Sci. 54–55 76–127 (2016) ttps://doi.org/10.1016/j.progpolymsci.2015.10.006

Ion beam patterning for the fabrication of Nanoelectronic and Nanomechanical devices

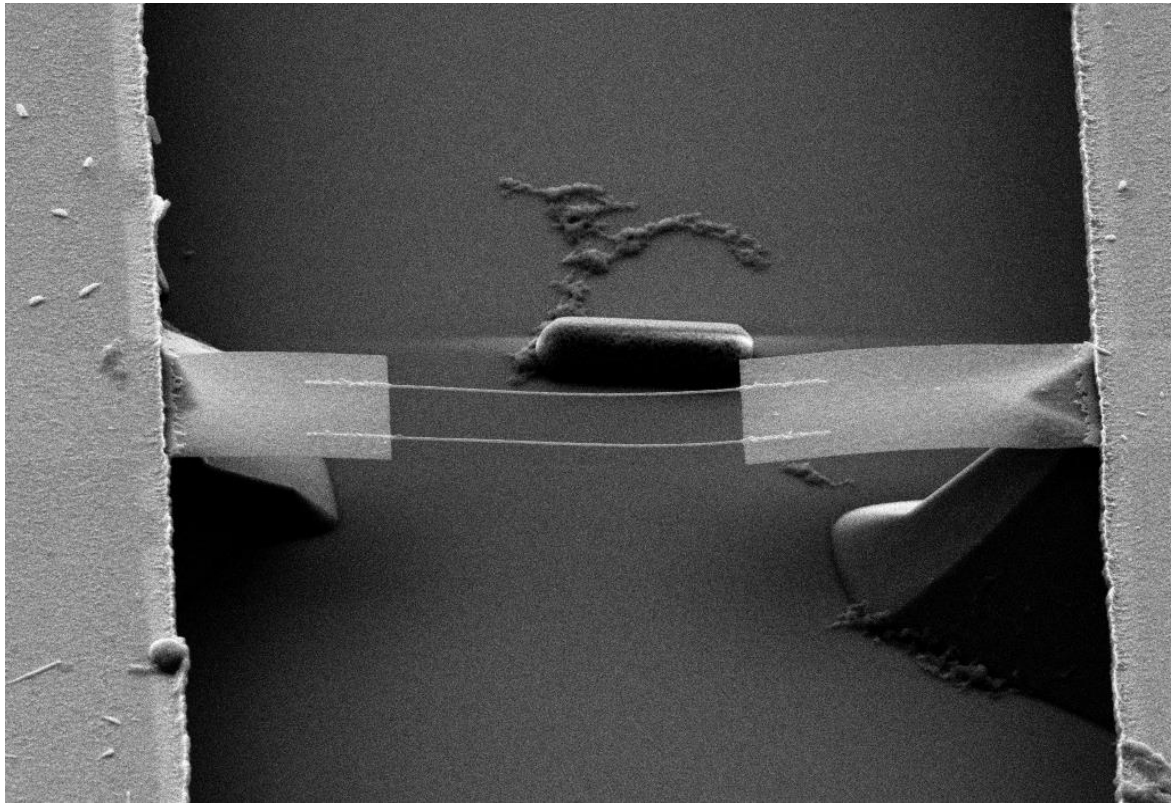

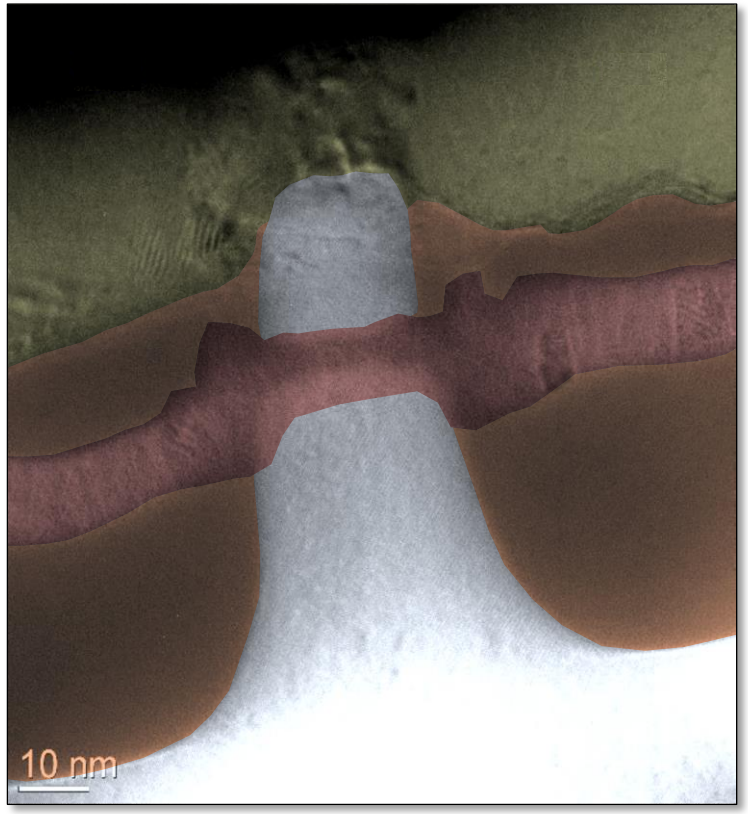

Focused Ion Beam (FIB) fabrication

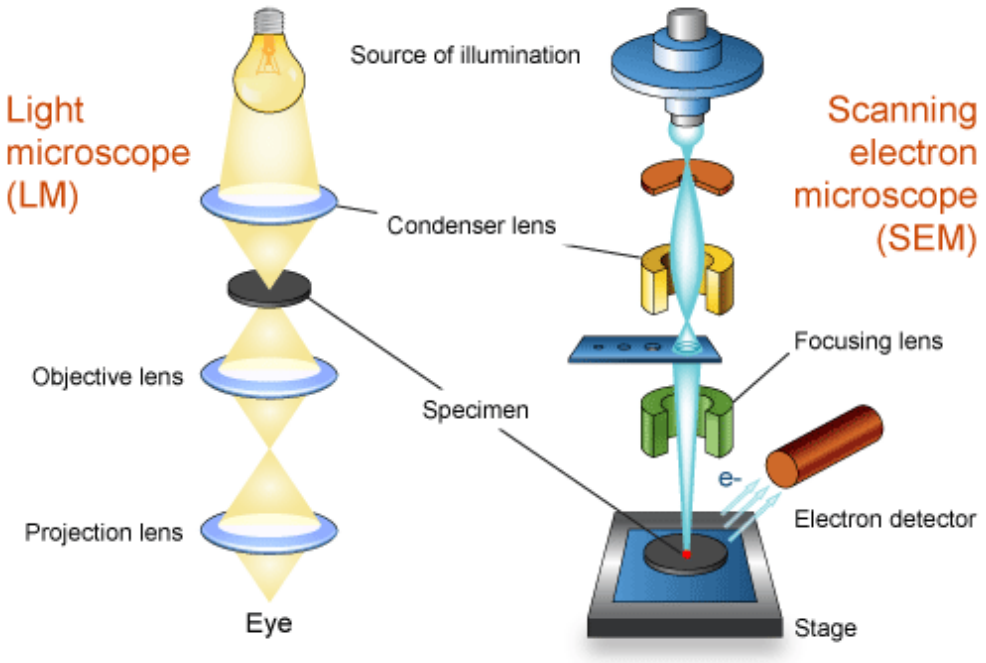

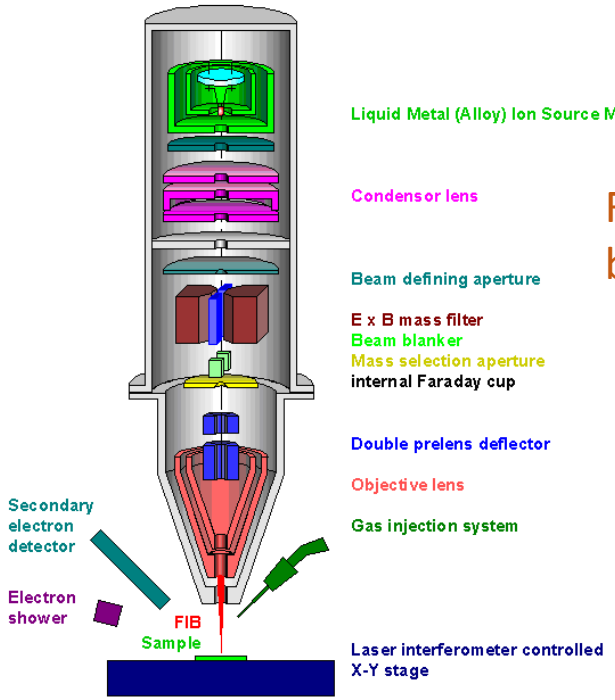

Focused ion beam system

Concept:

- Exposure of a surface by a focused ion beam
- Multiple modes of operation: Resist exposure (lithography), direct writing (milling), induce reactions, doping, …
- Ions have much large mass than electrons

FIB TOP-DOWN PROTOTYPING OF NANOSTRUCTURES

Modes of Operation

Direct Writing
- **Lithography** — *Resist exposure*
- **Irradiation** — *Material structure or property modification*

Subtractive
- **Milling** — *3D or quasi 3D nanostructuring*
- **Sputtering** — *Thin films High resolution*

Additive
- **Implantation** — *Material doping Amorphization*
- **FIBID** — *Functional layer Etching masking*

Fabrication & Integration

Mix and Match
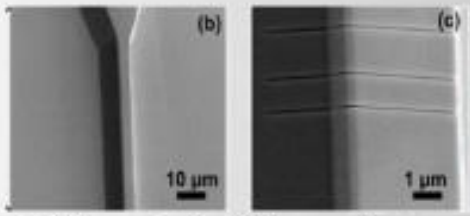

Milling + Optical lithography
[Kildishev; Lebedev 2021]

Hybrid Processing
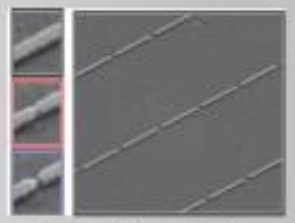

Sputtering + EBL
[Hentschel 2020]

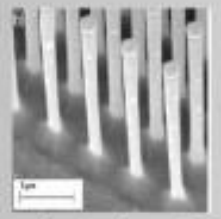

Implantation + RIE
[Chekurov 2009]

Heterogenous Tech.
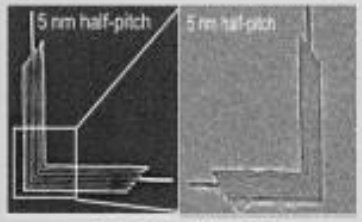

FIB Mould + NIL
[Li 2012]

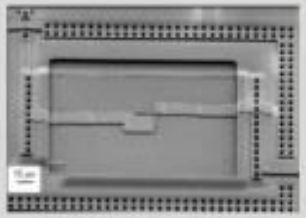

FIB NEMS + CMOS
[Rius 2011]

Fields of Application

Plasmonics


3D Janus structures
[Chen 2019]

Quantum
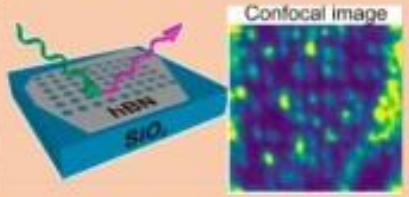

Quantum emitter
[Ziegler 2019]

Photonics
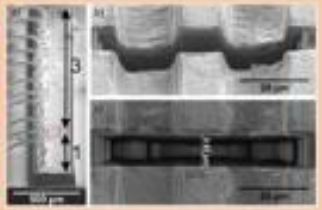

Coupled-cavity lasers
[Pierscinski 2018]

NEMS


Mechanical resonators
[Llobet 2018]

AFM tool
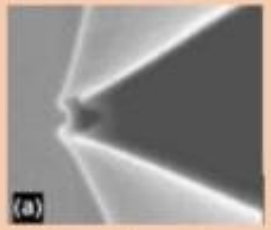

Nanodispensing
[Meister 2004]

Lab-on-a-chip
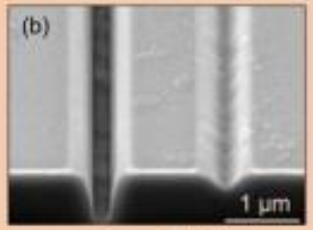

Nanofluidics
[Esmek 2019]

Lothar Bischop et al. In preparation

Ion beam interaction processes with surfaces

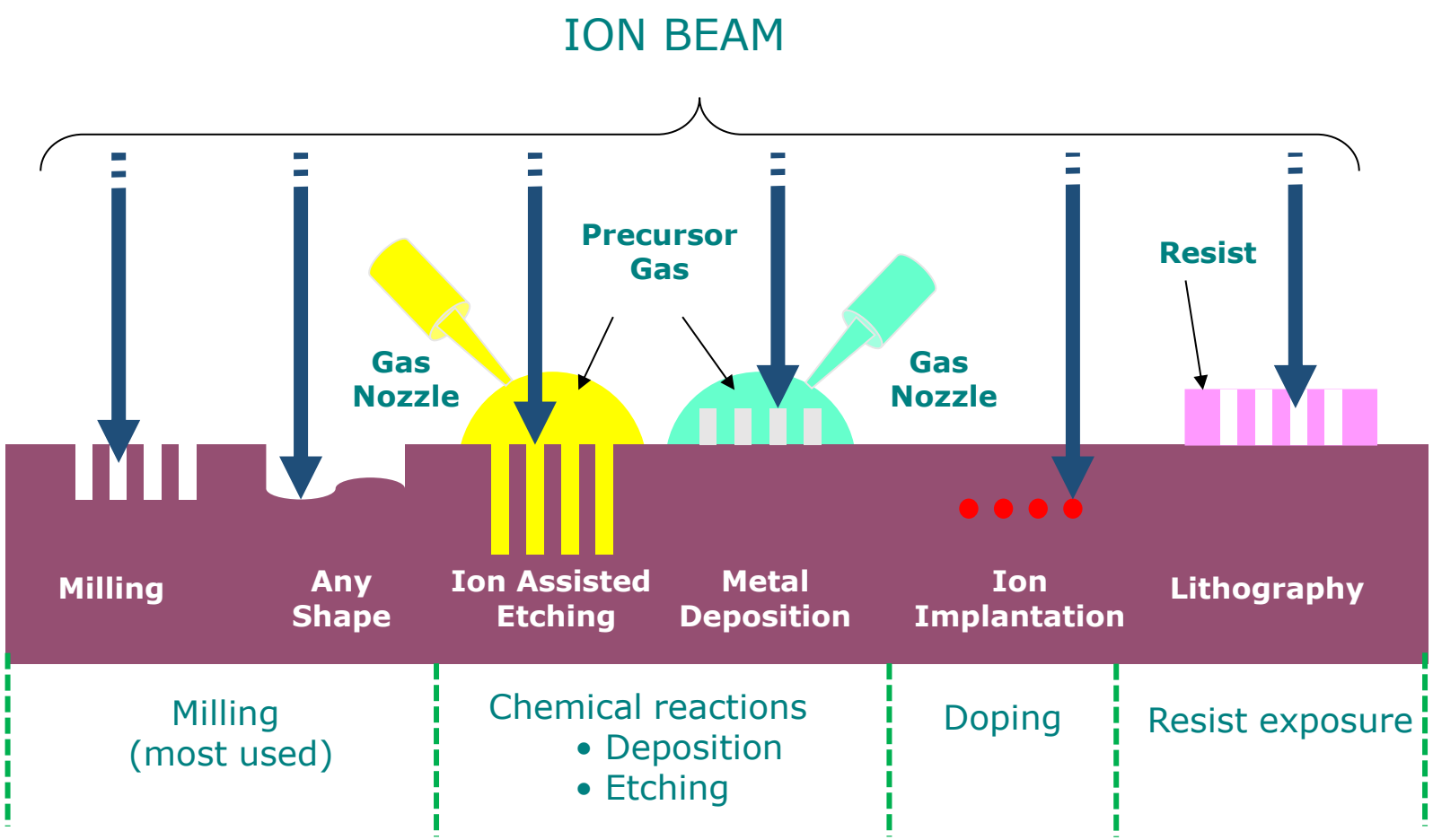

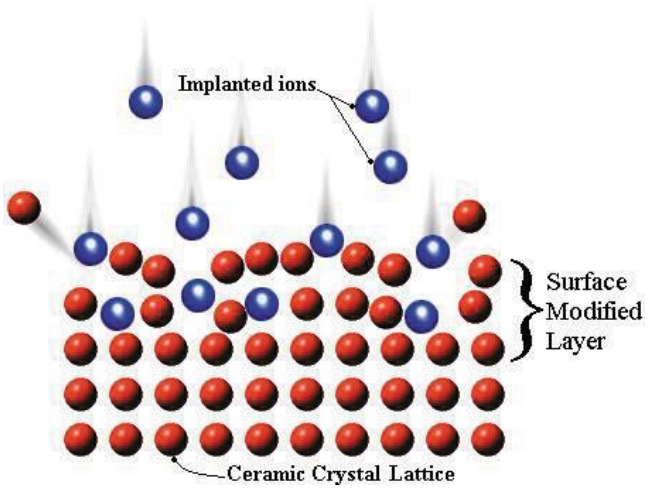

Ion implantation

Widely used in Microelectronics to locally modify the conductivity with electrons (type N) or holes (type P).

Type N: donor of electrons (e.g. phosphorus)

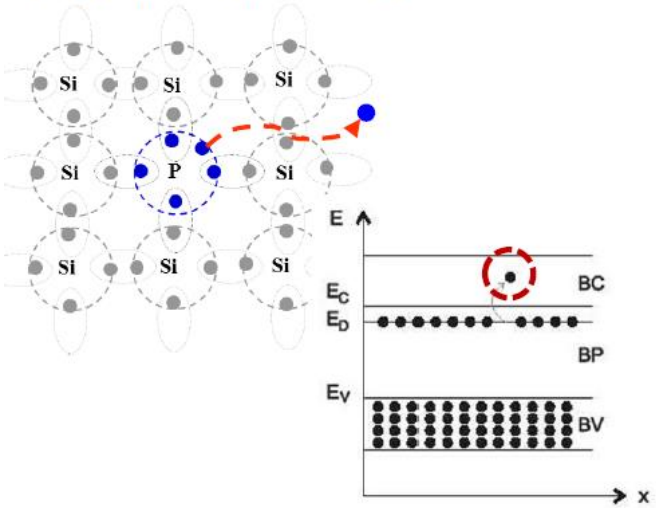

Type P: acceptor of electrons (e.g. boron) → generates holes

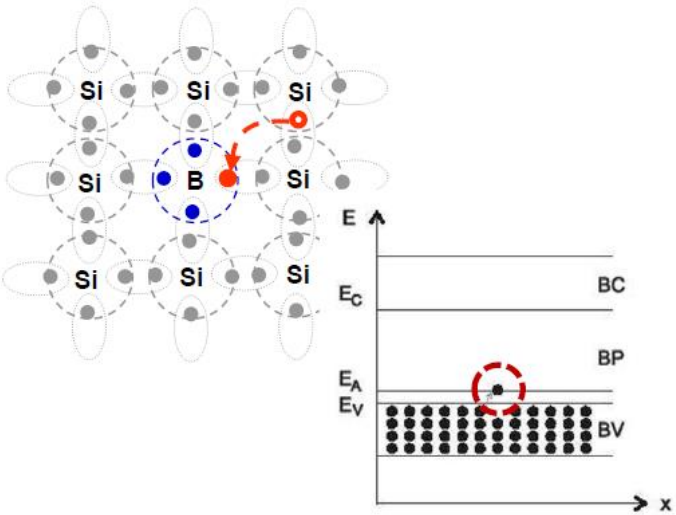

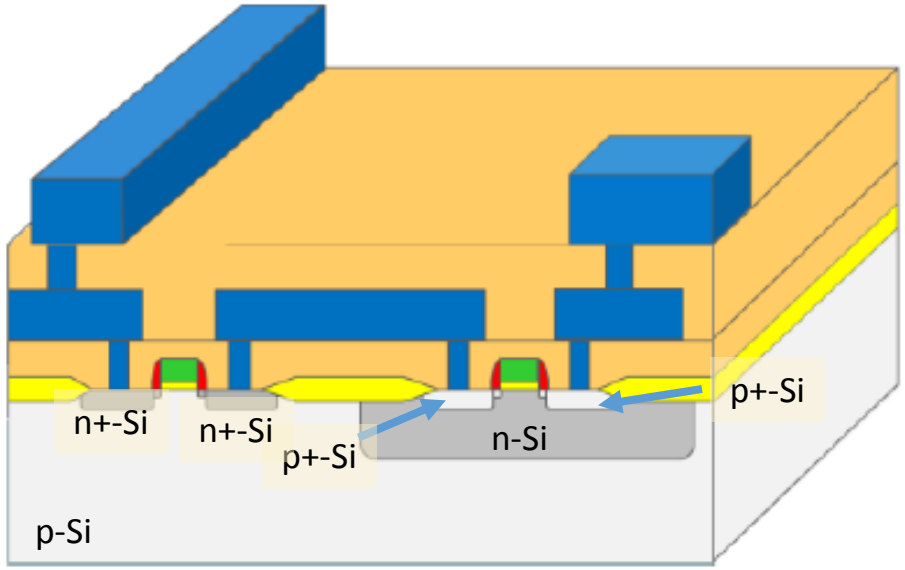

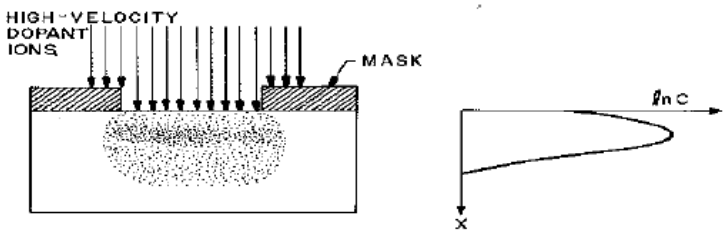

(+) control # dopants (10^{10} - 10^{16} cm^{-2})

Ion implantation

- The target (wafer) is bombarded by energetic doping ions
- Ion energy: 1 keV to 1 MeV, typically in standard implanters 10 to 200 keV

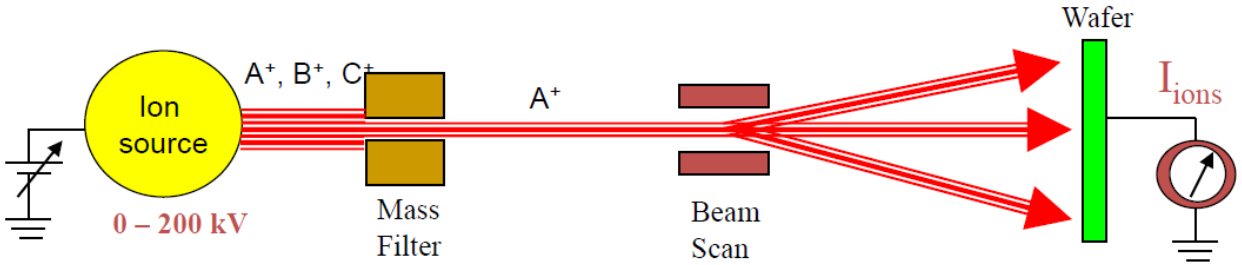

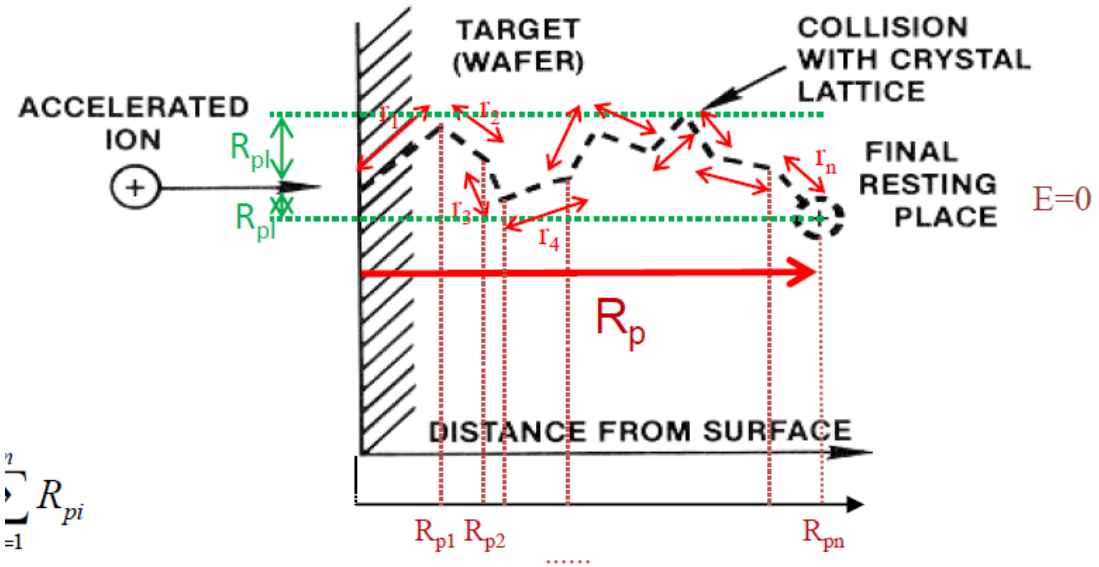

Total Range $R = \sum_{i=1}^{n} r_i$

Projected range (in NORMAL direction) $R_p = \sum_{i=1}^{n} R_{pi}$

Ion implantation

Profile of implanted ions

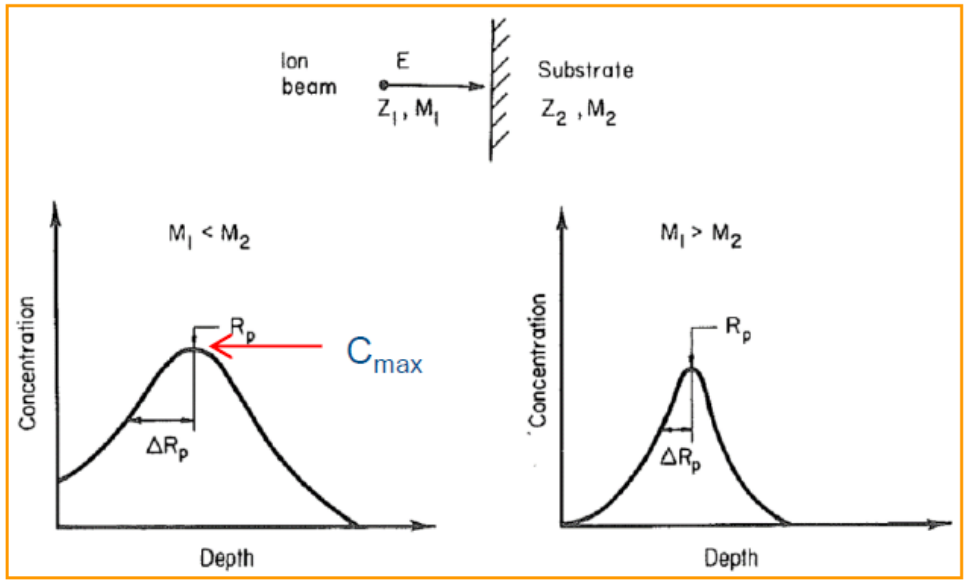

First approximation: Gaussian Distribution

$$C(x) = \frac{N_{Dose}}{\sqrt{2\pi}\,\Delta R_p} \exp\left[-\frac{(x-R_p)^2}{2\,\Delta R_p^2}\right]$$

Two first momenta:

Rp : projected range

ΔRp : projected standard deviation (or range straggling)

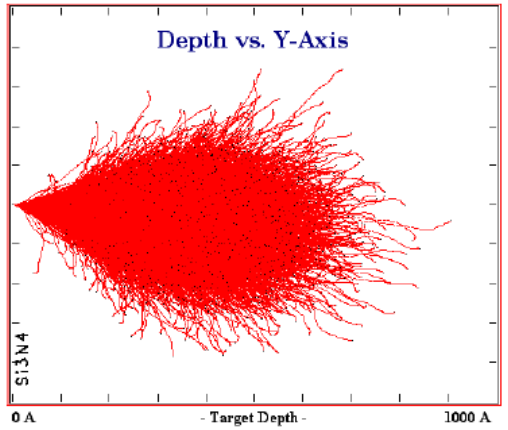

Hypothesis: (approximation!!)

$$N_{Dose} \equiv \int_{-\infty}^{+\infty} C(x)dx = \sqrt{2\pi}\,\Delta R_p\, C_{max}$$

Note that:

$$C_{max} = \frac{N_{Dose}}{\sqrt{2\pi}\,\Delta R_p} \approx 0.4\,\frac{N_{Dose}}{\Delta R_p}$$

Ion implantation

Projected ranges in Si and SiO_2

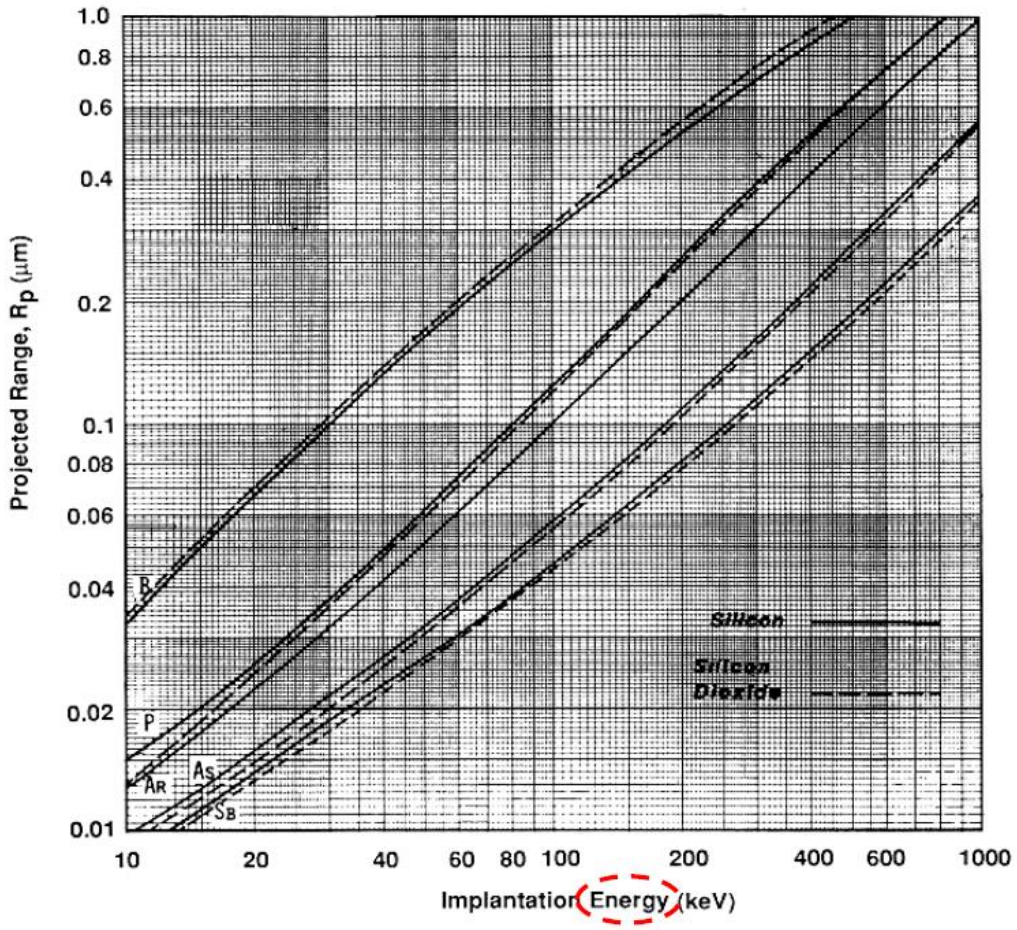

Projected standard deviations in Si and SiO_2

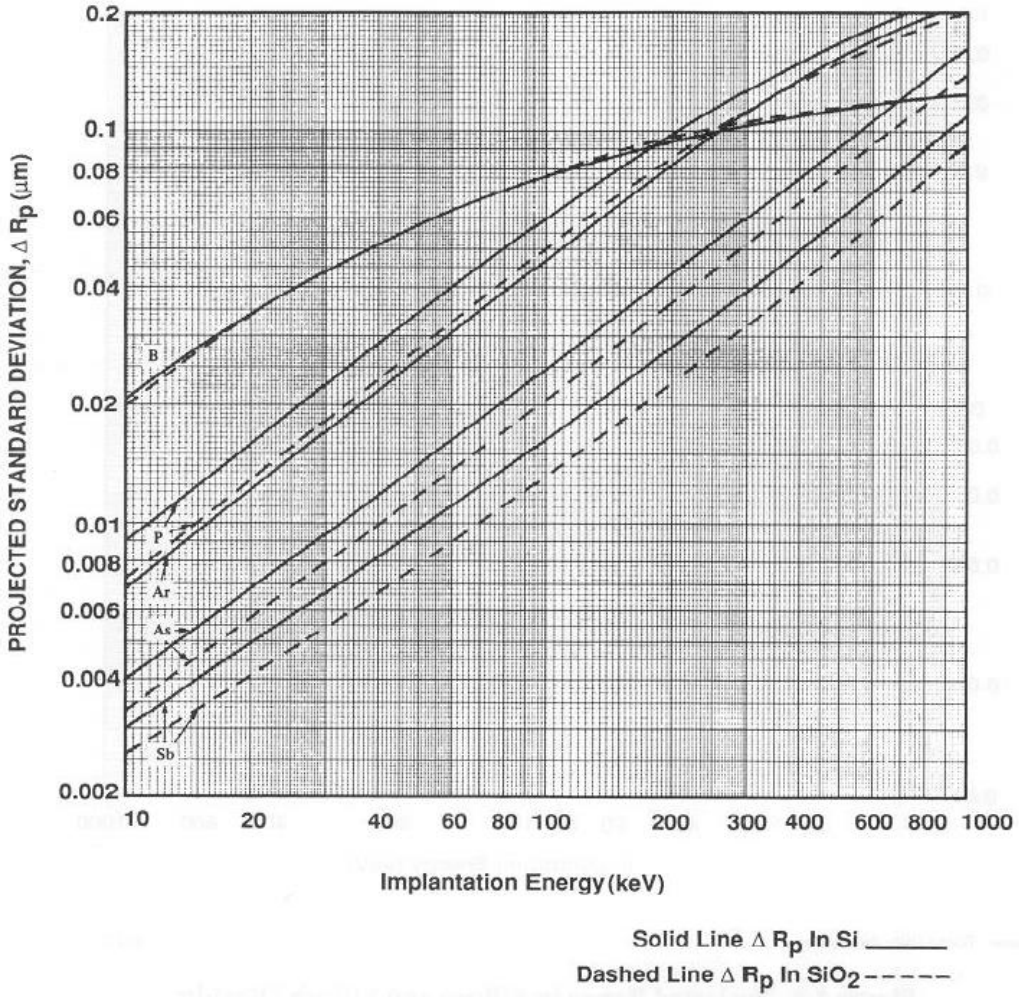

Ion implantation

$$N_{Dose} = \frac{I \times t}{q}$$

I.I. Doses and Energies (for CMOS technology)

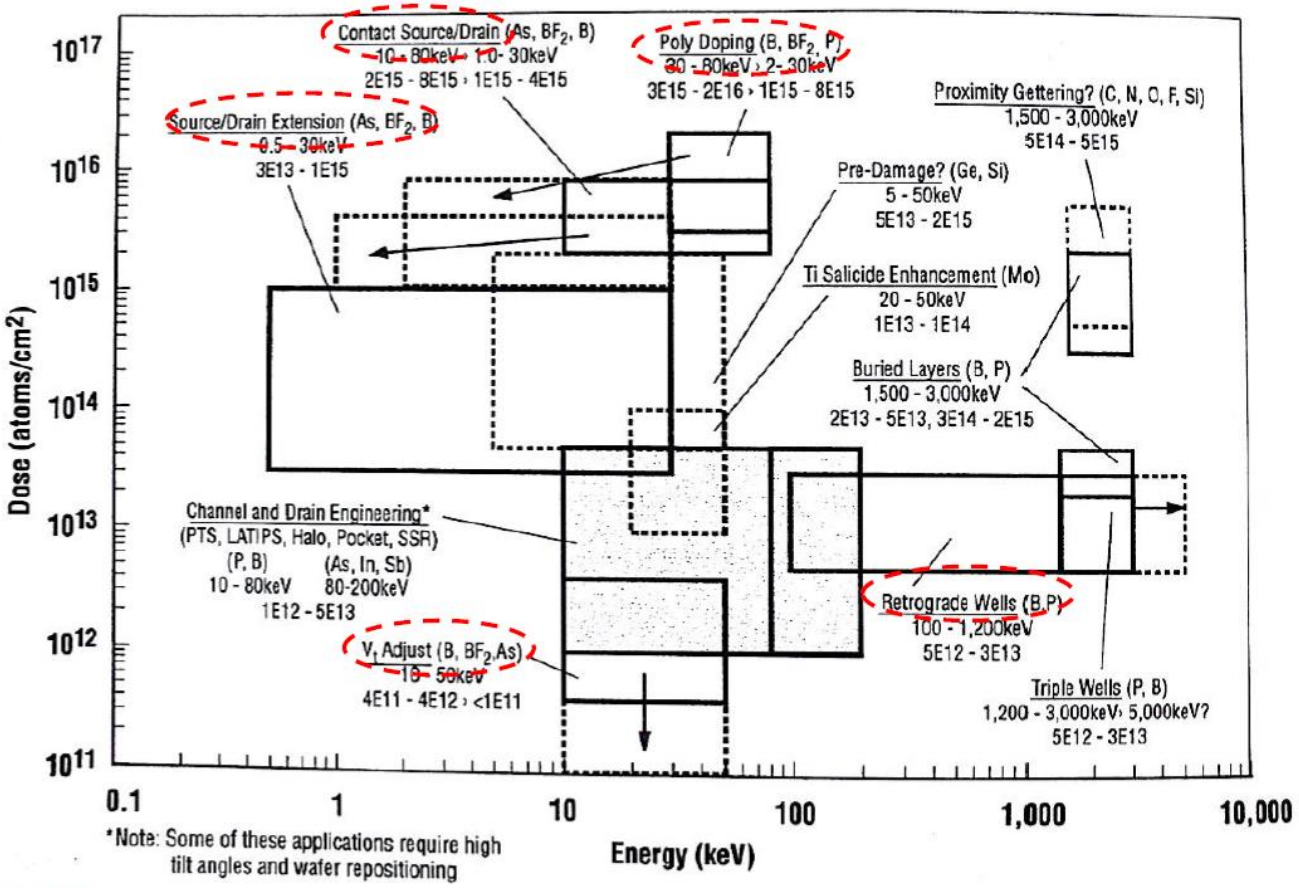

Dose (nº ions/cm²) = (t_{impl} x J_{ions}) / q

where: $J_{ions} = I_{ions}$/(scan area) (i.e. A/cm²)

$$I = \frac{Q}{t} = \frac{N\,q}{t}$$

Ion implantation vs Focused ion beam implantation

Energy: 3 – 300 keV
Typical corrent: 0.1-100 µA
Beam size: 1 cm^2

Current density : 1-10^3 A/m^2

Energy: 3 – 35 keV
Typical corrent: 0.1 – 100 nA
Beam size: 10 nm^2

Current density : 10^6-10^9 A/m^2

Ion implantation by Focused Ion Beams

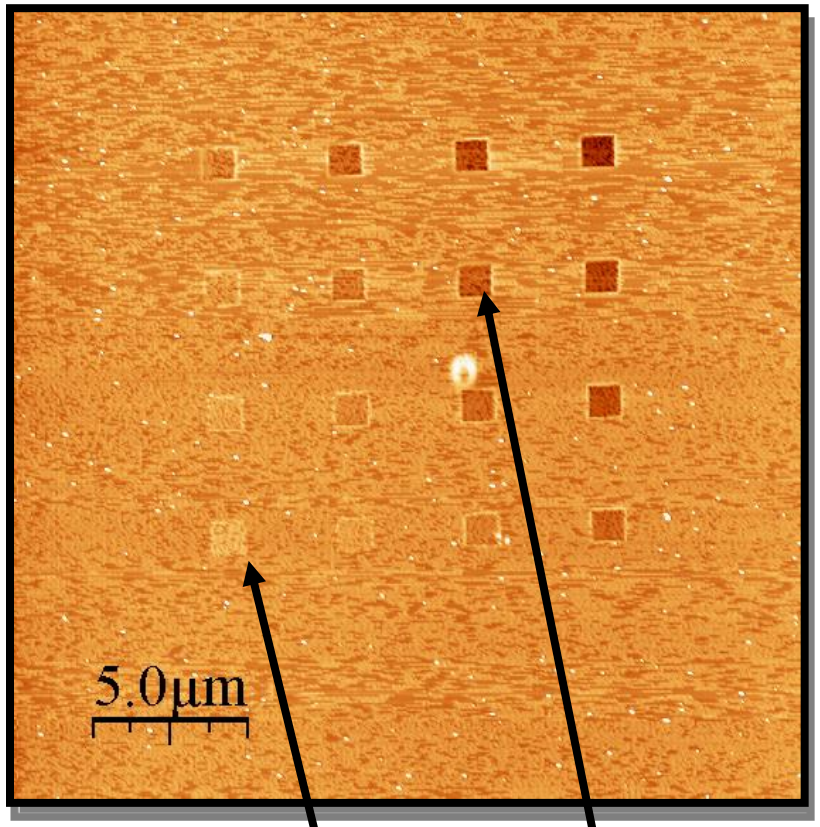

Ga^+ exposure
Dose: $1.5 \cdot 10^{16}$ Ions/cm²
1-2 nm height

Ga^+ exposure
Dose: $2 \cdot 10^{16}$ Ions/cm²
1-2 nm depth

SWELLING:
Amorphization + implantation

Etching:
Sputtering + Amorphization + implantation

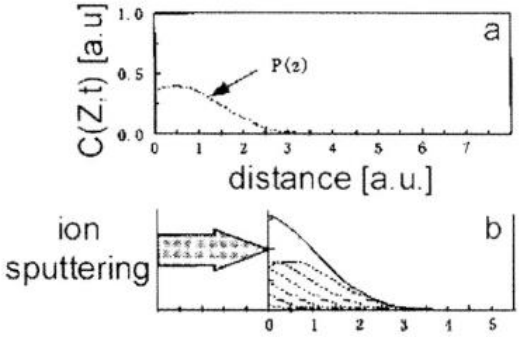

Implant profile without sputtering

Impt profile with steady state sputteringlan

L.A. Gianuzzo and F.A. Stevie, Ed. Introduction to focused ion beams. Springer. 2005

Dose	ions/nm2	3,000
Depth	nm	100
Beam diameter	nm	20
Area	nm2	1,257
ions incident	ions	3.77E+06
Volume	nm3	1.26E+05
Silicon density	atoms/nm3	49.9
atoms ejected	atoms	6.27E+06
Yield	**atoms ejected/ion**	**1.66E+00**

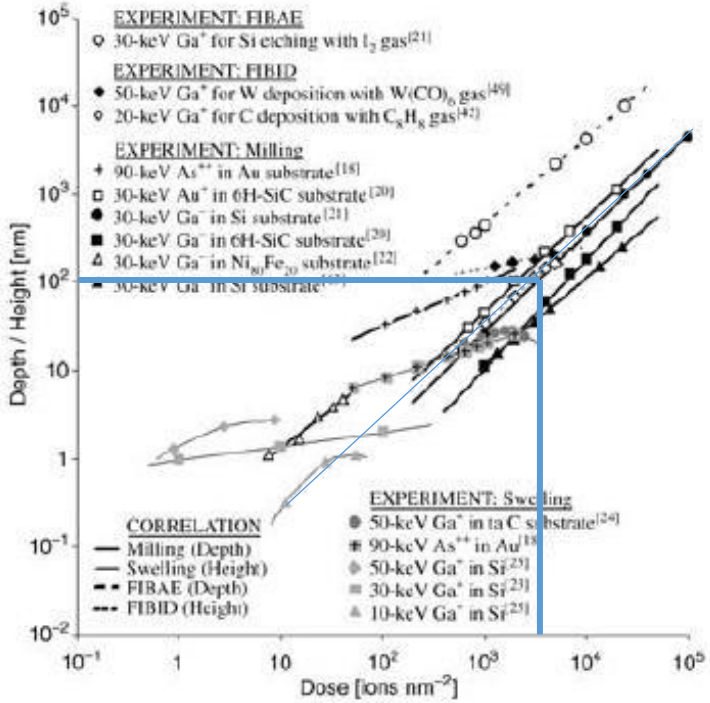

Figure 3. Relationship between feature size (depth by milling and etching or height by swelling and deposition) and ion doses for various ion species and materials.

Ion implantation by Focused Ion Beams

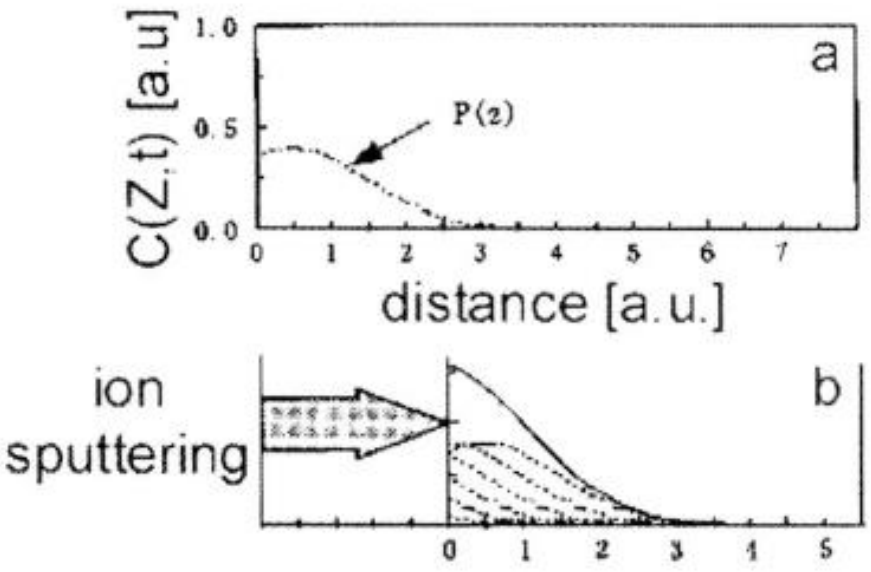

Implant profile without sputtering

Implant profile With steady state sputtering

L.A. Gianuzzo and F.A. Stevie, Ed. Introduction to focused ion beams. Springer. 2005

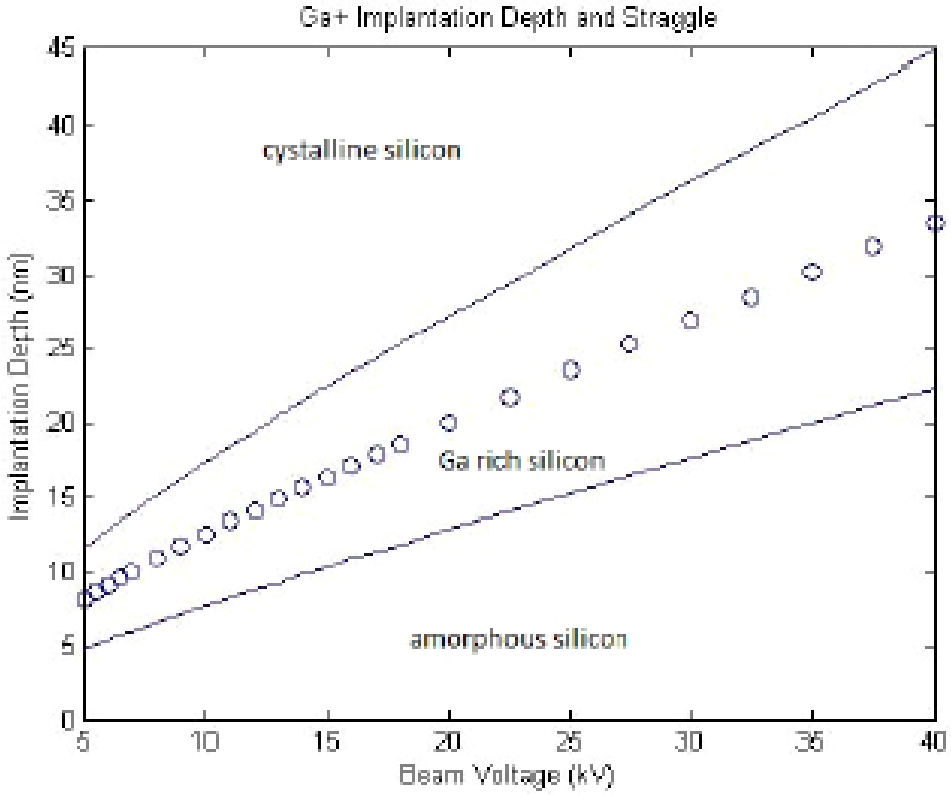

Figure 1. Ga^+ implantation depth, denoted by circles, for varying FIB beam voltages as simulated using TRIM. The straggle length, defined as one standard deviation from the mean dose, is denoted by the solid lines. The etch mask thickness is approximated here by two times the straggle length.

Increasing dose does not implant more ions to the surface, but rather, only recedes the "same" steady state surface with time

30 keV Ga Ion Range at 0 degrees on silicon: 15- 30 nm

Ion implantation by Focused Ion Beams

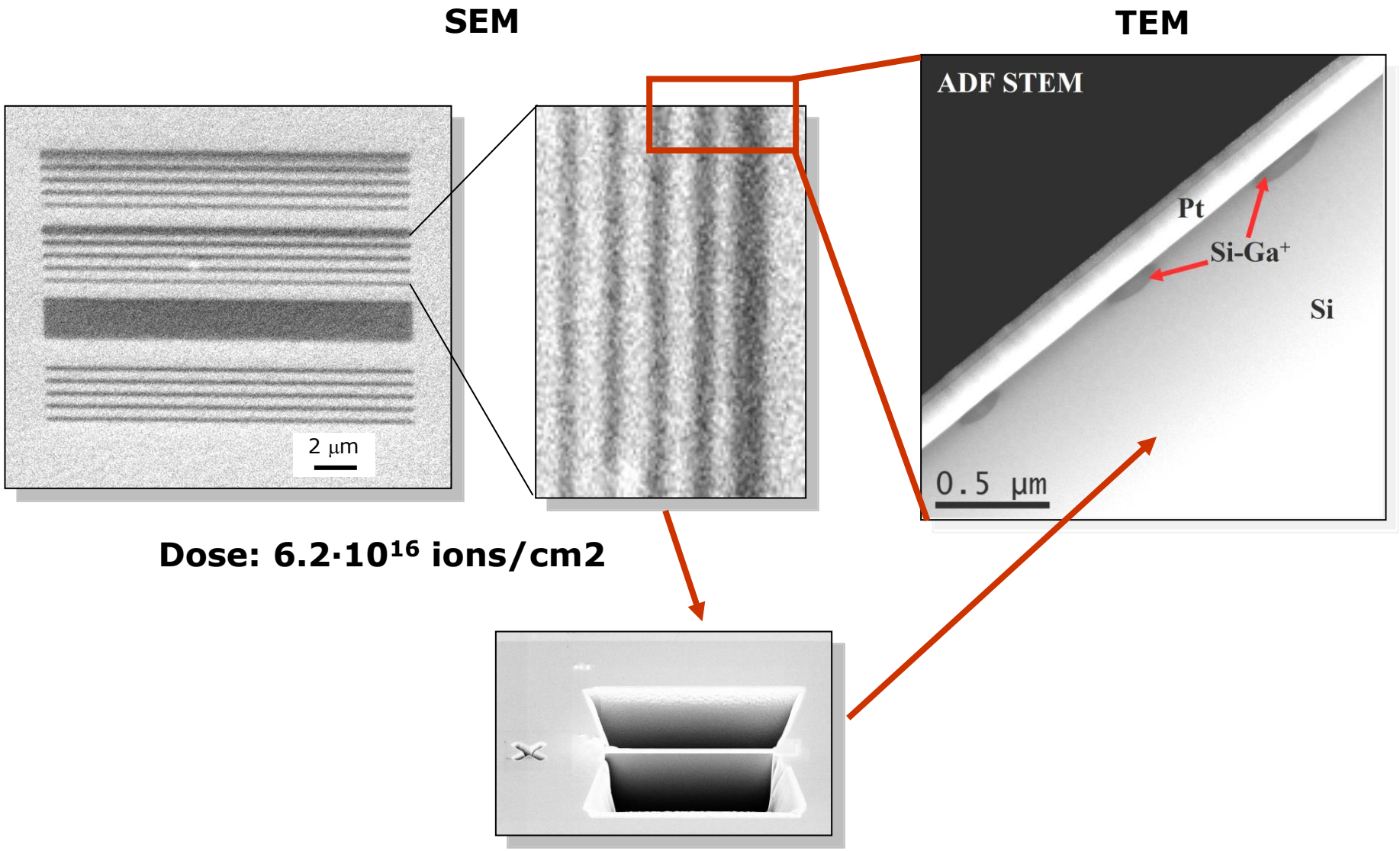

Dose: $6.2 \cdot 10^{16}$ ions/cm2

Ion implantation by Focused Ion Beams

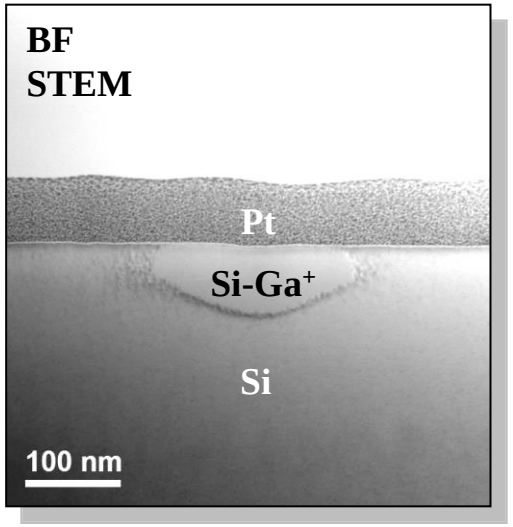

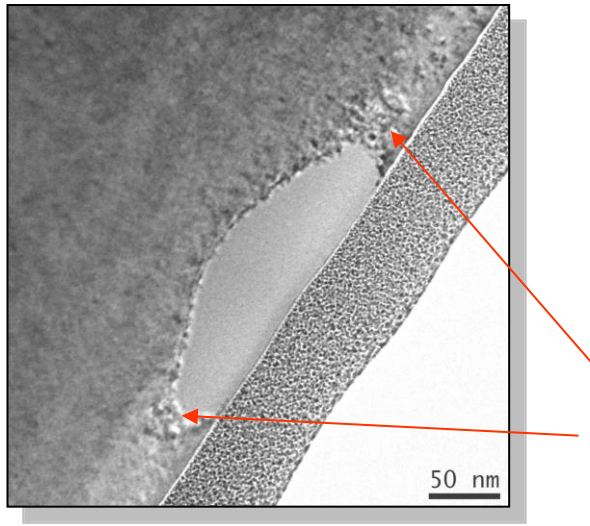

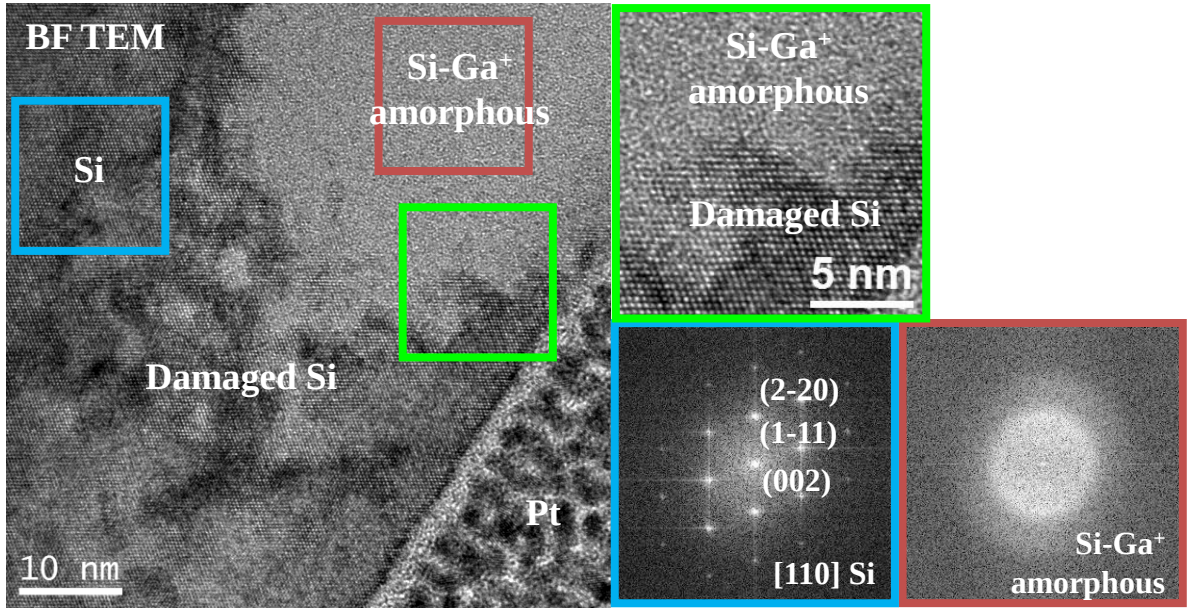

- Crystallization of the Si in the substrate far away from the Ga+ implanted area.
- In the Ga+ implanted area, the material is amorphous.
- Next to the borders, the Si structure is damaged with rough areas of mixed amorphous and crystalline Si.

How did our interest in this method start?

ELSEVIER

Available online at www.sciencedirect.com
ScienceDirect
Microelectronic Engineering 84 (2007) 1215–1218

MICROELECTRONIC ENGINEERING
www.elsevier.com/locate/mee

Fabrication of nanogaps for MEMS prototyping using focused ion beam as a lithographic tool and reactive ion etching pattern transfer

Maria Villarroya [a,*,1], Nuria Barniol [a], Cristina Martin [b], Francesc Pérez-Murano [b], Jaume Esteve [b], Lars Bruchhaus [c], Ralf Jede [c], Eric Bourhis [d], Jacques Gierak [d]

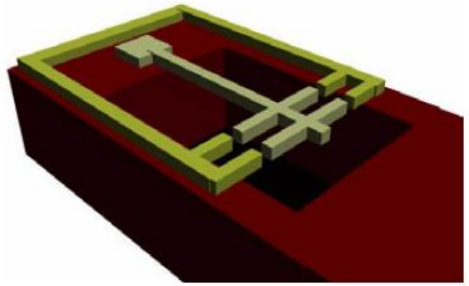

(a) Cantilever in rest

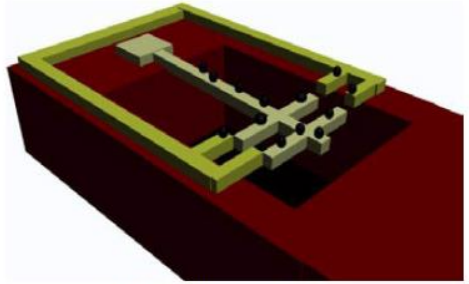

(b) Cantilever deflected

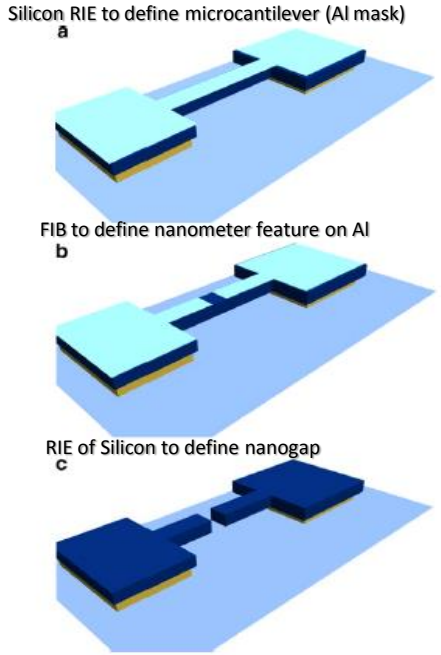

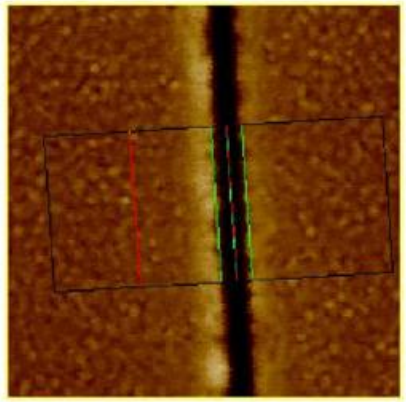

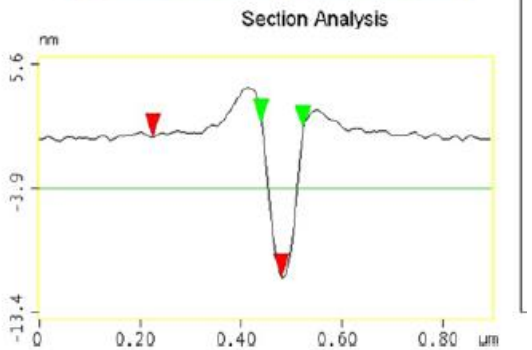

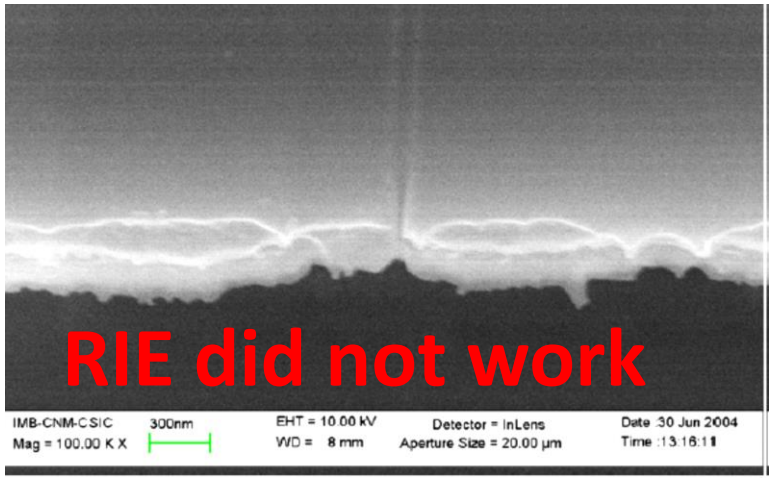

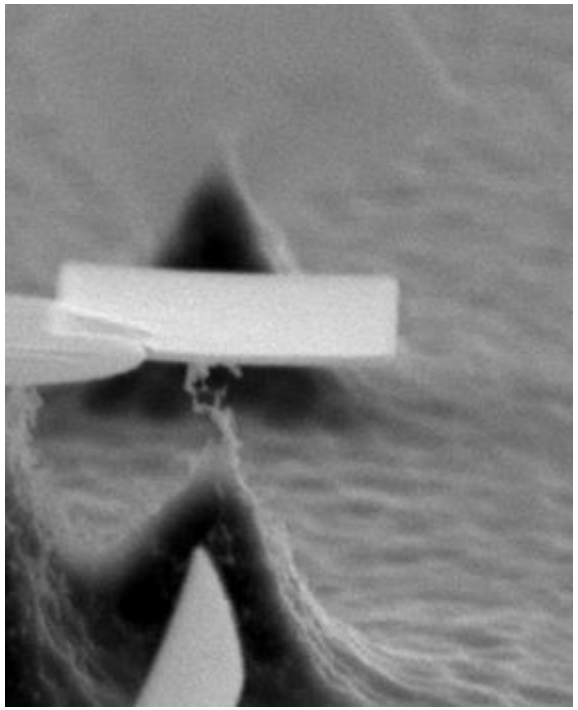

However…..

Ion beam implantation for nanopatterning

Ga^+ induced amorphization

<u>Isotropic</u> RIE reveals:

- **mask robustness**
- **thickness**
- **selectivity**

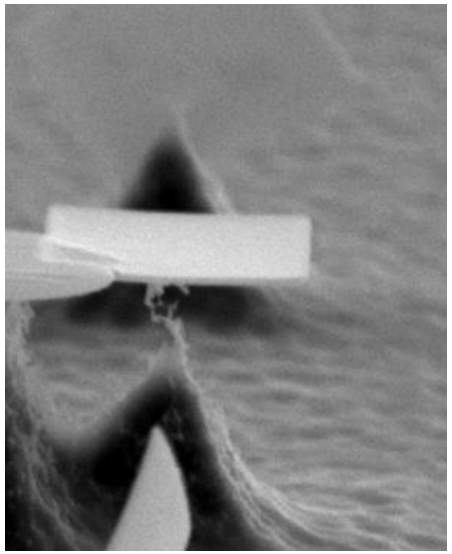

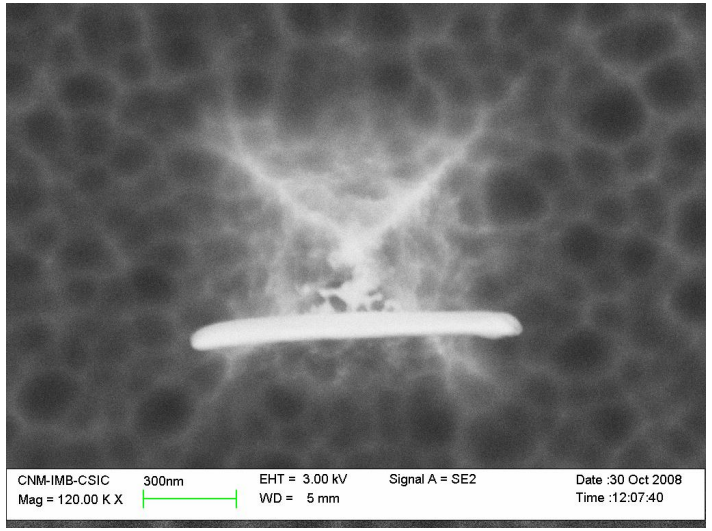

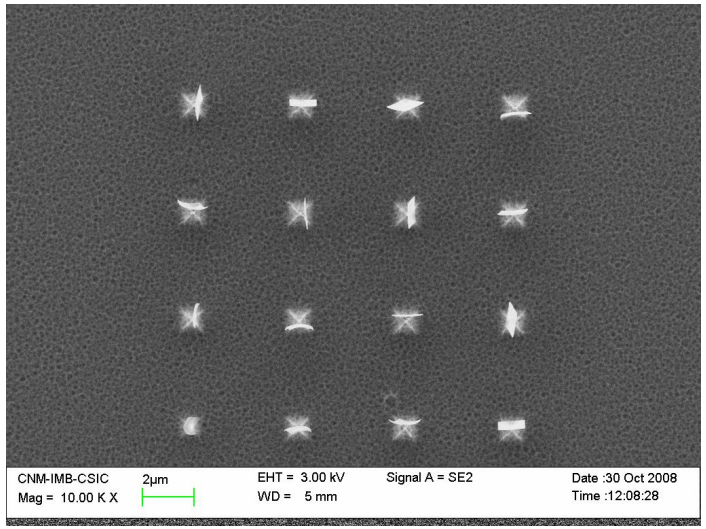

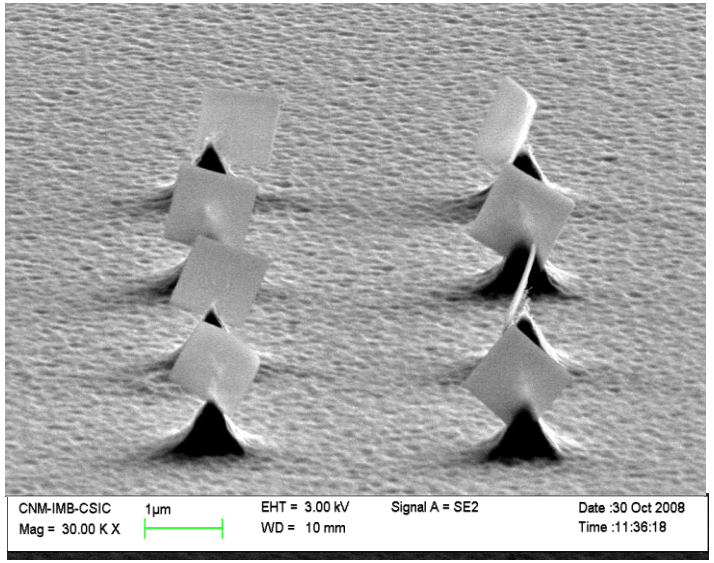

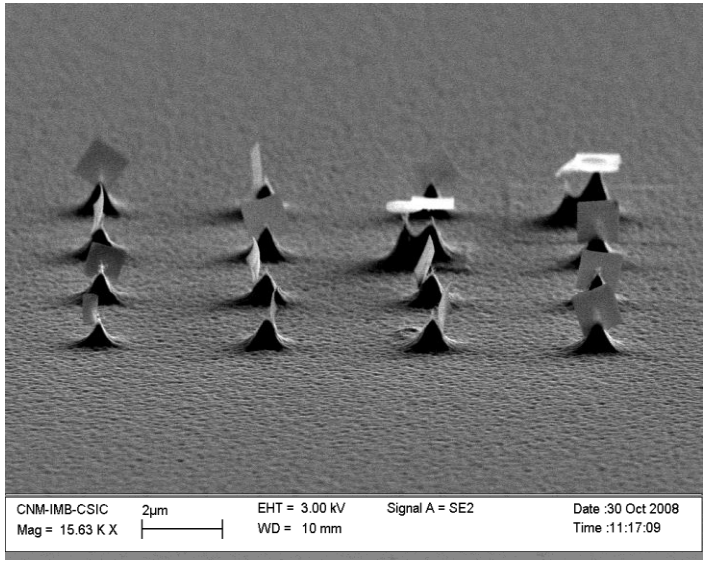

Ion beam implantation for nanopatterning

Irradiation :30 keV Ga^+ 5000 mC/cm^2; 50 – 100 nc/cm

After FIB

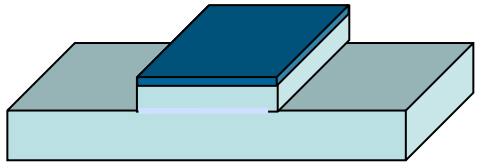

After RIE

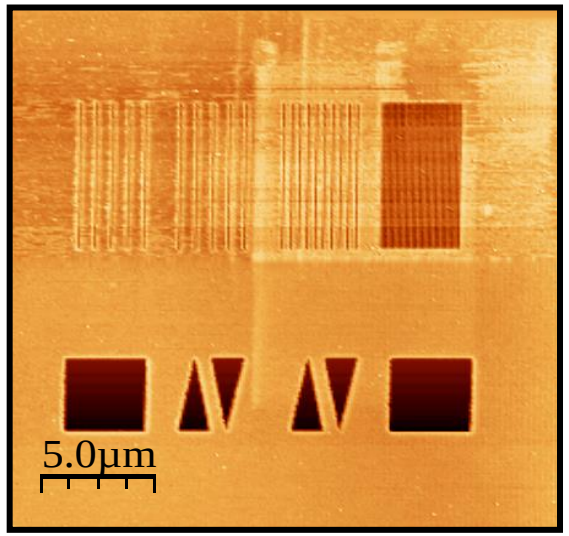

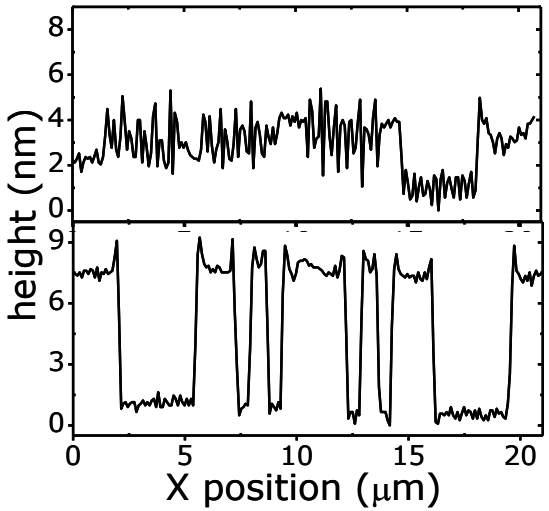

SEM and AFM images after RIE: SF6 (20 sccm) and C4F8 (30 sccm)

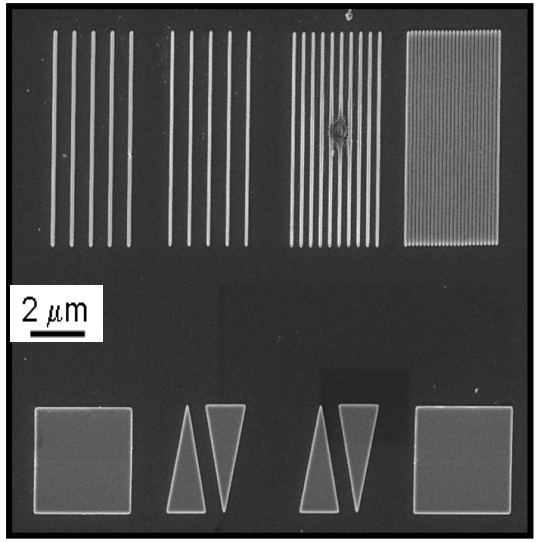

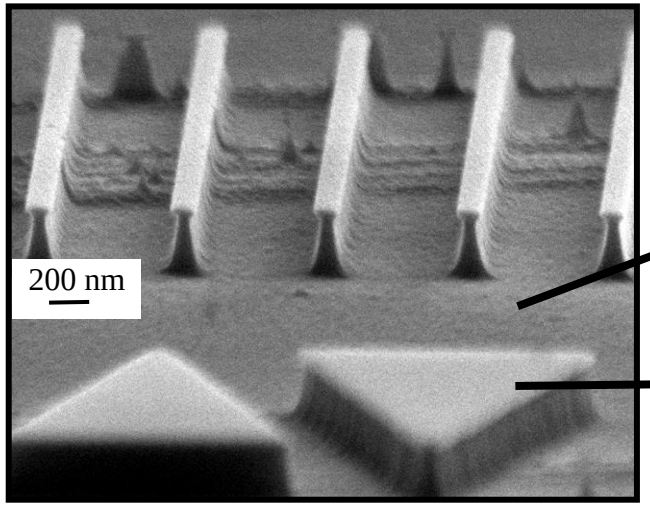

Etched surface: 1.4 nm rms

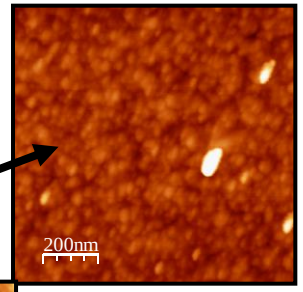

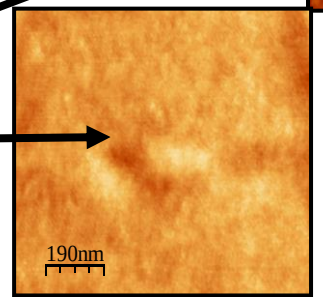

Non etched surface: 0.4 nm rms

Ion beam implantation for nanopatterning

- Effect that Ga implanted regions show reduce etching rate **in silicon** first published in 1983:
  1. Komuro et al., J. Vac. Sci. Technol. B 1, 985 (1983)
  2. La Marche et al., J. Vac. Sci. Technol. B, 1, 1056 (198
  3. Berry et al., J. Vac. Sci. Technol. B, 1, 1059 (1983)

Fully under-etched features → "free-standing"

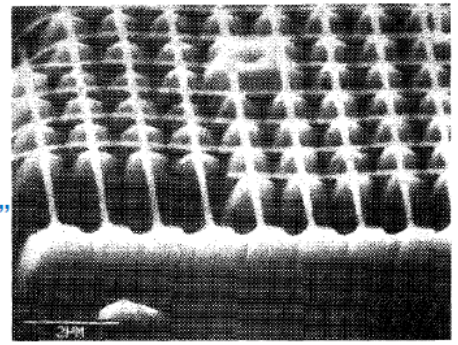

Ga-doped Si lines (140 nm wide, 20 nm thick) [3]

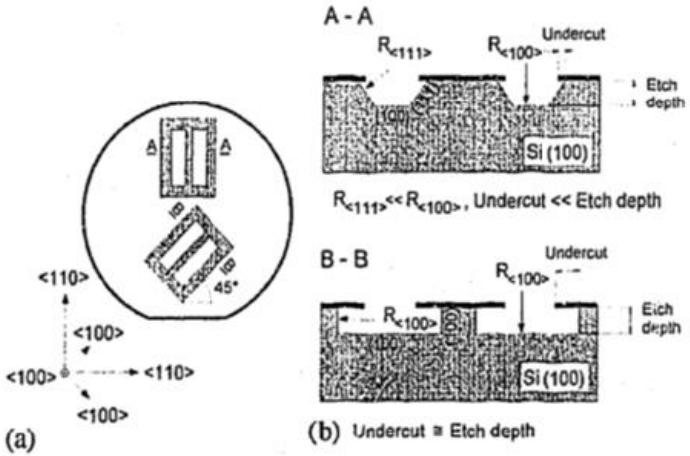

Schmidt, B., Bischoff, L. & Teichert, J. Writing FIB implantation and subsequent anisotropic wet chemical etching for fabrication of 3D structures in silicon. *Sens. Actuators Phys.* **61,** 369–373 (1997).

Use of Si_3N_4 together with optimized (but slow) etching process (pure CF4)

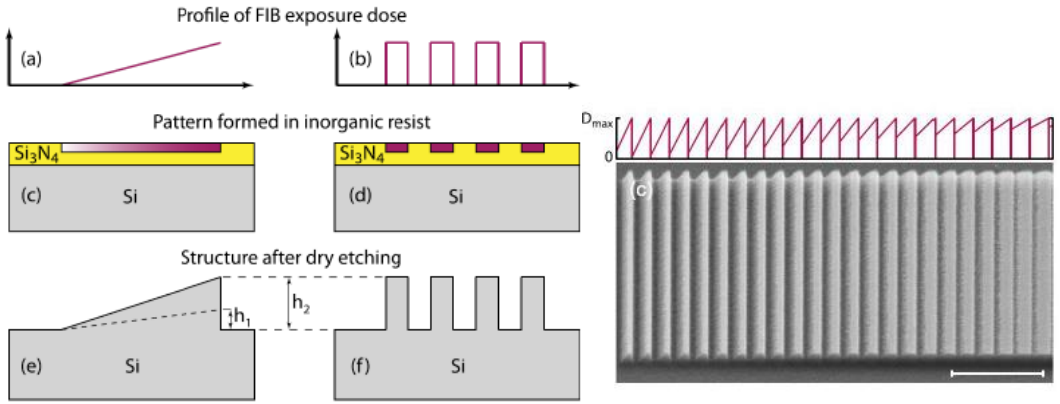

Erdmanis et al., Appl. Phys. Lett. 104, 073118 (2014)

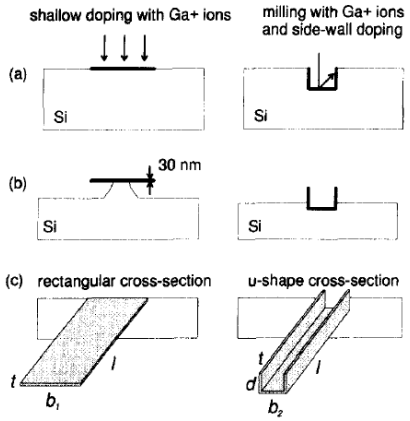

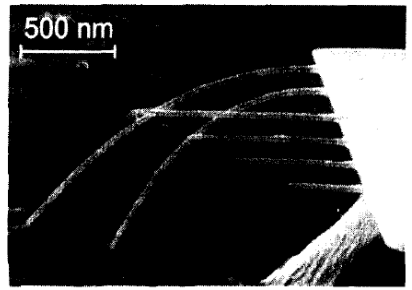

Figure 2. SEM of a series of 30 nm thin and 100 nm wide Si cantilevers with length ranging from 0.5 – 2 μm. Only the shorter beams are stable enough to withstand the surface tension during the rinsing process.

J. Brugger, et al, Microelectronic Engineering, 35, 401-404, 1997,

- **Si: Cryogenic or mixed mode etching (DRIE) enables structures with very high aspect ratios (AR) and vertical sidewalls**

AR ~ 10-14

- 120 °C

SF_6/O_2

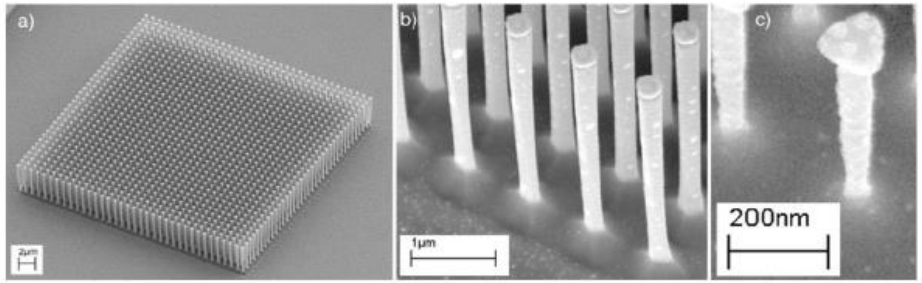

Chekurov et al. Nanotechnology (2009)

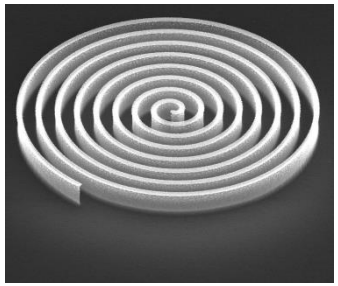

M. Rommel. IISB-Franhofer

Ion beam implantation for NEMS

General approach for the fabrication process

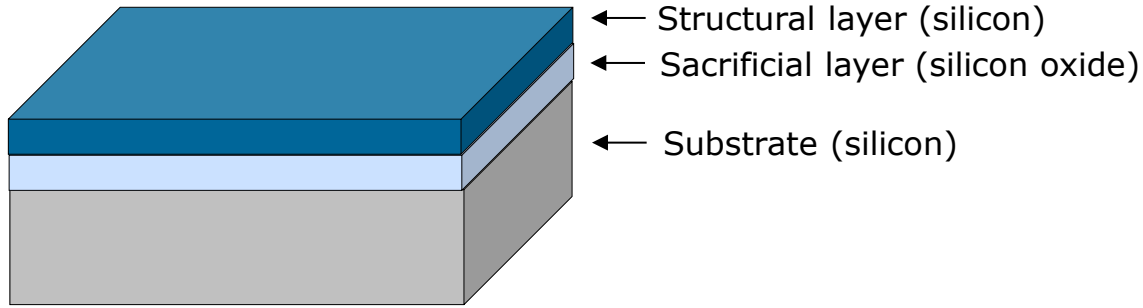

1. Lithography and etching

Patterning and transfer

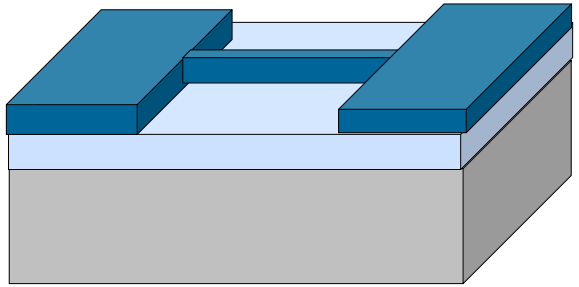

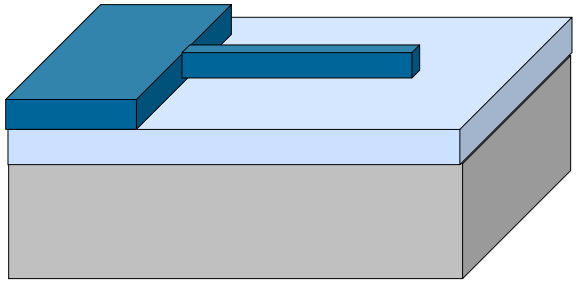

2. Under-etching

Release of the structure

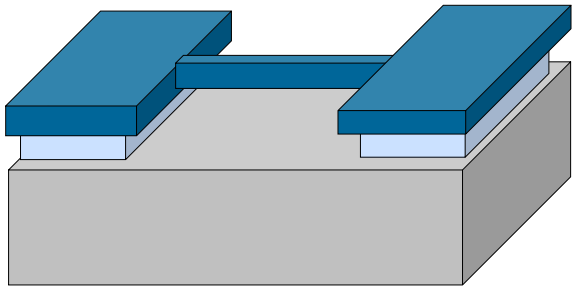

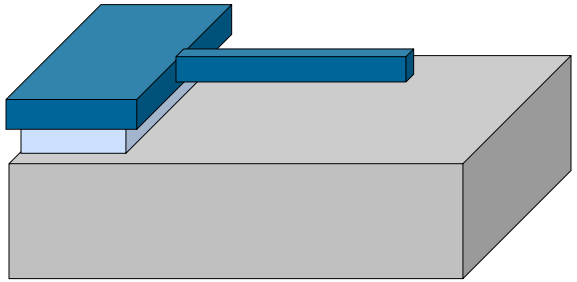

Double-clamped beam

Free-standing cantilever

Ion beam implantation for NEMS

Wet etching (KOH or TMAH)

Isotropic etching

($HF + HNO_3 + H_2O$)

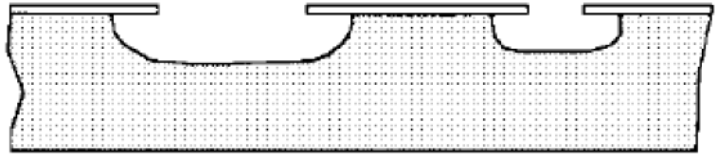

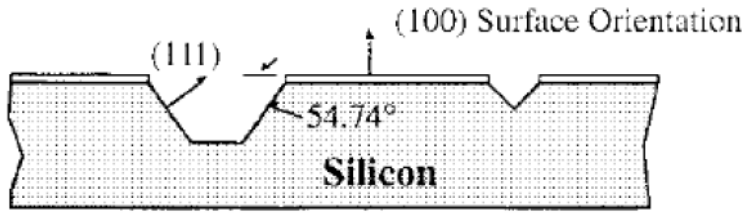

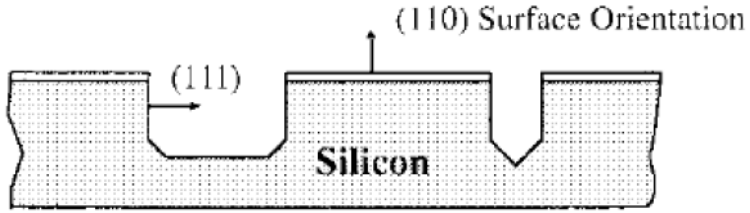

Anisotropic etching
(basic solutions)

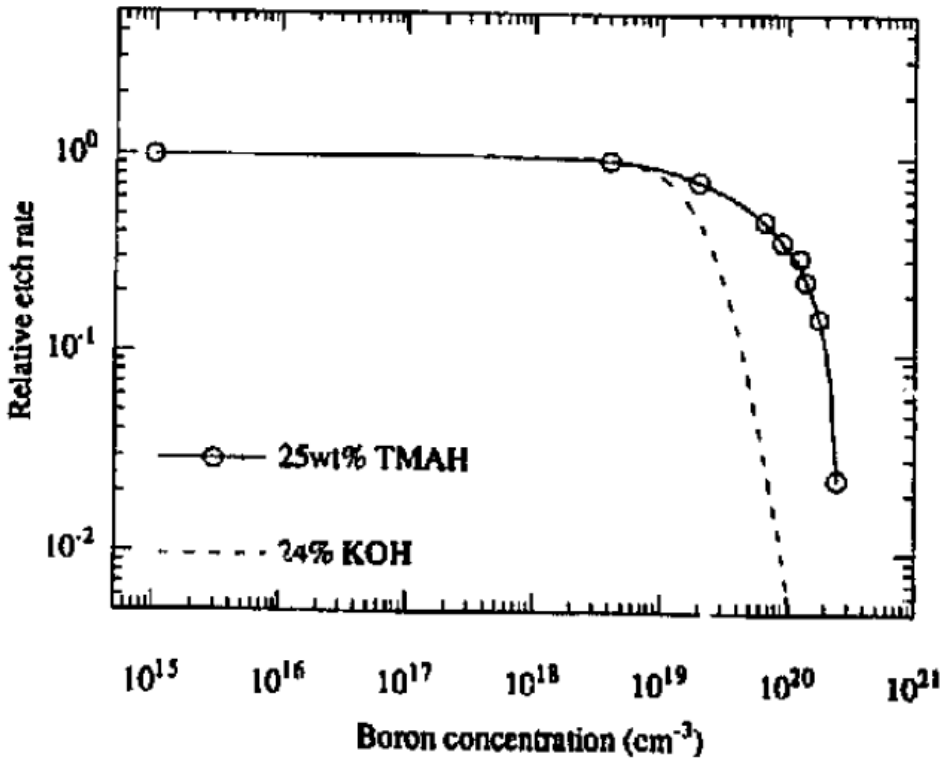

Ion beam implantation for NEMS

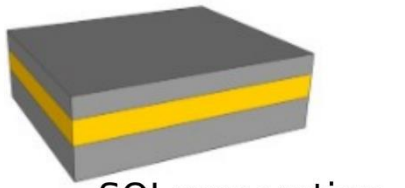

SOI preparation

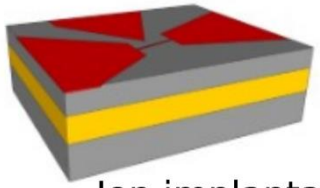

Ion implantation

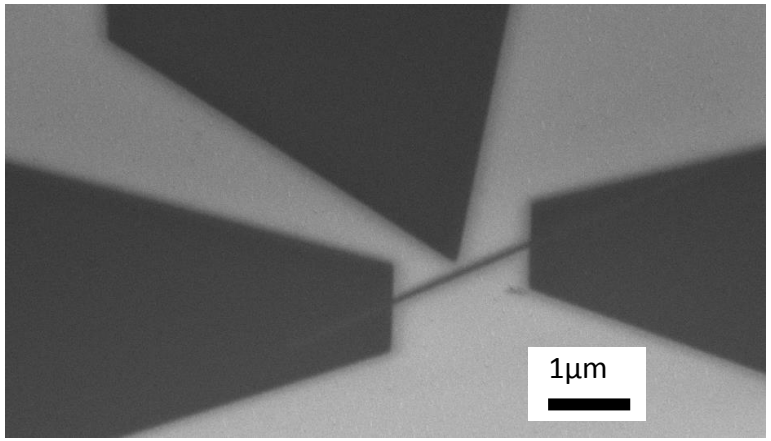

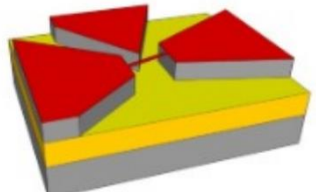

Silicon etching

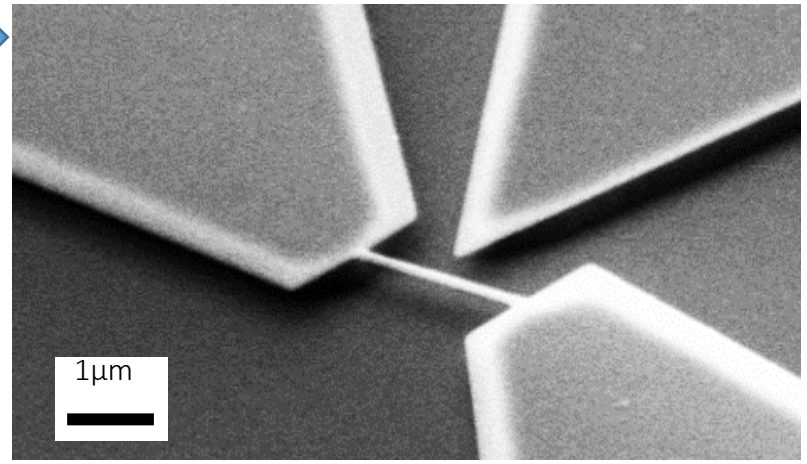

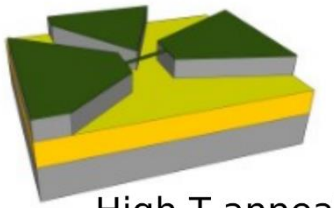

High T annealing

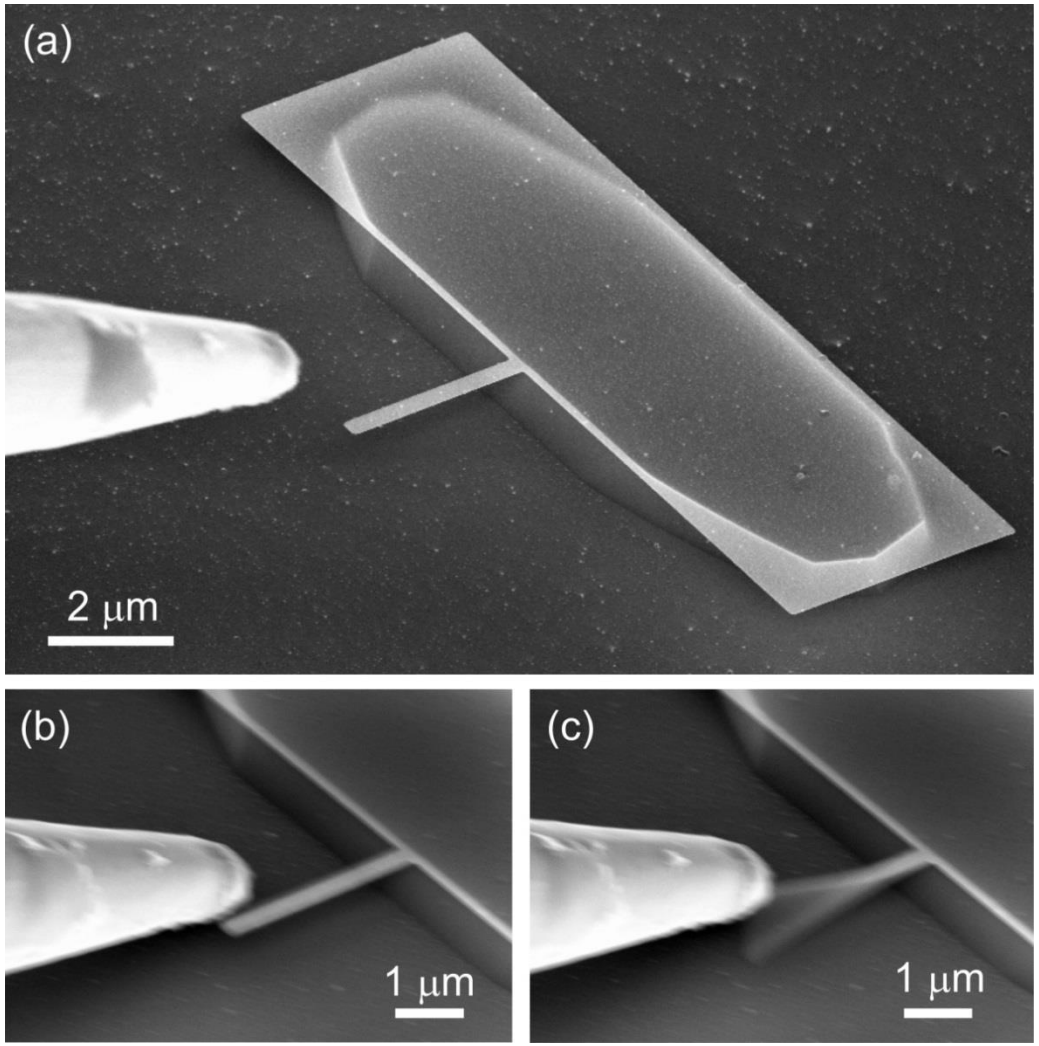

Ga implanted silicon	SiO_2
Si p-type doped (B)	Si

Free standing nano-cantilever

Thickness: 30 nm
Width: 200 nm

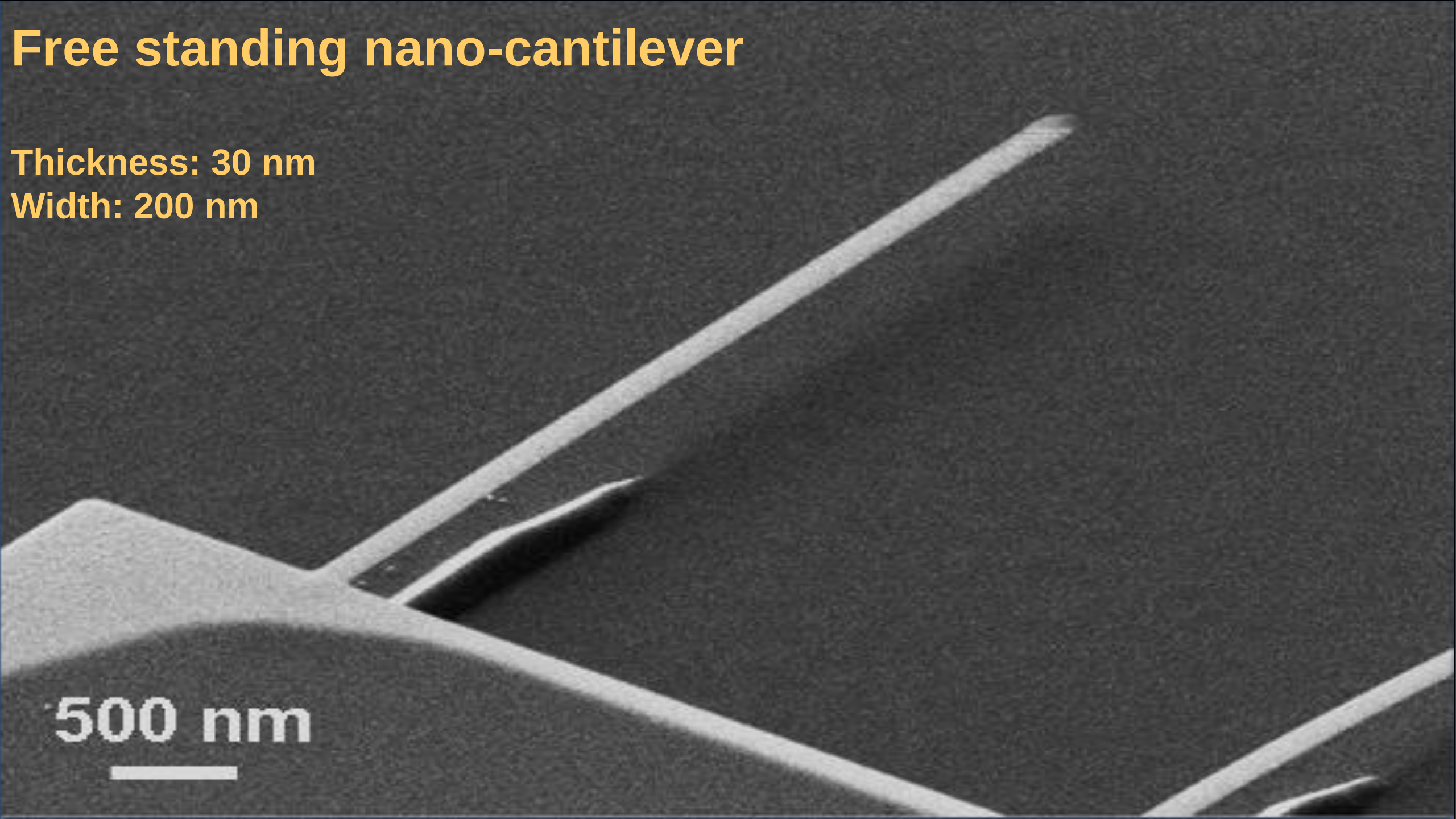

Released silicon nano-beams

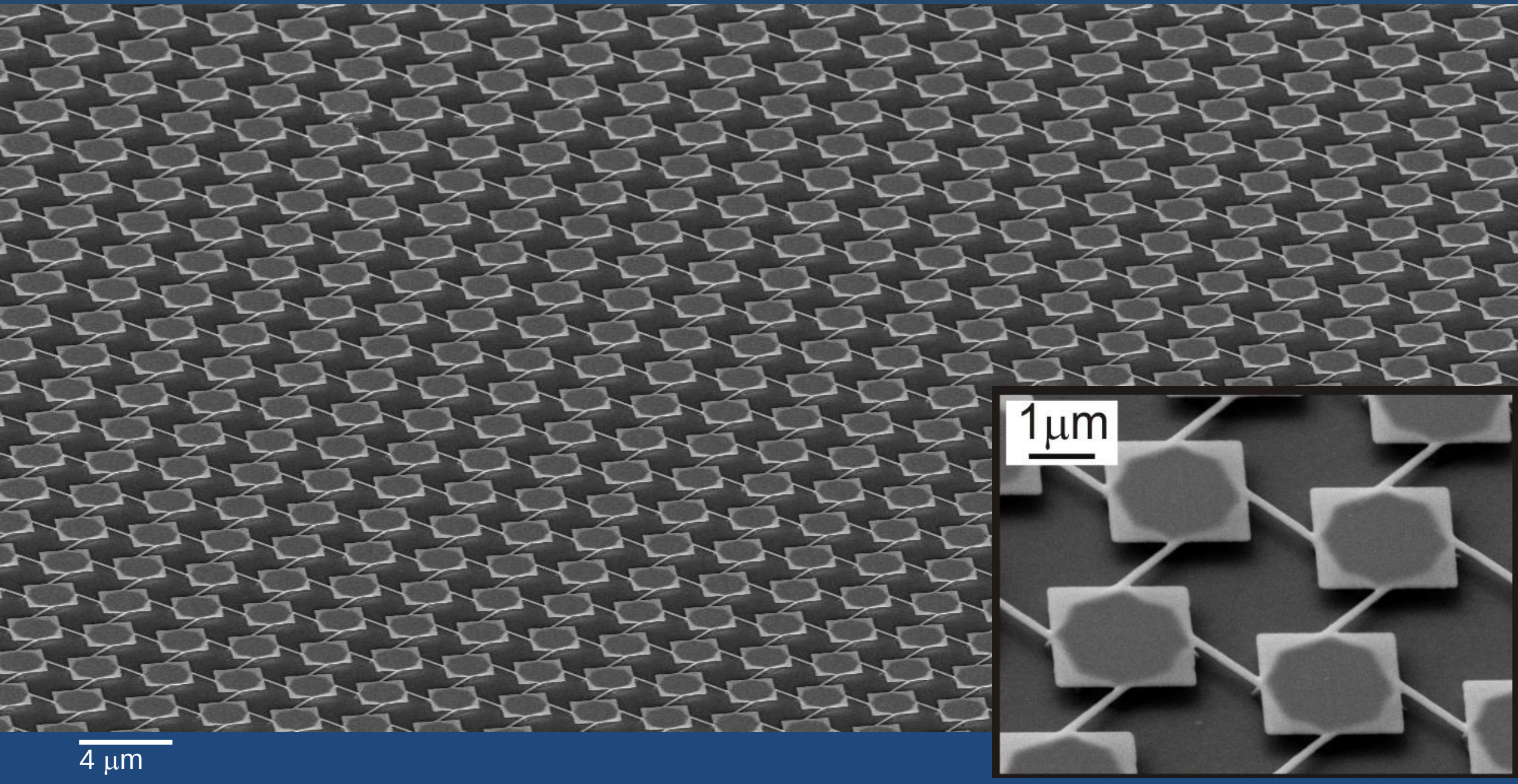

Test platform for nano-mechanical characterization

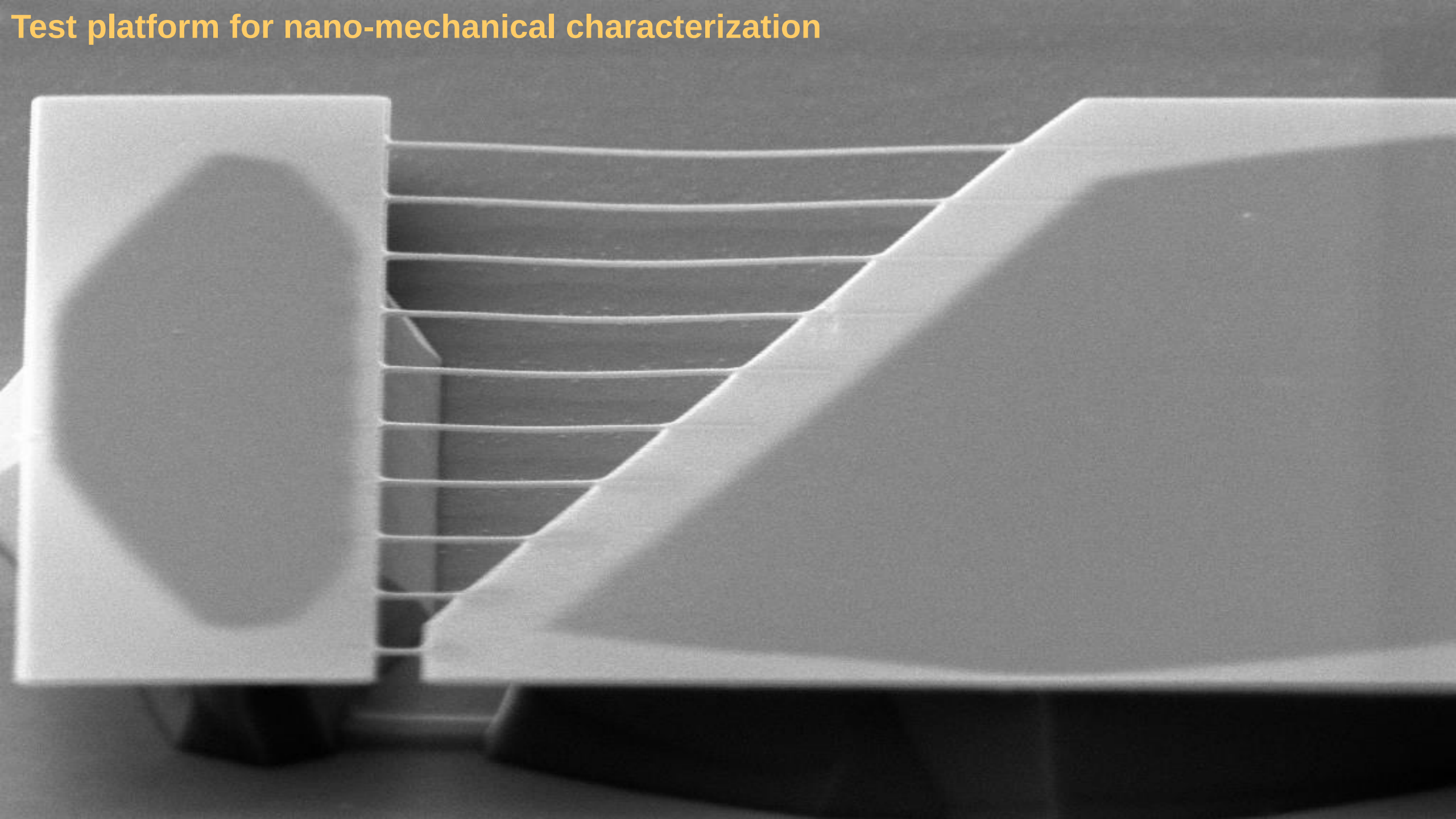

Array of nanowires

Diameter: 25 nm

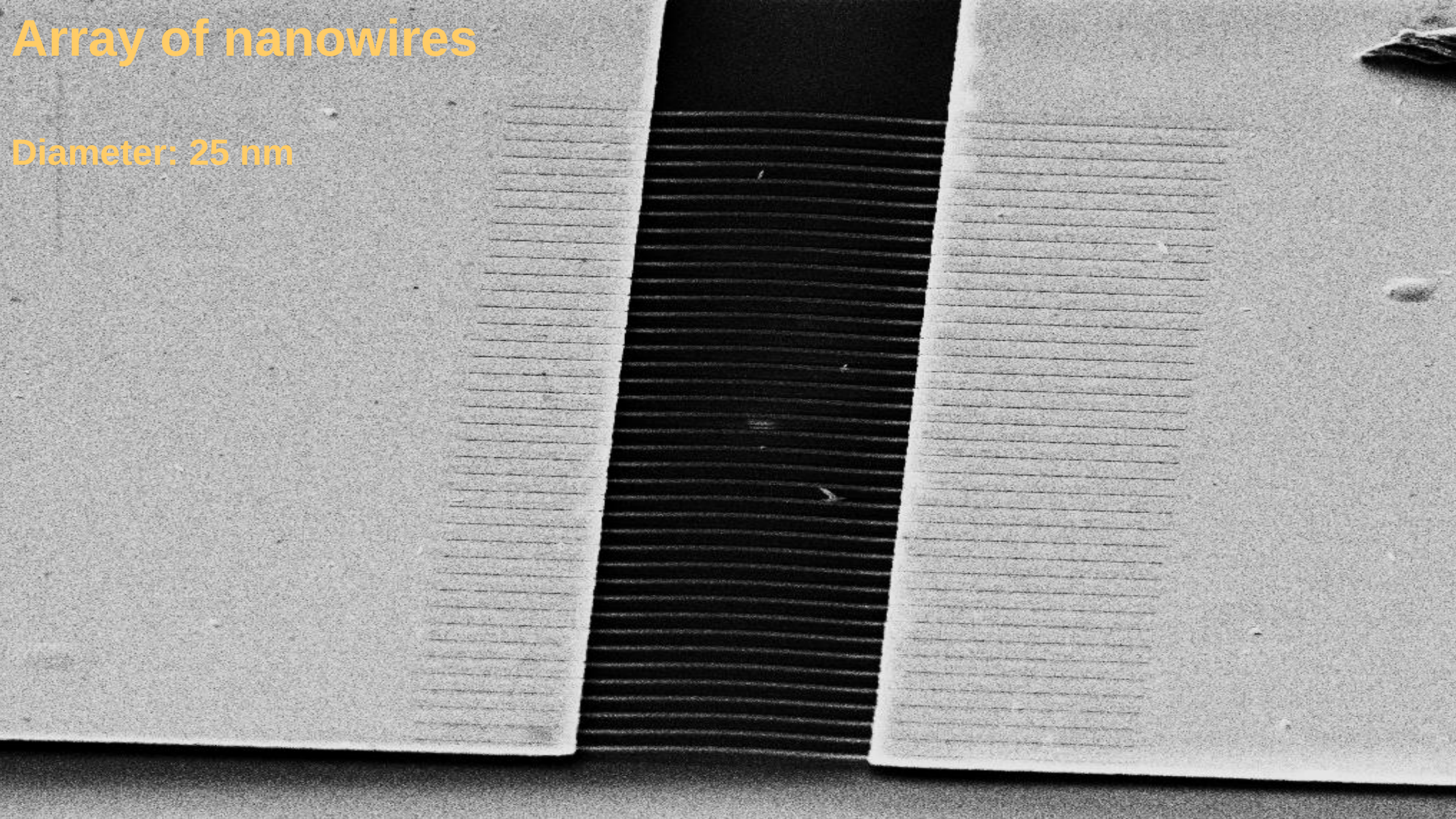

Coupled nanomechanical structures

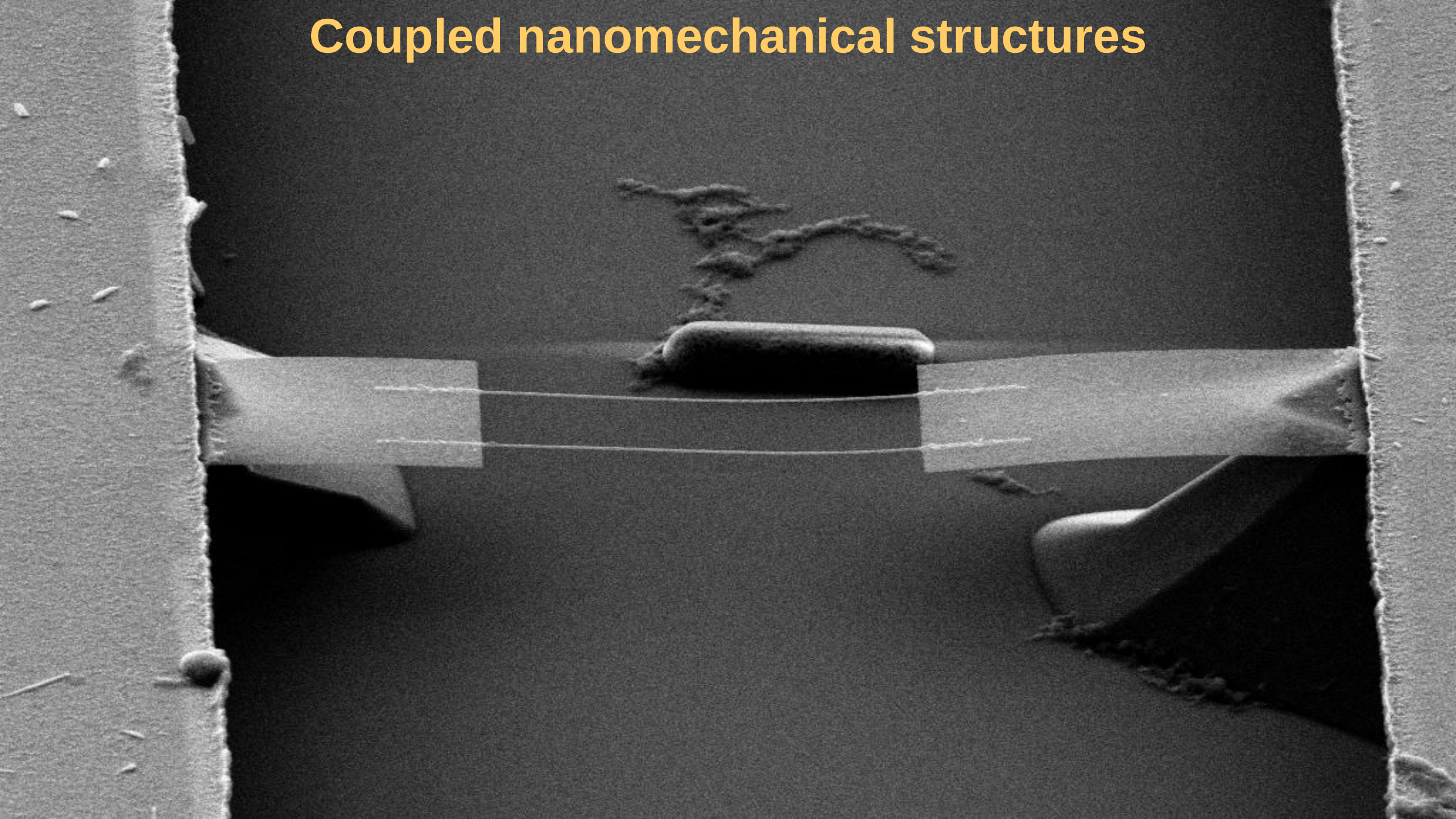

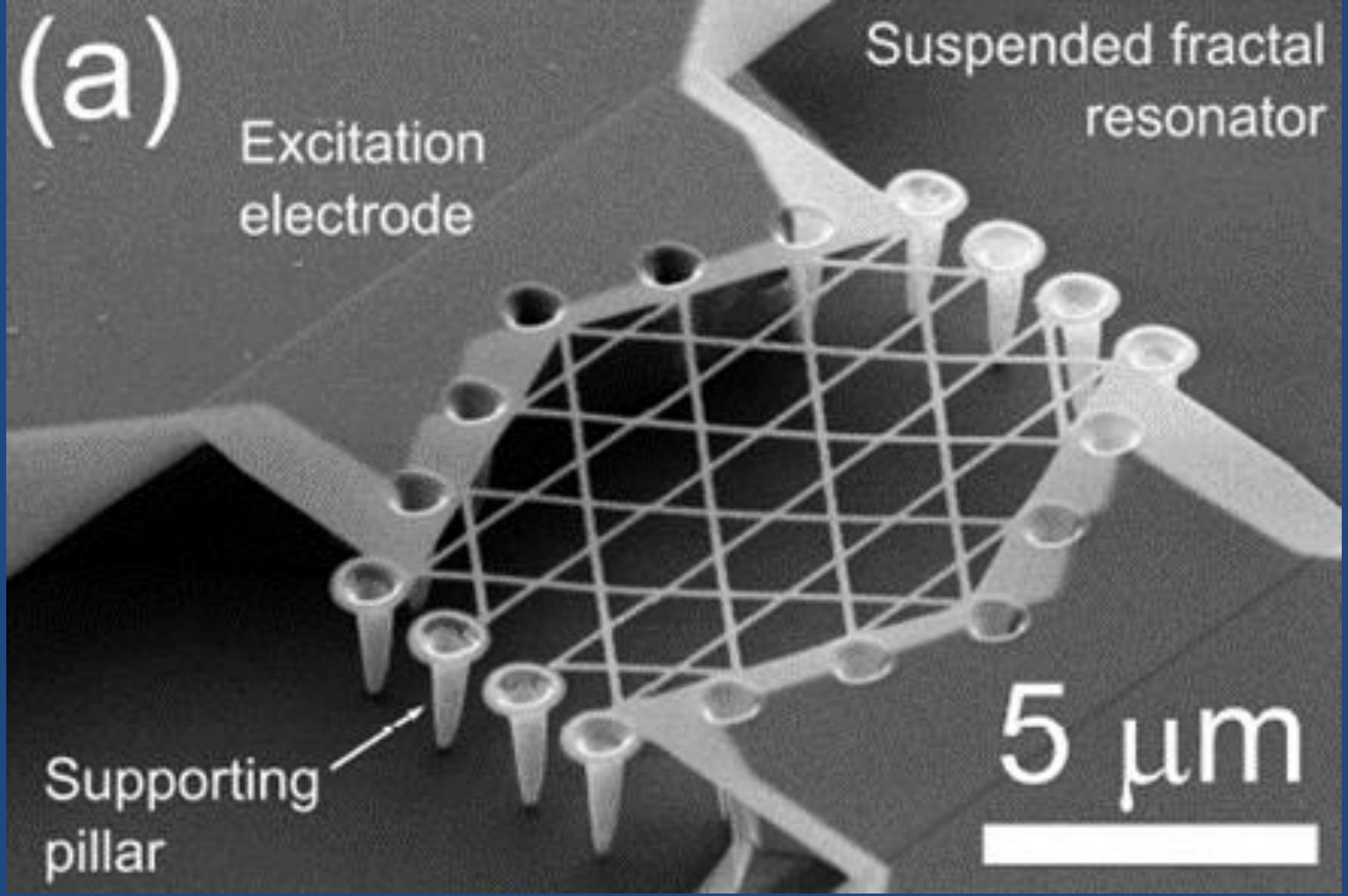
(a)
Excitation electrode
Suspended fractal resonator
Supporting pillar
5 μm

Ion beam implantation for NEMS

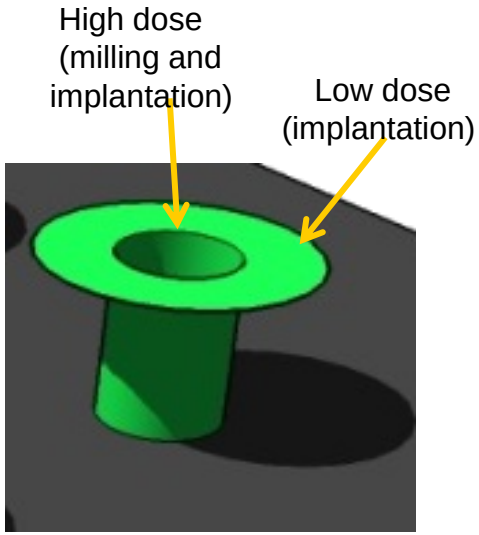

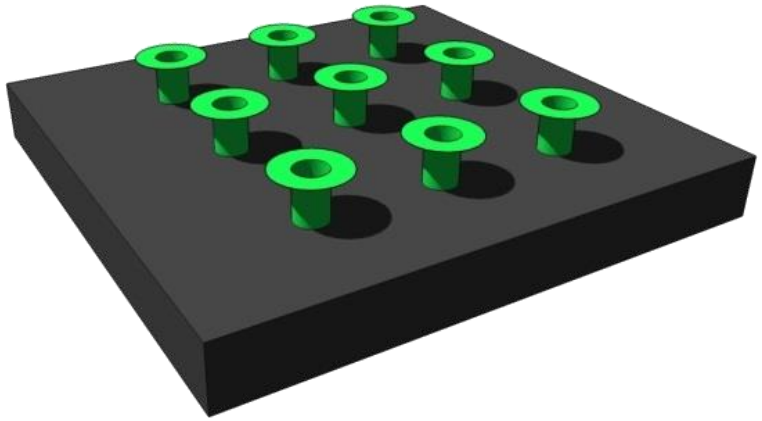

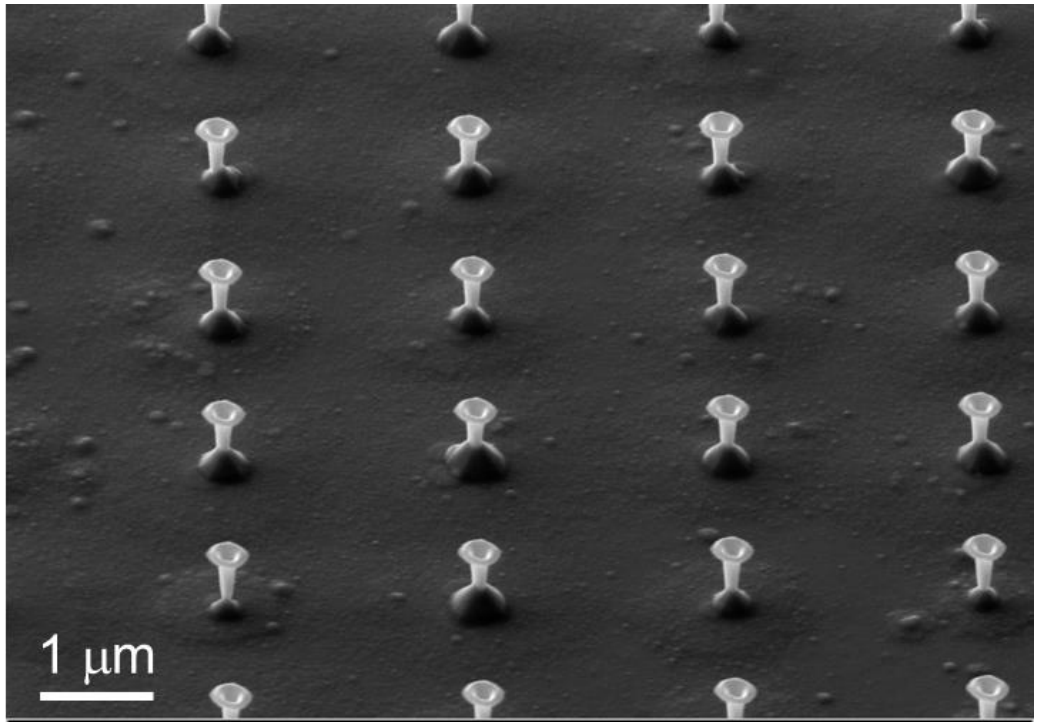

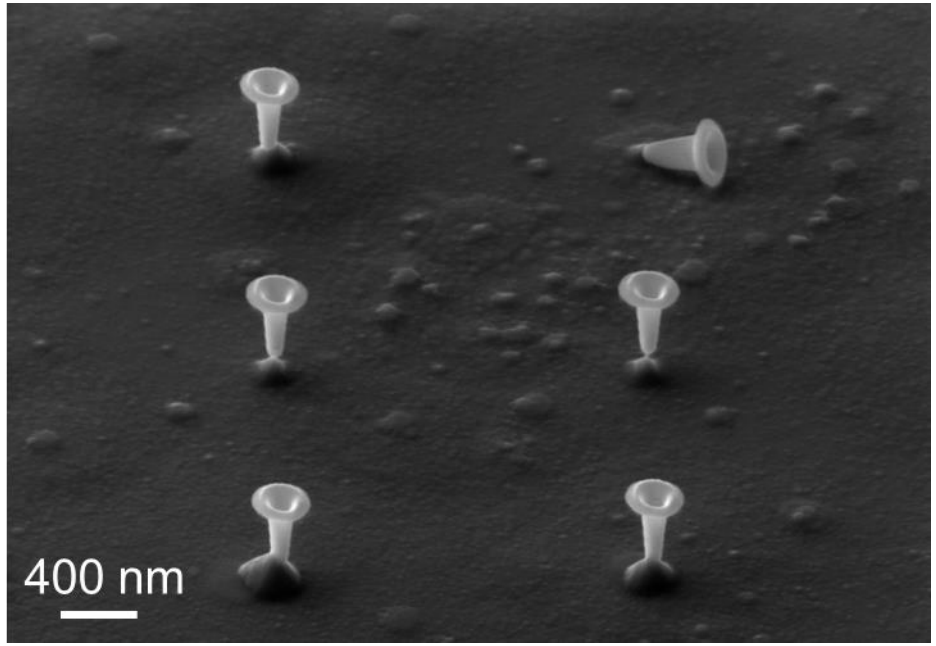

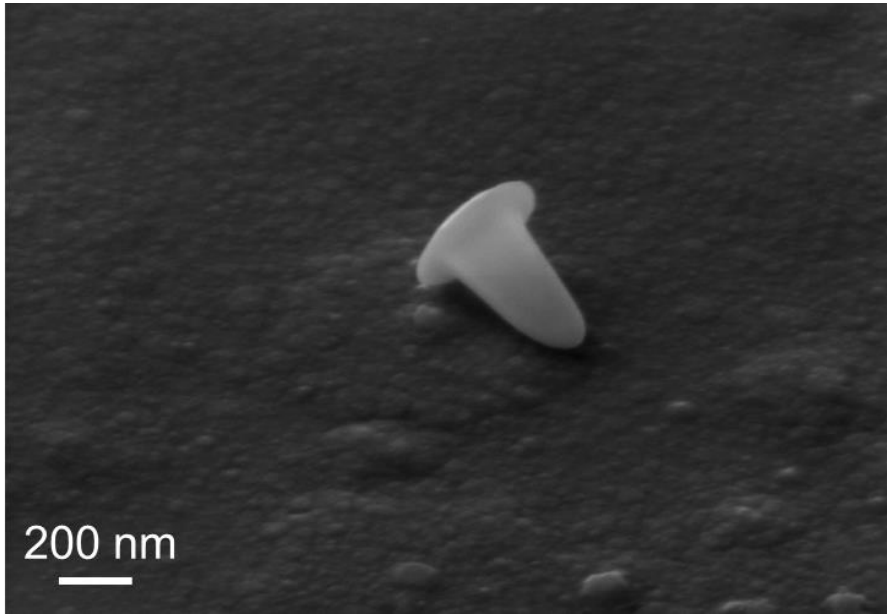

Ion beam implantation for NEMS

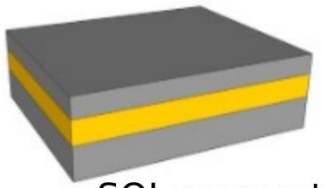

SOI preparation

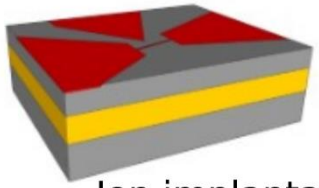

Ion implantation

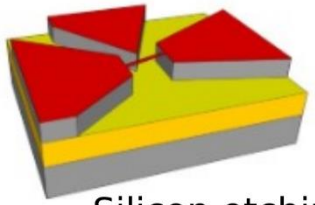

Silicon etching

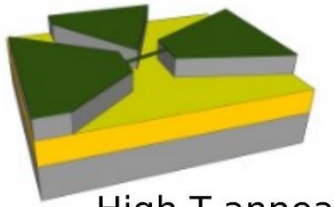

High T annealing

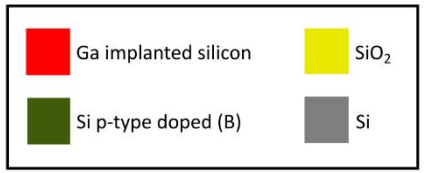

Effect of annealing:

- **Recovery of crystallinity**
- **Activation of electrical conductivity**

Recovering crystallinity

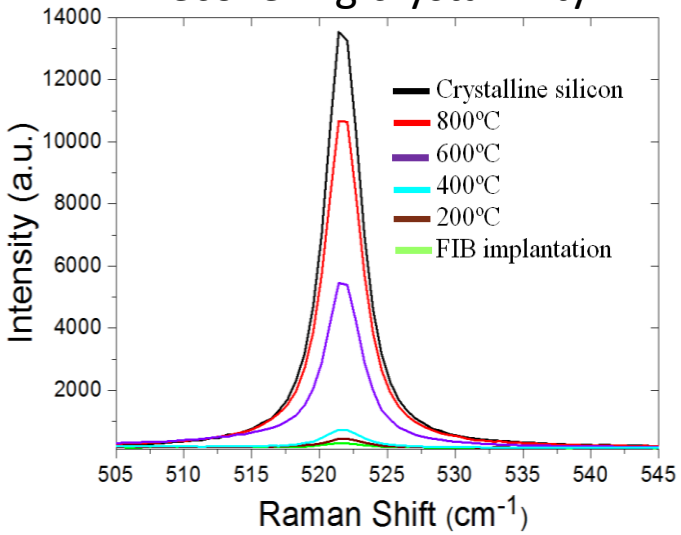

Out-diffusion of gallium

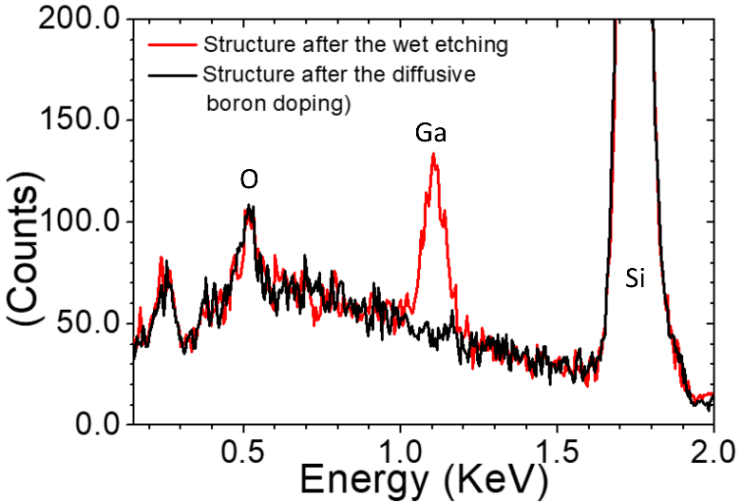

Recovering conductivity

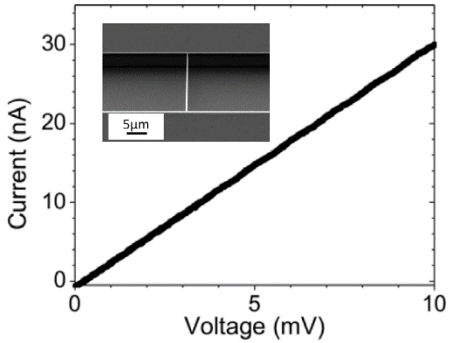

Before annealing:
$\rho = 3.11\ \Omega\cdot m$

↓

After annealing:
$\rho = 3.4\cdot10^{-4}\ \Omega\cdot m$

- J Llobet, M Sansa, M Gerbolés, N Mestres, J Arbiol, X Borrisé, F Pérez-Murano *Nanotechnology* 25, 135302 (2014)
- J Llobet, M Gerbolés, M Sansa, J Bausells, X Borrisé, F Pérez-Murano *J. Micro/Nanolith. MEMS MOEMS* 14, 031207 (2015)
- J Llobet, G Rius, A Chuquitarqui, X Borrisé, R Koops, M van Veghel, F Perez-Murano *Nanotechnology* 29, 155303 (2018)

Ion beam implantation for NEMS

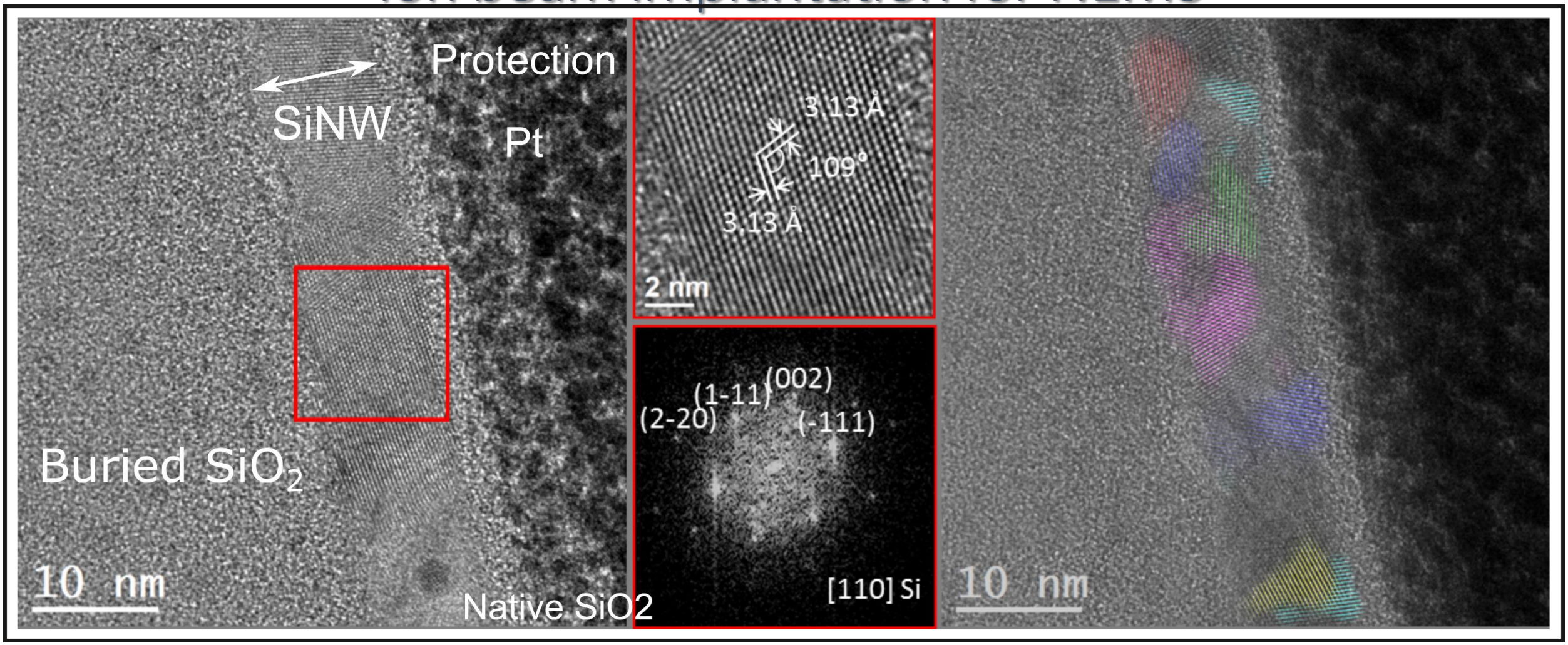

Annealing in N2 environment promotes:

- Elimination of gallium
- Re-crystallization of silicon (nanocrystals)

- J. Llobet 2016. 'Focused ion beam implantation as a tool for the fabrication of nano electromechanical devices.' PhD thesis. Universitat Autònoma de Barcelona
- In collaboration with J. Arbiol

Ion beam implantation for NEMS

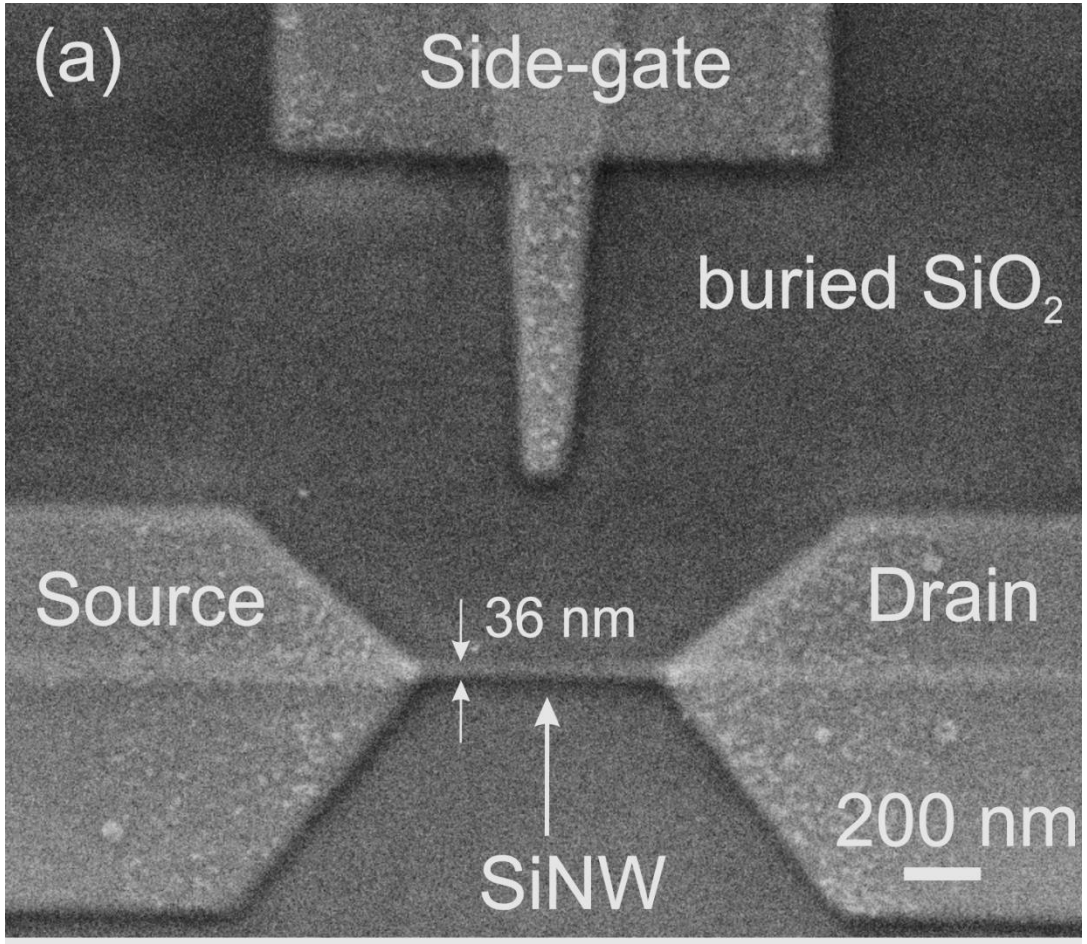

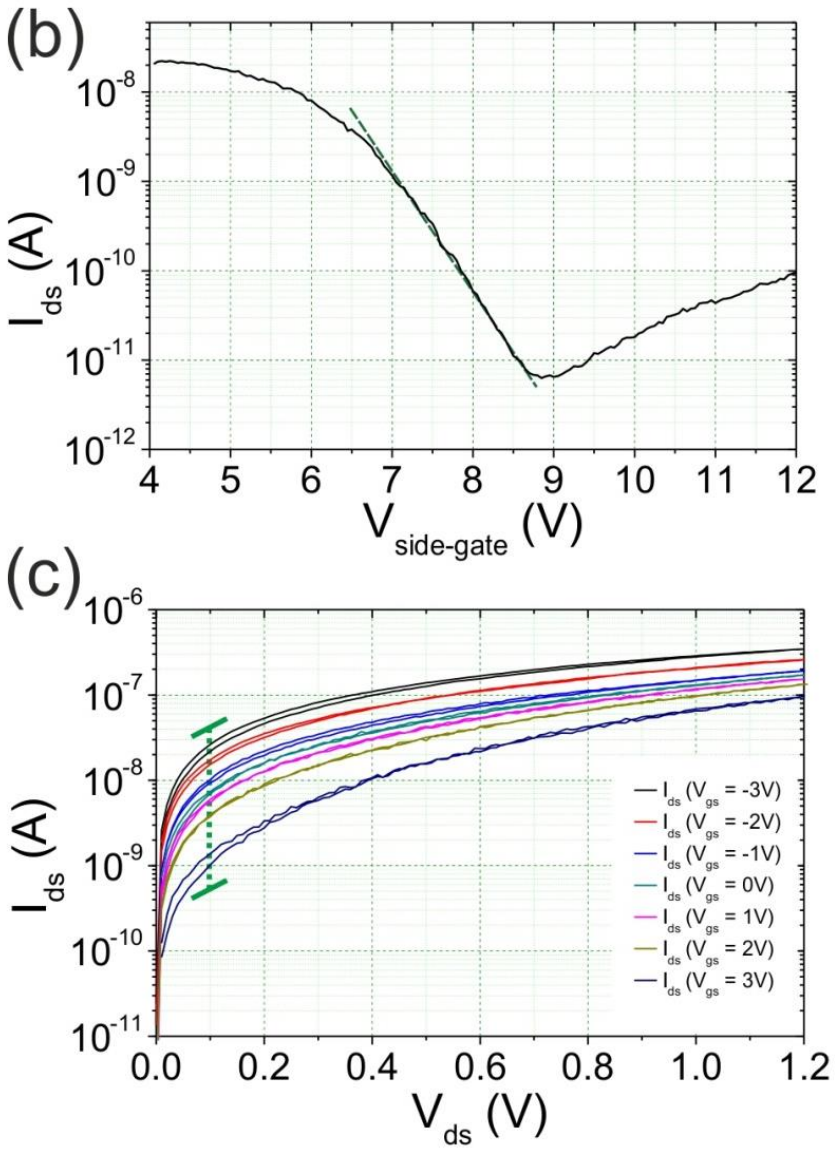

Ion beam implantation for NEMS

Integration of QDs into a SiNW (SET/SHoT)

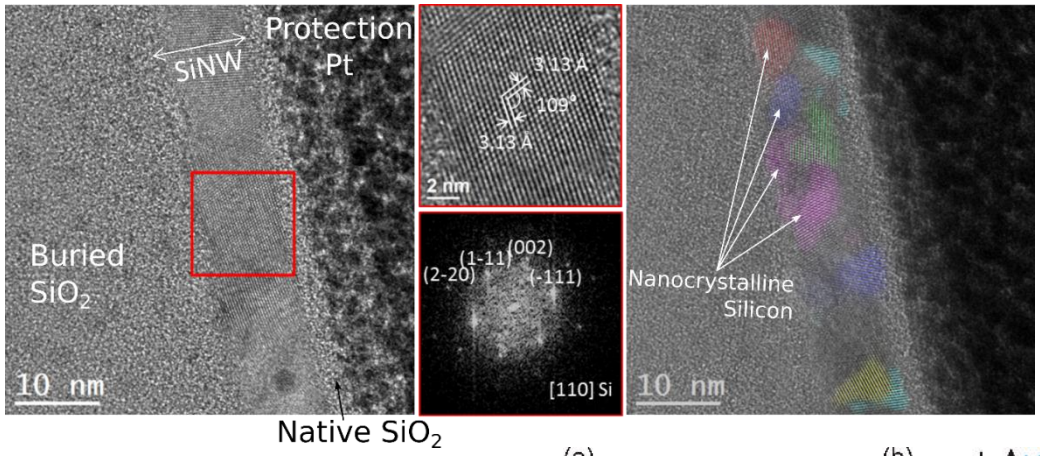

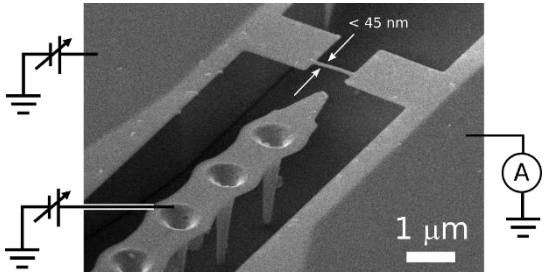

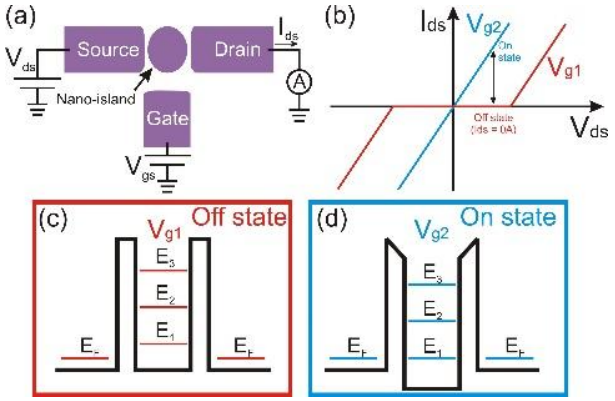

Durrani, Z.A.K. Single-electron devices and circuits in silicon, Imperial College Press, London 2010

1. Gate capacitance:

$C_G = e/(V_{Gu} - V_{Gw}) = 0.023$ aF

2. Total QD capacitance:

$|V_{Dv}| = |V_{Dx}| = e/C_T = 0.053$ V

$\Rightarrow C_T = C_1 + C_2 + C_G = 3$ aF

3. Tunnel capacitances:

$V_{Dy} = e/(2C_2 + C_G) = 0.043$ V

$\Rightarrow C_2 = 1.85$ aF

$\Rightarrow C_1 = 1.13$ aF

4. Coulomb charging energy:

$E_C = e^2/2C_T = 27$ meV

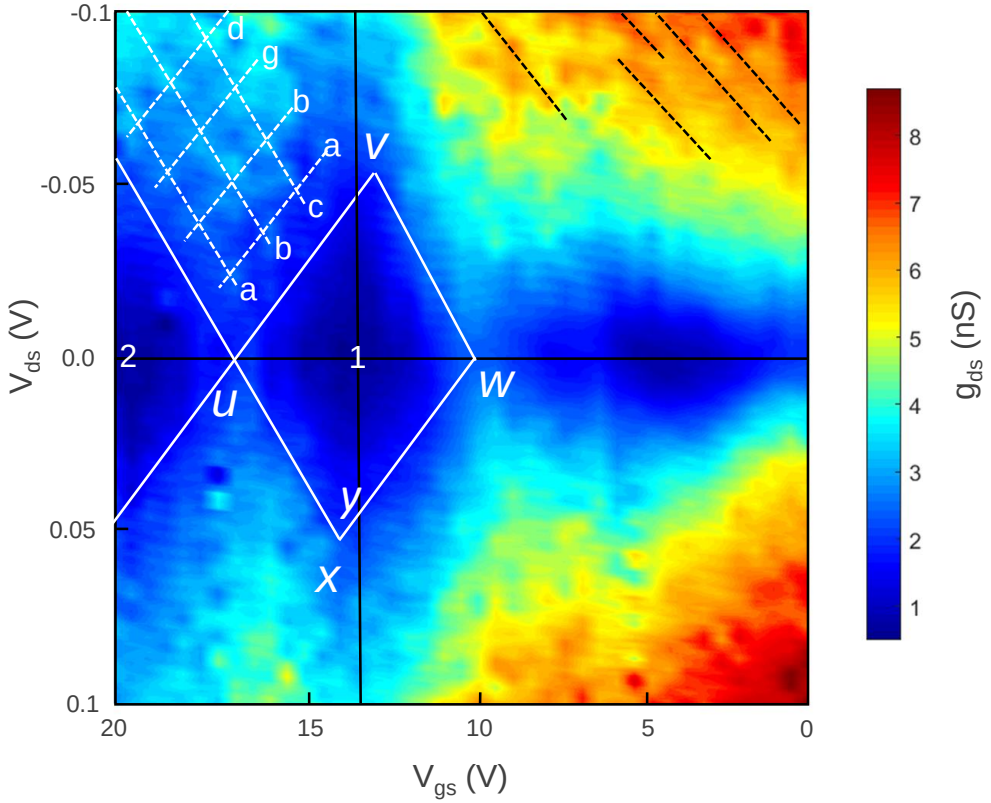

Ion implantation for creating nanoelectronic devices

- Self-assembly of quantum dots

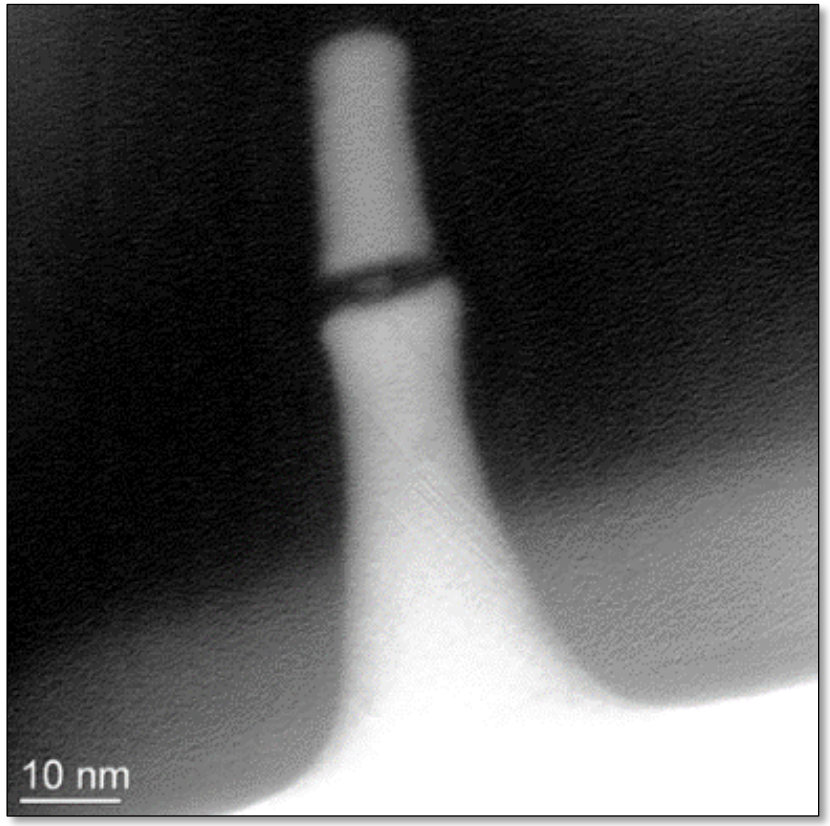

- Deterministic dopant implantation

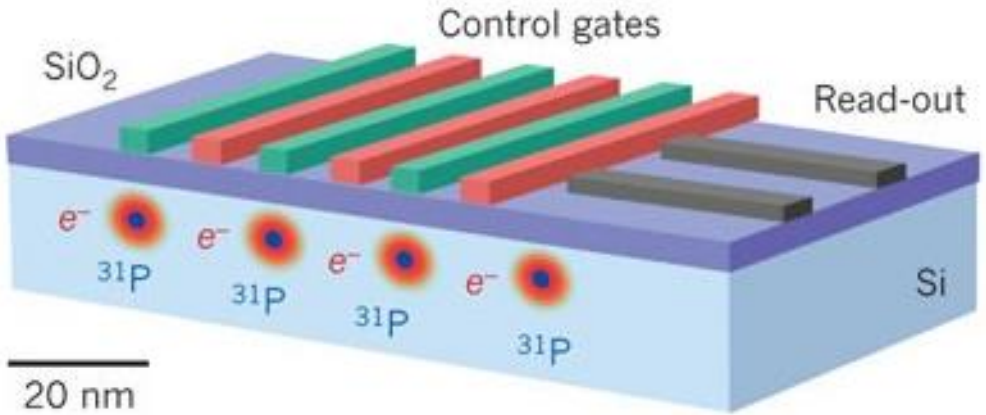

Ion implantation for creating nanoelectronic devices

Self-assembly of quantum dots

Si nanoclusters can be form from an excess Si in SiO_2:

- ion-induced mixing at a Si/SiO_2 interface,
- Subsequent thermal phase decomposition of the supersaturated oxide layer.

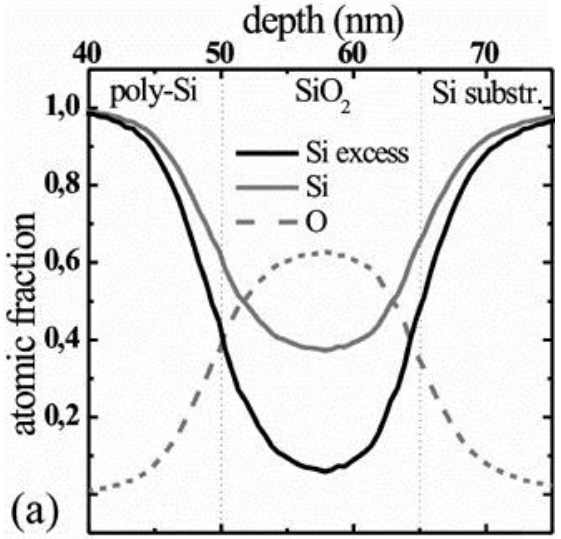

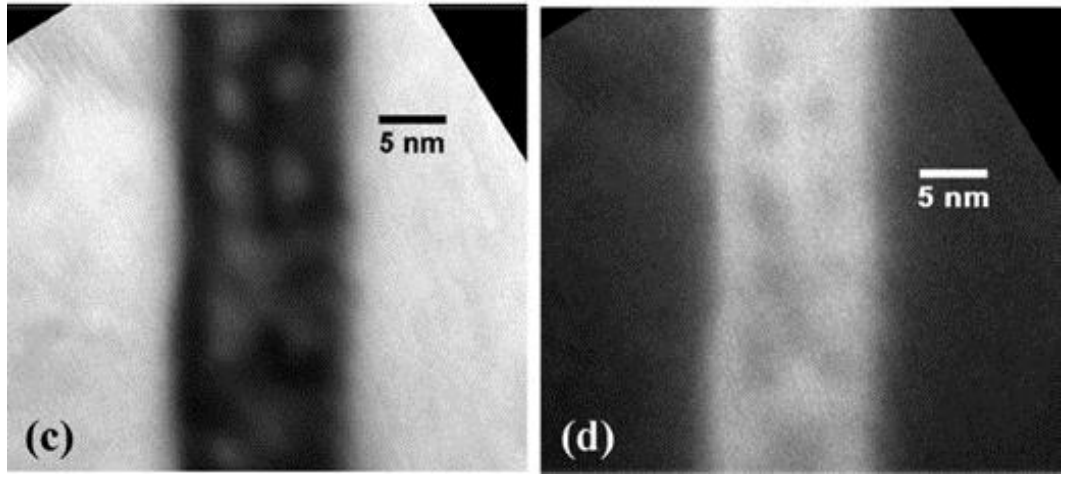

L. Rontzsch, K. H. Heinig, B. Schmidt, A. Mucklich, W. Moller, A. Thomas, and T. Gemming, Phys. Status Solidi A 202, R170 (2005). https://doi.org/10.1002/pssa.200521399

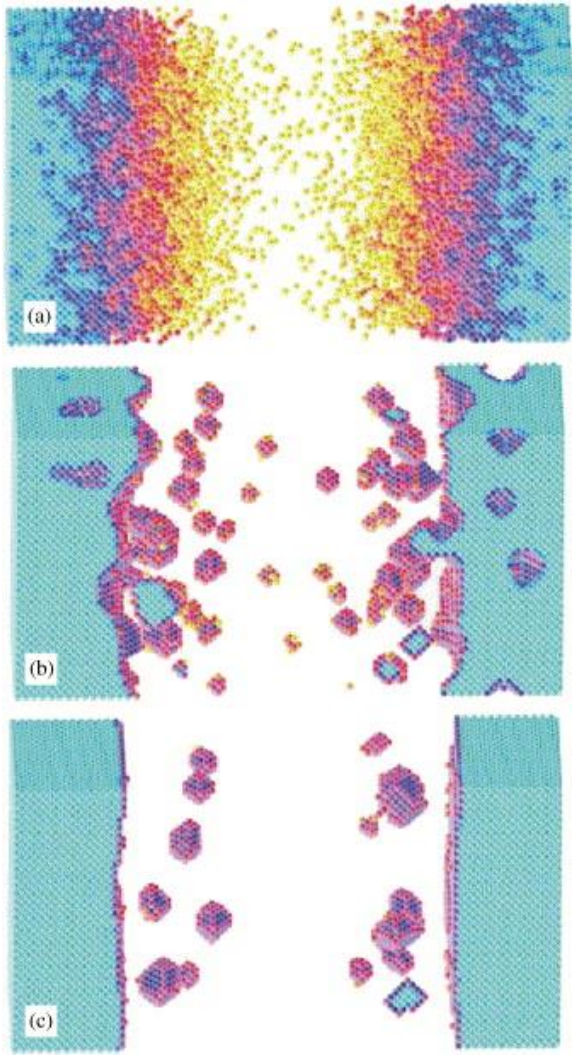

L. Rontzsch, K. H. Heinig, and B. Schmidt, Mater. Sci. Semicond. Process. **7**, 357 (2004). https://doi.org/10.1016/j.mssp.2004.09.098

Ion implantation for creating nanoelectronic devices

Self-assembly of quantum dots

Si NC formation after Si^+ irradiation of a-Si/SiO_2/c-Si layer stack and rapid thermal annealing at 1050 °C in a N_2 atmosphere

ion energy: 50 keV

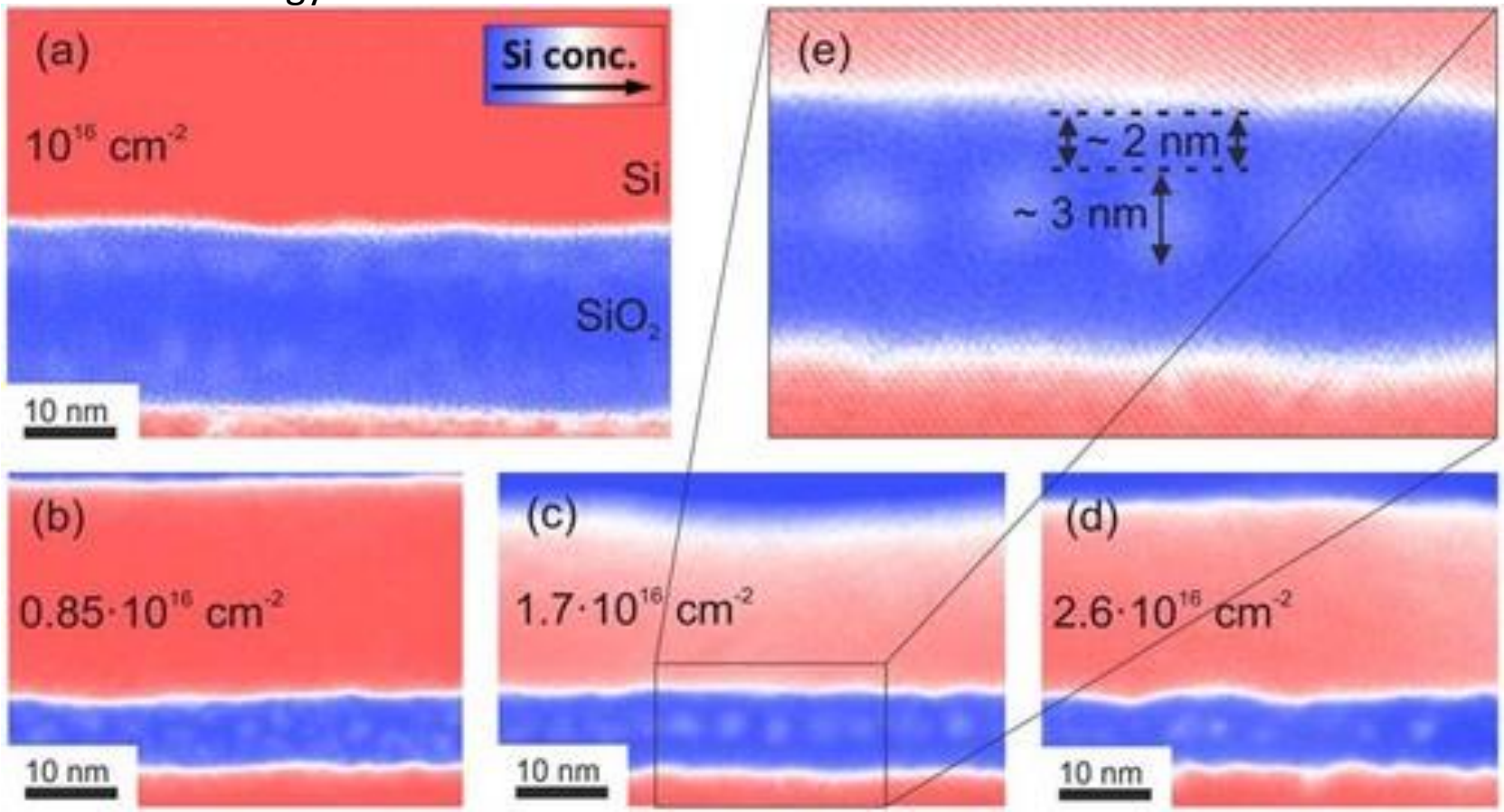

ion energy: 60 keV

(a) Top Si thickness 50 nm, oxide interlayer thickness 14 nm

(b)–(d) top Si thickness 30 nm, oxide interlayer thickness 7 nm

Prüfer, T., *et al.*, *Journal of Applied Physics*, *125*(22), 225708 (2019).

Ion implantation for creating nanoelectronic devices

Quantum dot single electron device

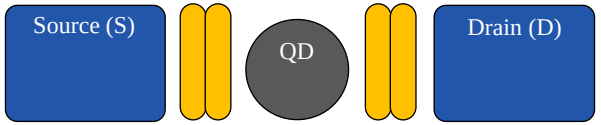

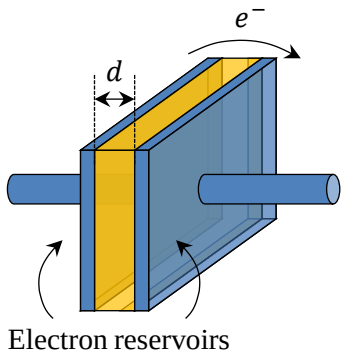

Coulomb blockade: quantization of electrical current given a low-capacitance tunnel junction. $W = \frac{Q^2}{2C}$

Discretization of the energy levels. By applying a bias voltage the energy levels can be shifted.

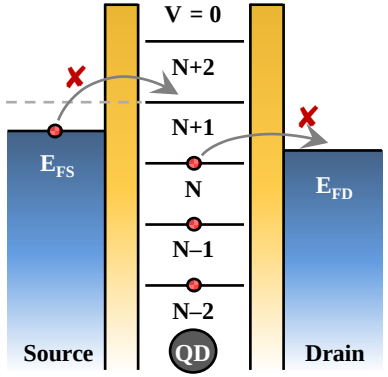

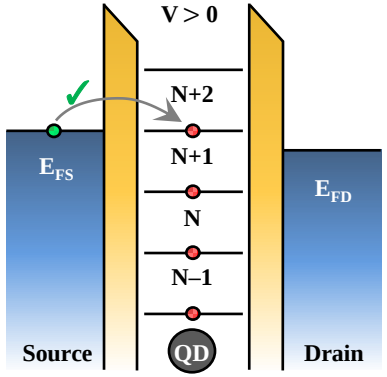

Quantum dot single electron transistor

Single Electron Transistor (SET) is a configuration based on a QD separated from tunnel reservoirs by tunnel junctions in which gate action is provided

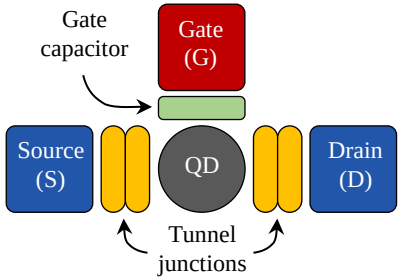

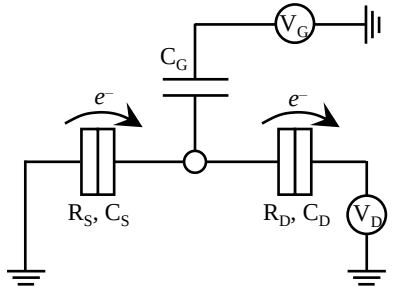

Charging current occurs at discrete voltage steps.

Gate bias shifts the charging energy levels of the QD.

Combination of Coulomb blockade with QD energy levels.

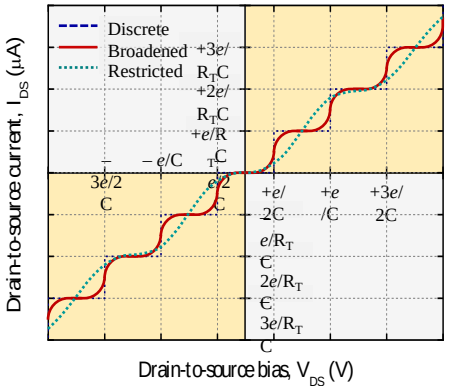

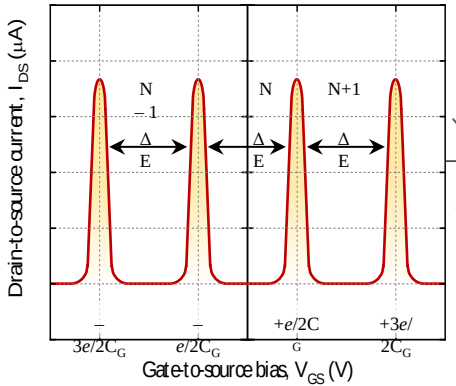

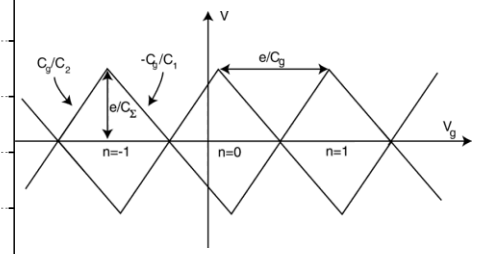

Ion implantation for creating nanoelectronic devices

Si NDs self assembly

Concept for Si NDs self-assembly

- **Si NDs irradiation is…**
  - a two-step process.
  - a self-assembly method.

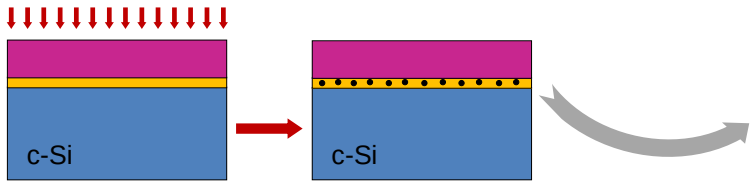

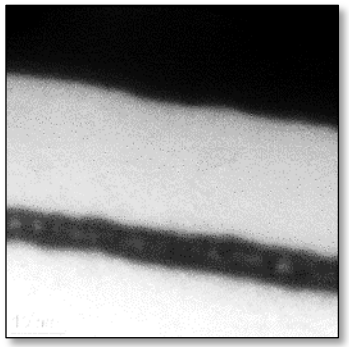

Ion irradiation

50 keV, 1.2×10^{16} Si^+/cm^{-2}

Interface mixing turns finite volumes of SiO_2 into a SiO_x metastable form

Rapid thermal annealing (RTA)

60s at 1050°C in N_2

Induces a phase separation ($SiO_x \rightarrow Si + SiO_2$)

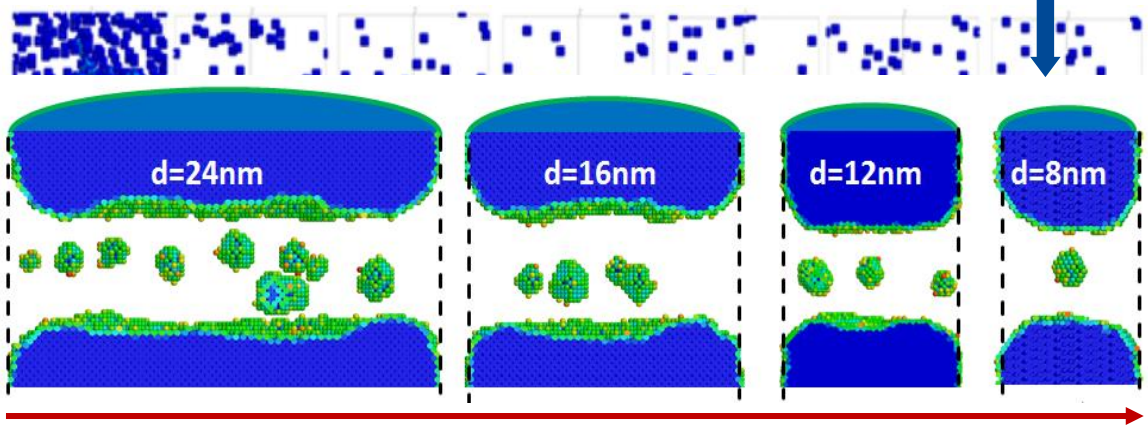

Annealing time

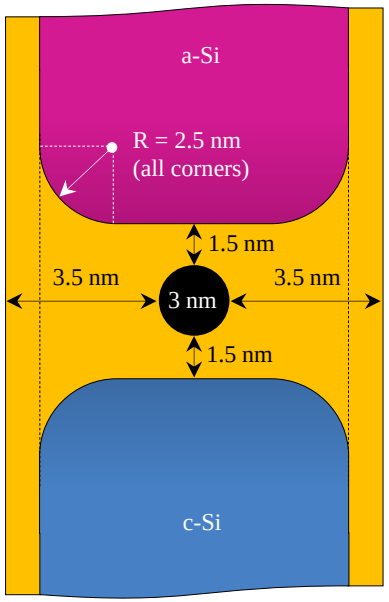

Prüfer, T., *et al.*, *Journal of Applied Physics*, *125*(22), 225708 (2019).

Ion implantation for creating nanoelectronic devices

Concept for Si NDs self-assembly

- **The ions4SET proposal…**

Vertical SET, CMOS compatible, room temperature and scalable.

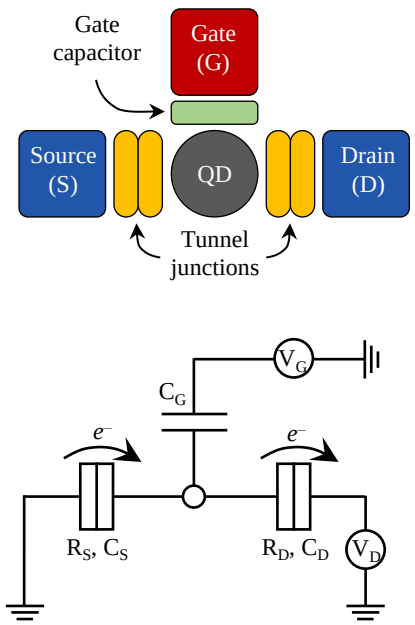

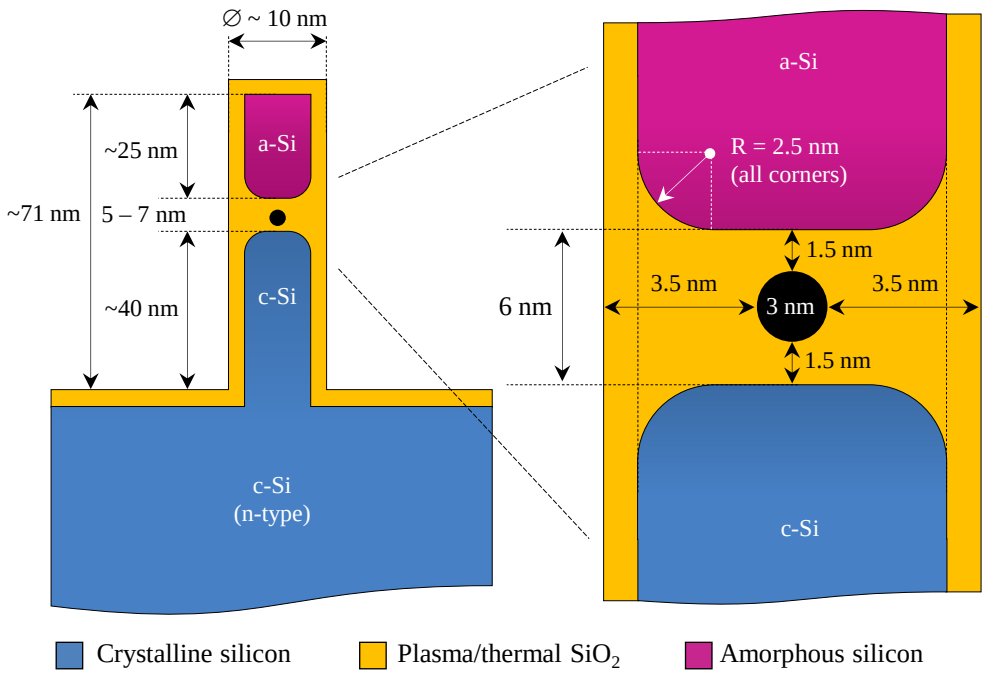

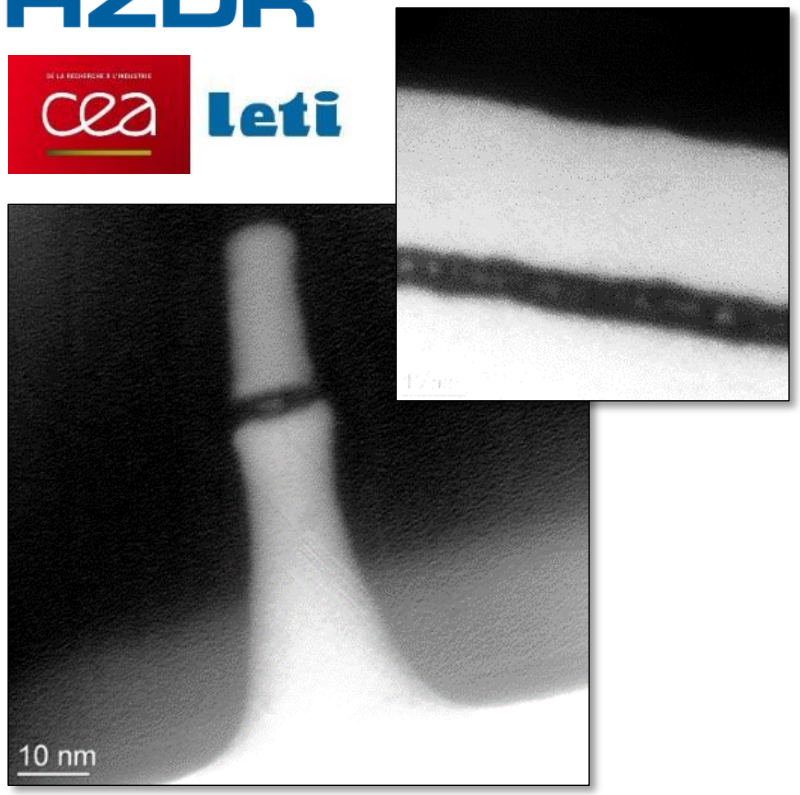

Pourteau, M. L., et al. (2020). *Micro and Nano Engineering*, *9*, 100074.

Ion implantation for creating nanoelectronic devices

Fabrication of pillars

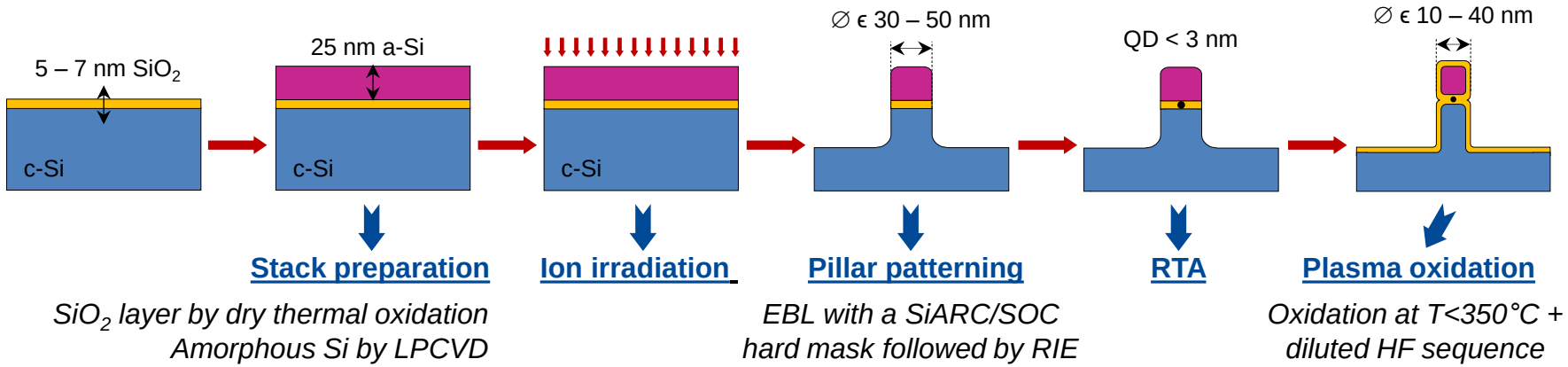

SiO_2 layer by dry thermal oxidation
Amorphous Si by LPCVD

EBL with a SiARC/SOC
hard mask followed by RIE

Oxidation at T<350°C +
diluted HF sequence

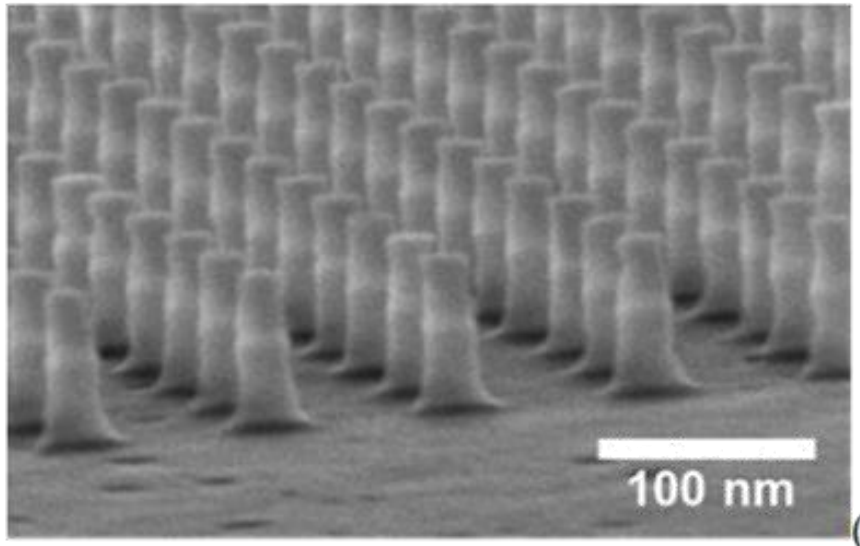

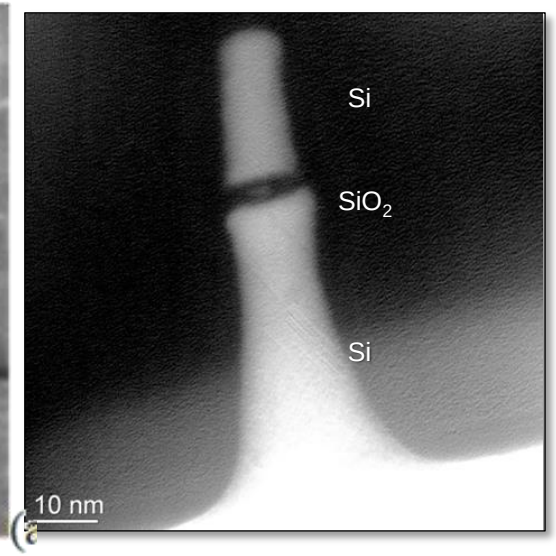

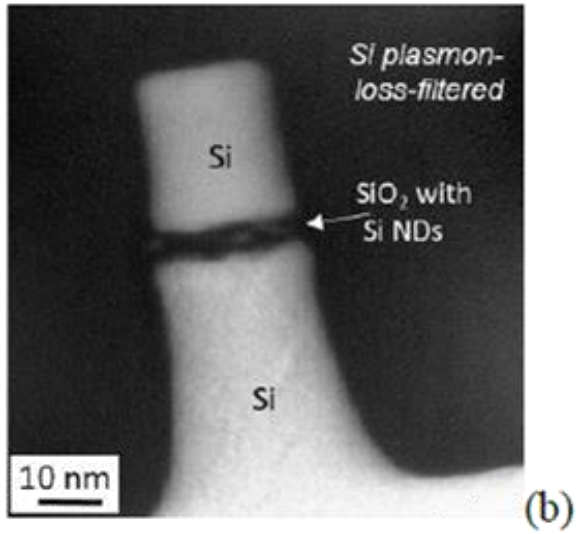

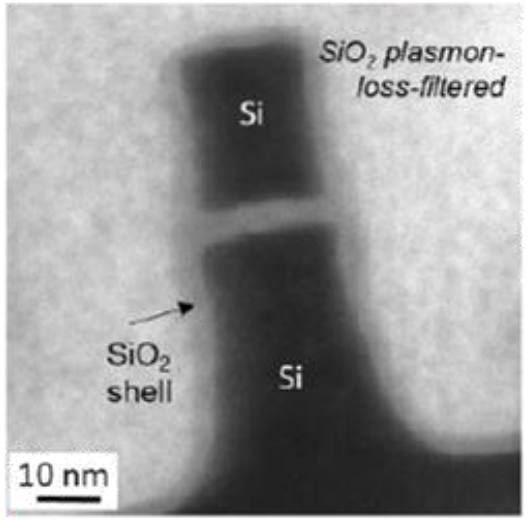

Von Borany et al. Submitted to SST.

Ion implantation for creating nanoelectronic devices

Vertical SET integration

Contacting of pillars

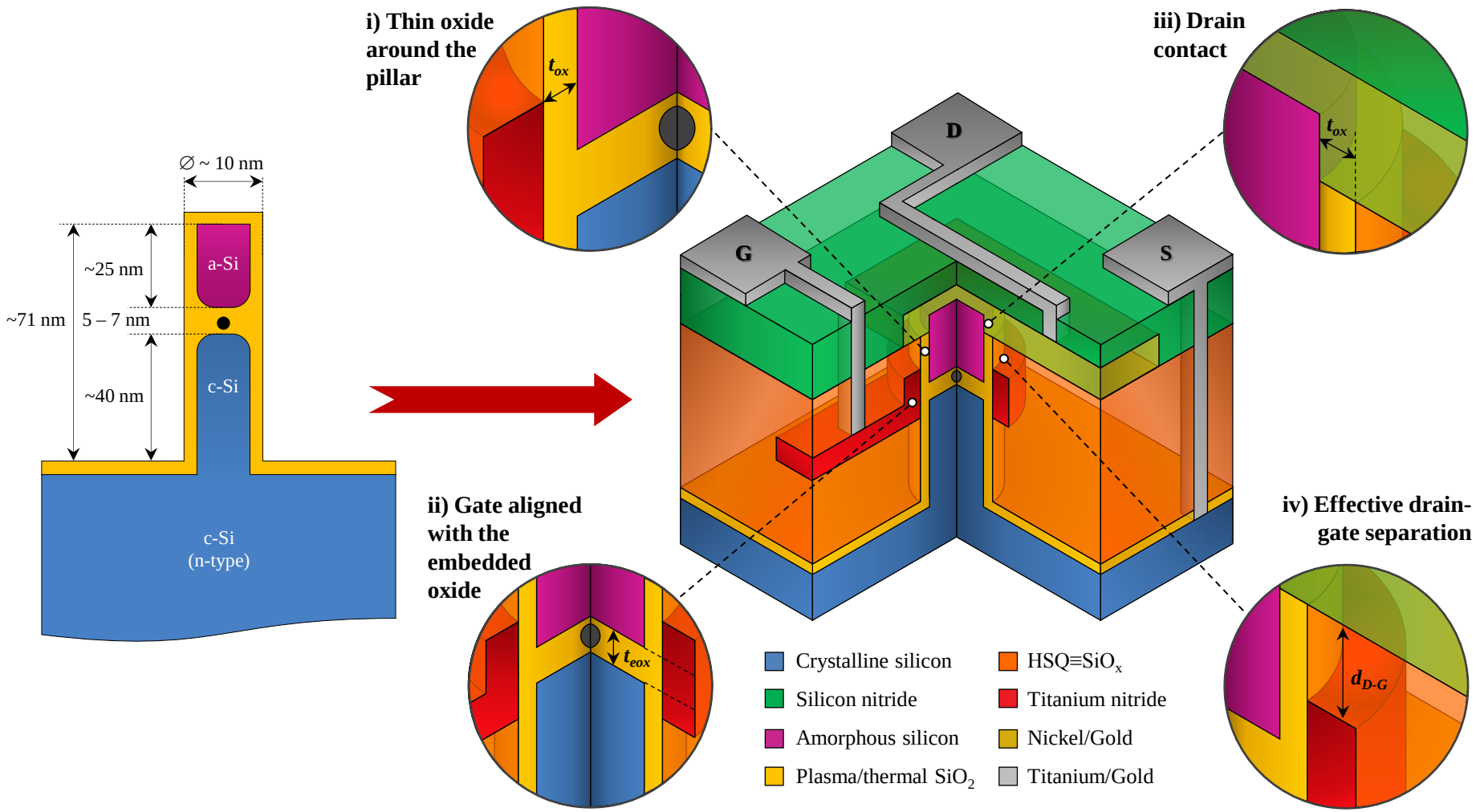

Ion implantation for creating nanoelectronic de

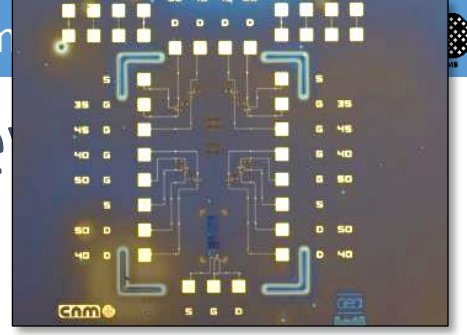

Vertical SET integration

Concept for Si NDs self-assembly

ions4SET

- Design, optimization and development of a complete technological process: more than 40 individual steps

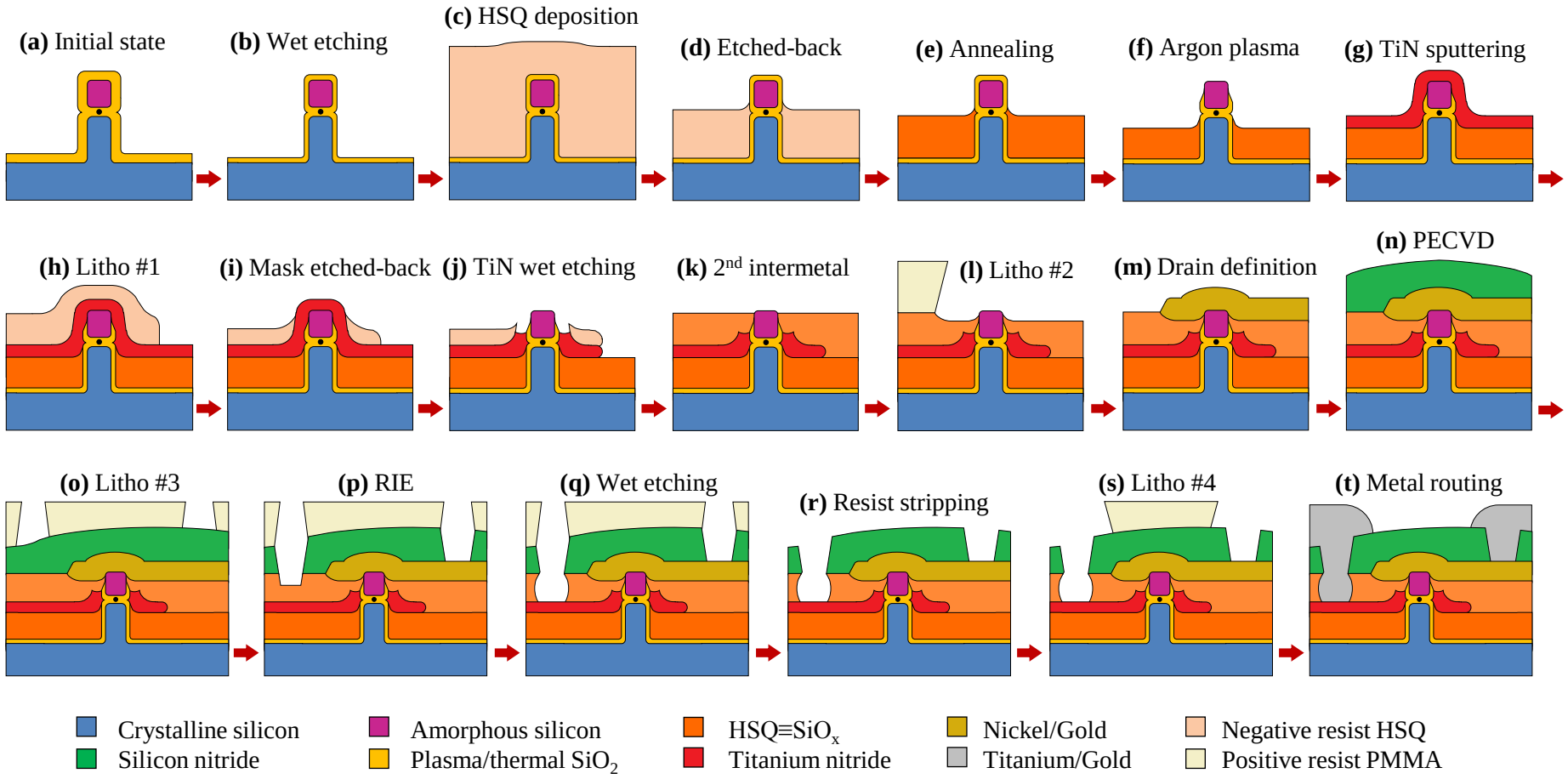

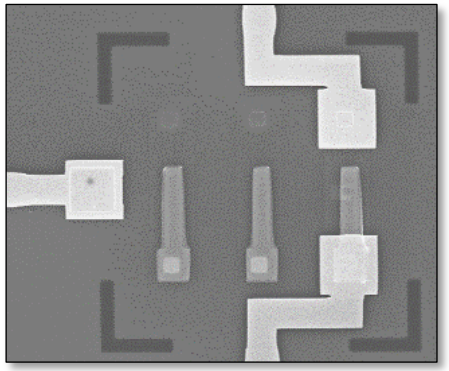

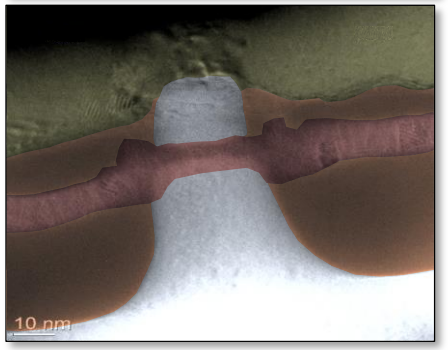

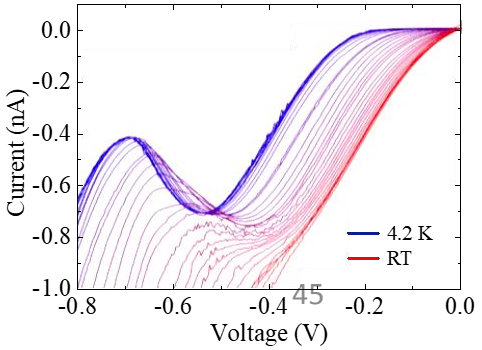

A del Moral et al. Submitted to SST

Ion implantation for creating nanoelectronic devices

Si quantum technologies

Donor based qubit

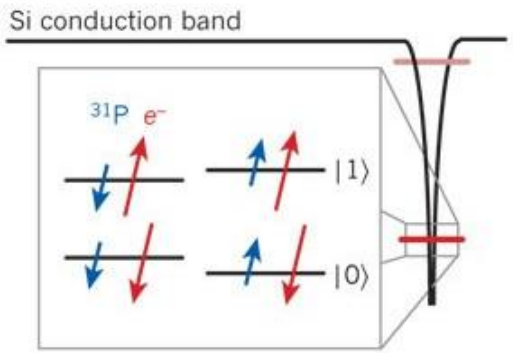

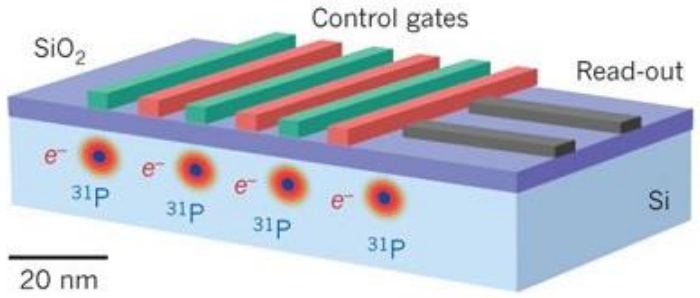

Morton JJL, McCamey DR, Eriksson MA, Lyon SA.
Nature 479, 345–353. (2011)

STM lithography

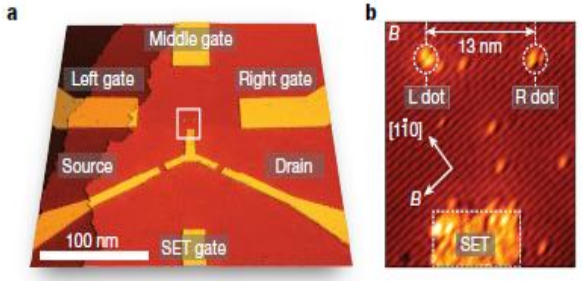

Y He et al.
Nature 571, 371-375 (2019)

Localized implantation

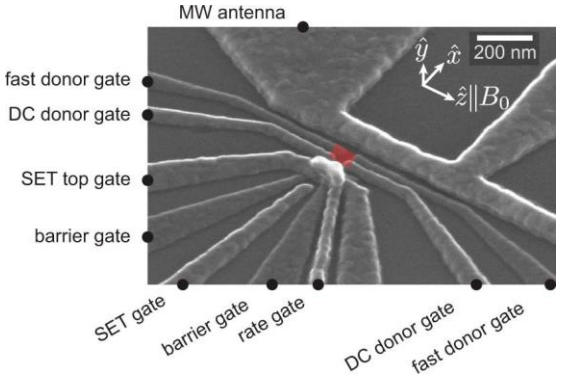

Mądzik, M.T et al.
Nature 601, 348–353 (2022)

Electrostatic quantum dot qubit

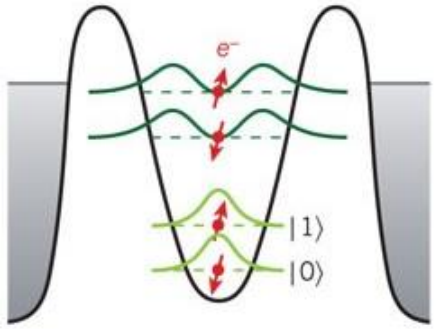

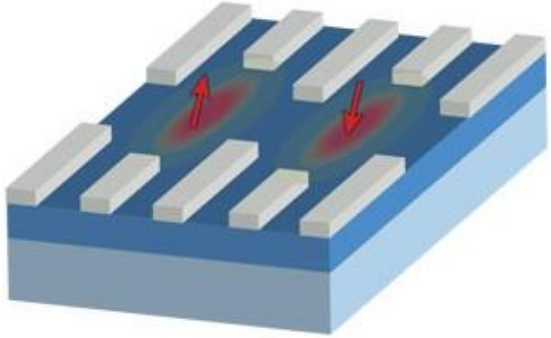

Morton JJL, McCamey DR, Eriksson MA, Lyon SA.
Nature 479, 345–353. (2011)

Quantum dots in Si/SiGe

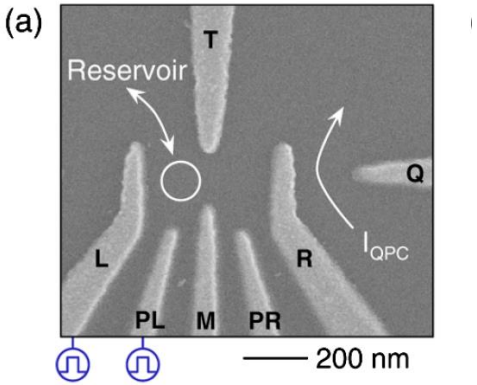

C. B. Simmon et al. Phys. Rev. Lett. (2011)

Quantum dots in silicon nanowire

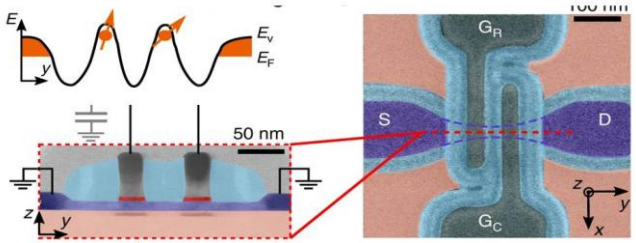

Crippa et a.
Nature communications, (2019)

Ion implantation for creating nanoelectronic devices

Donor based silicon qubits

Stocastic

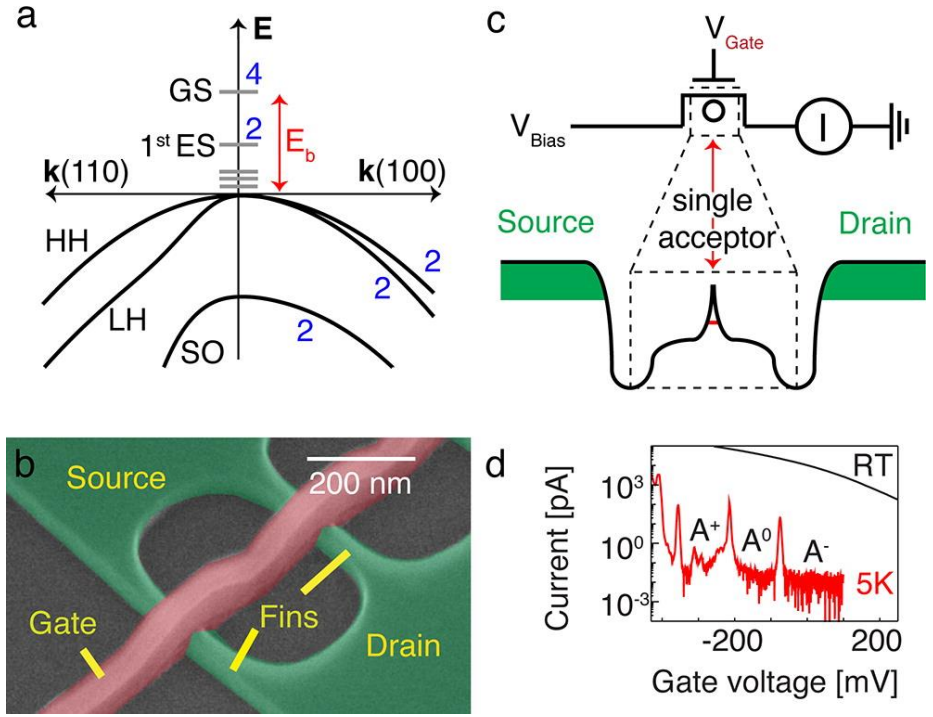

Not scalabe

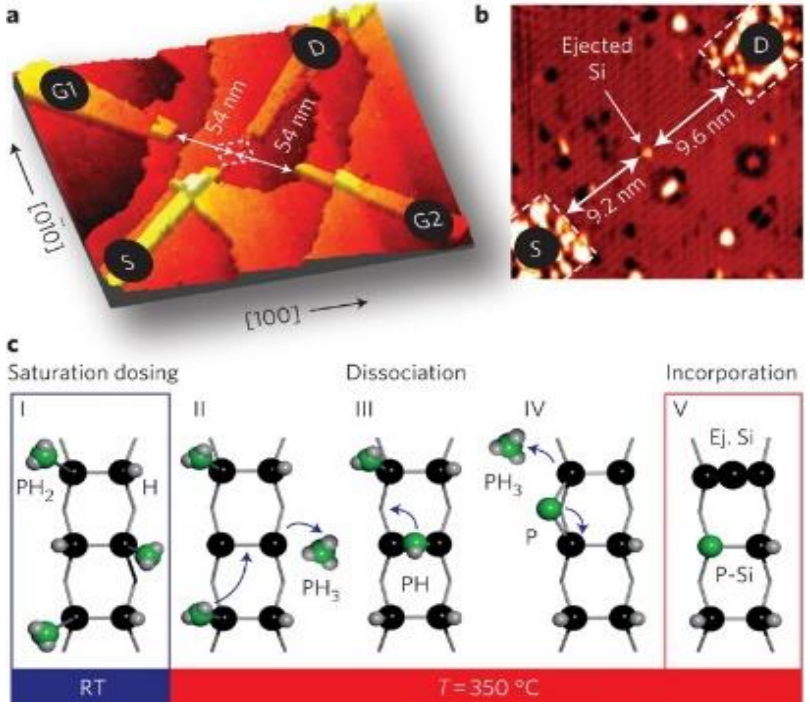

Van Der Heijden J, Salfi J, Mol JA, Verduijn J, Tettamanzi GC, Hamilton AR, et al. Probing the spin states of a single acceptor atom. Nano Lett 2014;14:1492–6. https://doi.org/10.1021/nl4047015.

Fuechsle M, …., Michelle Y. Simmons. A single-atom transistor. Nat Nanotechnol 2012;7:242–6. https://doi.org/10.1038/nnano.2012.21

Deterministic doping challenges: Positioning, Straggle, diffusion and statistics

Single Dopant Atom Lithography Tool

TECHNISCHE UNIVERSITÄT ILMENAU

Courtesy : nano analytik GmbH

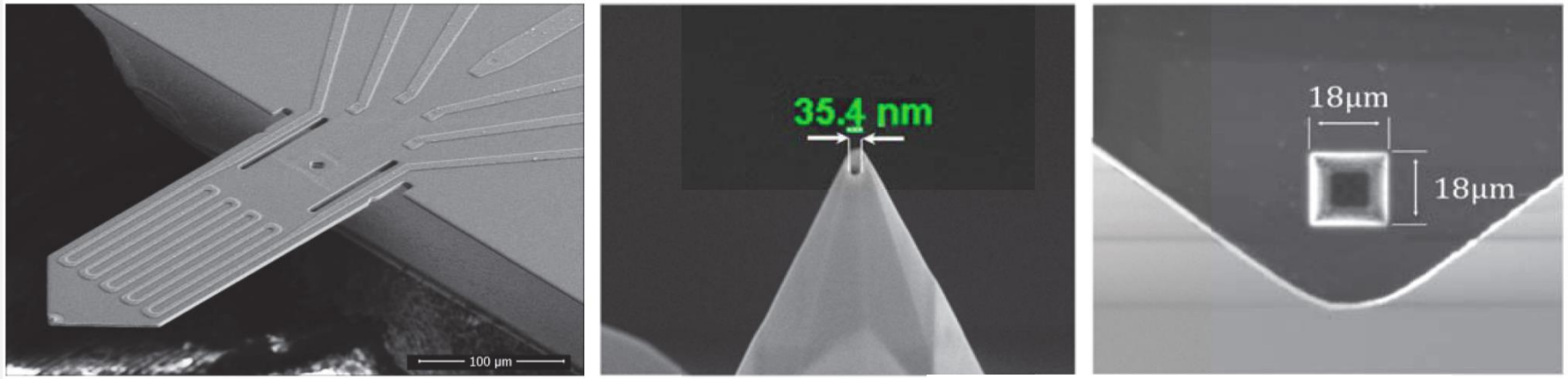

Towards the implanting of ions and positioning of nanoparticles with nm spatial resolution

[1] RUBION, Ruhr-Universität Bochum, 44780 Bochum, Germany
[2] Department of Micro- and Nanoelectronical Systems, Institute of Micro- and Nanoelectronics, Technical University of Ilmenau, PF 10 05 65, 98684 Ilmenau, Germany
[3] Institut für Verbrennung und Gasdynamik, Universität Duisburg-Essen, 47057 Duisburg, Germany
[4] 3. Physikalisches Institut, University Stuttgart, Pfaffenwaldring 57, 70550 Stuttgart, Germany
[5] Institut für Quanteninformationsverarbeitung, University Ulm, Albert-Einstein-Allee, 89069 Ulm, Germany

Appl. Phys. A 91, 567–571 (2008)

I.W. Rangelow
WEBINAR SERIES ON ADVANCED NANOFABRICATION (2020-2021)

Single Donor-Atom Lithography Lab

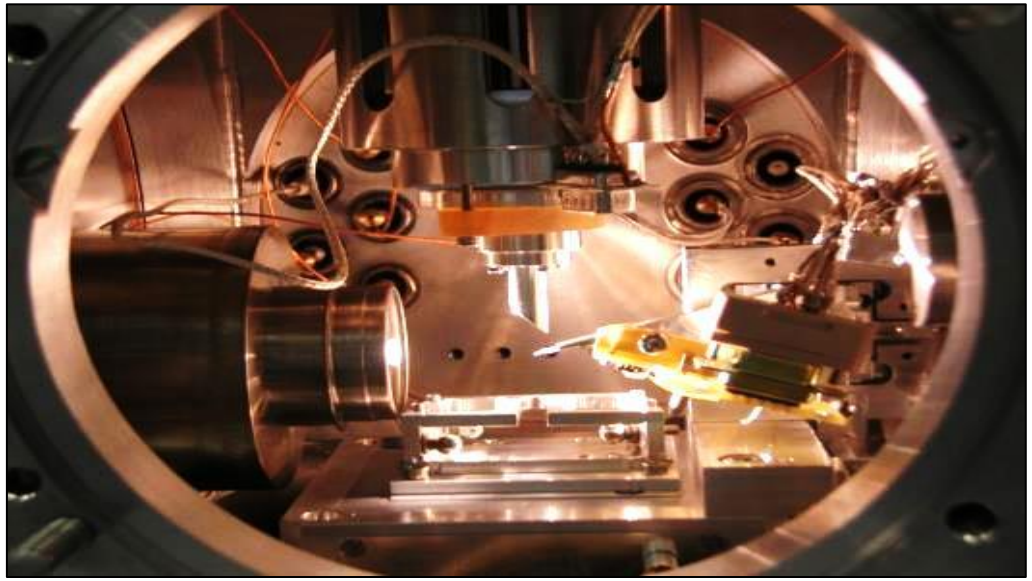

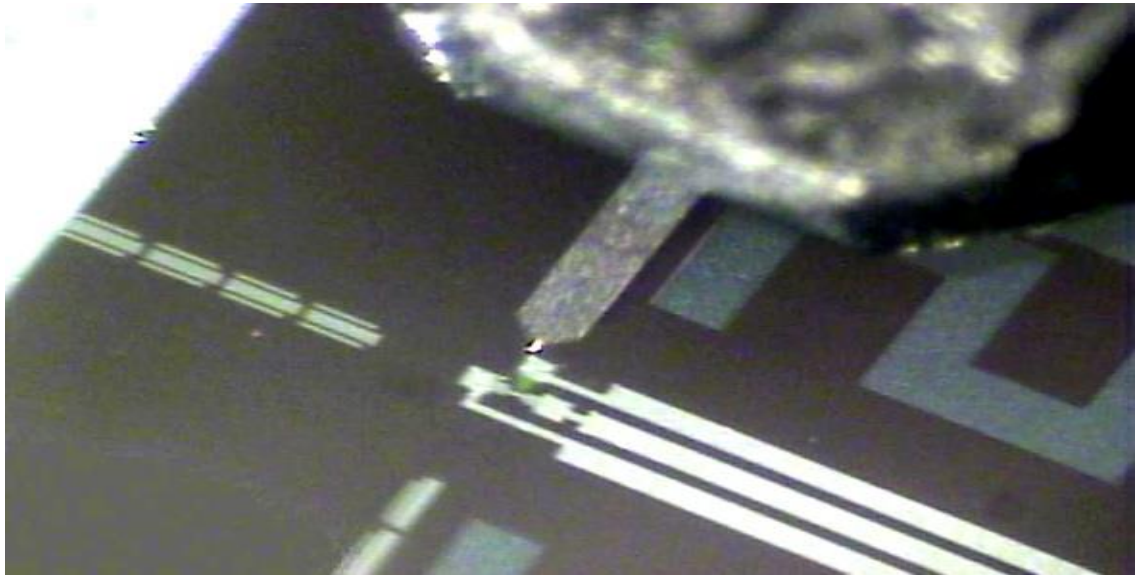

Single atom doping for quantum device development in diamond and silicon

C. D. Weis and A. Schuh
Lawrence Berkeley National Laboratory, 1 Cyclotron Road, Berkeley, California 94114 and Technical University Ilmenau, D-98684 Ilmenau, Germany

A. Batra and A. Persaud
Lawrence Berkeley National Laboratory, 1 Cyclotron Road, Berkeley, California 94114

I. W. Rangelow
Technical University Ilmenau, D-98684 Ilmenau, Germany

J. Bokor
Department of Electrical Engineering and Computer Science, University of California, Berkeley, California

Top 20 Most Downloaded Articles Journal of Vacuum Science & Technology B: Microelectronics and Nanometer Structures -- January 2009

Arbeitsgruppe Nanoskalige Systeme

Lawrence Berkeley National Laboratory

TECHNISCHE UNIVERSITÄT ILMENAU

Deterministic doping challenges
Positioning, Straggle, diffusion and statistics

- Poisson statistics in timed ion implantation

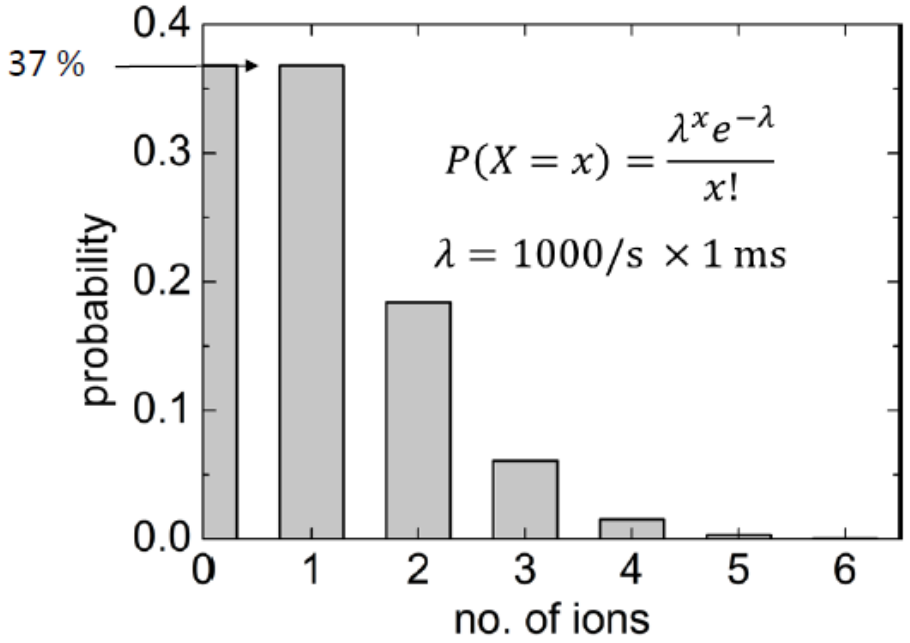

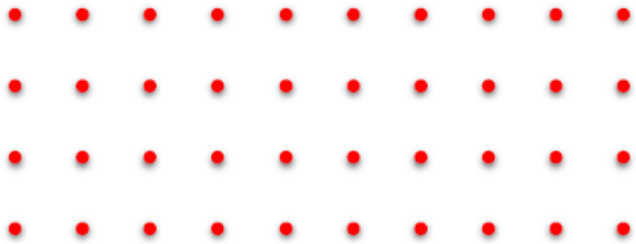

Number of placed atoms	Success probability
2	0.14
6	2×10^{-3}
40	4×10^{-18}

- Deterministic ion implantation requires detection of each individual ion

Deterministic Single Dopant Ion Results

~ 4 ions/interval ~ 1 ion/interval

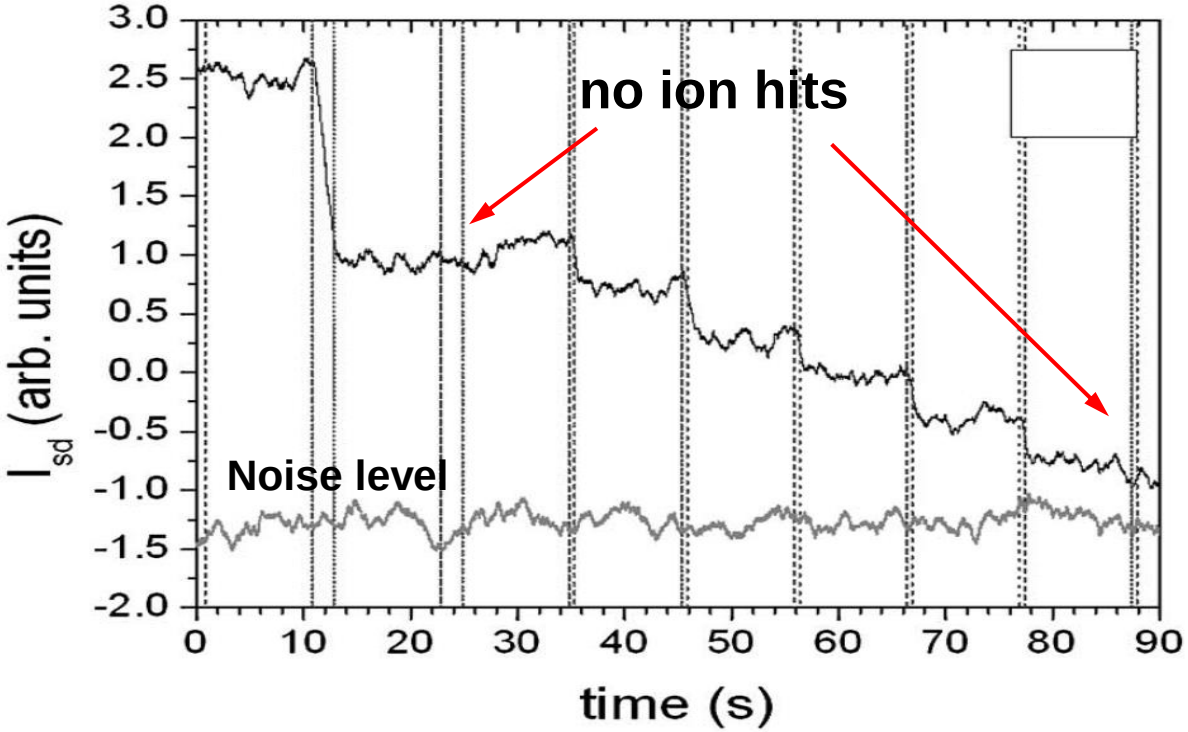

I_{sd}~ 200µA; Ion effect ~ 20nA (10^{-4})
~ 0.2 ions/interval

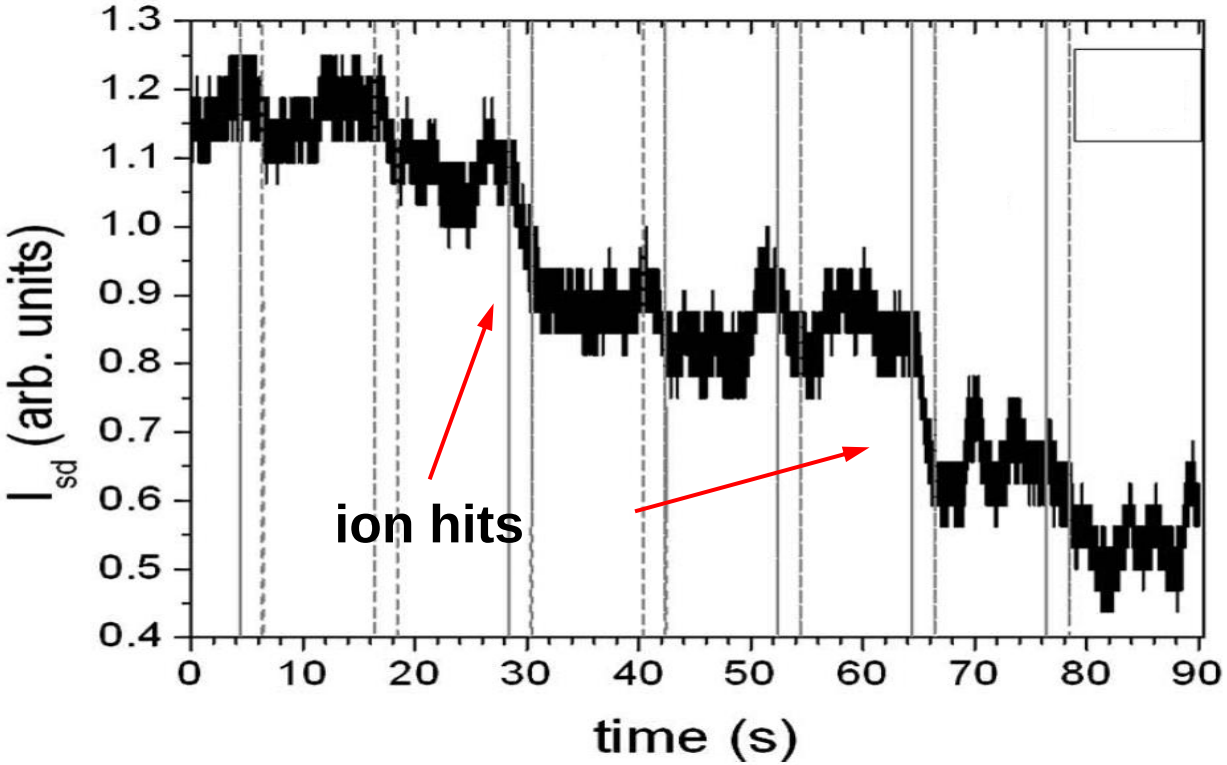

Improved single ion implantation with scanning probe alignment, Michael Ilg, et. al. J. Vac. Sci. Technol. B 30(6), Nov/Dec 2012 2166-2746/2012/30(6)/06FD04/5/$30.00 VC 2012 American Vacuum Society

approach 1: use signals from ion impact ("post-detection")

electron-hole pairs

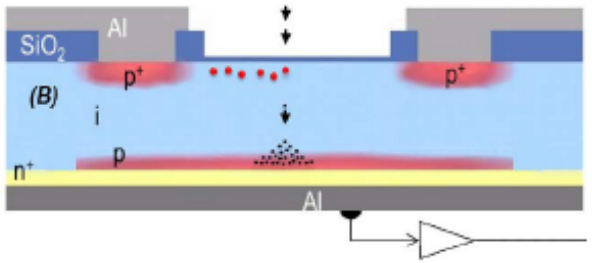

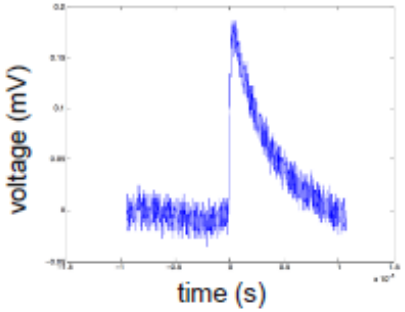

J. van Donkelaar et al., New J. Phys. **12**, 065016 (2010)
J. van Donkelaar et al., J. Phys.: Condens. Matter **27**, 154204 (2015)
D. N. Jamieson et al., Mater Sci Semicond Process **62**, 23 (2017)
A.M. Jakob et al., arXiv:2009.02892 (2020)

Prof. David Jamieson et al (University of Melbourne)

secondary electrons

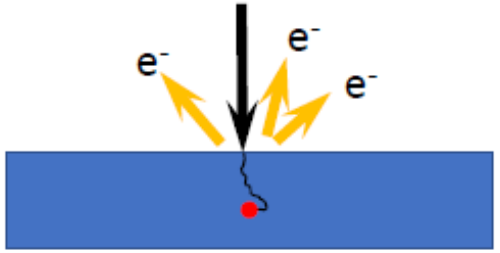

T. Matsukawa et al., Appl. Surf. Sci. **117/118**, 677-683 (1997)
T. Shinada et al., Nature **437**, 1128 (2005)
N. Cassidy et al., phys stat sol (a) **218**, 2000237 (2021)

challenge: detection efficiency close to 100% required

P. Räcke et al. Nanoscale ion implantation using focussedhighly charged ions. New J. Phys. **22**083028 (2020)

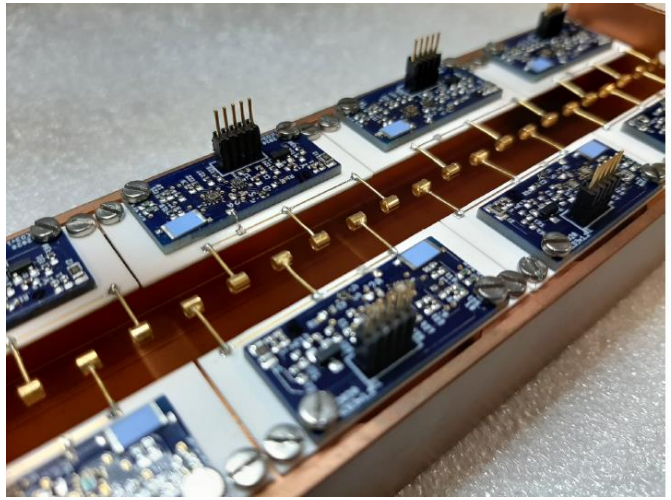

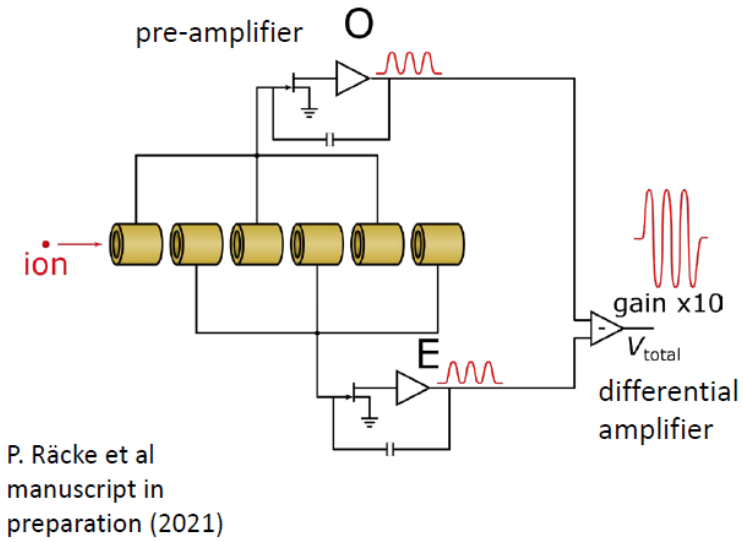

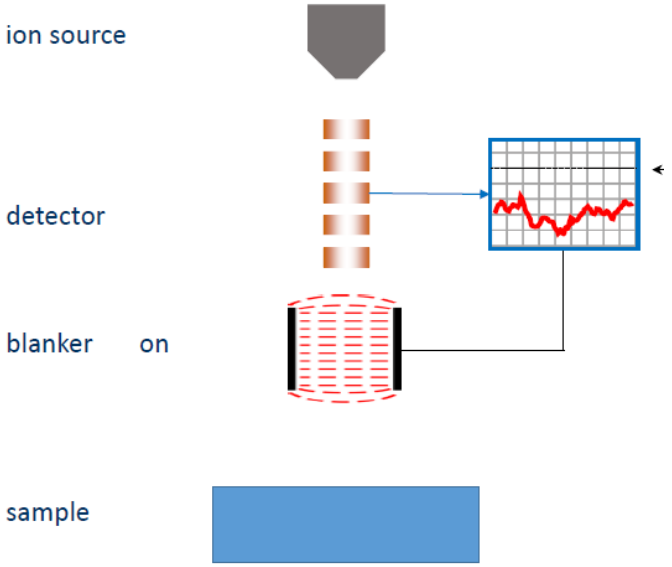

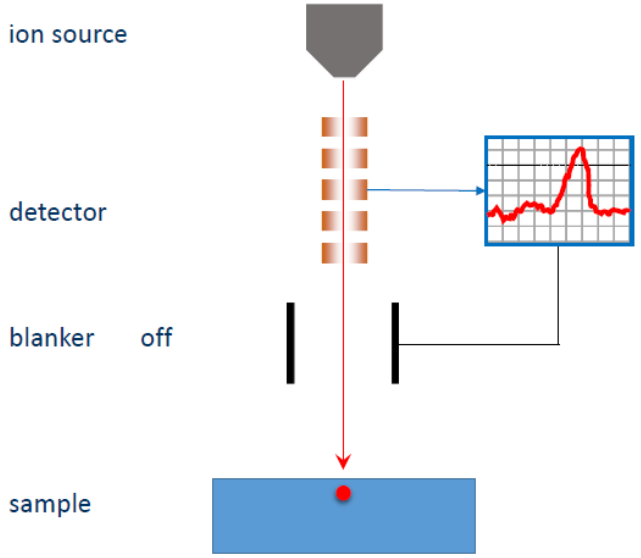

Current status of the detector development

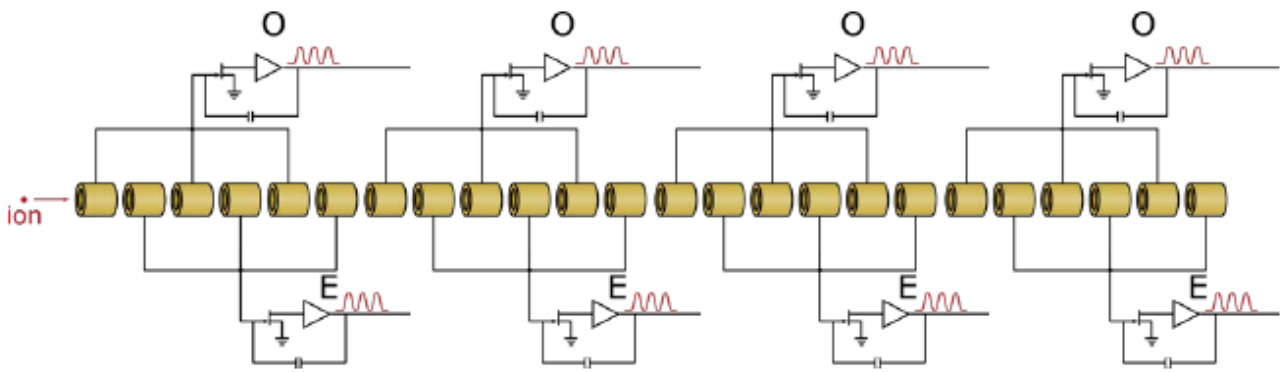

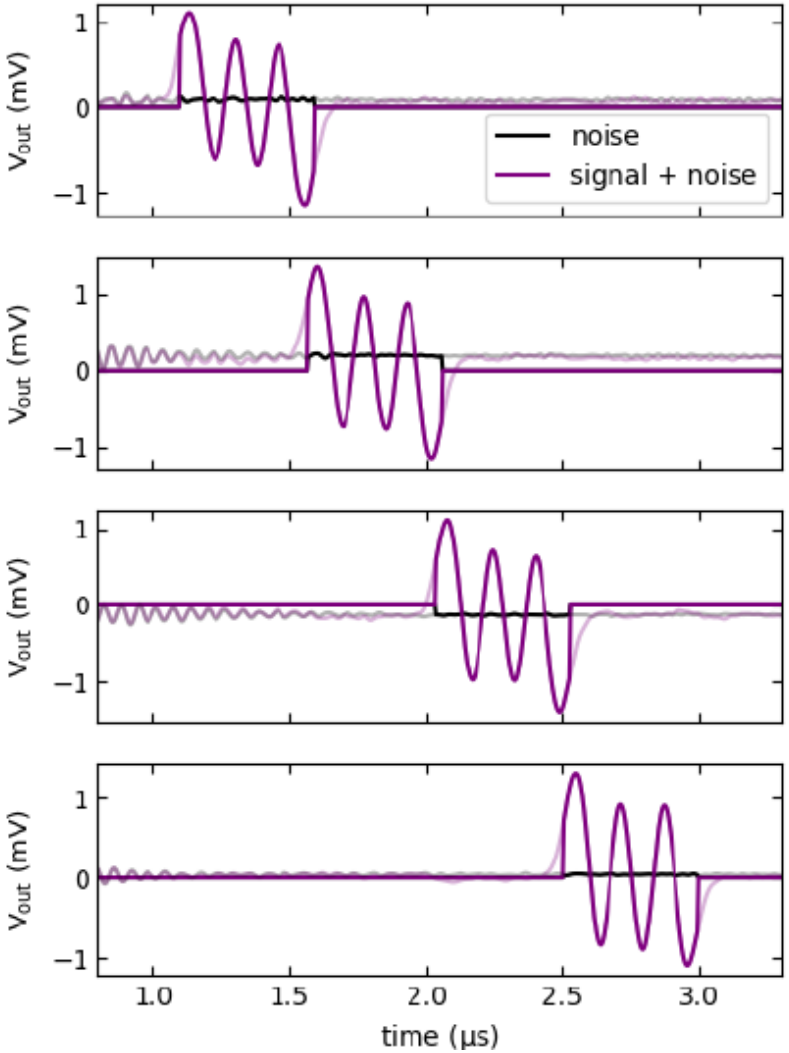

→ gain SNR x √4 = 2

P. Räcke et al
manuscript in
preparation (2021)

Take home messages

Message

- Nanoelectronic devices are always using the ultimate performance of available fabrication methods

- Future evolution of semiconductor devices requires the development of improved fabrication methods

Botom-up fabrication

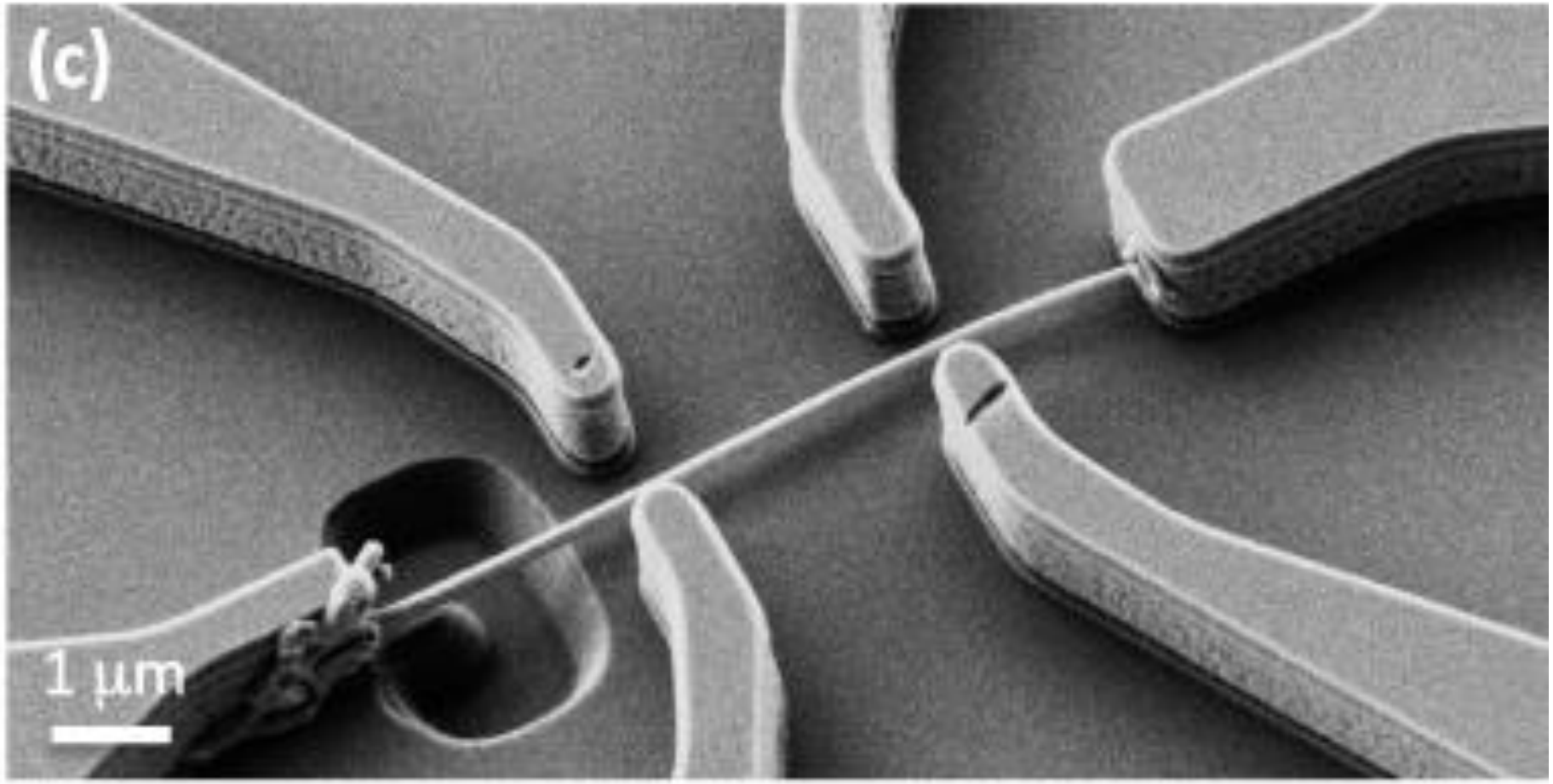

Fernandez-Regulez et al (2013)

Limits of optical lithography

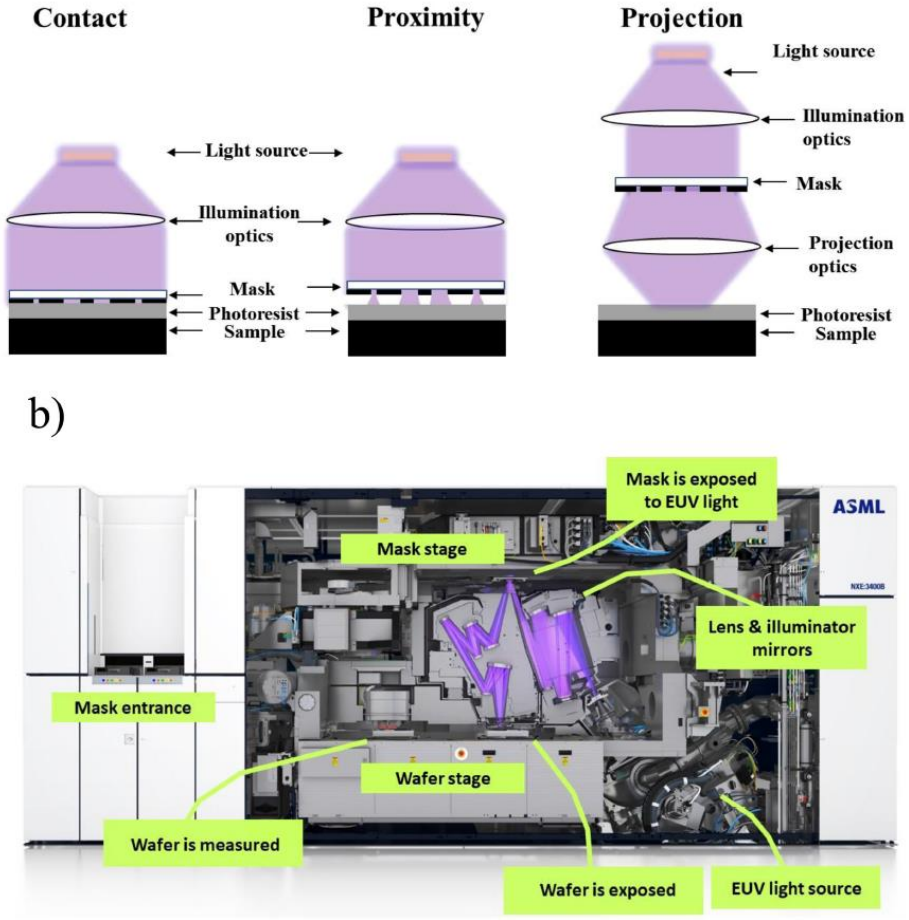

Figure 2.3. (a) Optical lithography modes using an optical mask: contact, proximity and projection. (b) Photograph of an extreme-UV optical lithography system. The main elements are labelled.

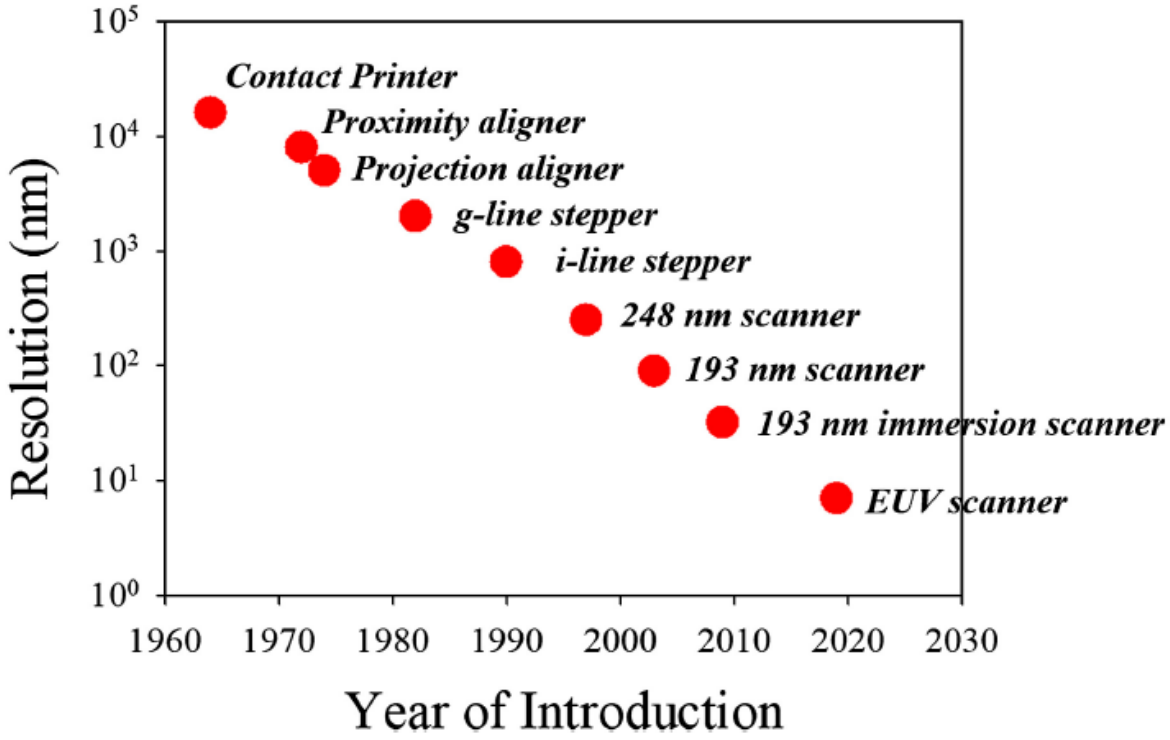

Figure 2.4. Evolution of the optical resolution during the years. Data extracted from [2].

Figures extracted from: Francesc Perez-Murano, José Ignacio Martín y José María de Teresa. Optical Lithgroaphy, Chapter 2. Nanofabrication. IOP books

Patterning resolution vs Throughput

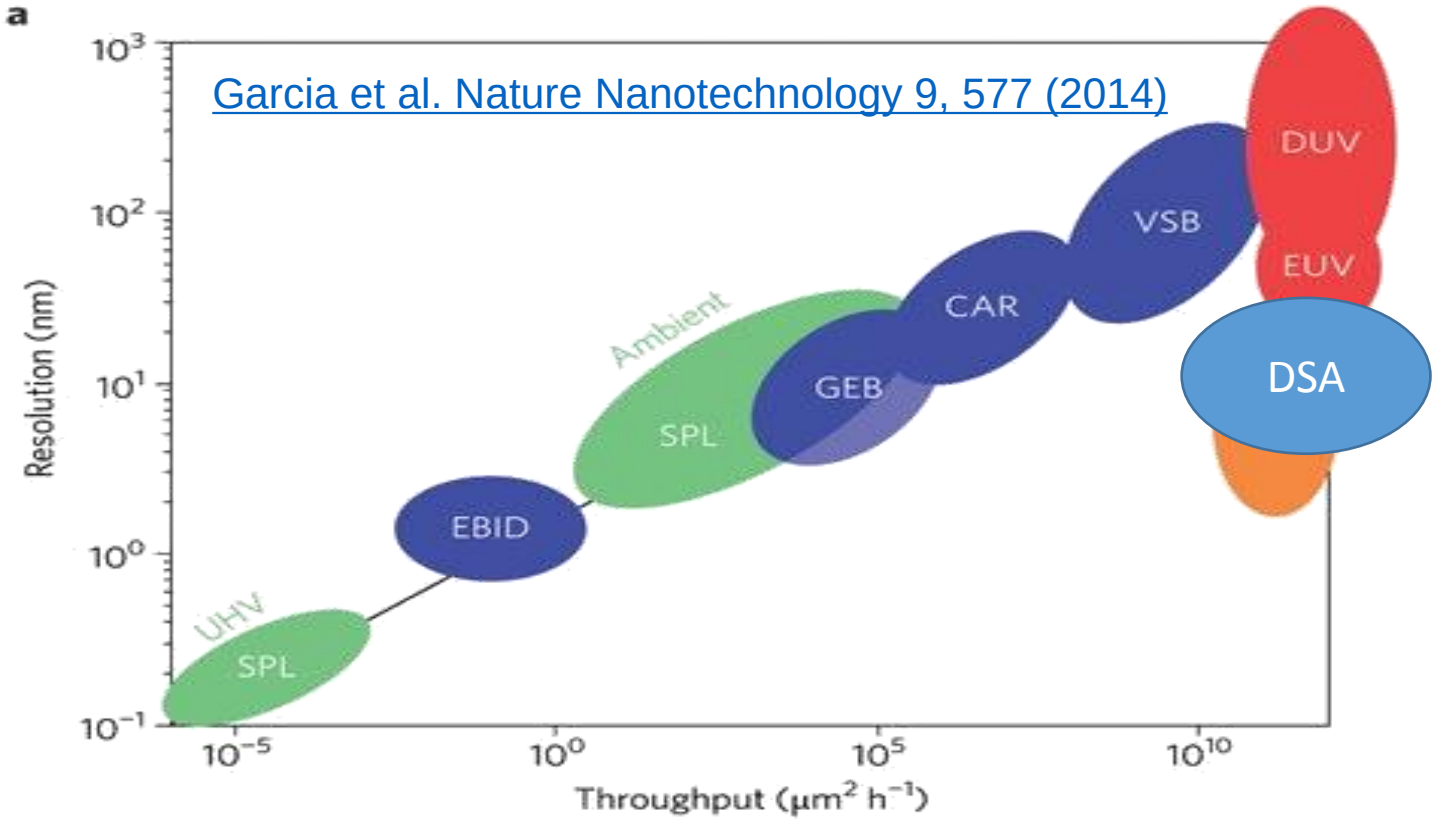

SEQUENTIAL LITHOGRAPHY

- Scanning probe lithography
- Electron beam lithography

PARALLEL LITHOGRAPHY

- Optical lithography
- Directed self assembly

Examples of bottom-up fabrication

Carbon nanotubes transistors

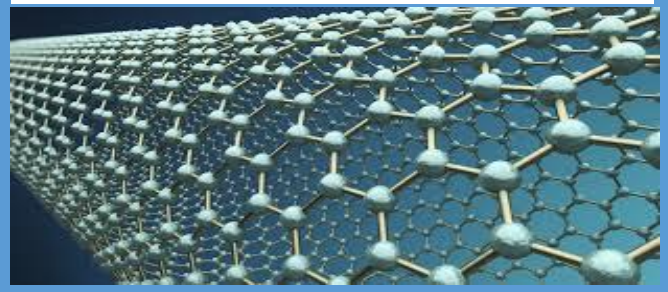

Logic Circuits with Carbon Nanotube Transistors

Bachtold et al. Science. 2001

Silicon nanowire resonators

Sansa et al. Nature comm 2014.

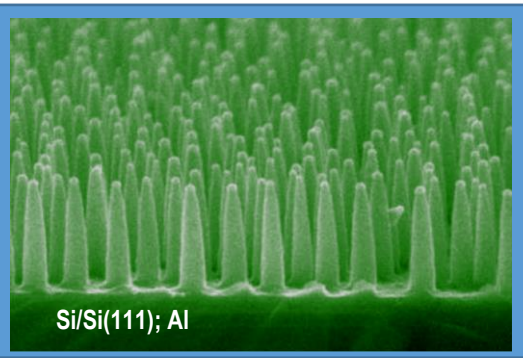

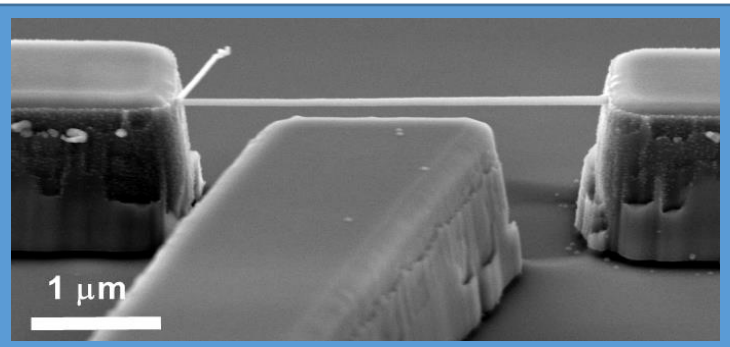

Block copolymer self-assembly

Oria et al. Microelectronic Engineering 2006

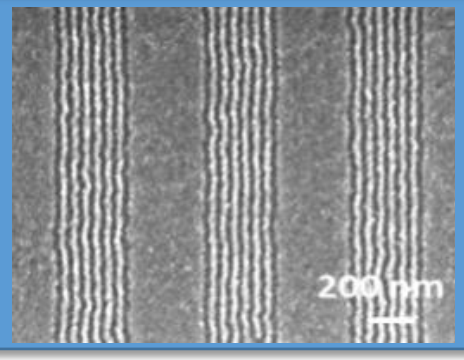

Assembly of DNA

DNA Origami

P. Wang et al. J.Am.Chem.Soc. 2016.

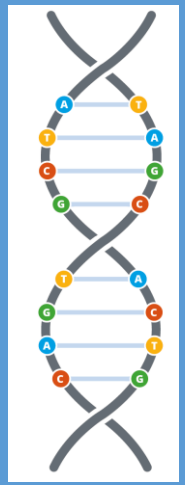

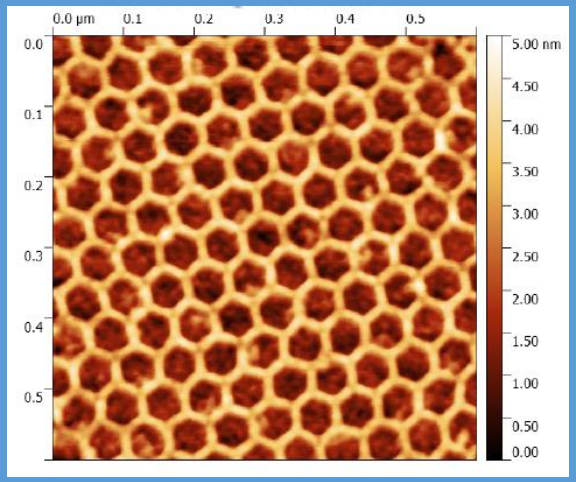

Assembly of nanocrystals

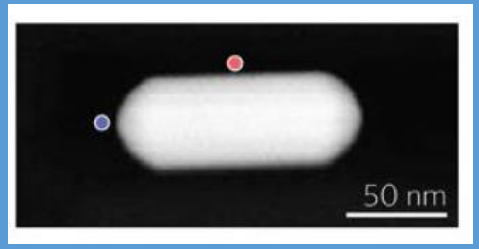

Flauraud et al. Nat.Nanotech. 2016

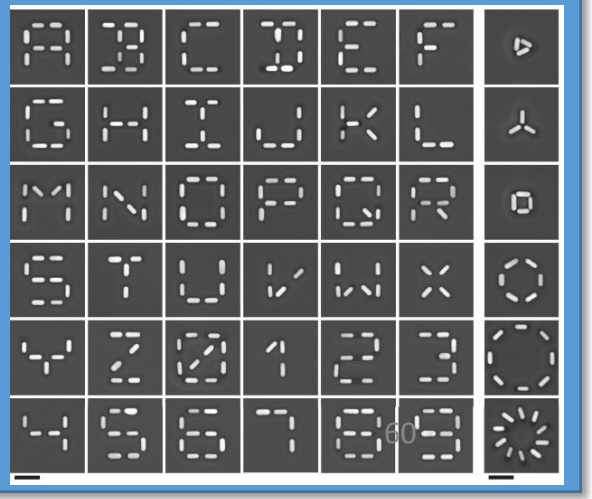

Directed self-assembly of block copolymers

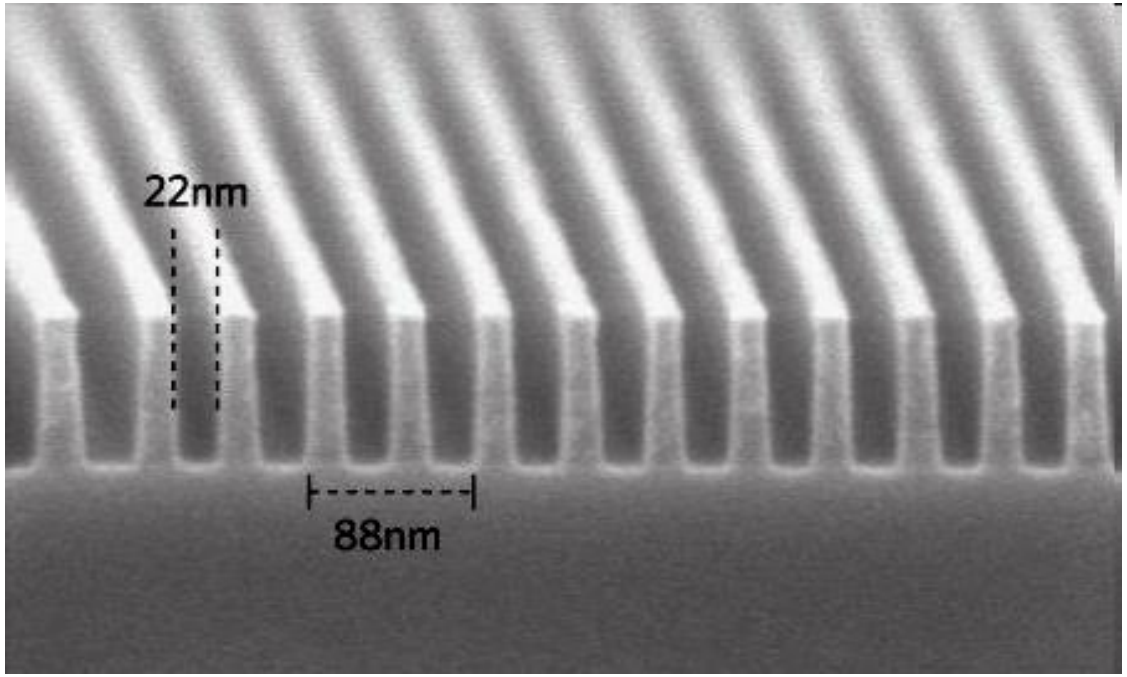

By optical lithography

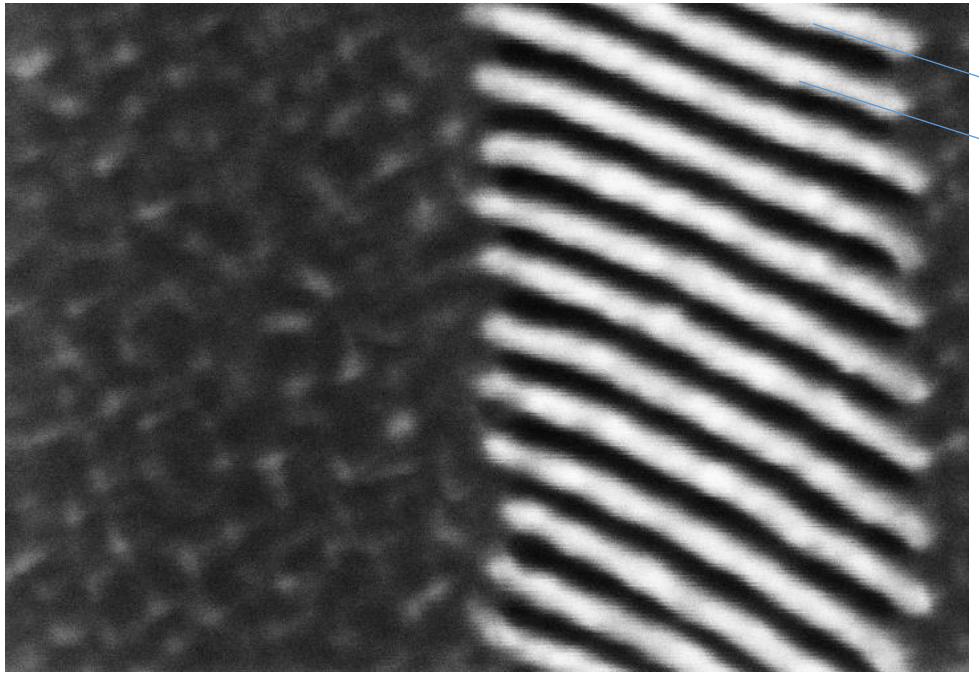

By directed sef-assembly of block copolymers

IEEE IRDS ROADMAP 2021

https://irds.ieee.org/

The IRDS™ is a set of predictions that intent to provide a clear outline to simplify academic, manufacturing, supply, and research coordination regarding the development of electronic devices and systems.

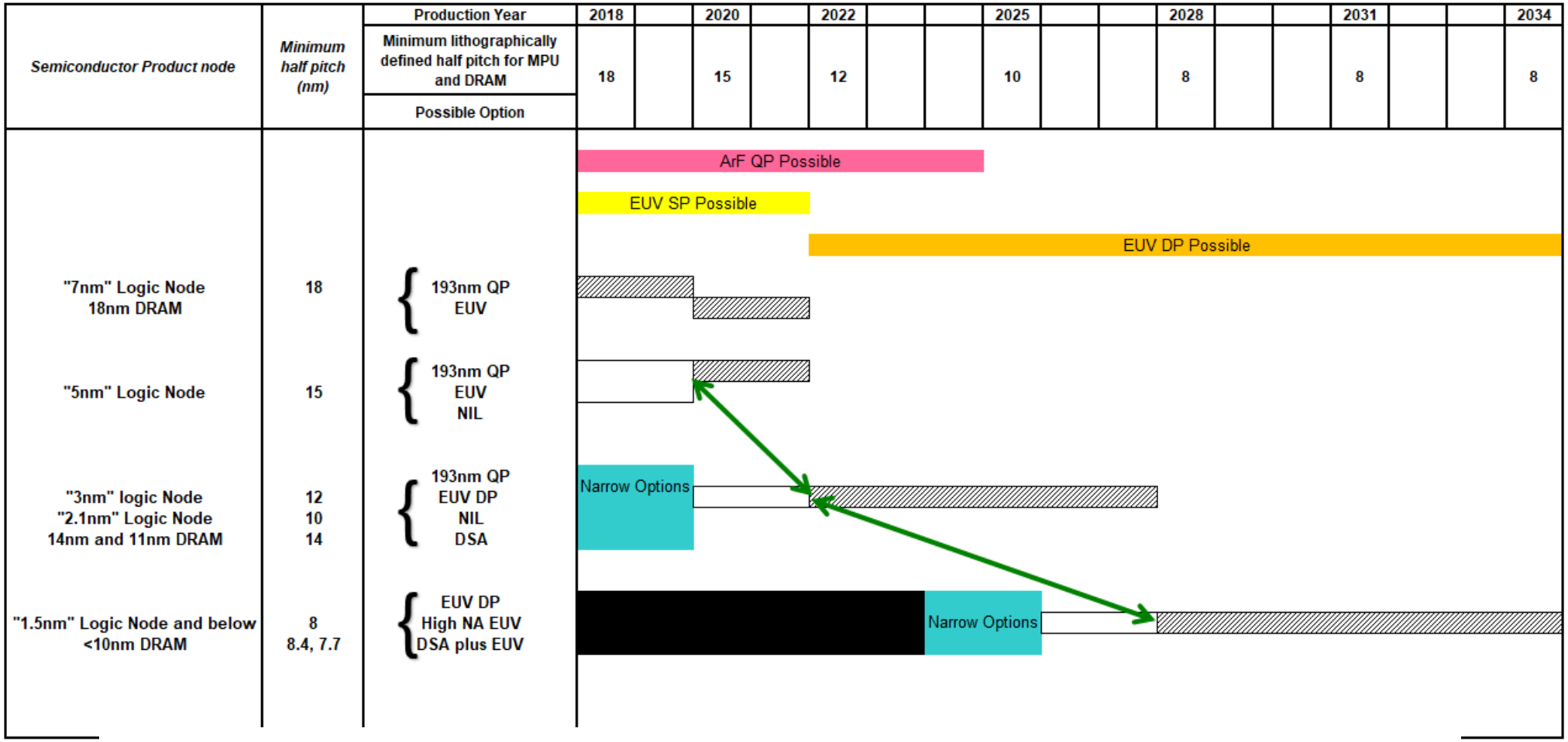

LINE AND SPACE POTENTIAL SOLUTIONS

BLOCK CO-POLYMER SELF-ASSEMBLY

- ***What are block copolymers?***

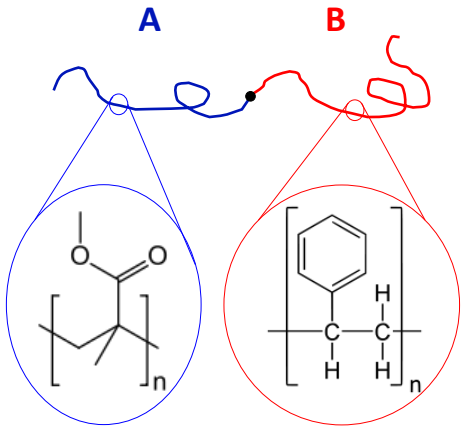

f: Volume fraction of one block in a BCP

χ: Flory-Huggins interaction parameter

N: Polymerization index

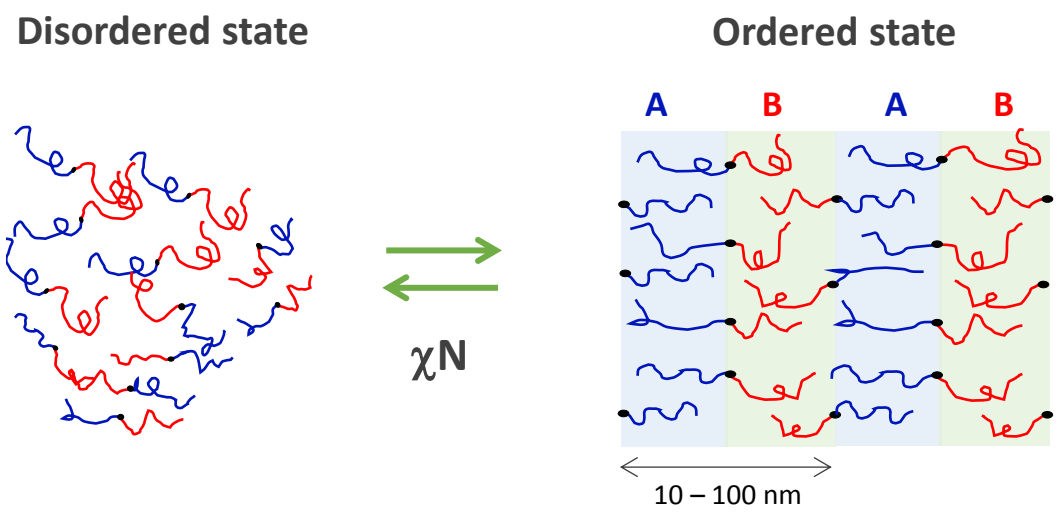

- ***Phase diagram of A-B diblock copolymer***

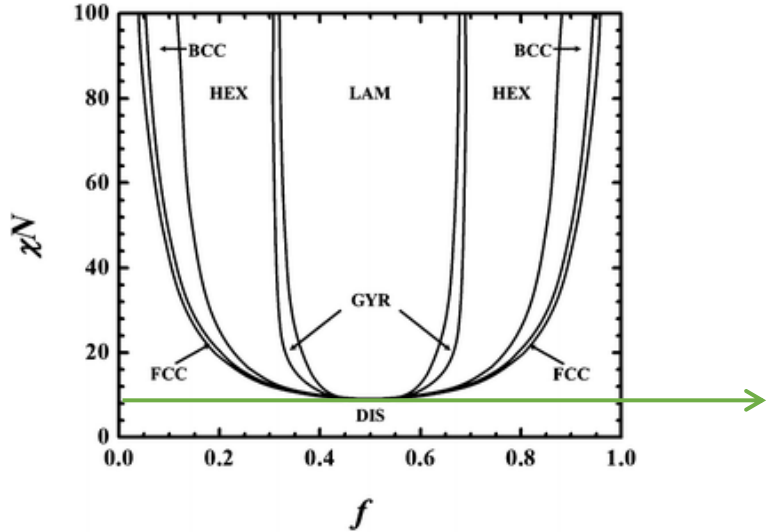

χN = 10.5

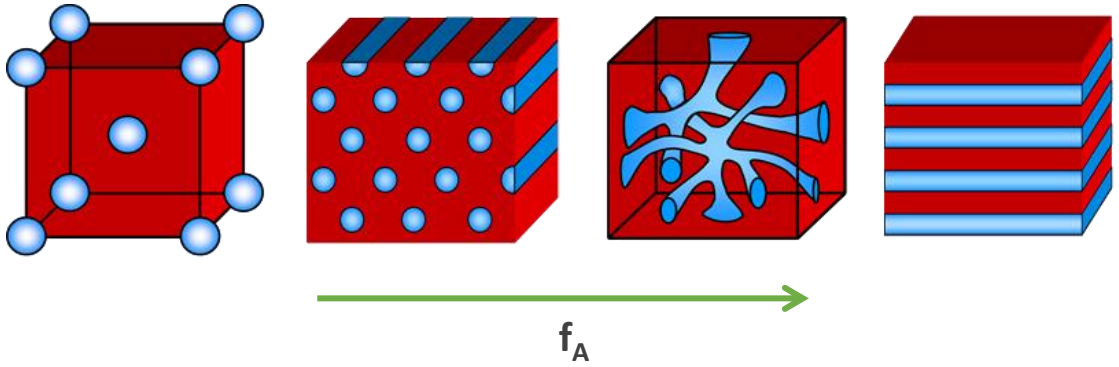

Bates, F.S. and Fredrickson, G.H. "Block Copolymers – Designer Soft Materials", Physics Today, 52, 2 (1992)

Examples of phase segregation
Lamellar forming block copolymers

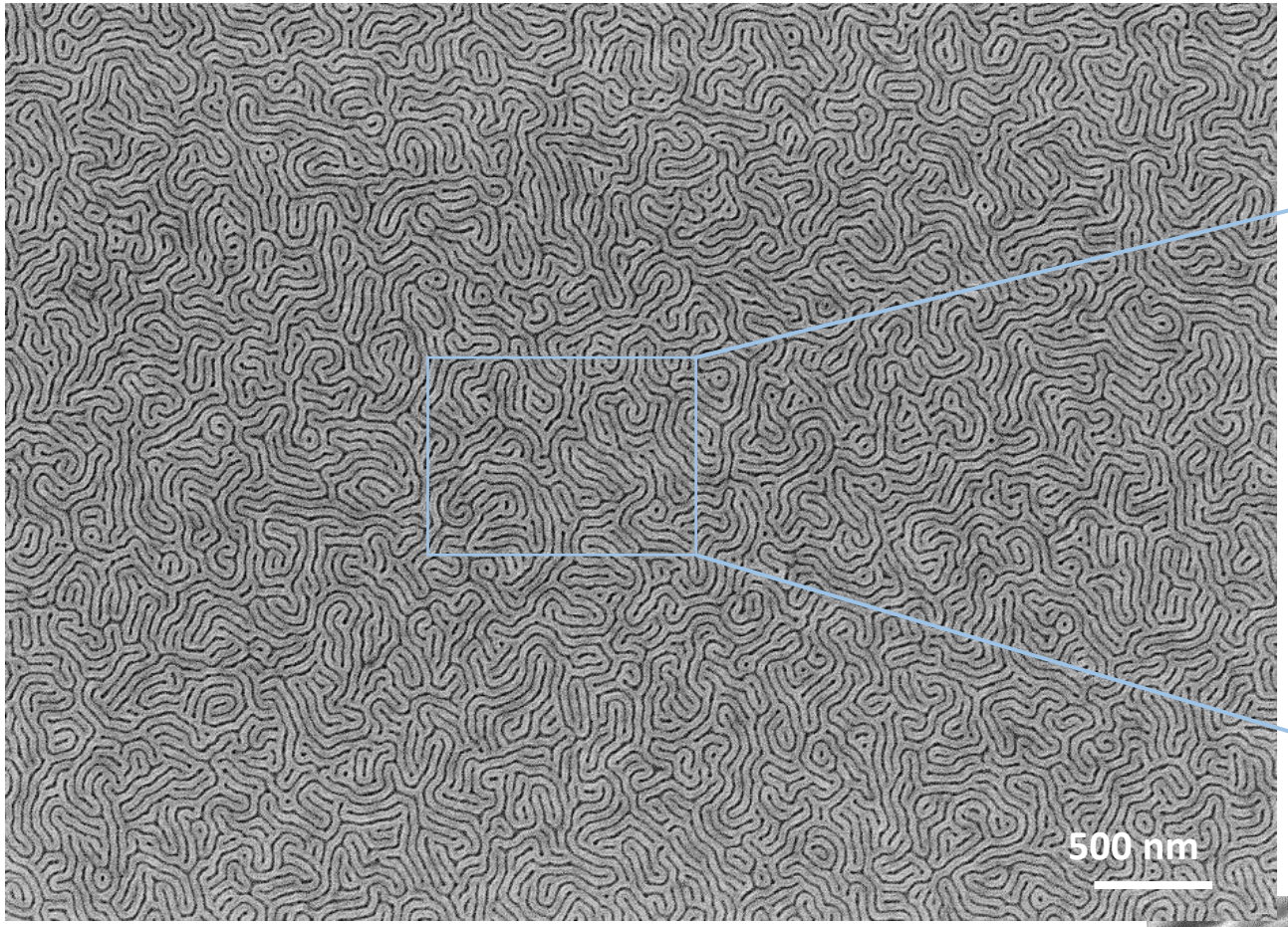

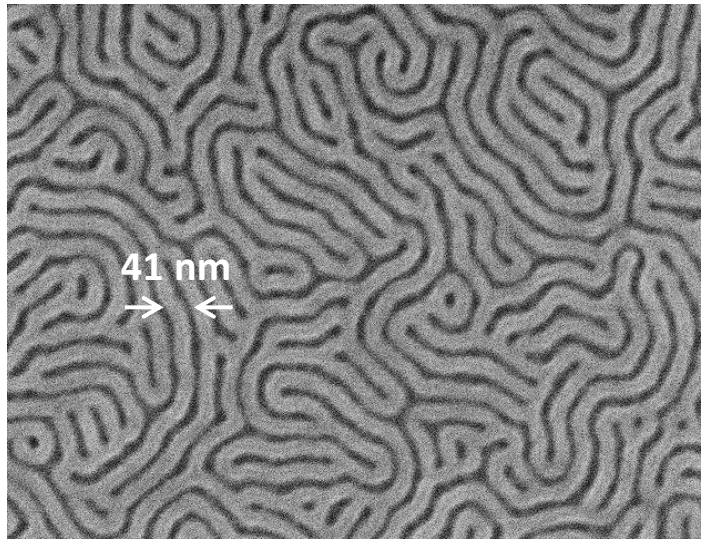

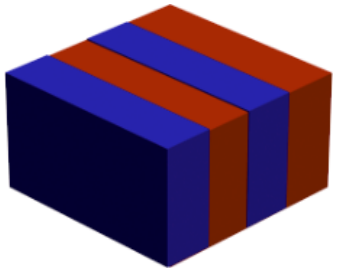

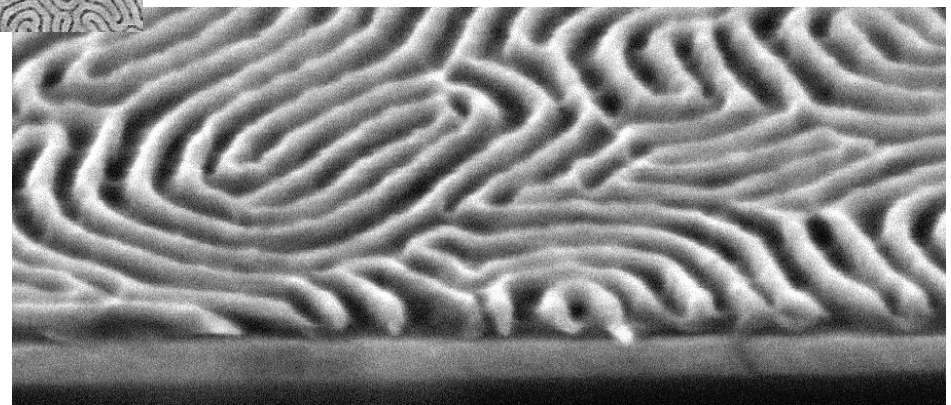

Cylindrical forming of block copolymers

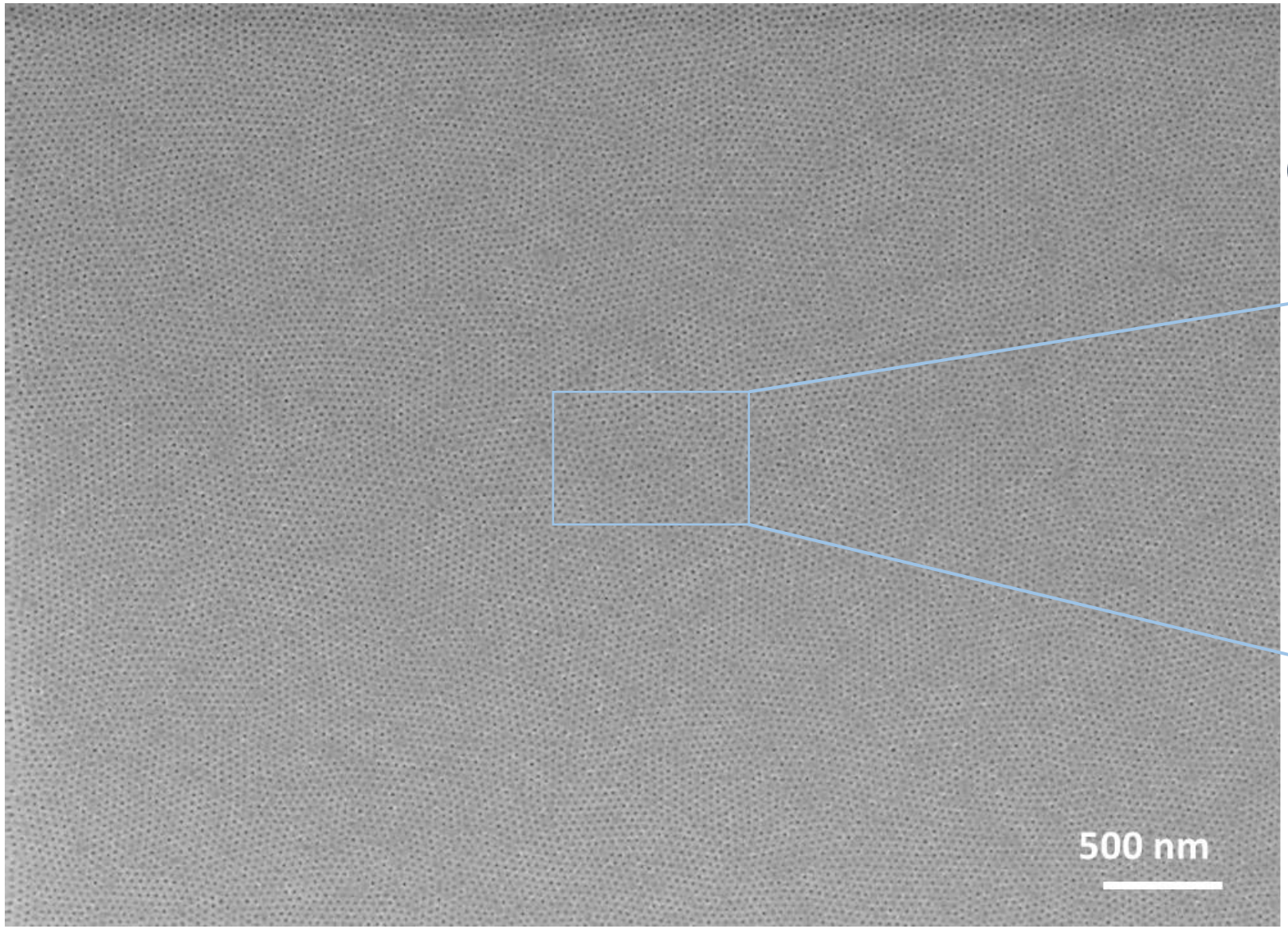

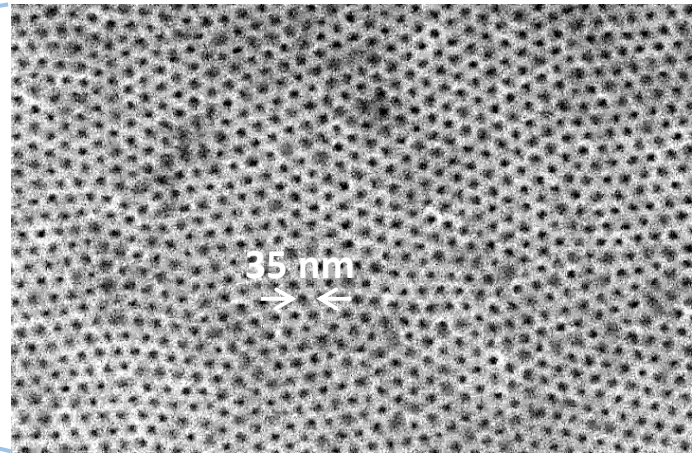

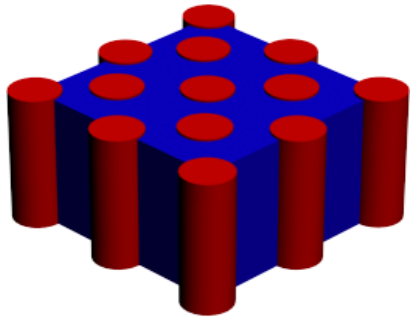

BLOCK CO-POLYMER SELF-ASSEMBLY

The pitch of the features depends on the molecular

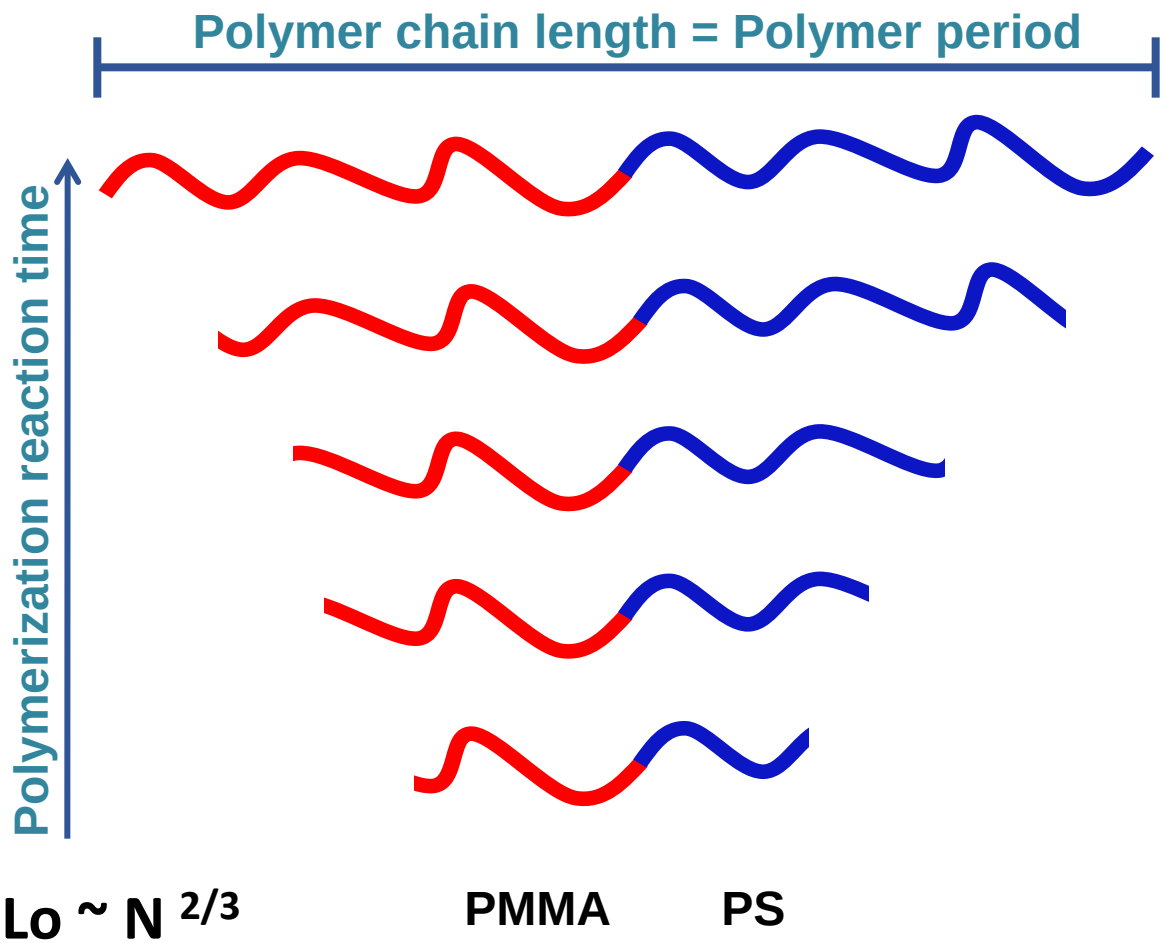

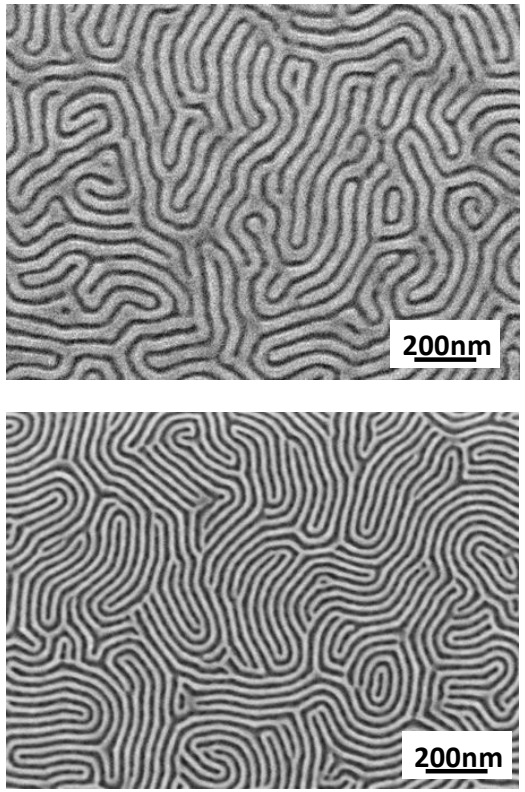

19 nm half pitch

11 nm half pitch

Thin film preparation of block co-polymers

1. Preparation of a surface with the proper interface energy (usually, deposition of a monolayer of molecules)
2. Dissolution of the block co-polymer in a solvent
3. Spinning of the solution
4. Annealing (Thermal annealing or solvent annealing)

Thin film preparation of block co-polymers

In order to promote and **enhance** the **ordering** of BCP microdomains it is necessary to **induce some mobility** on polymer chains to facilitate the microphase separation process.

Thermal annealing

Solvent annealing

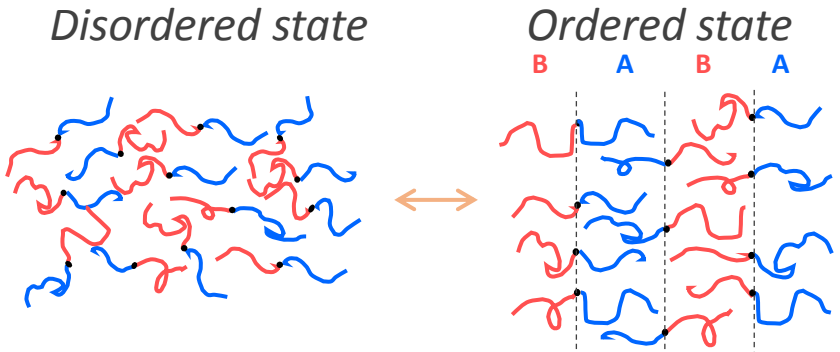

Thermal annealing

Heating **above T_g** and **below degradation** T

$$D = D_0 e^{-0.28\cdot(\chi N - 3.5)}$$

$$\chi_{AB} = \frac{Z}{k_B T}\left[\varepsilon_{AB} - \frac{\varepsilon_{AA} + \varepsilon_{BB}}{2}\right]$$

T ↑ χ ↓

✓ Equipment already implemented in the industry

✓ No waste stream

✗ Systems which undergo degradation at high temperatures

Solvent annealing

Exposure to a solvent **below T_g** to form a swollen and mobile polymer film

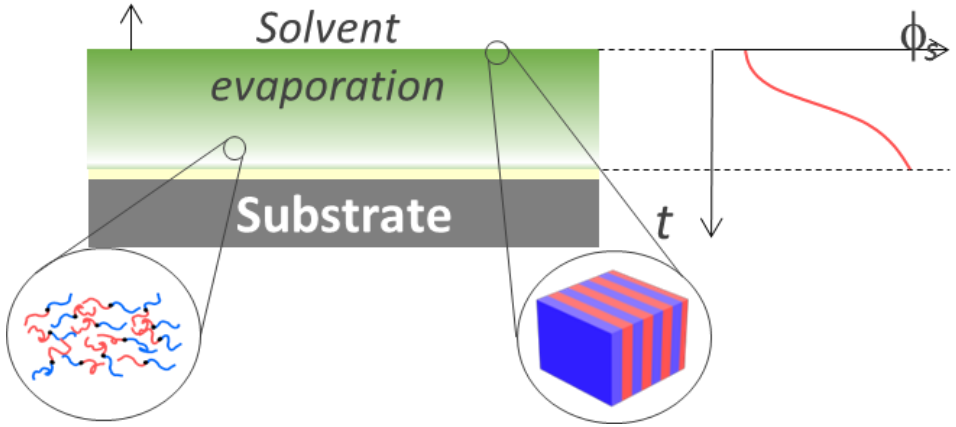

Thin film preparation of block co-polymers

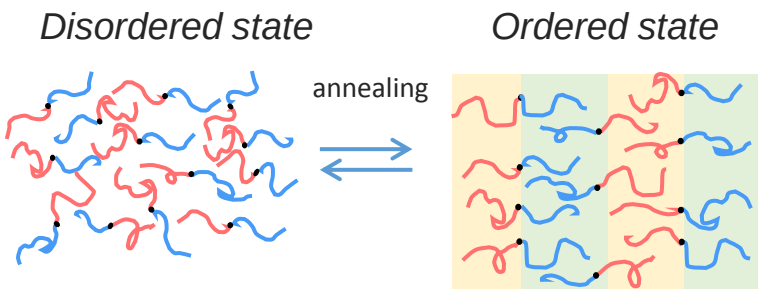

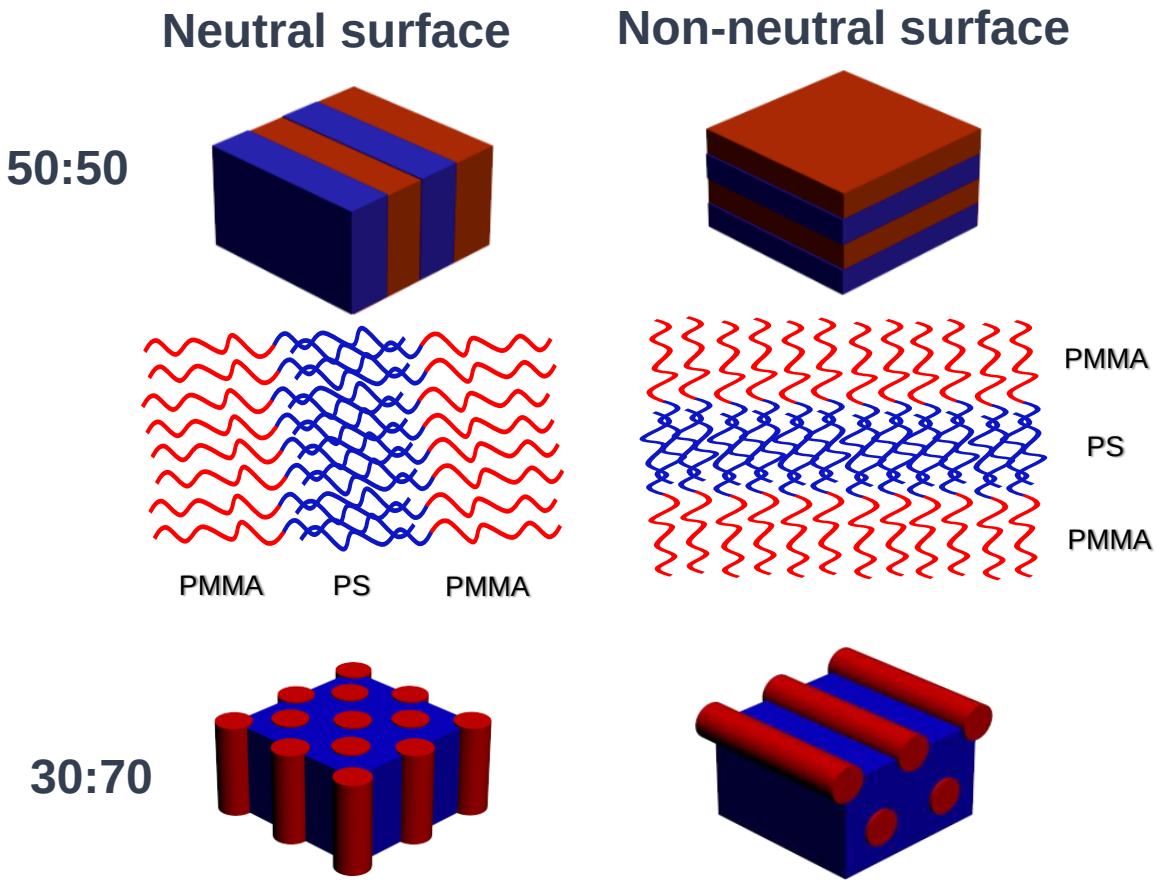

The **surface affinity** is usually controlled by a polymer monolayer

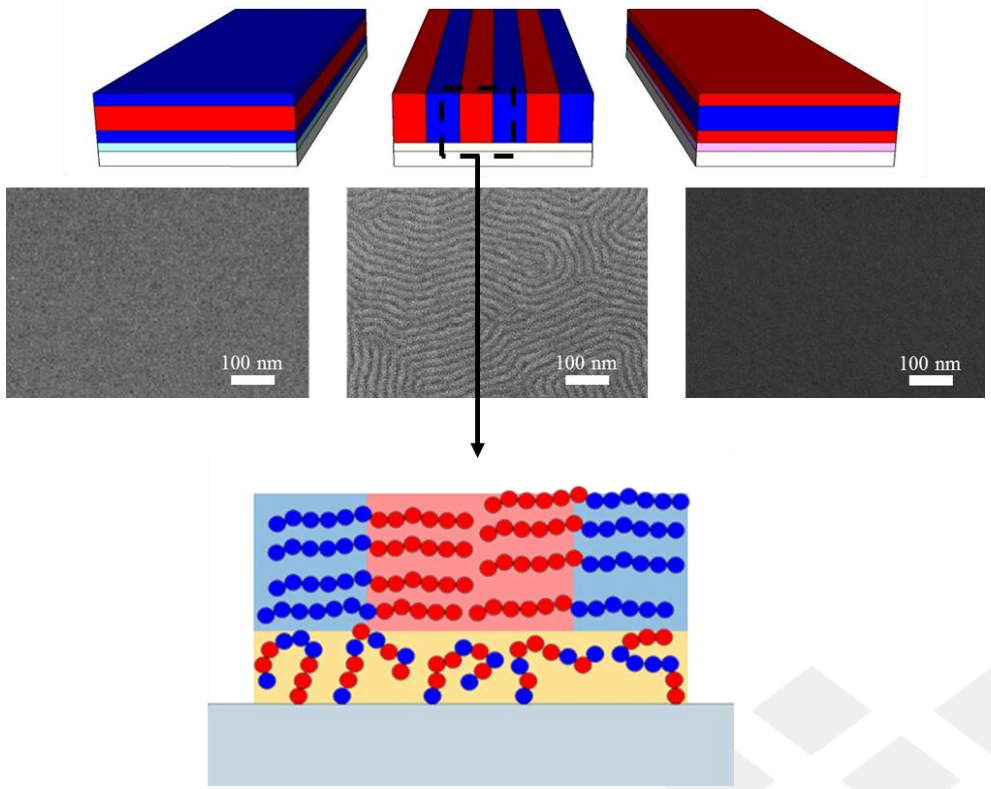

$$E_{tot} = \sum E = E_{stretch} + E_{curvature} + E_{interblock} + E_{surface}$$

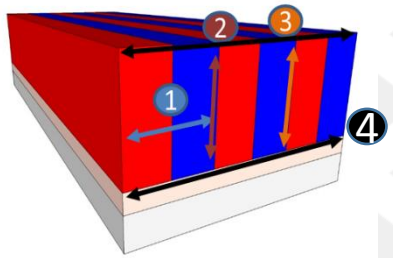

Surface neutralization

For technological applications there is the need to control the BCP morphology, and thus **avoid wetting morphologies** at the polymer-brush interface.

Use of **brush polymer** to create a neutral layer which balances the surface free energy between the BCP domains

Mansky, P., "Controlling polymer-surface interactions with random copolymer brushes", Science, 275, 1458-1460 (1997)

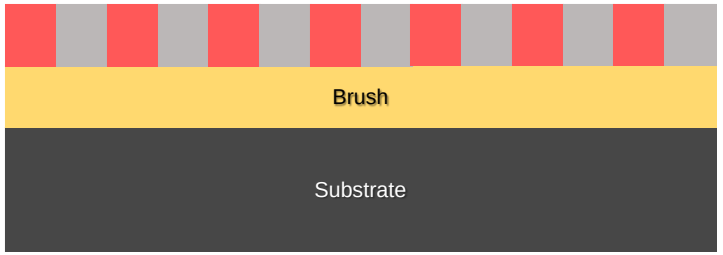

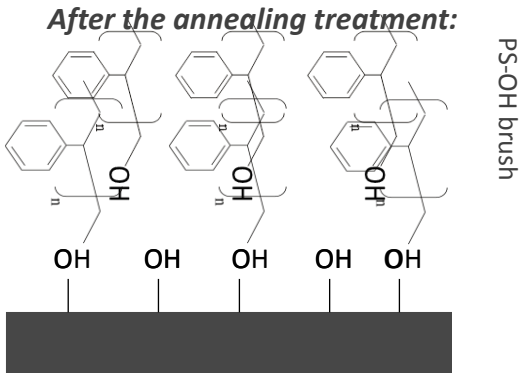

% PMMA (PS-r-PMMA)

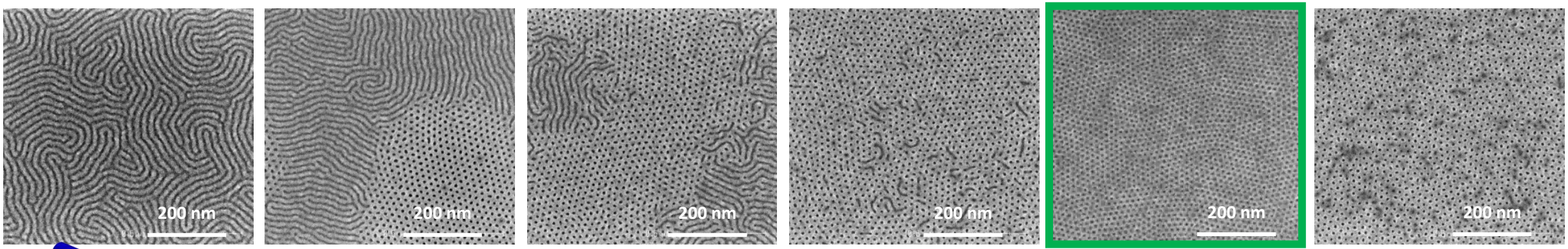

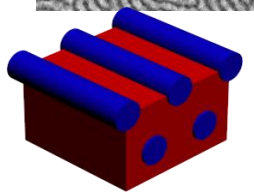

Cylindrical PS-b-PMMA

SEM images taken after PMMA removal

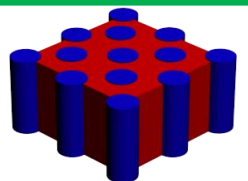

Block copolymer – surface interaction: *Role of surface affinity*

Interaction energies $E = \boxed{(E_{A/B} + E_{conf})} + \boxed{(E_{A/Subs} + E_{B/subs} + E_{A/air} + E_{B/air})}$

Neutral surface

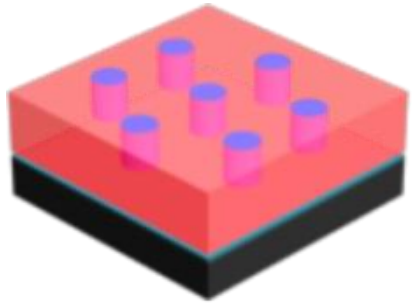

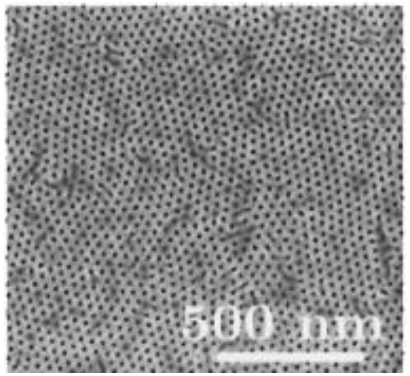

Neutral surface

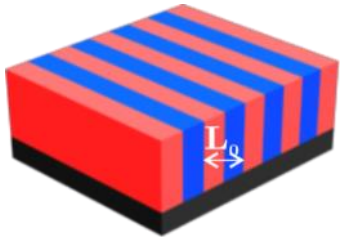

$\gamma_{A\text{-air}} \approx \gamma_{B\text{-air}}$

$\gamma_{A\text{-subs}} \approx \gamma_{B\text{-subs}}$

AFFINE SURFACE

$\gamma_{A\text{-air}} < \gamma_{B\text{-air}}$

$\gamma_{A\text{-subs}} < \gamma_{B\text{-subs}}$

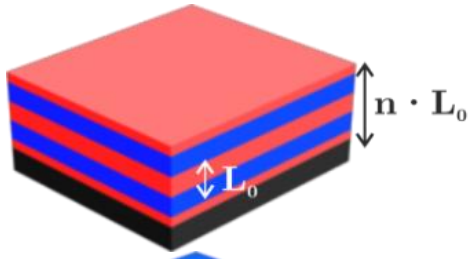

$\gamma_{A\text{-air}} > \gamma_{B\text{-air}}$

$\gamma_{A\text{-subs}} < \gamma_{B\text{-subs}}$

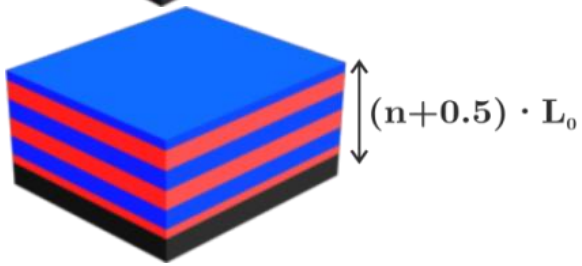

Affine surface

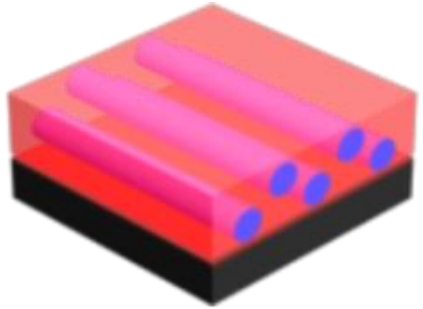

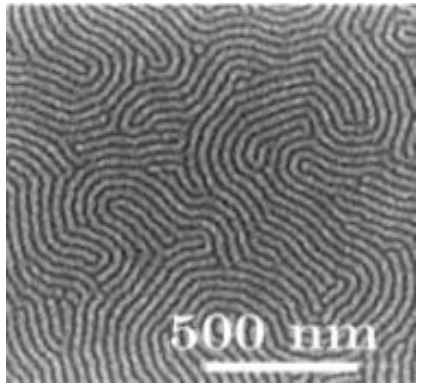

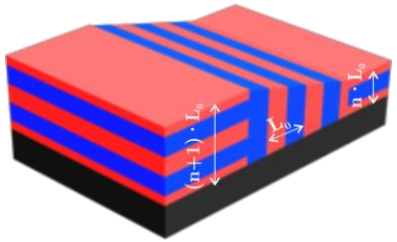

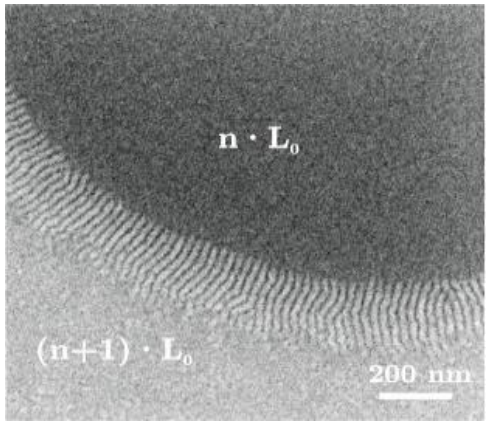

When the BCP **does not** fulfill the film thickness **commensurability** condition, the BCP tend to create some **holes** or **terraces**

Directed self-assembly (DSA)

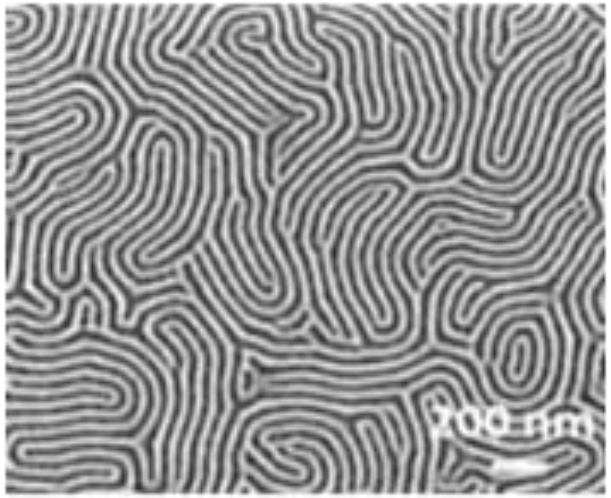

Intrinsic property of BCP to self-assemble

+

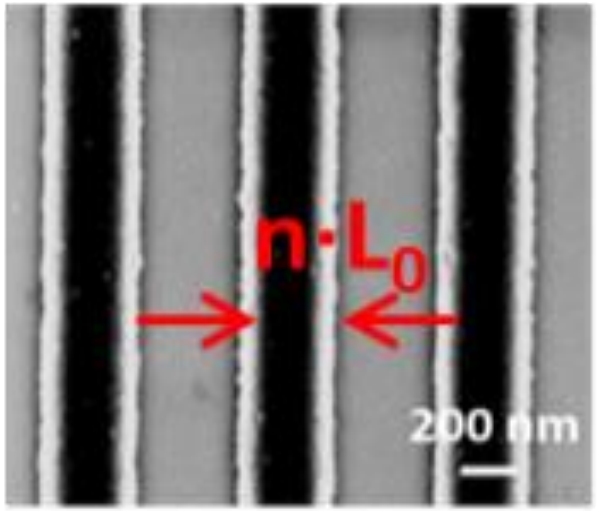

=

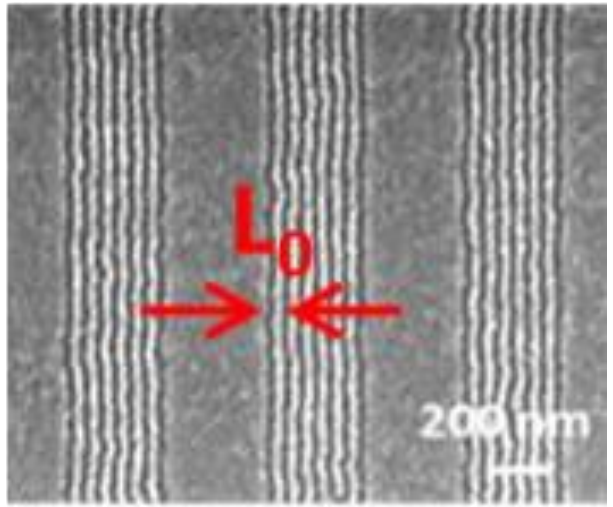

Density multiplication factor: n

Directed self-assembly: guiding patterns

Graphoepitaxy

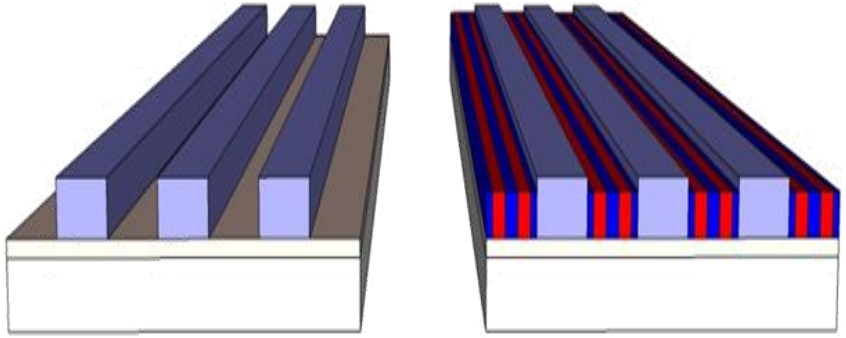

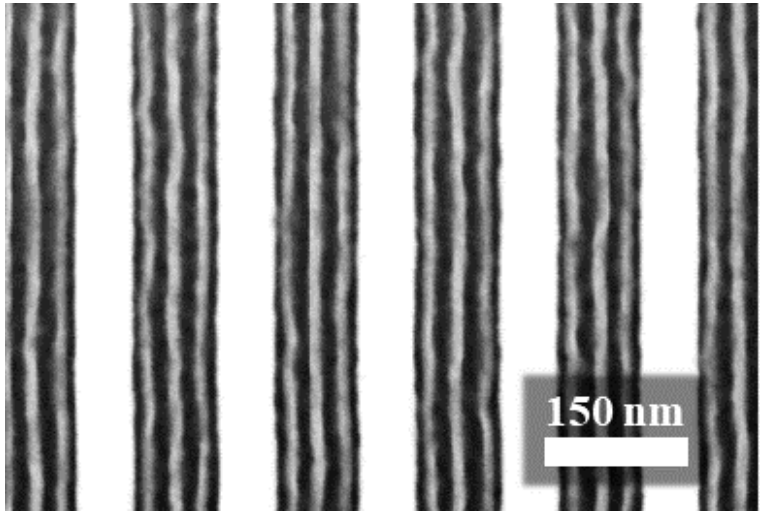

Chemoepitaxy

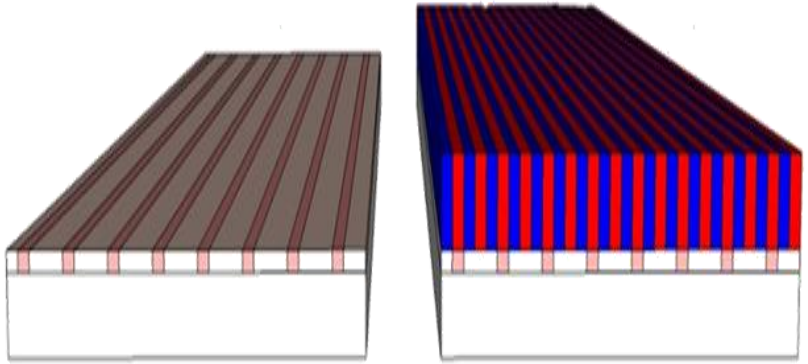

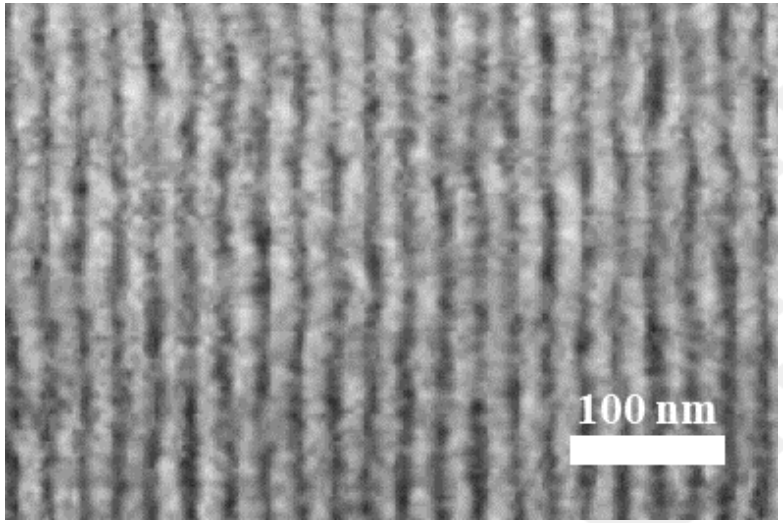

Graphoepitaxy process

Graphoepitaxy consists in creating **topographical features** on the substrate to enforce the self-assembly of block copolymers, thus enhancing the lateral order on the BCP nano-domains.

Graphoepitaxy overall process

1. E-beam lithography

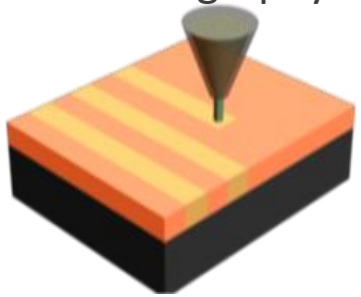

2. PMMA development + Si etching

3. Resist stripping

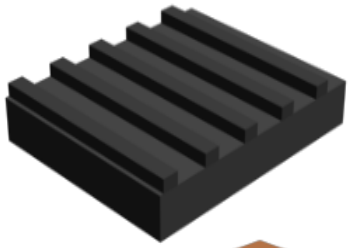

4. Brush deposition

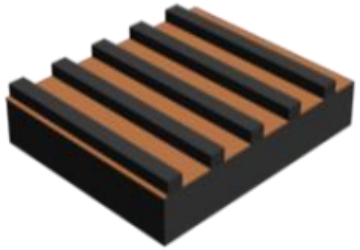

5. BCP spin-coating

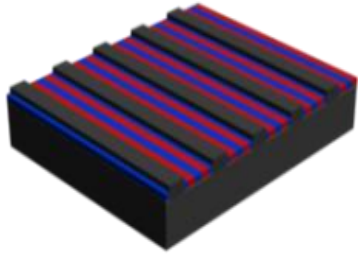

The chemical affinities between the **walls** and the **bottom** with the **BCP nanodomains** are the ones which determine the orientation the BCP will take after self-assembly.

Neutral bottom and **neutral** walls

↓

Perpendicular morphology **perpendicularly** oriented to trenches

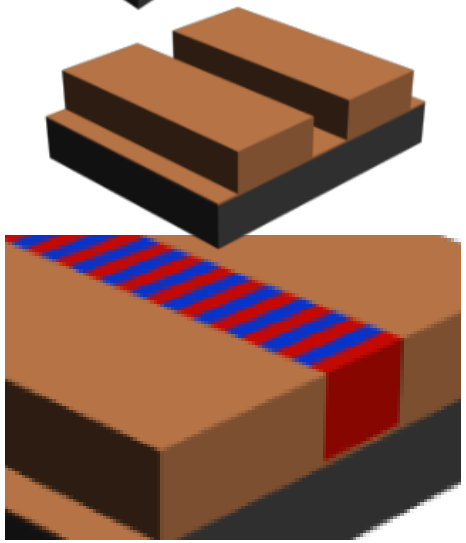

Neutral bottom and **preferential** walls

↓

Perpendicular morphology **parallely** oriented to trenches

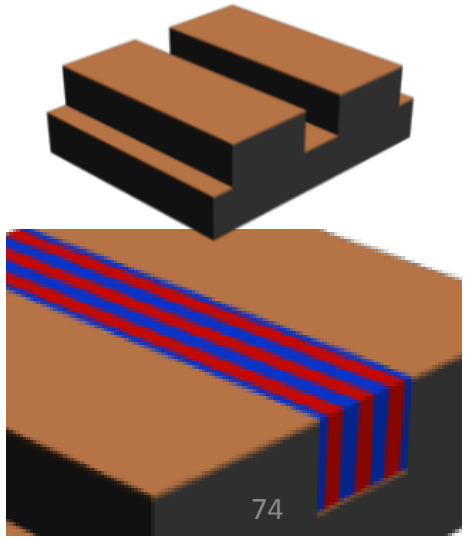

Examples of grapho-epitaxy

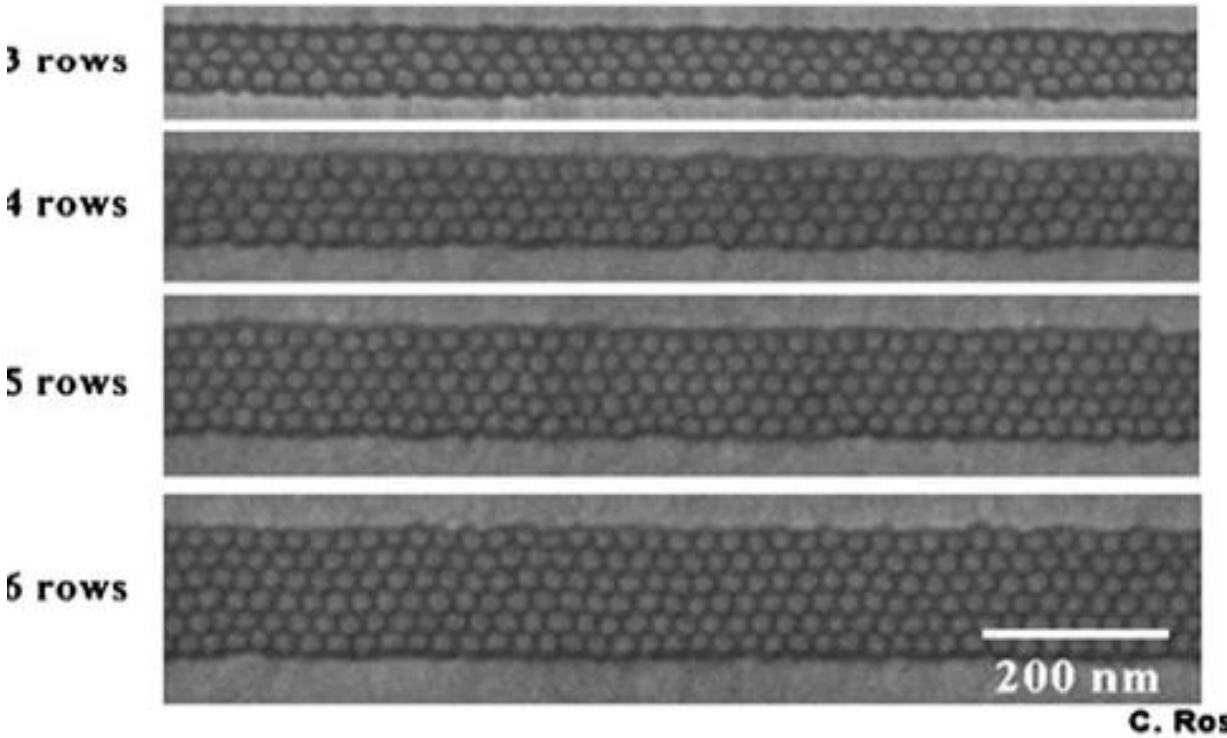

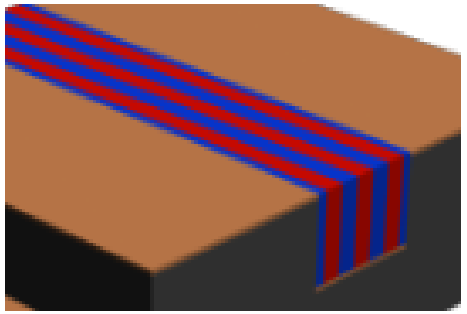

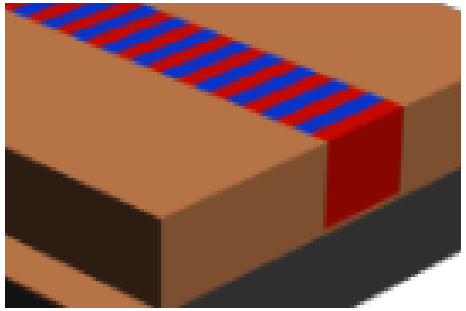

Directed block copolymer self-assembly for nanoelectronics fabrication.
Daniel J.C. Herr. Mater. Res., 26, 122, , 2011

e this: DOI: 10.1039/c8sm01045e

Nano-confinement of block copolymers in high accuracy topographical guiding patterns: modelling the emergence of defectivity due to incommensurability†

Steven Gottlieb,[a] Dimitrios Kazazis,[b] Iacopo Mochi,[b] Laura Evangelio,[a] Marta Fernández-Regúlez,[a] Yasin Ekinci[b] and Francesc Perez-Murano[a]

(a)

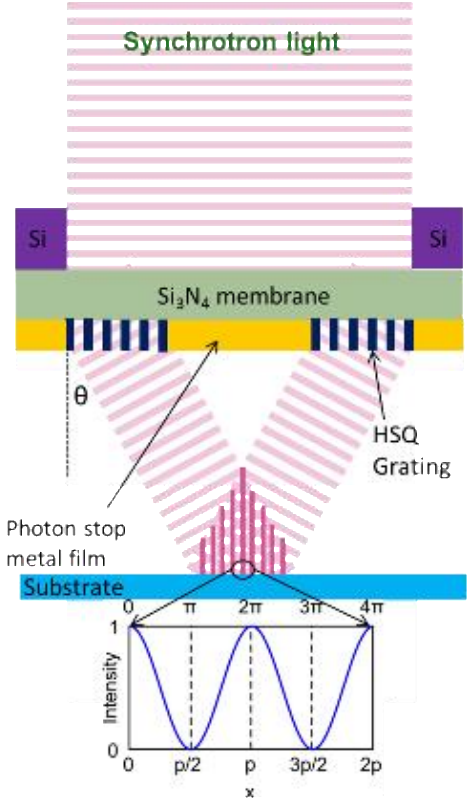

(b)

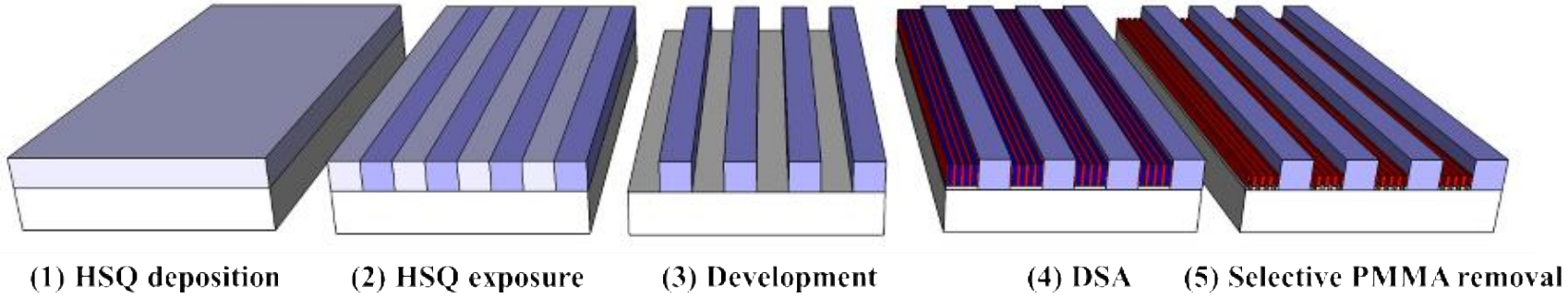

(c)

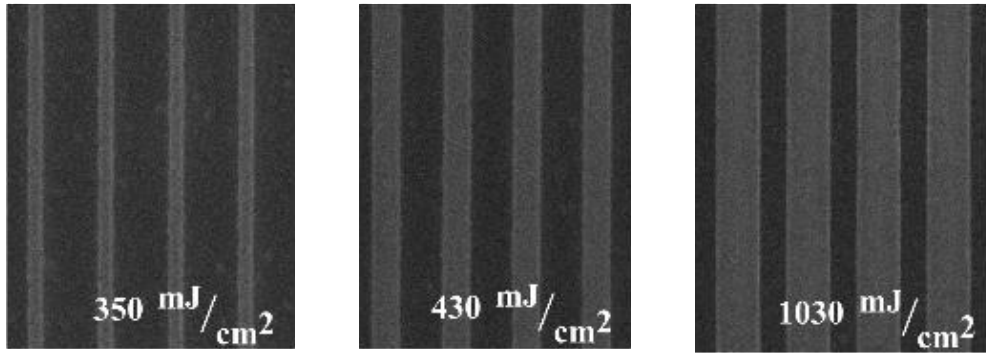

(d)

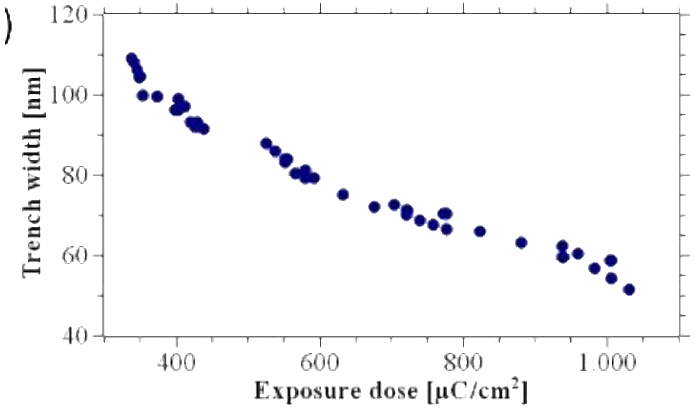

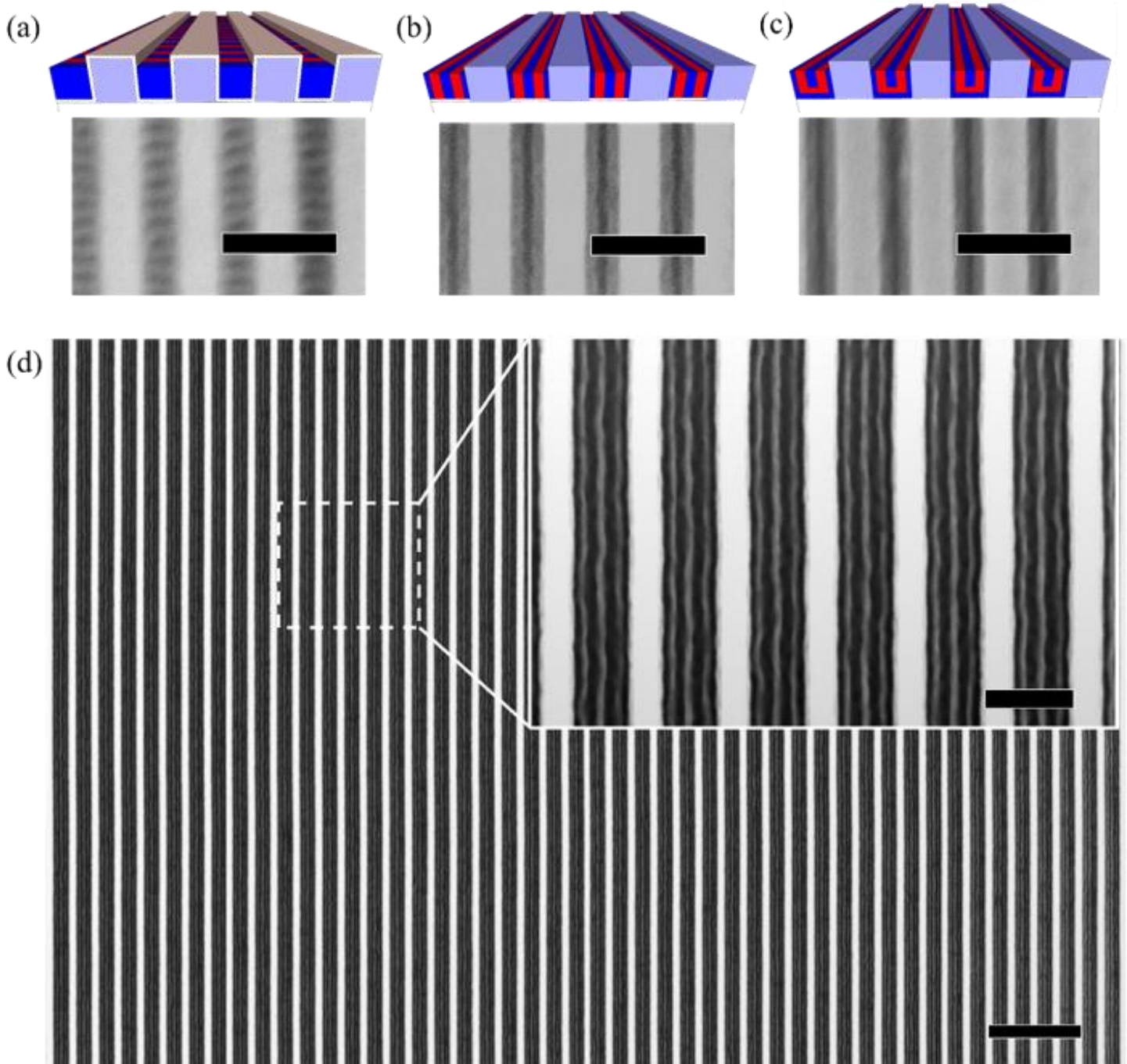
(a)
(b)
(c)
(d)

Examples of grapho-epitaxy

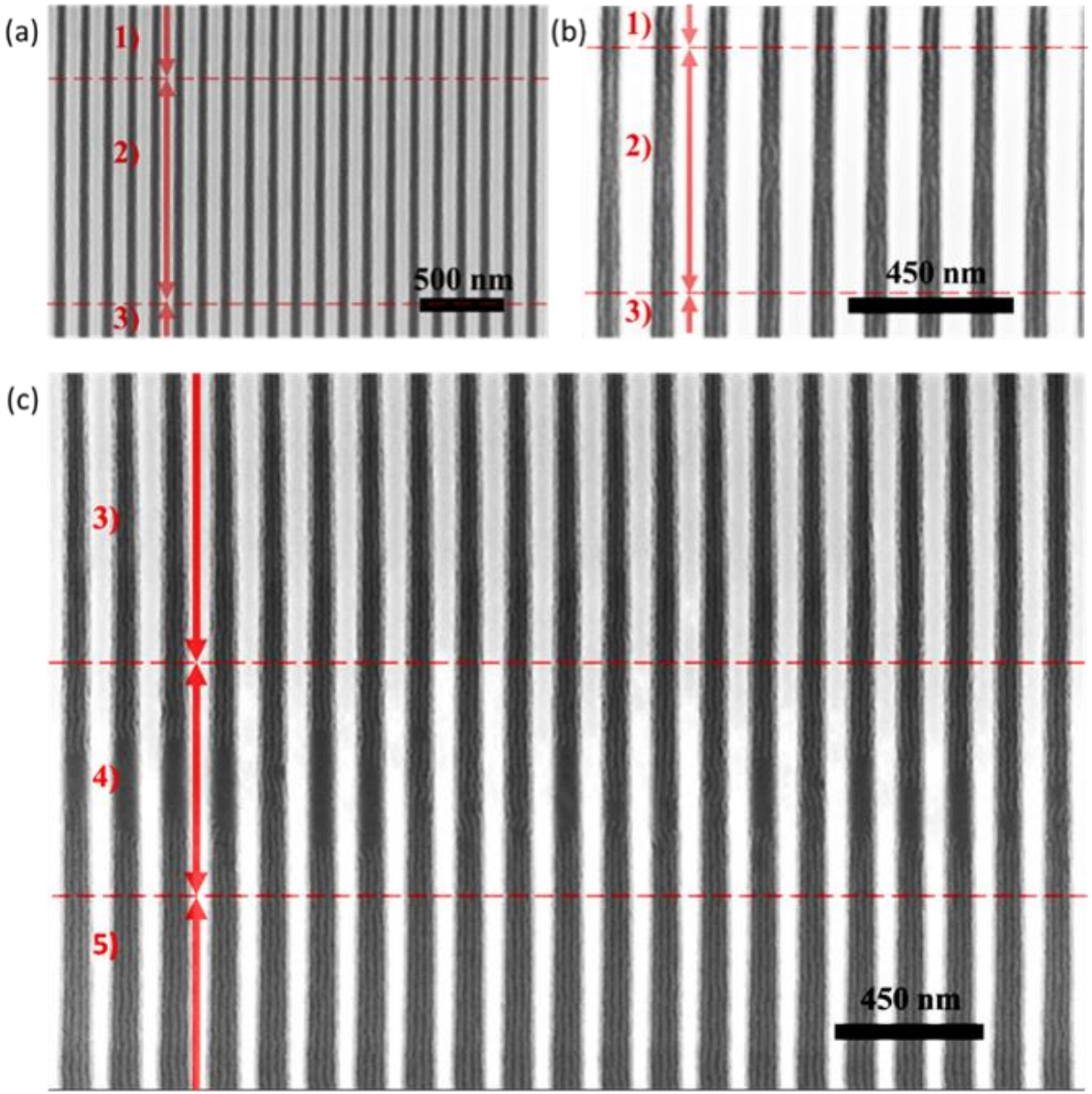

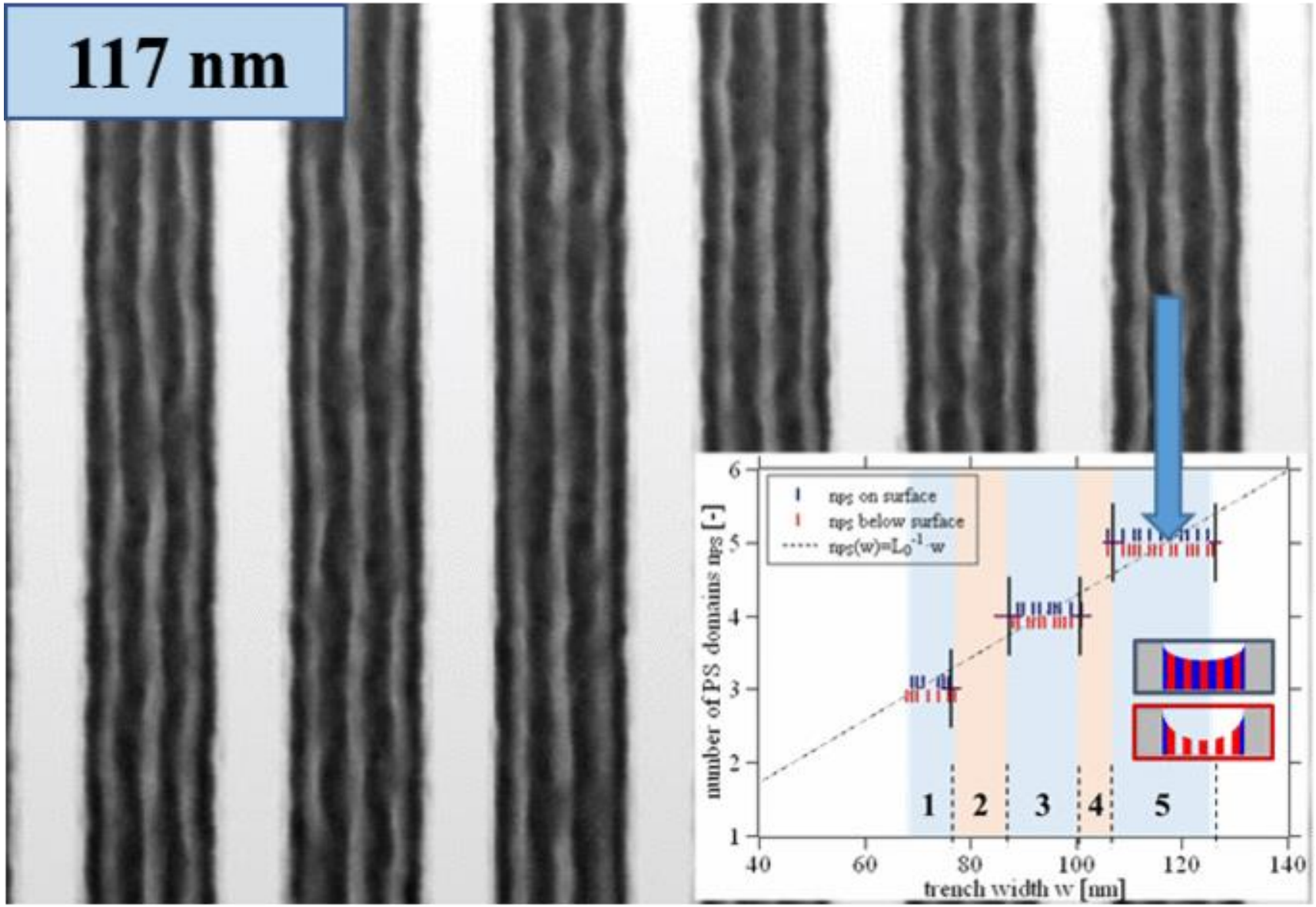
117 nm
nps on surface
nps below surface
nps(w)=L0-1·w
number of PS domains nps [-]
trench width w [nm]
1
2
3
4
5
40
60
80
100
120
140

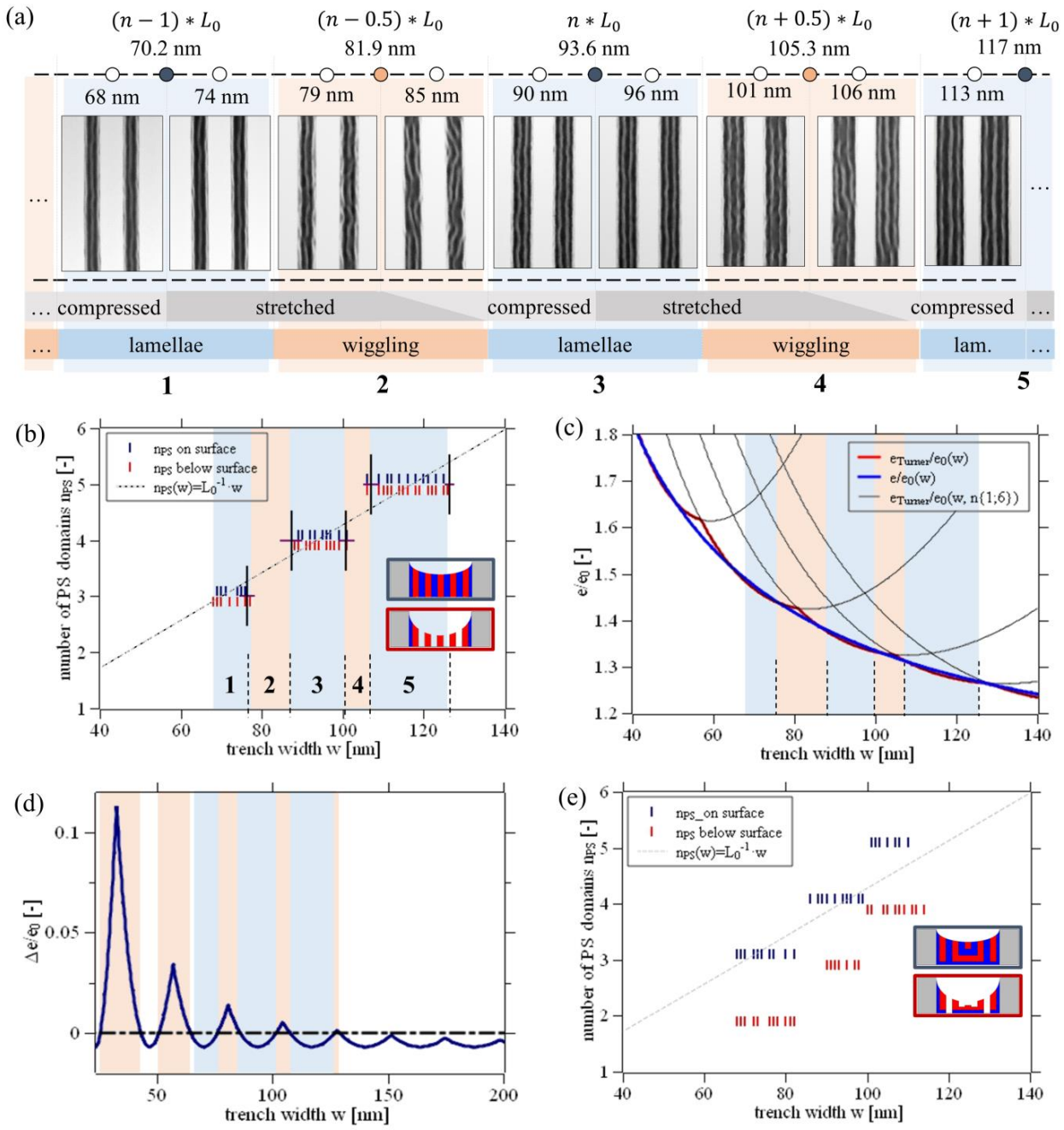
(a)
$(n-1)*L_0$ 70.2 nm
$(n-0.5)*L_0$ 81.9 nm
$n*L_0$ 93.6 nm
$(n+0.5)*L_0$ 105.3 nm
$(n+1)*L_0$ 117 nm
68 nm
74 nm
79 nm
85 nm
90 nm
96 nm
101 nm
106 nm
113 nm
… compressed
stretched
compressed
stretched
compressed …
… lamellae
wiggling
lamellae
wiggling
lam. …
1
2
3
4
5
(b)
nPS on surface
nPS below surface
nPS(w)=L0-1·w
number of PS domains nPS [-]
trench width w [nm]
(c)
eTurner/e0(w)
e/e0(w)
eTurner/e0(w, n{1;6})
e/e0 [-]
trench width w [nm]
(d)
Δe/e0 [-]
trench width w [nm]
(e)
nPS_on surface
nPS below surface
nPS(w)=L0-1·w
number of PS domains nPS [-]
trench width w [nm]

Graphoepitaxy process: Contact Shrink

guiding pattern ***RCP & BCP processing*** ***BCP self-assembly***

Guiding pattern

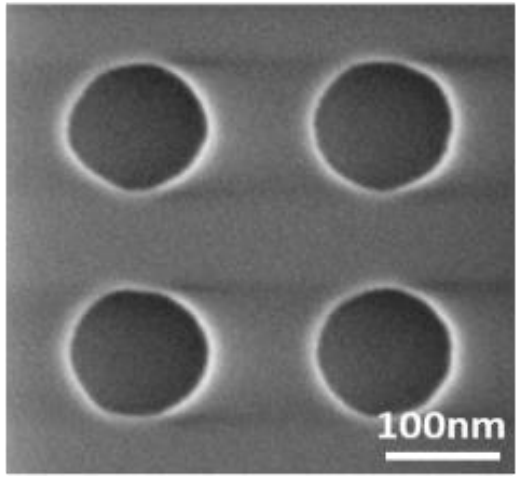

Self-assembled pattern

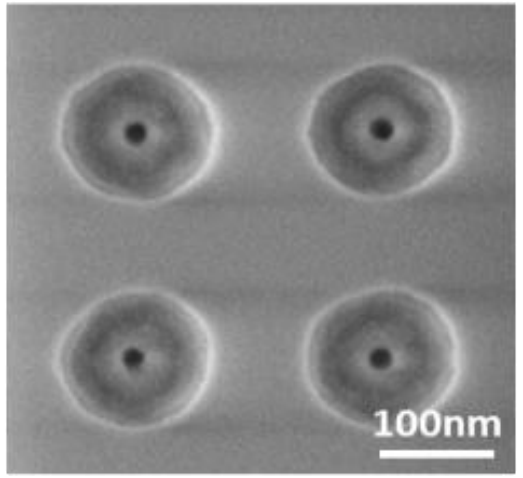

Tiron, R. et al. , “The potential of BCP’s DSA for contact hole shrink and contact multiplication”, Proc. SPIE, 8680, p. 868012 (2013)

Graphoepitaxy process: Contact Shrink

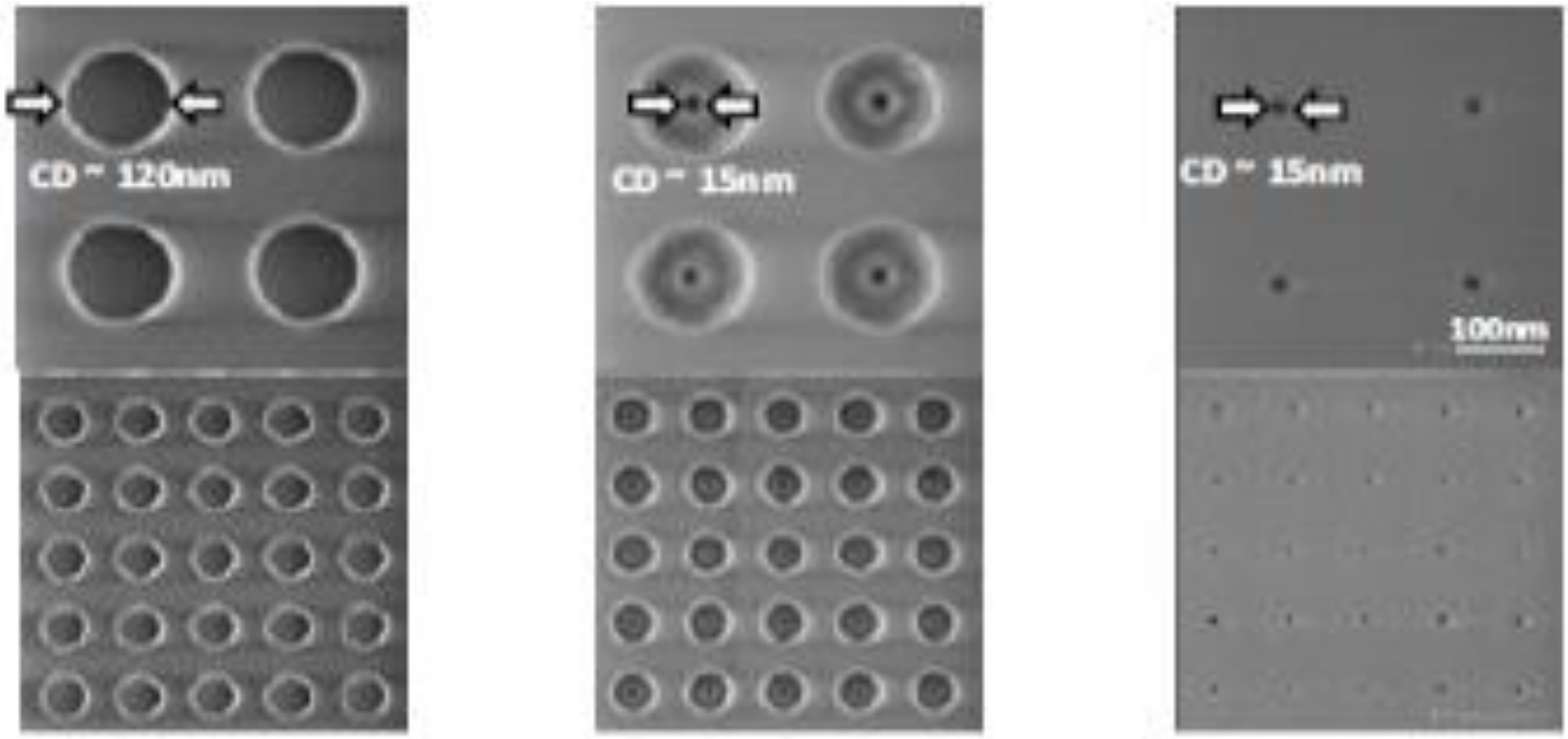

Tiron, R. et al. , “The potential of BCP’s DSA for contact hole shrink and contact multiplication”, Proc. SPIE, 8680, p. 868012 (2013)

Directed self-assembly: guiding patterns

Graphoepitaxy

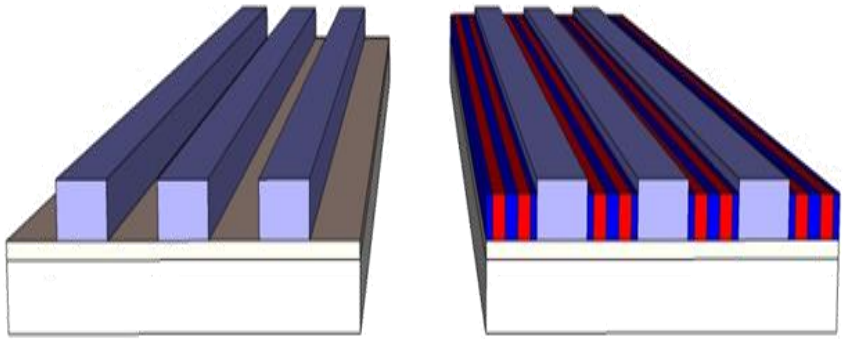

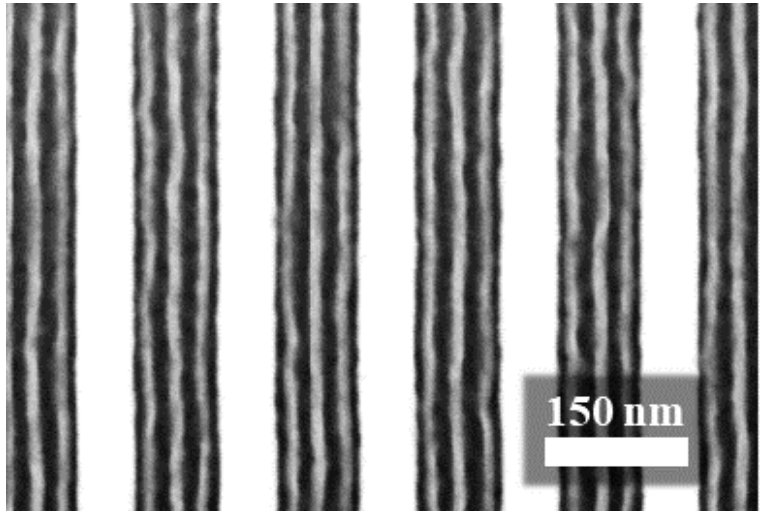

Chemoepitaxy

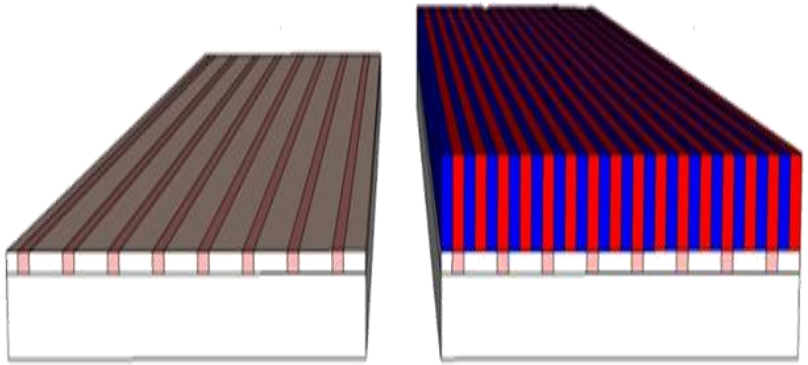

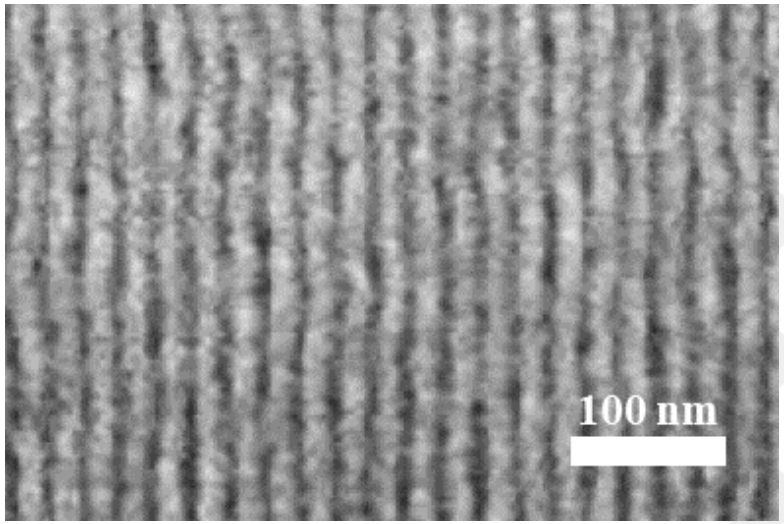

Chemical epitaxy process (i)

First chemoepitaxy approach: SAM functionalization

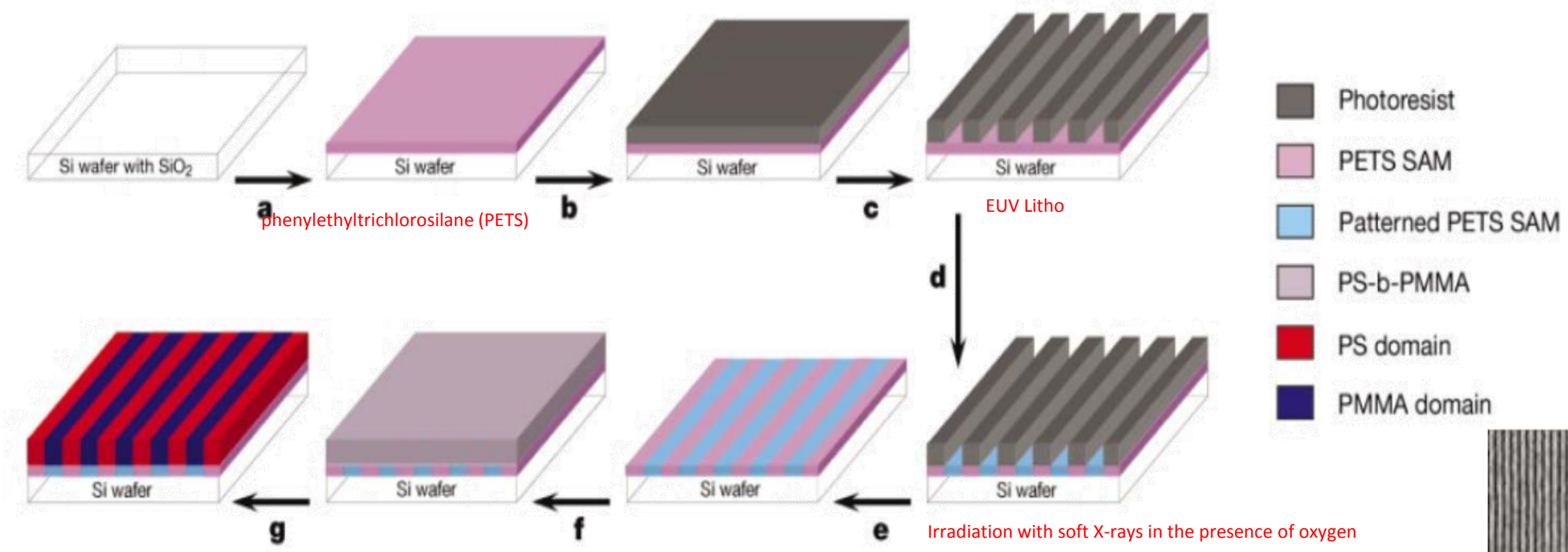

PS-b-PMMA copolymer
(Lo = 48 nm,film thickness of 60 nm)

Kim, S.O. de Pablo, Nealey. , "Epitaxial self-assembly of block copolymers on lithographically defined nanopatterned substrates", Nature, 424, 411-414 (2003)

Chemical epitaxy process (ii)

Creation of chemical guiding patterns by means of EBL and oxygen plasma functionalization

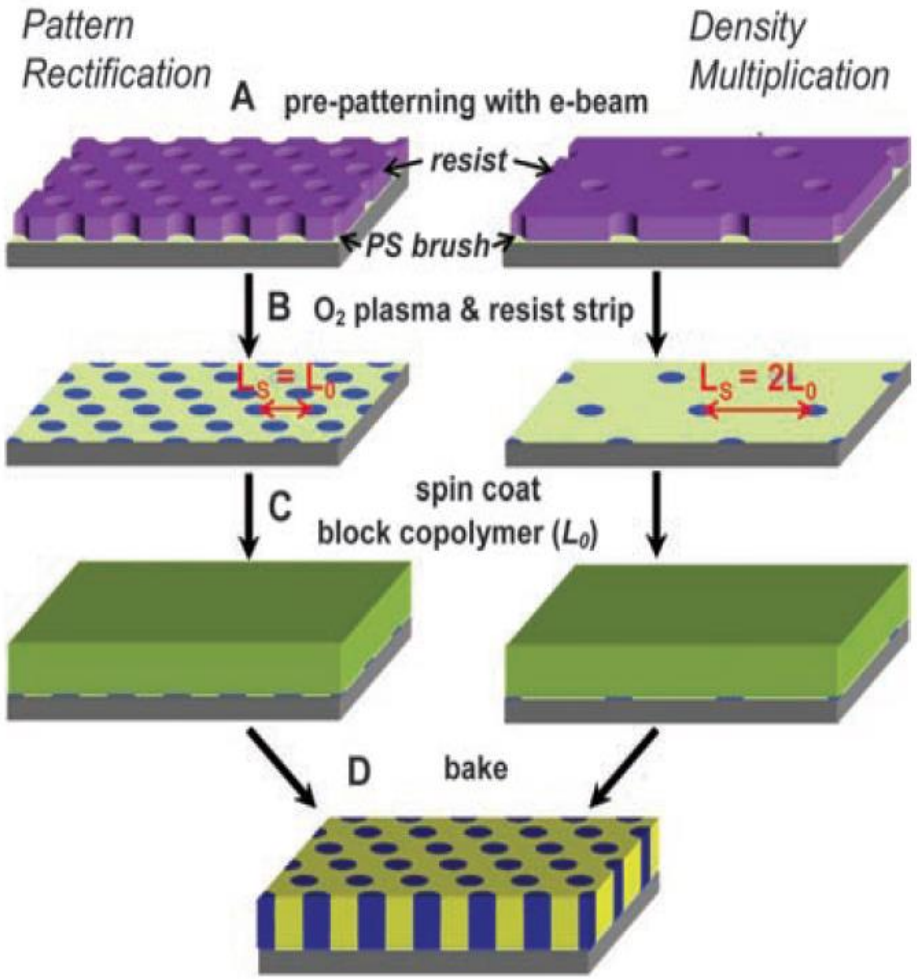

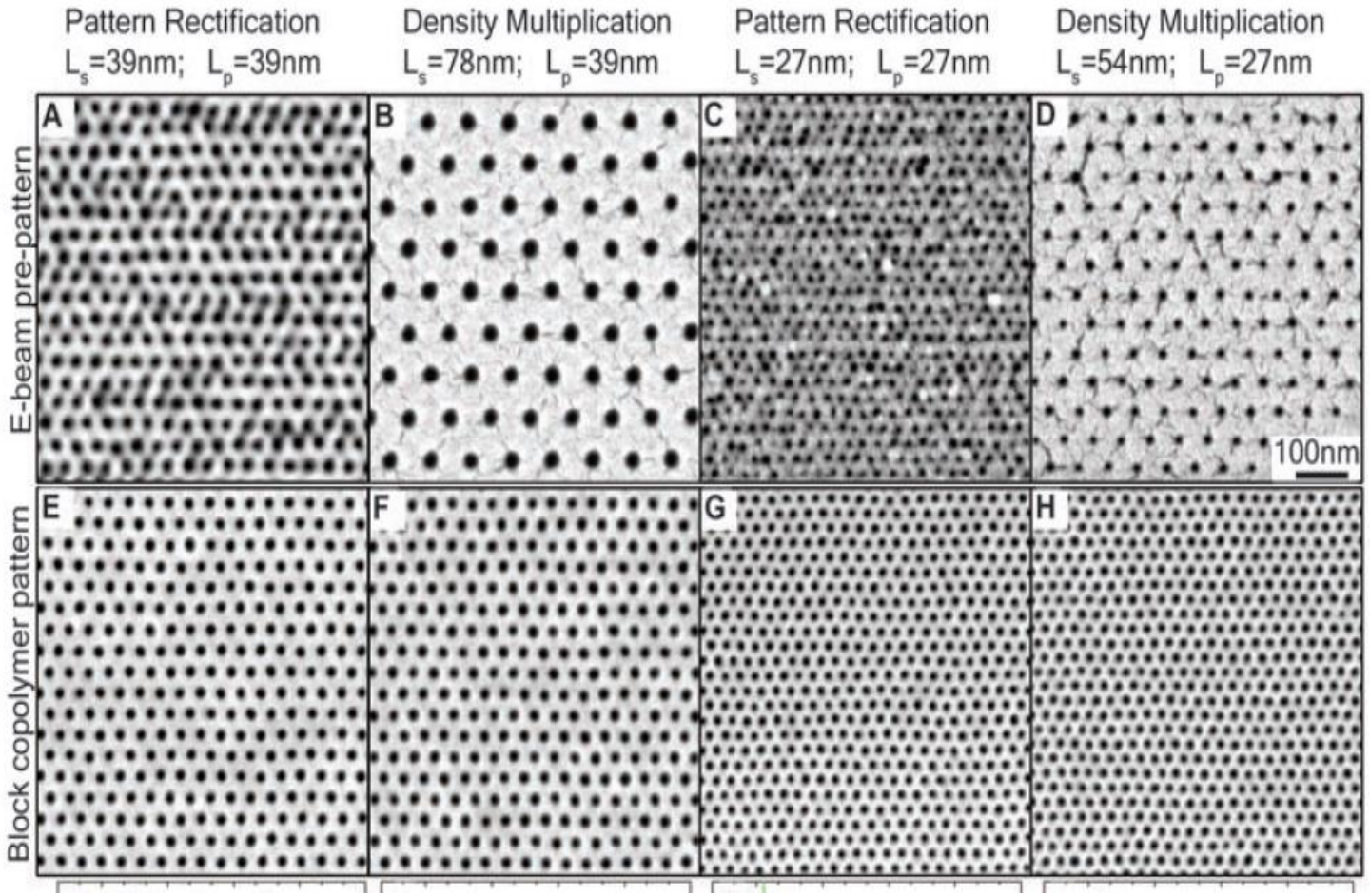

Ruiz, R. et al., "Density multiplication and improved copolymer assembly", Science, 321, 936-940 (2008)

Chemical epitaxy process (ii)

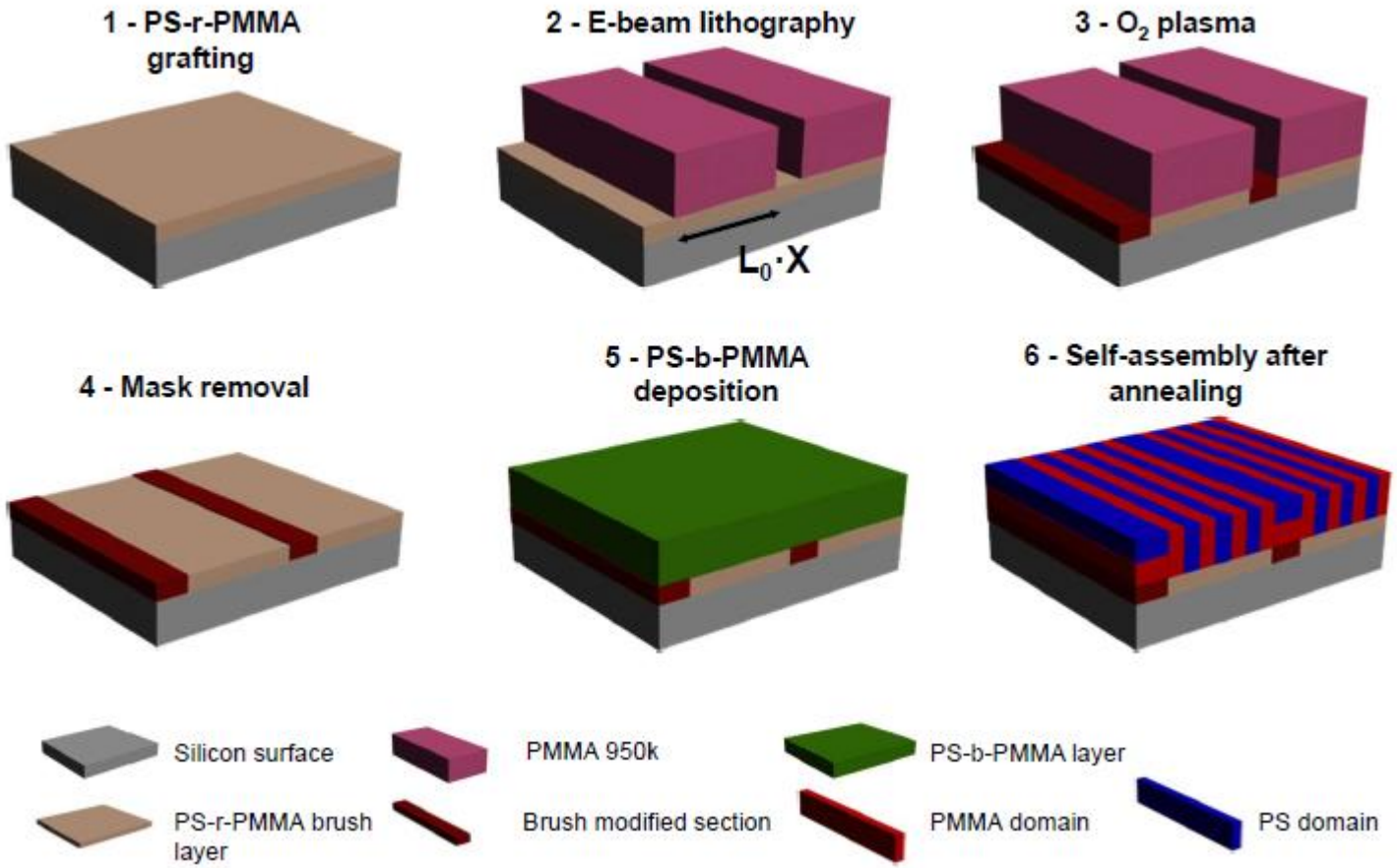

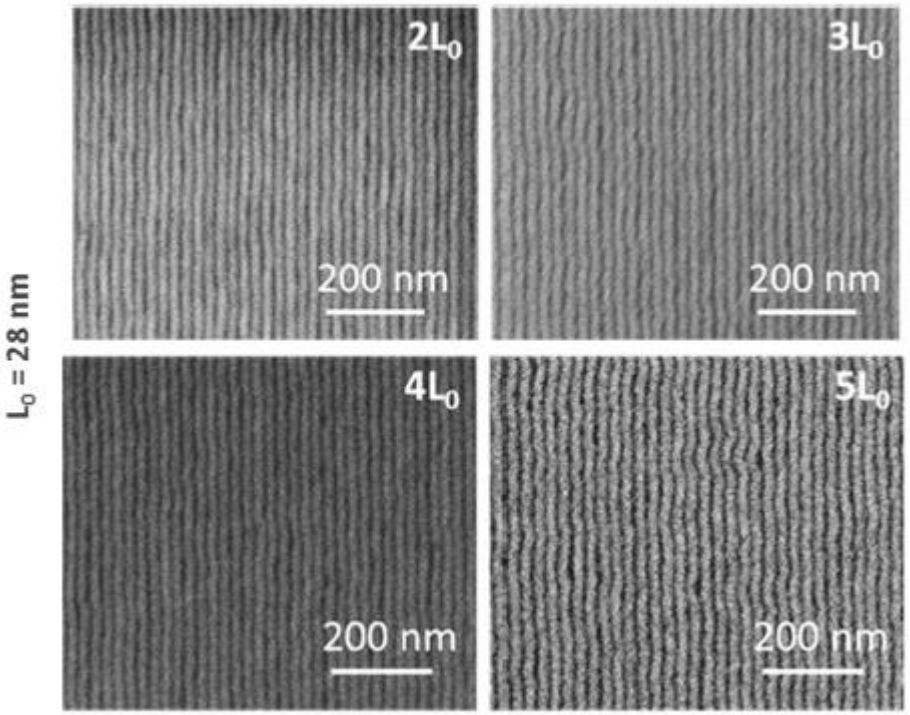

Oria et al. Microelectronic Engineering 2006

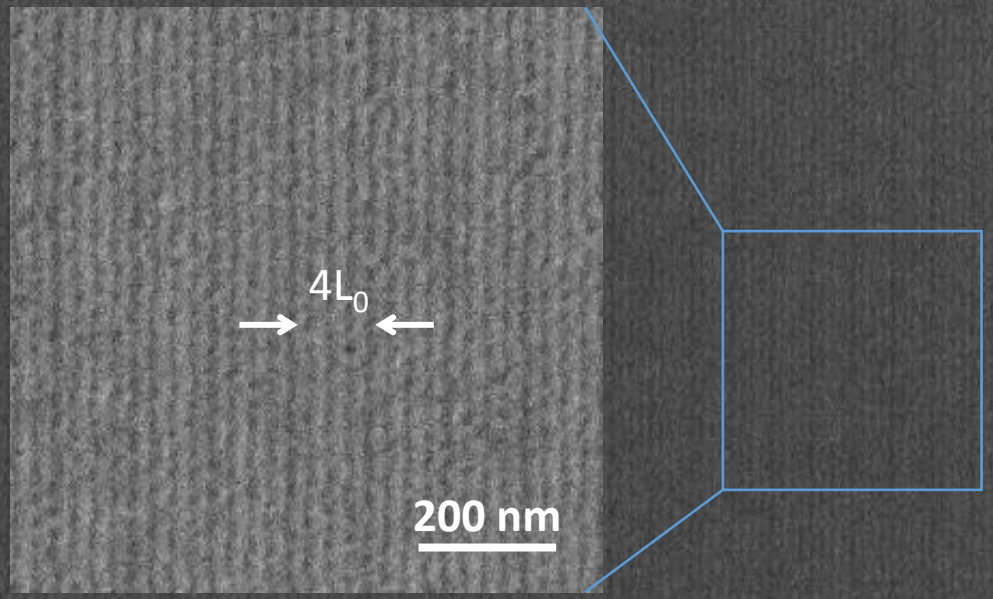

1 µm

Chemical epitaxy process (iii)

Creation of a layer of two polymers (LINE process)

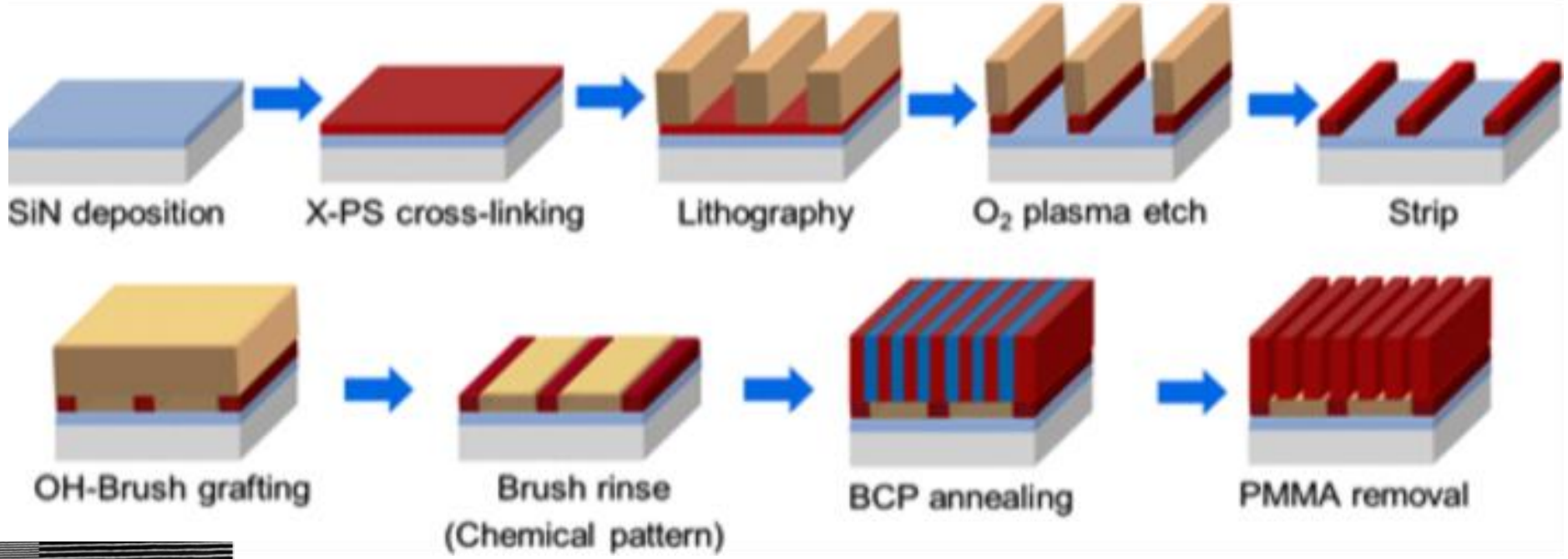

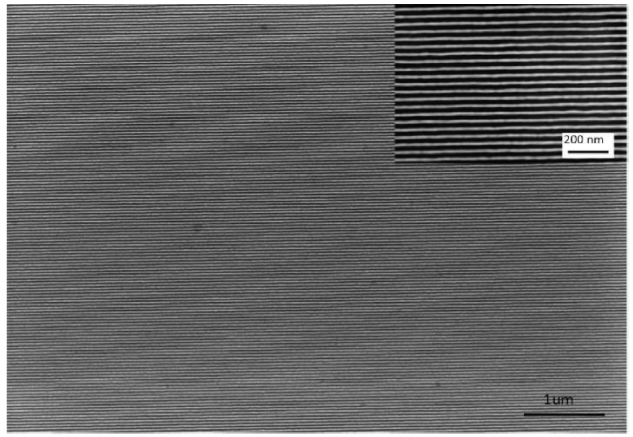

Liu, C-C. et al. , “Fabrication of Lithographically Defined Chemically patterned polymer brushes and Mats”, Macromolecules, 44, 1876-1885 (2011)

Chemical epitaxy process (iv)

Creation of pinning sites in a neutral layer(AZ Smart process)

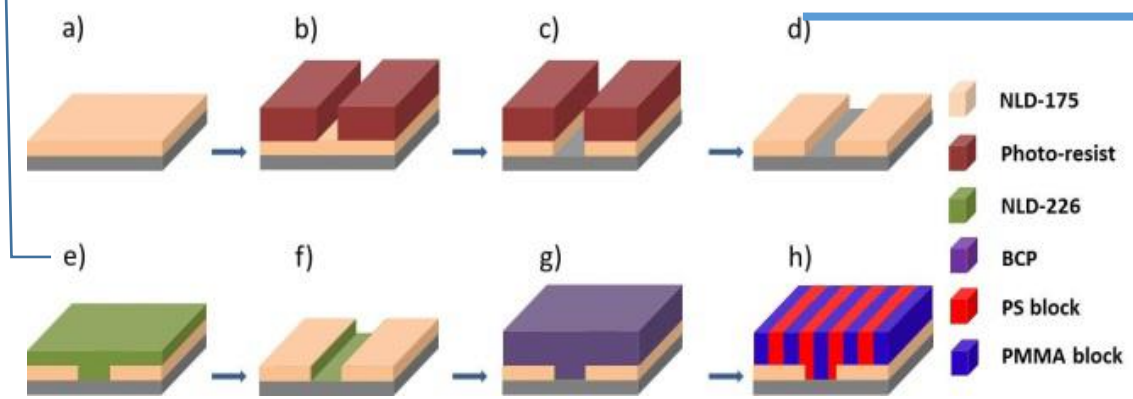

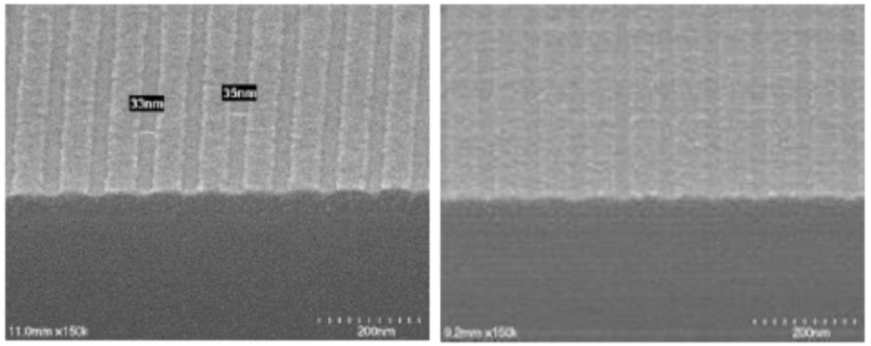

Fig. 7. xSEM of AZ SMART chemical pre-pattern structure a) before pinning material brushing and b) after pinning material brushing.

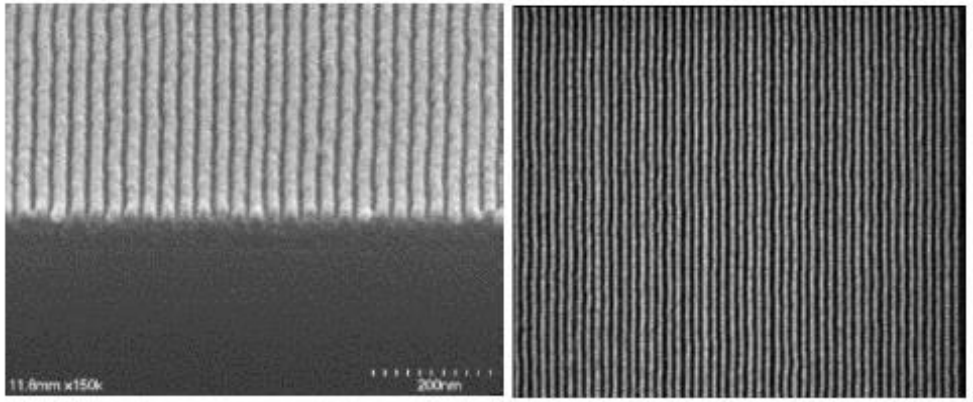

Kim, Jihoon et al., "The Smart TM process for Directed Block Co-Polymer Self-Assembly". Journal of Photopolymer Science and Tecnology, 26, 573-579 (2013)

Pattern transfer

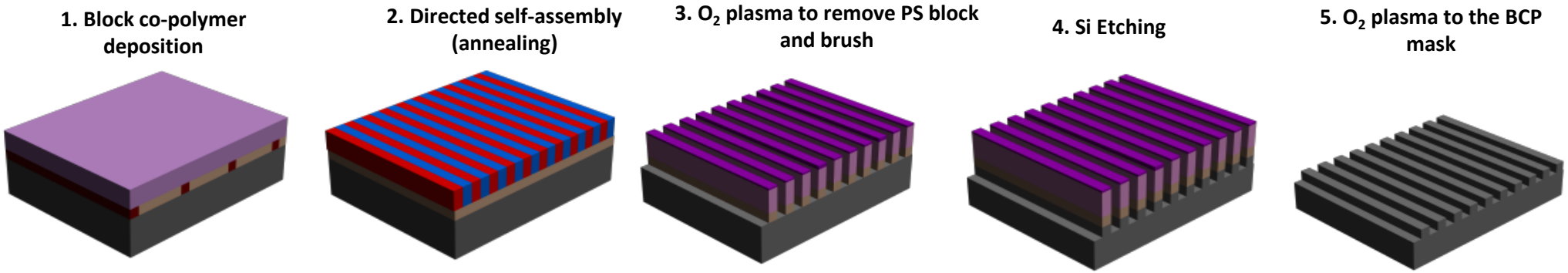

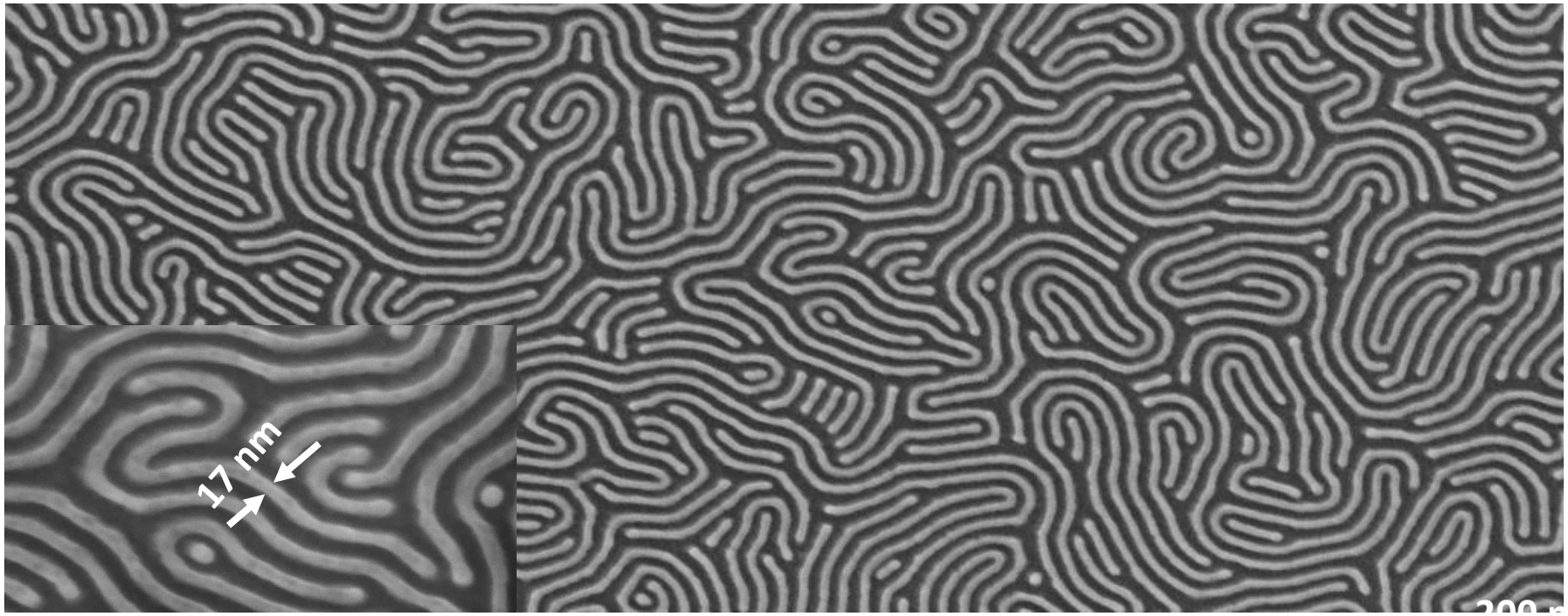

Pattern transfer. Atomic layer deposition (ALD)

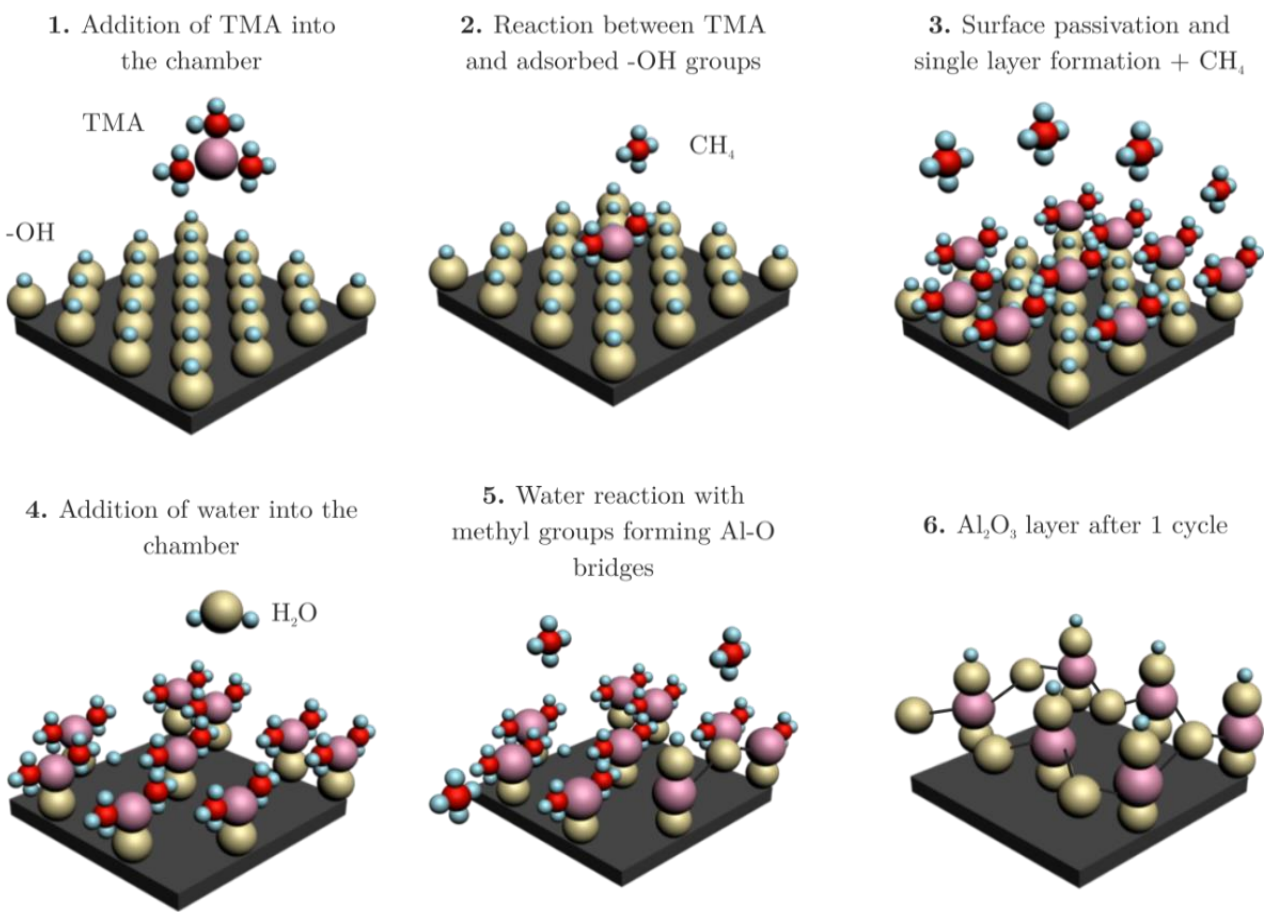

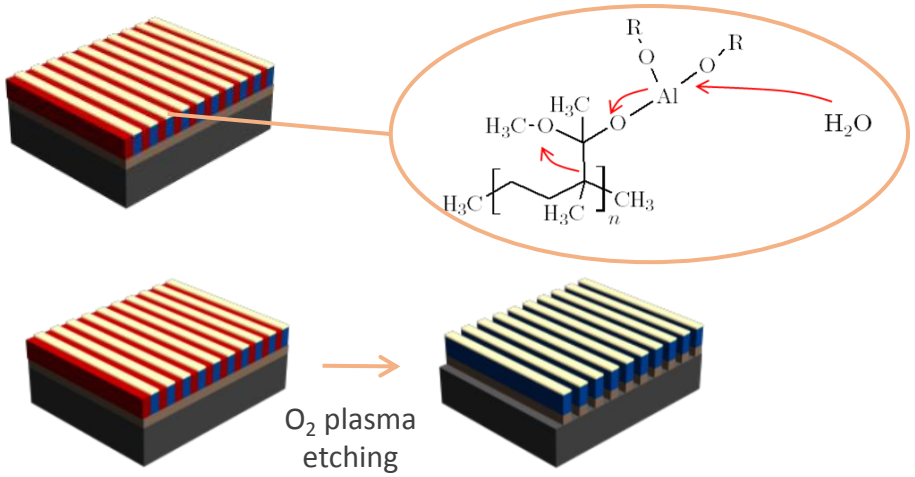

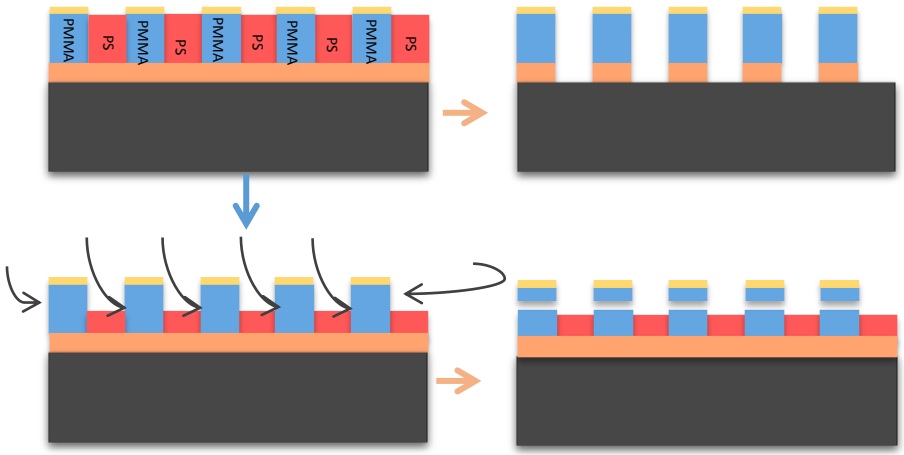

$Al(CH_3)_{3(g)} + 3/2\ H_2O_{(g)} \rightarrow 1/2\ Al_2O_{3(s)} + 3CH_{4(g)}$,

$|\text{-OH} + Al(CH_3)_{3(g)} \rightarrow |\text{-O-}Al(CH_3)_2 + CH_{4(g)}$,

$|\text{-O-}Al(CH_3)_2 + 2H_2O_{(g)} \rightarrow |\text{-O-}Al(OH)_{2\ (s)} + 2CH_{4(g)}$,

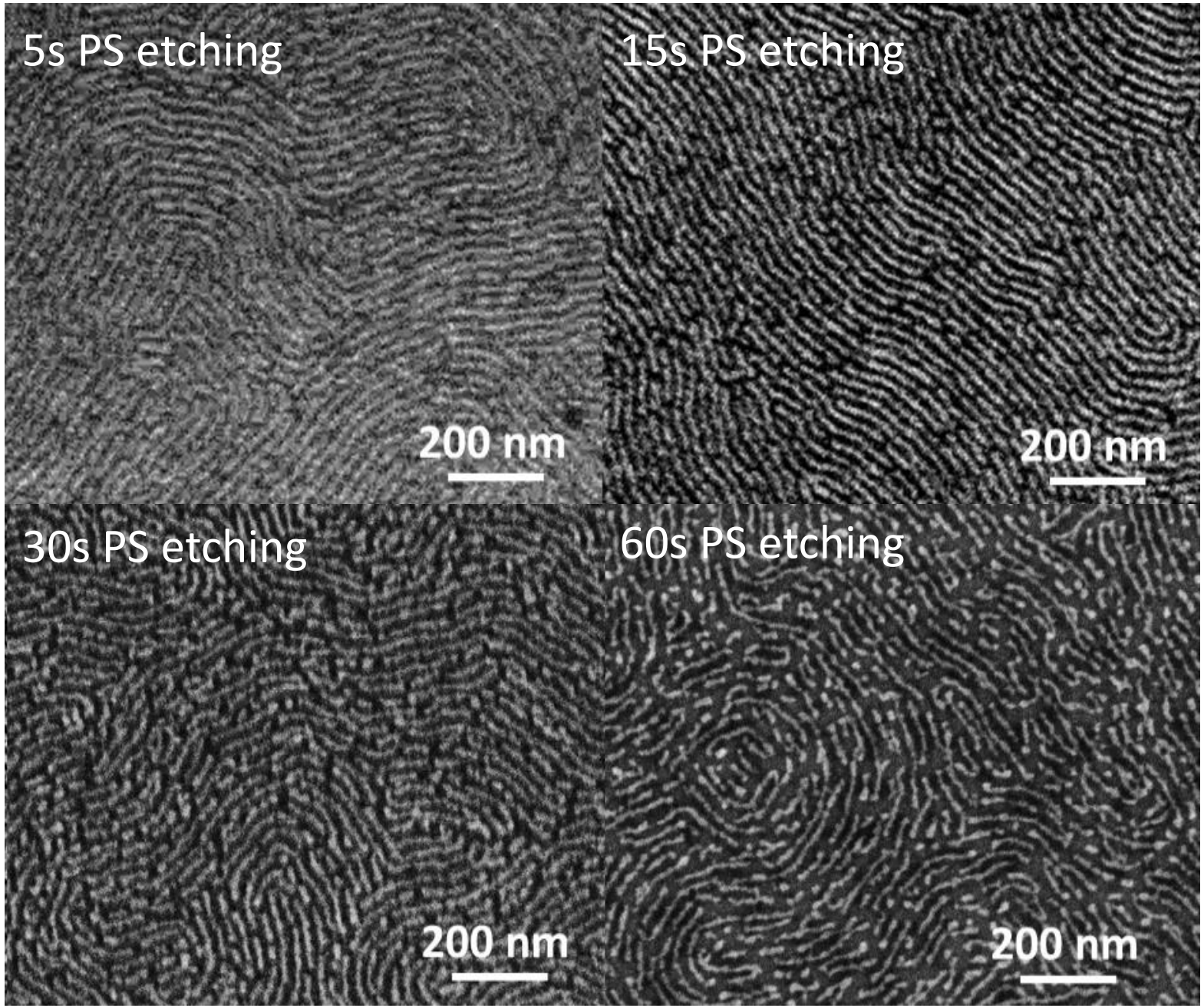
5s PS etching
200 nm
15s PS etching
200 nm
30s PS etching
200 nm
60s PS etching
200 nm

Pattern transfer. Sequential infiltration synthesis (SIS)

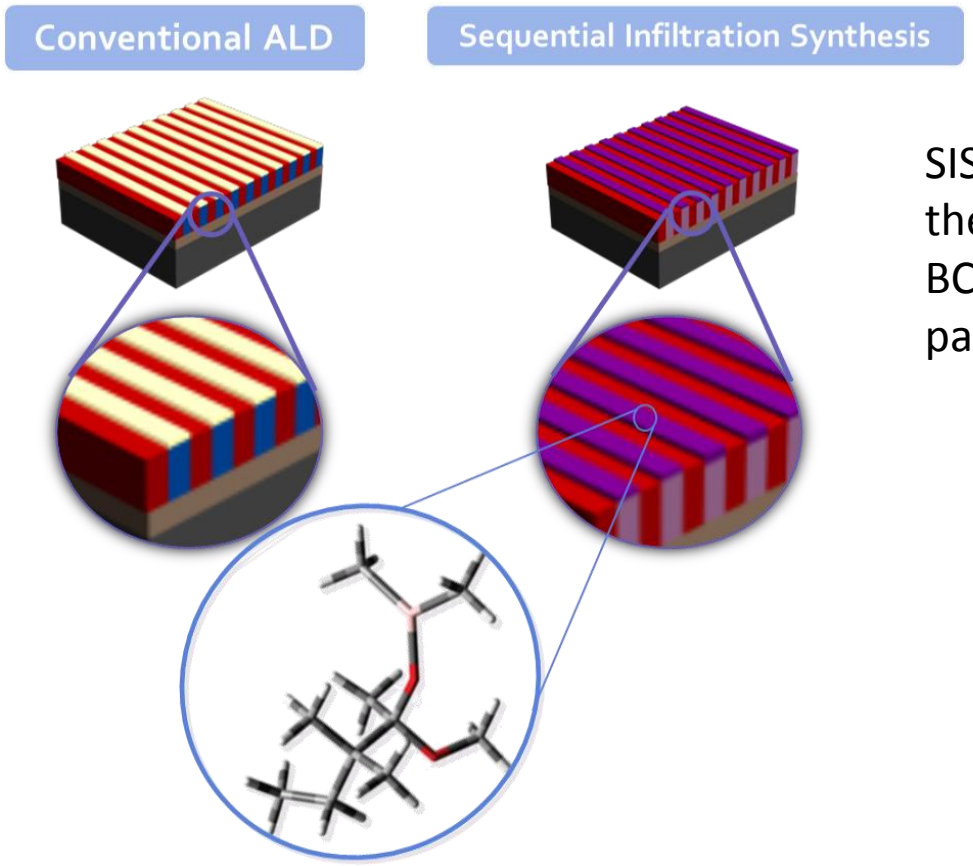

SIS offers an alternative ALD mechanism which allows the infiltration of the precursors into the polymer. It is used to selectively infiltrate one BCP domain, and use this protective component as a hard mask to pattern transfer

Tseng, Y.-C., *et al.* Enhanced Block Copolymer Lithography Using Sequential Infiltration Synthesis. *J. Phys. Chem. C* **115,** 17725–17729 (2011).

- The dosage times are of the order of several minutes to ensure diffusion into the bulk
- By using SIS the bulk of **PMMA** domains become **harder** (not only the surface)

Pattern transfer (ii). Sequential infiltration synthesis (SIS)

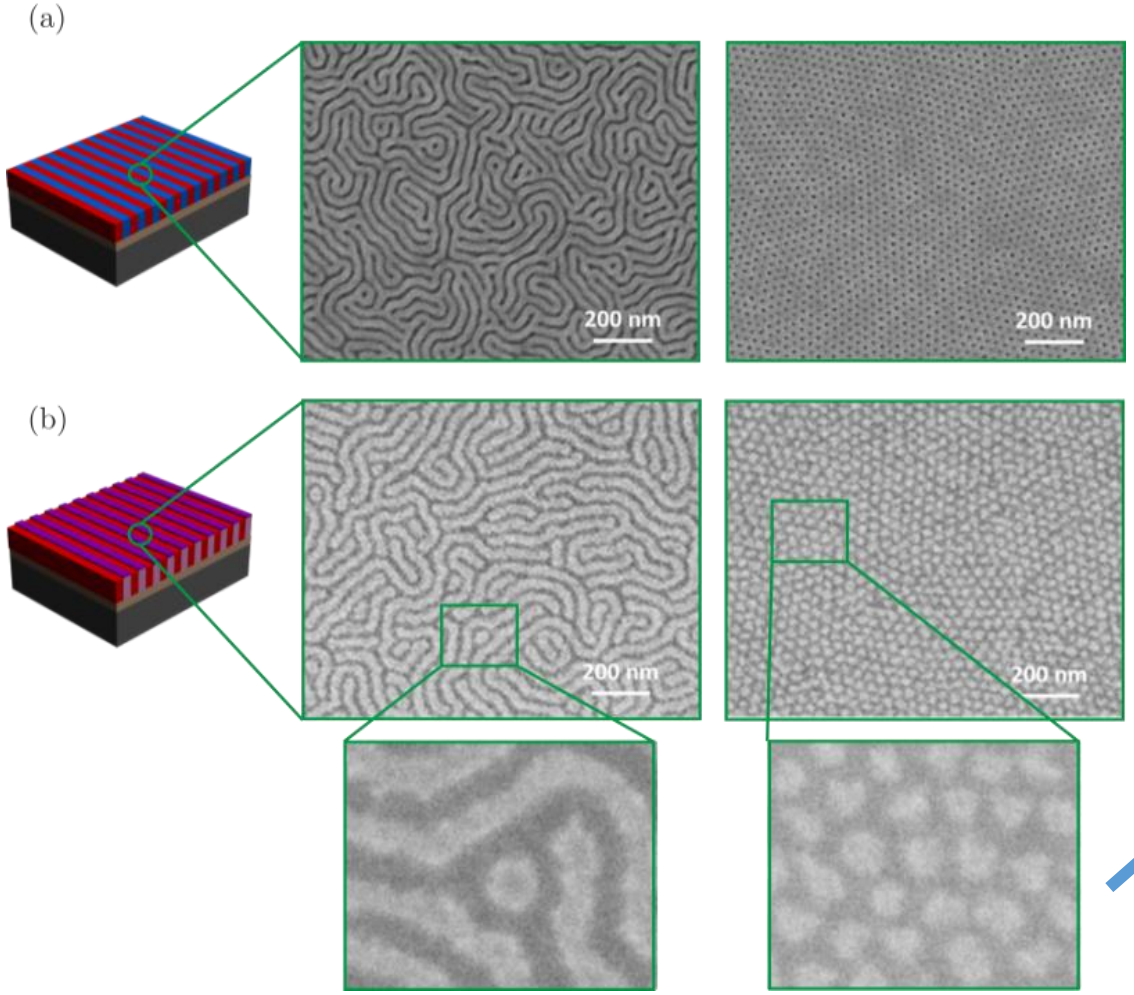

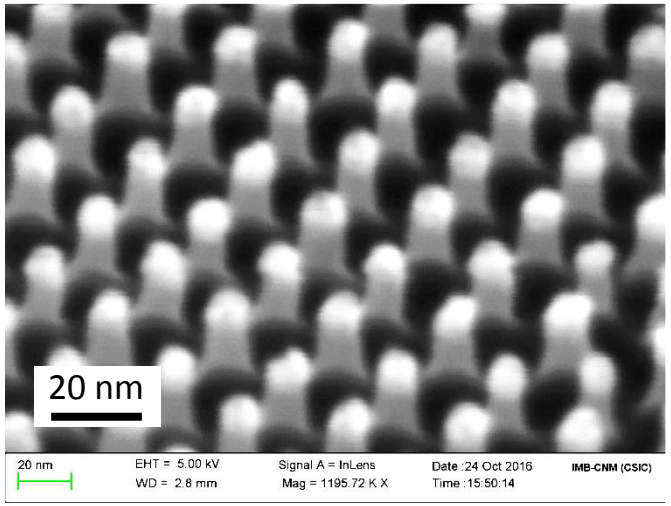

PMMA modification by Sequential Infiltration Synthesis (SIS)

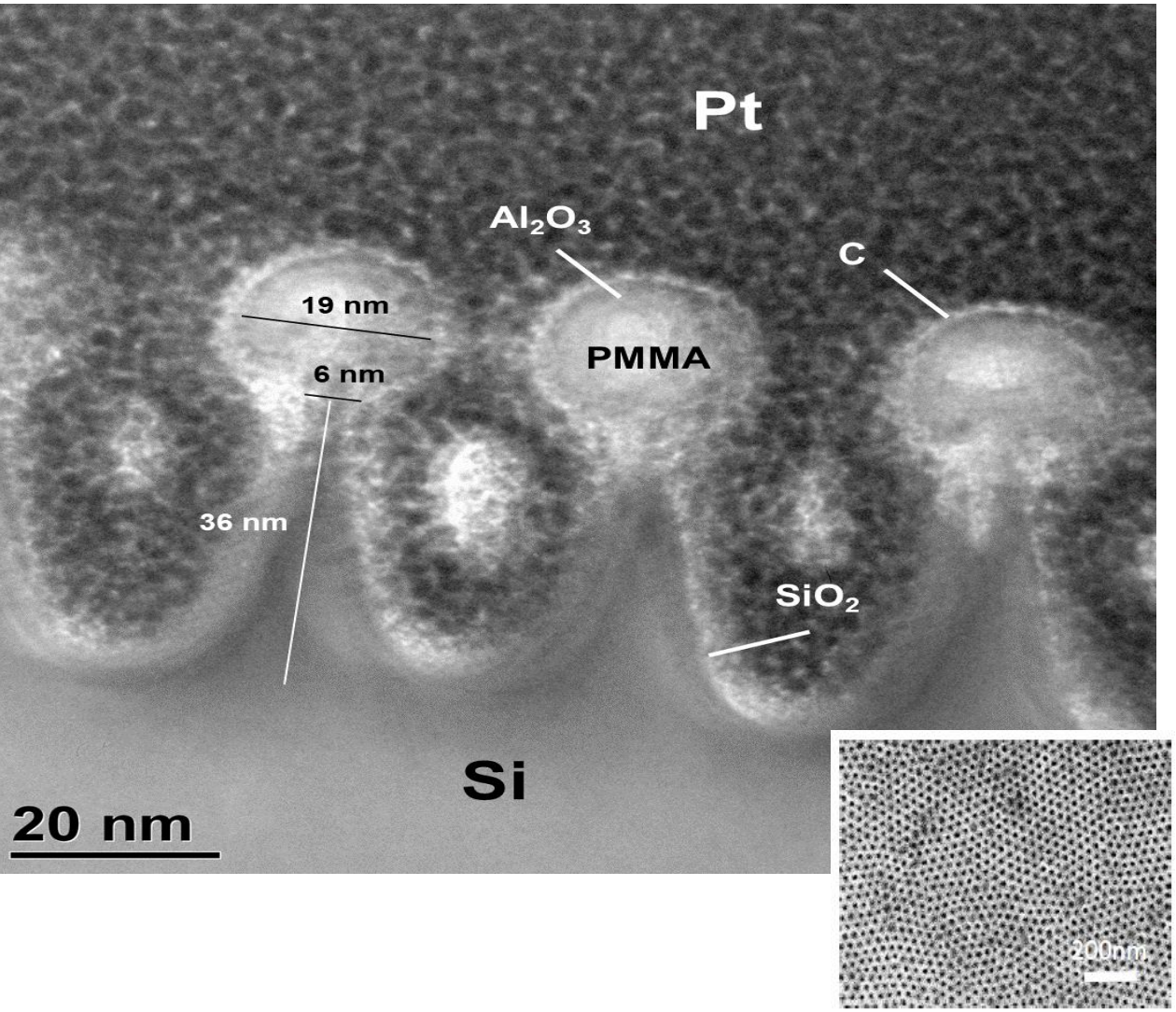

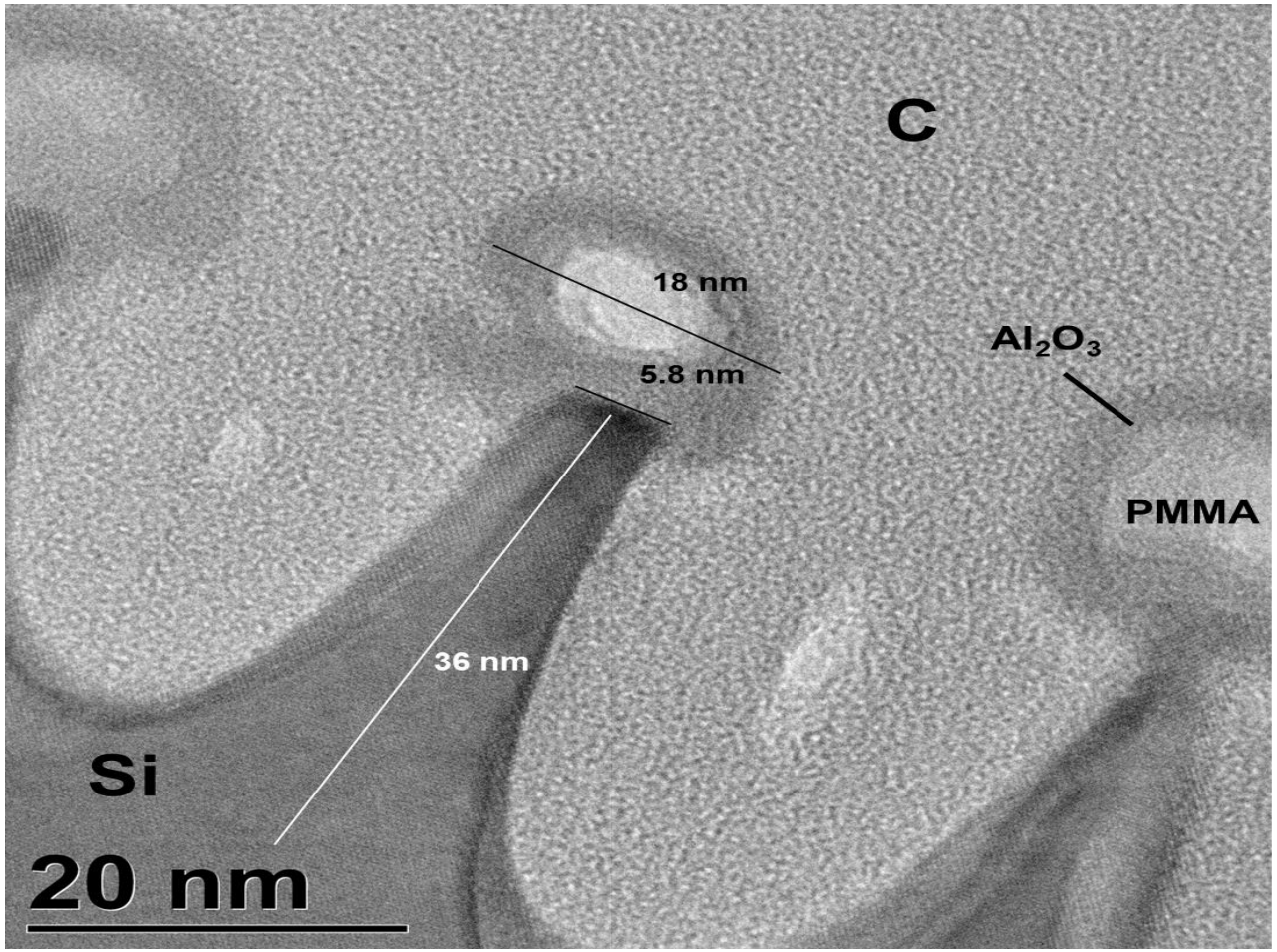

DSA applications

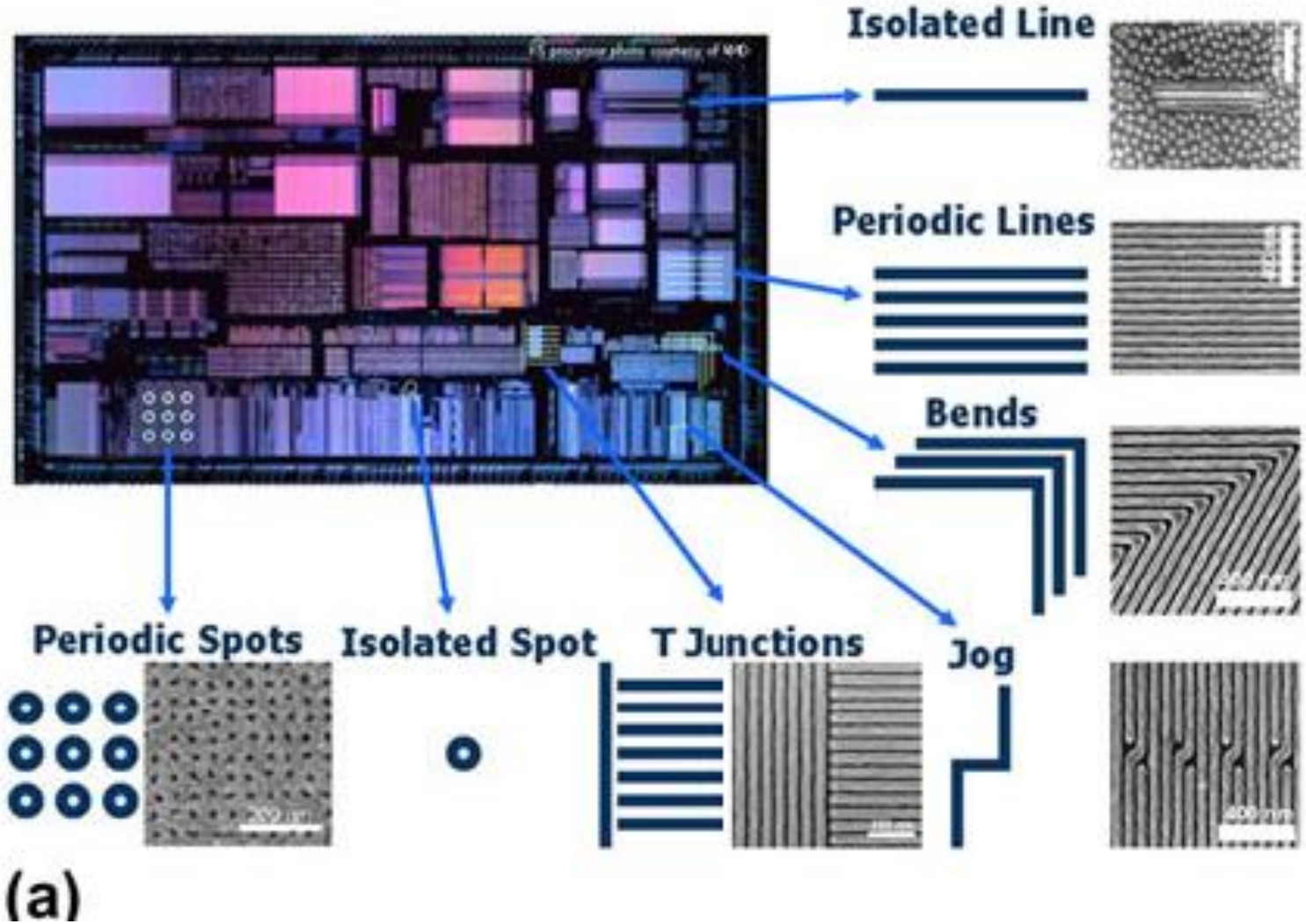

Directed block copolymer self-assembly for nanoelectronics fabrication.
Daniel J.C. Herr. J. Mater. Res., 26, 122, , 2011

Applications

Bit patterned media

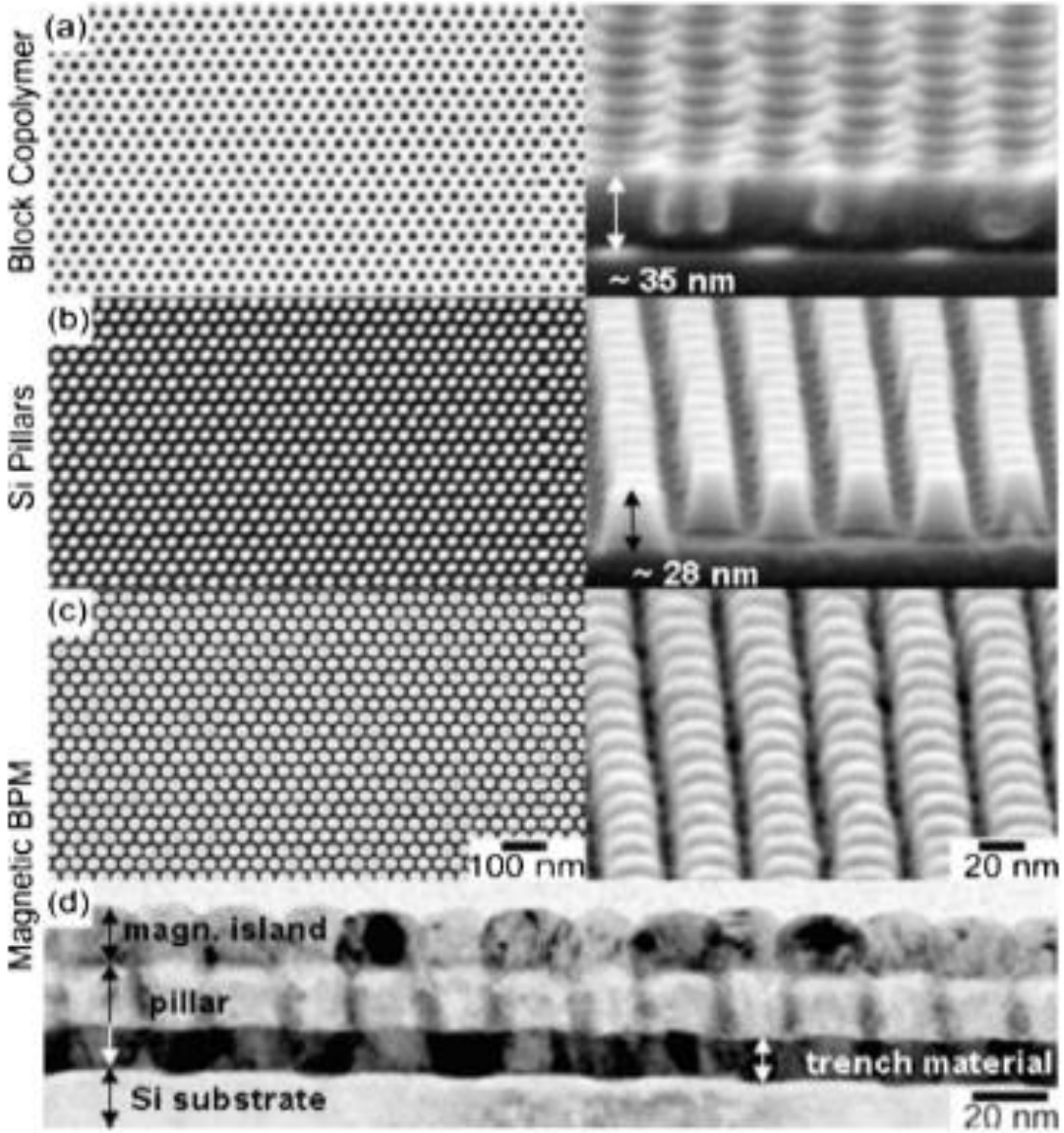

FIG. 1. 0.5 Tbit/in^2 (L_o=38 nm) BPM array consisting of MLs deposited onto Si pillar substrates fabricated via e-beam directed assembly of block copolymer films. SEM micrographs of (a) the block copolymer film after selective removal of the PMMA cylinder cores, (b) Si pillars after Cr lift-off using the template in (a) and subsequent reactive ion etching, and (c) magnetic BPM after depositing a Co/Pd ML thin film onto the pillar structures (left: top view, right: section view at 85° angle). (d) Bright field TEM cross-sectional image through two consecutive rows of bits (into the image plane) that are 180° phase shifted with respect to each other.

O. Hellwig, …, R: Ruiz (Htachi). Appl.Phys.Lett. 96, 052511 (2010)

Two-Dimensional Pattern Formation Using Graphoepitaxy of PS-b-PMMA Block Copolymers for Advanced FinFET Device and Circuit Fabrication

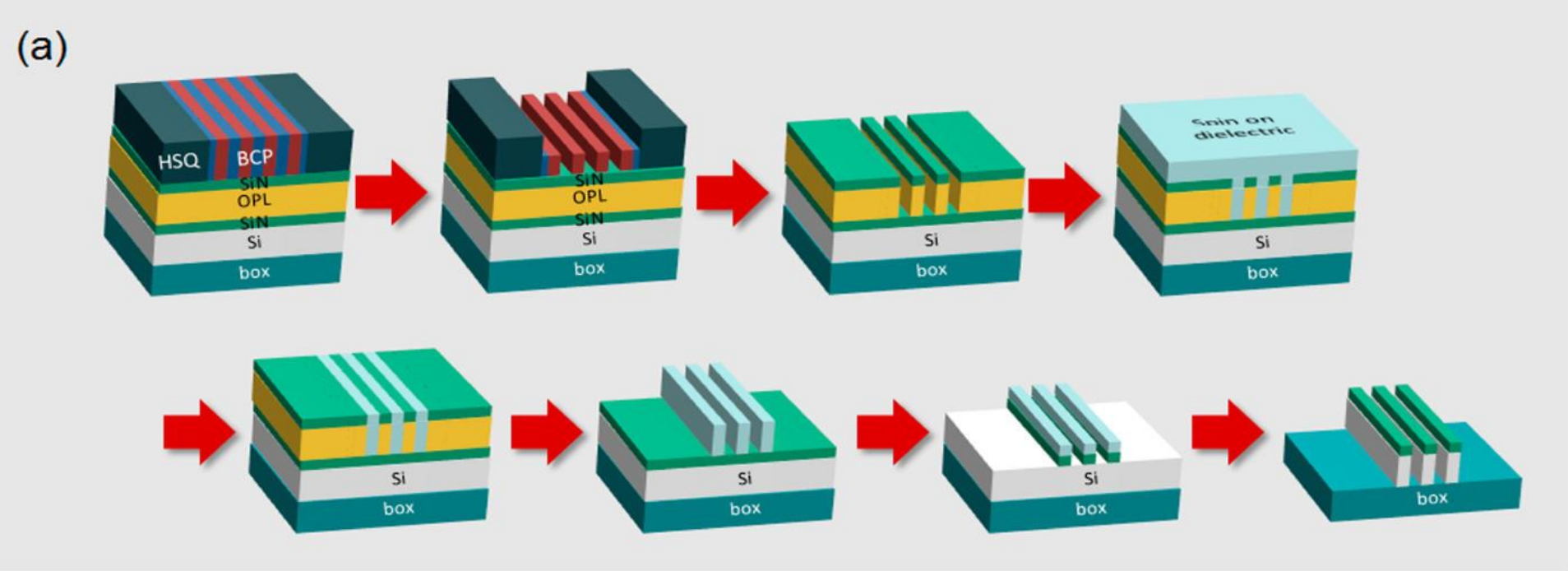

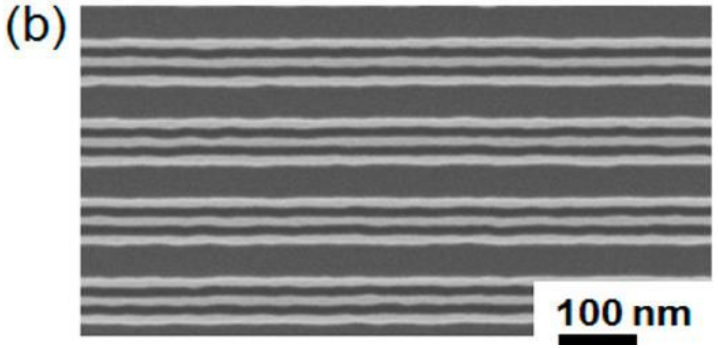

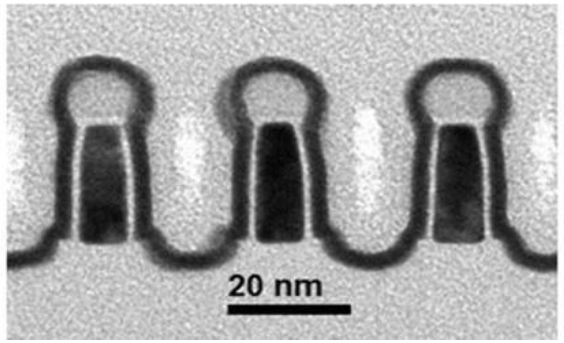

H. Tsai et al. Nanoletters 8, 5227 (2014) (IBM)

Two-Dimensional Pattern Formation Using Graphoepitaxy of PS-b-PMMA Block Copolymers for Advanced FinFET Device and Circuit Fabrication

(a)

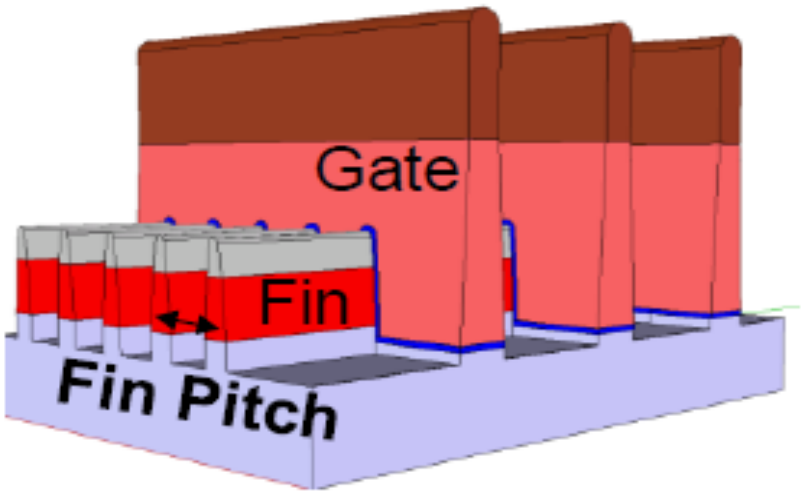

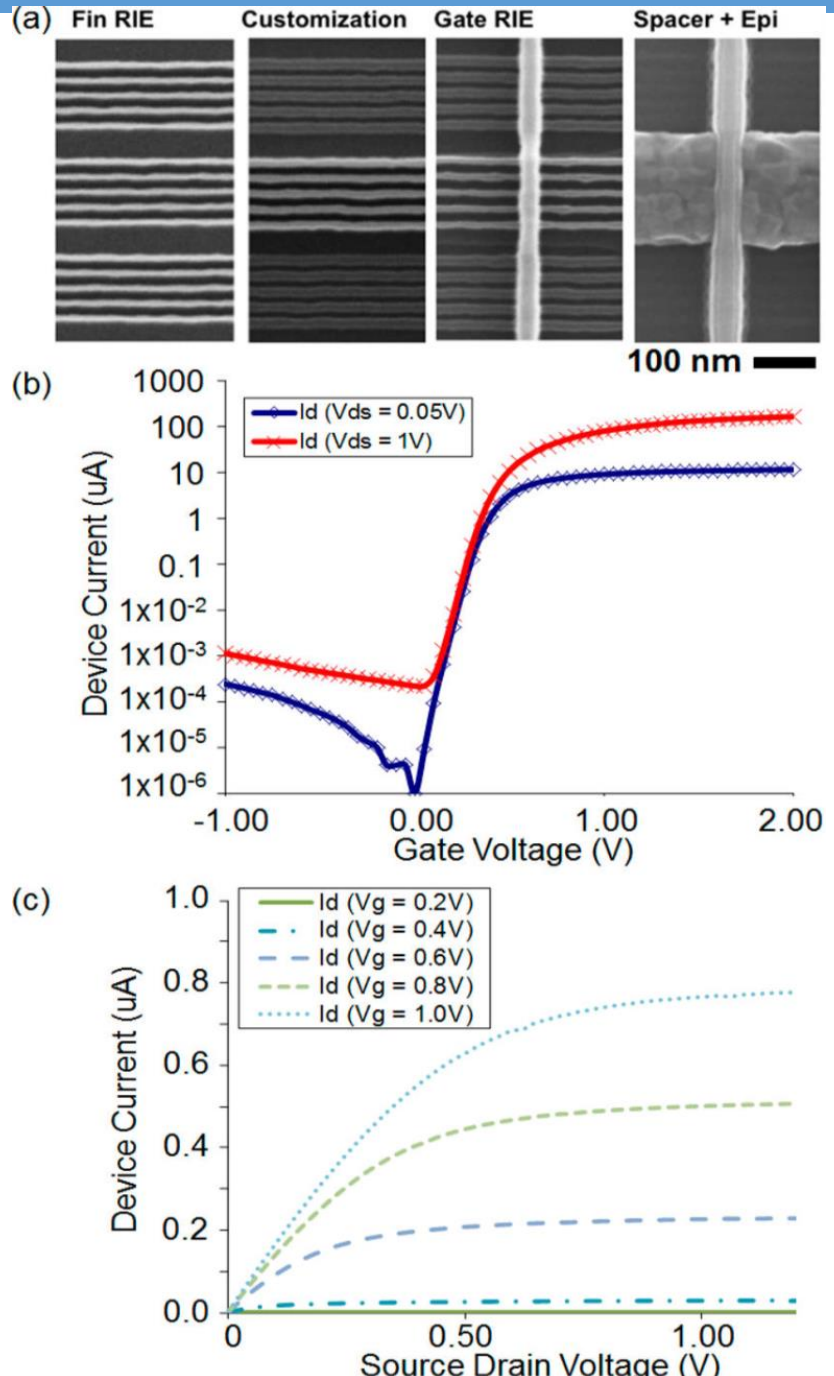

H. Tsai et al. Nanoletters 8, 5227 (2014) (IBM)

GRAPHENE NANOMESH

Graphene has significant potential for application in electronics, but cannot be used for effective field-effect transistors operating at room temperature because it is a semi-metal with a zero bandgap.

Processing graphene sheets into nanoribbons with widths of less than 10 nm can open up a bandgap that is large enough for room-temperature transistor operation, but nanoribbon devices often have low driving currents or transconductances

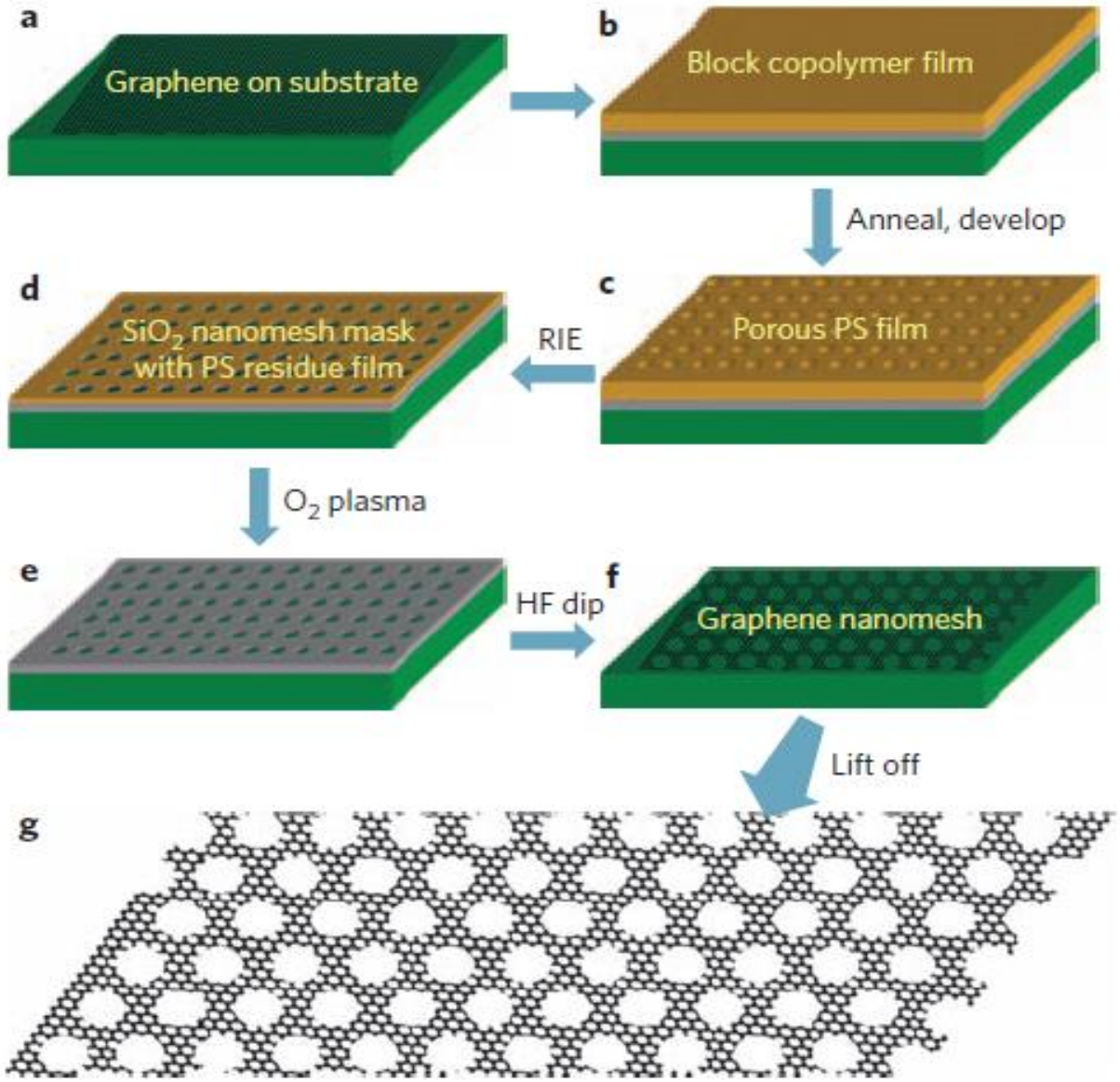

J. Bai et al. Nature Nanotechnology 5, 190 (2010)

J. Bai et al.
Nature Nanotechnology 5, 190 (2010)

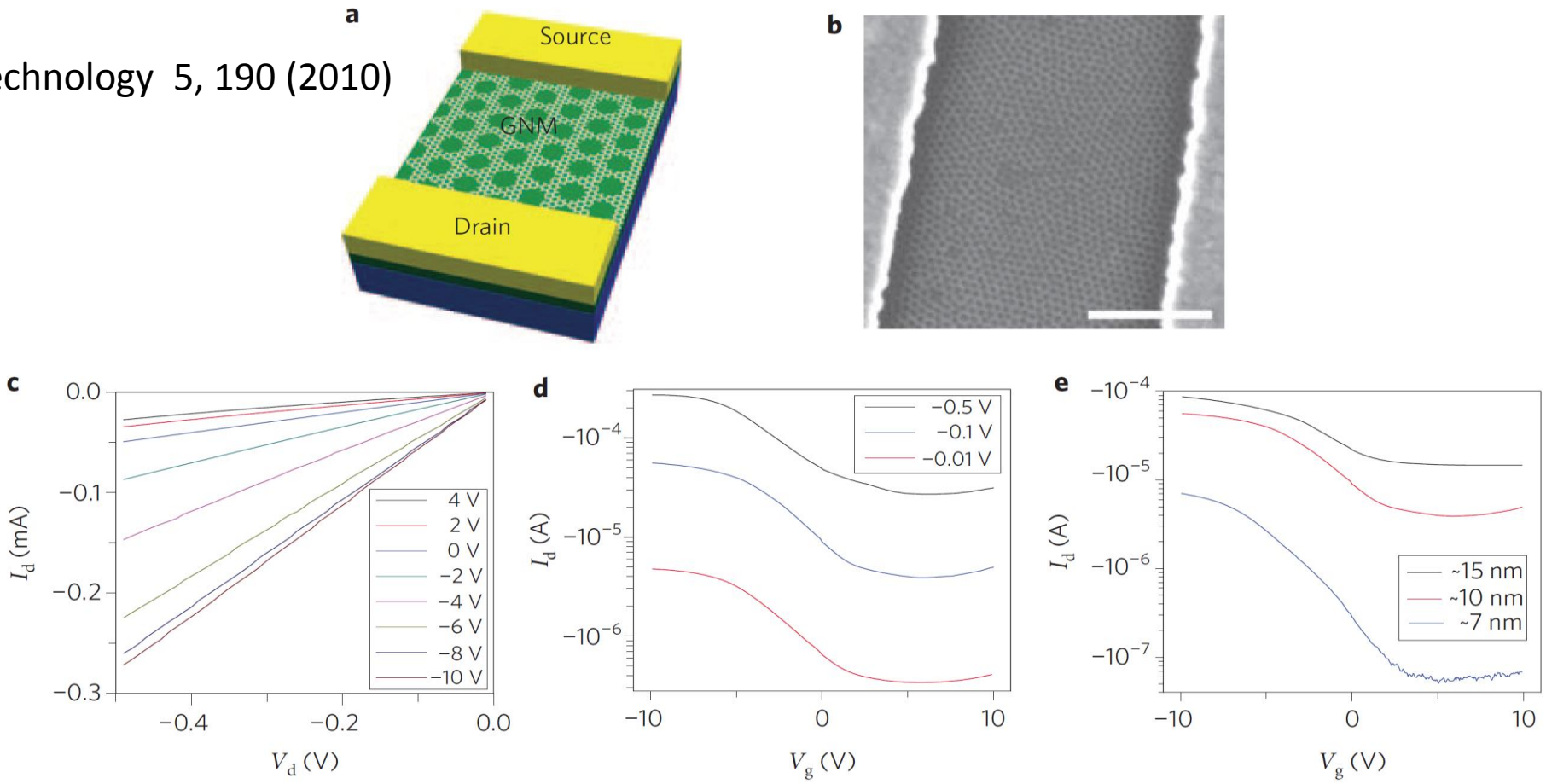

Figure 4 | Room-temperature electrical properties of a graphene nanomesh device. a, Schematic of a GNM-FET. The device is fabricated on a heavily doped silicon substrate with 300-nm SiO_2 as the gate dielectric. The electronic measurement was carried out in ambient conditions at room temperature, without removing the top oxide layer. **b**, SEM image of a GNM device made from nanomesh with a periodicity ~39 nm and neck width of ~10 nm. Scale bar, 500 nm. **c**, Drain current (I_d) versus drain-source voltage (V_d), recorded at different gate voltages for a GNM device with a channel width of ~2 μm and channel length of ~1 μm. The on-state conductance at $V_g = -10$ V is comparable to an array of 100 parallel GNR devices. **d**, Transfer characteristics for the device in **c** at $V_d = -10$ mV, −100 mV and −500 mV. The ratio between I_{on} and I_{off} for this device is ~14 at $V_d = -100$ mV. **e**, Transfer characteristics at $V_d = -100$ mV for GNMs with different estimated neck widths of ~15 nm (device channel width 6.5 μm and length 3.6 μm), ~10 nm (channel width 2 μm and length 1 μm) and ~7 nm (channel width 3 μm and length 2.3 μm).

Nanomechanical resonator based on suspended nanowires

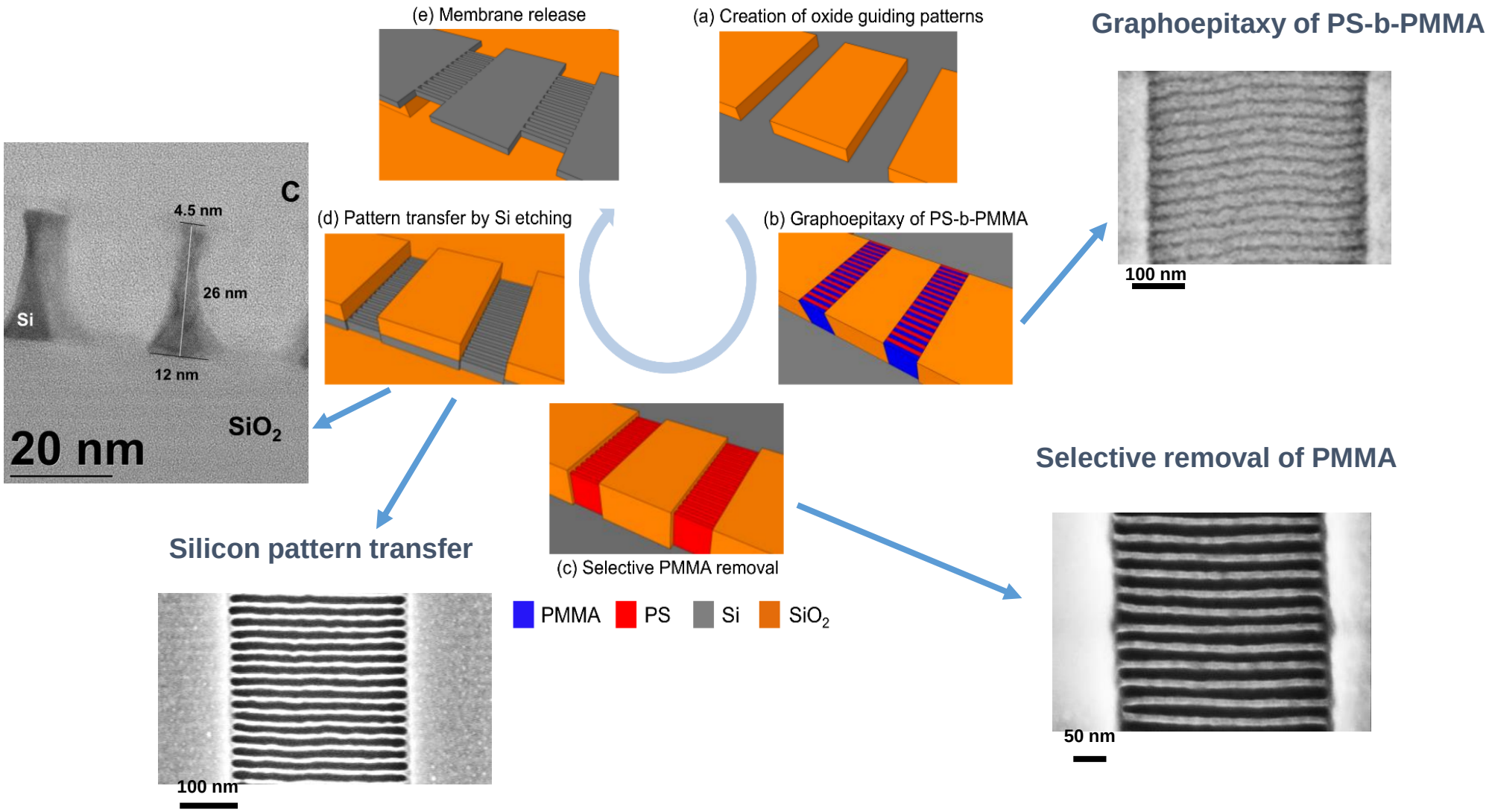

Directed self-assembly of block copolymers for the fabrication of functional devices . C. Pinto-Gómez, F. Pérez-Murano, J. Bausells, L. G. Villanueva, M. Fernández-Regúlez Polymers 2020, 12(10), 2432

Nanomechanical resonator based on suspended nanowires

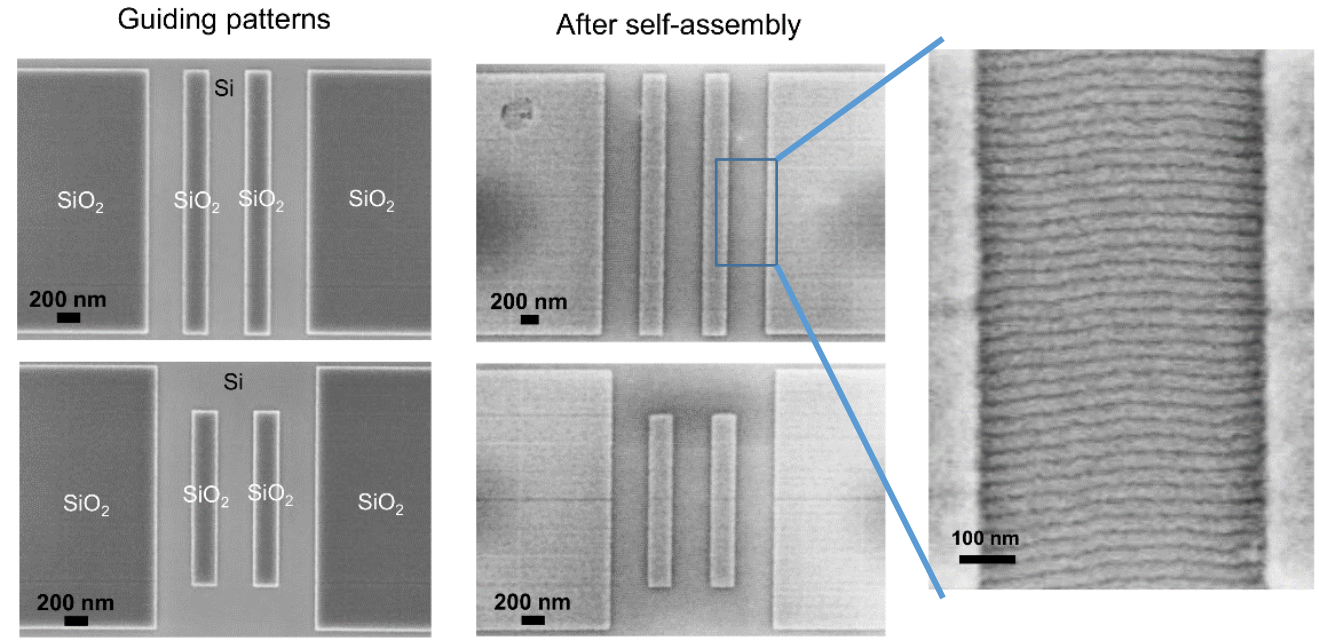

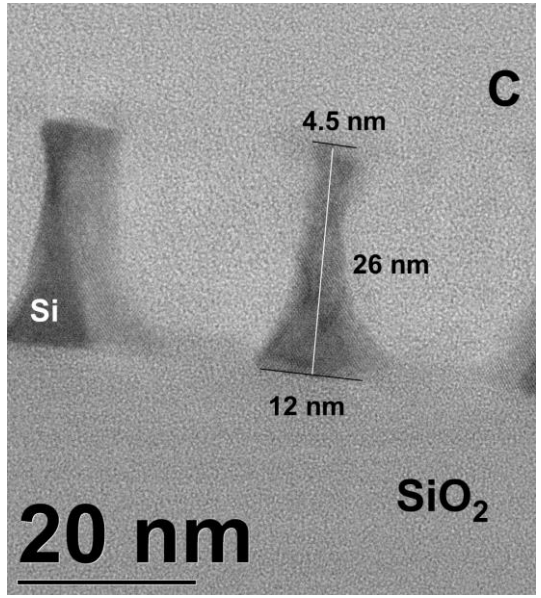

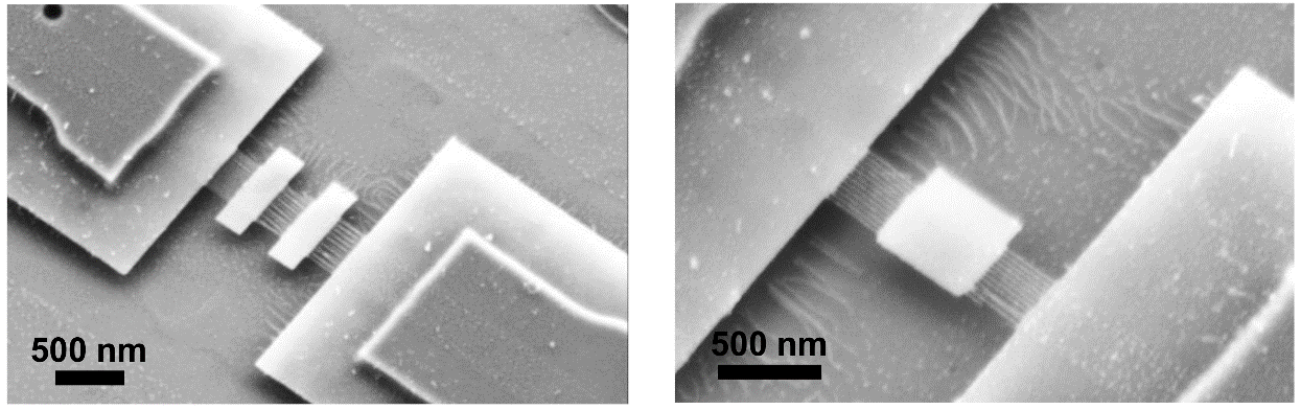

Directed self-assembly of block copolymers for the fabrication of functional devices . C. Pinto-Gómez, F. Pérez-Murano, J. Bausells, L. G. Villanueva, M. Fernández-Regúlez Polymers 2020, 12(10), 2432

Take home message

- Block copolymers are made of two or more distinct homopolymers linked end to end through covalent bonds. Upon annelaing, they suffer a micro-phase separation, creating nanoscale patterns.
- Thin films of self-assembled block copolymers can be used as lithographic masks. The resolution is dictated by the size of the block copolymer molecules.
- By means of guiding patterns, the orientation and position of the self-assembled patterns can be controlled: graphoepitaxy and chemoepitaxy
- Wide application range: magnetic media, electronics, graphene, ….